TARGETING *TOUSLED-LIKE KINASE 1* SIGNALLING PATHWAYS IN GLIOBLASTOMA MULTIFORME THERAPY

KAMARIAH BINTI IBRAHIM

UNIVERSITI KEBANGSAAN MALAYSIA

TARGETING *TOUSLED-LIKE KINASE 1* SIGNALLING PATHWAYS IN GLIOBLASTOMA MULTIFORME THERAPY

KAMARIAH BINTI IBRAHIM

THESIS SUBMITTED IN FULFILMENT OF THE REQUIREMENT FOR THE DEGREE OF DOCTOR OF PHILOSOPHY

MEDICAL MOLECULAR BIOLOGY INSTITUTE
UNIVERSITI KEBANGSAAN MALAYSIA
KUALA LUMPUR

2017

DECLARATION

I hereby declare that the work in this thesis is my own except for quotations and summaries which have been duly acknowledged.

14 March 2017

KAMARIAH BINTI IBRAHIM
P64523

ACKNOWLEDGEMENT

In the name of Allah most gracious and most merciful. Thank you Allah for this great opportunity that I can complete my Phd thesis. I would like to thank many people who helped me going through this journey. I am very fortunate to have Dr Roslan Harun as a research supervisor throughout this project. Although he has retired now, but all the knowledge he has taught me are very valuable. Throughout his supervision, I have improved myself in many ways, especially analytical skills and the passion to love science. My second supervisor, Dr Nor Azian Abdul Murad have also contributed so much in this project. She thought me that with hardwork, everything can be achieved.

Not to forget, all senior research fellows that have helped me to become a better scientist especially Professor Datuk Dr Rahman Jamal, Dato' Dr Wan Zurinah Wan Ngah and Associate Professor Dr Norfilza Mokhtar. Their thoughts and scientific arguments are very valuable to me. I would like to thank all UMBI research fellows for being supportive and helpful throughout my PhD. Moments in UMBI will not be great without these people with different unique characteristics and approach to make me mature enough in my scientific journey.

I would also like to express my high appreciation to all UMBI staffs; scientific officers, research officers and medical laboratory technologists. I would like to make my sincere gratitude especially to these people, the cell culture lab staffs, Hanif, Nurmi, and Raziff who will never say no to any kind of help that I needed. Cik Rosniza and Pn Norshahidah who have being helping me with my animal work. Not to forget Pn Zuraini from the Biobank PPUKM-UMBI. Others, like Sri Noraima, Riya and Encik Muhyiddin I will indeed remember you guys.

I would like to thank all the postgraduate students of UKM Medical Molecular Biology Institute especially Syazani, Amirah, Nadia, Rozita, Rashidah and Fateen. Others that have not been named, you know who you are. You guys have been great friends. Best friends ever! Thank you for sharing the good and the bad times together. Without these people I don't know if I can make it till the end.

To my dearest husband, thank you very much for understanding me. Journey as a PhD student will not be completed without the understanding of a loving husband. My credit to you also for being my mentor especially improving my presentation skills and confidence to speak in front of the public. You have become my idol. This thesis is also dedicated to my dearest family, my mom, my parents in law, brothers, sisters and brothers in laws. You guys helped me in many ways. Thank you for understanding me. This thesis is especially dedicated to my late father, Allahyarham Ibrahim Amnan who was my greatest inspiration to pursue this journey and got me through the thick and thin.

Last but not least, I gratefully acknowledge the financial support from the Ministry of Higher Education through the Higher Institution Centre of Excellence (HICOE), Grant number JJ-012-2015. Great science just cannot happen without good financial support. Thank you.

ABSTRACT

Glioblastoma multiforme (GBM) is an aggressive and highly invasive brain tumour that commonly exhibits resistance to conventional chemotherapy and radiotherapy. It is a heterogeneous disease involving complex kinomic alterations causing aberrant dysregulation of signalling pathways. Although many specific kinase inhibitors have been developed, only 30% of patients' survived due to extreme proliferation, invasion and highly vascularized nature of GBM cells. The aim of this study was to explore novel kinome pathways and to identify potential therapeutic targets for GBM. Meta-analysis was performed by filtering significant genes having p-value <0.05 from the Oncomine database using a total of 415 glioblastoma versus normal samples. This analysis identified 113 significantly upregulated kinases. RNAi screening on identified 113 kinases was performed subsequently, using Dharmacon Custom siRNA SMARTpool^{TM} library on LN18 and U87MG cells. k-Median Absolute Deviation statistical analysis has identified Tousled-like kinase 1 *(*TLK1*)* as a potential molecular target. TLK1, a serine-threonine kinase, was selected for an *in vitro* functional validation as its role in GBM is still unknown. Silencing of *TLK1* using 25nM siRNA and shRNA in GBM cells resulted in a significant reduction in cell viability, clonogenicity and proliferation by inducing S-phase cell cycle arrest. In addition, inhibition of *TLK1* induced apoptosis signals in GBM cells. Silencing of *TLK1* also chemosensitised GBM cells towards sub-lethal dose of temozolomide (250µM). Invasion and migration of GBM cells were also inhibited ($p<0.05$). Interestingly, in normal human astrocytes, silencing of *TLK1* did not cause significant changes in cell viability, apoptosis, invasion as well as migration. The downstream pathways of *TLK1* in U87MG cells were interrogated using Illumina HumanHT12-12 v4 BeadChip microarray. WebGestalt pathways analysis on 2,632 significant probes with more than 1.1 fold change difference identified key signalling pathways involved in GBM cancer pathways including DNA replication, cell cycle, focal adhesion, TGF-beta, and integrin-mediated cell adhesion signalling pathways. Gene expression analysis using qPCR confirmed the differential expressions of Thrombospondin-2, Paxillin, Ras-related C3 botulinum toxin substrate 2 (RAC2), Collagen type IV α2, FYN proto-oncogene Src family tyrosine kinase and Rho associated coiled-coil containing protein kinase 2 which were involved in the focal adhesion pathway. *TLK1* was postulated to regulate invasion and migration of GBM cells through signalling with a small GTP binding protein, RAC2. RAC2 signal was significantly suppressed in both *TLK1* knockdown U87MG and LN18 cells using RAC2 activation assay. *TLK1* knockdown GBM cells also significantly reduced phosphorylated p70S6 kinase expression which acted downstream of the PI3K/AKT/mTOR signalling pathway. *In vivo* subcutaneous GBM xenograft of stably transfected U87MG cells with sh-*TLK1* in *balb/c* female nude mice showed significant difference ($p<0.05$) in tumour growth potential. Subsequent *in silico* homology modelling of TLK1 and high throughput virtual screening of protein-ligand docking identified two potential compounds that bound to catalytic site of TLK1 modelled protein. These findings suggest that TLK1 and its related pathways are potential molecular targets for GBM therapy.

ABSTRAK

Glioblastoma multiform (GBM) merupakan penyakit tumor otak yang sangat agresif dan sering mengalami kerintangan terhadap kemoterapi dan radioterapi. Ianya bersifat heterogen yang melibatkan pelbagai perubahan kinomik yang kompleks sekaligus menyebabkan perubahan pengawal aturan tapak jalan dalam sel GBM. Walaupun pelbagai penghambat kinase telah dibangunkan, hanya 30% pesakit dapat menjangkau hayat lebih lama selepas rawatan dan pembedahan. Objektif kajian ini adalah untuk mengenalpasti tapak jalan baru kinase sebagai sasaran yang berpotensi untuk merawat GBM. Meta-analisis daripada pangkalan data Oncomine ke atas 415 sampel glioblastoma dan normal telah mengenalpasti 113 kinase yang mengalami peningkatan pengekspresan gen ($p<0.05$). Ujian saringan kehilangan fungsi menggunakan kepustakaan RNAi Dharmacon Custom SMARTpool^{TM} terhadap 113 kinom telah dijalankan ke atas sel LN18 dan U87MG. Analisa menggunakan "k-Median Absolute Deviation" telah mengenalpasti Tousled-like kinase 1 (TLK1) sebagai sasaran penanda molekul. TLK1 merupakan serin-threonin kinase yang berperanan di dalam pembaikpulih dan replikasi DNA telah dipilih untuk analisis kefungsian secara *in vitro* kerana peranannya di dalam mengawal atur sel GBM tidak diketahui. Penyenyapan *TLK1* menggunakan siRNA and shRNA menunjukkan perencatan yang signifikan terhadap kebolehidupan, klonogenisiti dan percambahan sel GBM melalui proses peningkatan penyekatan kitaran sel fasa-S. Penyenyapan *TLK1* mengakibatkan peningkatan apoptosis. Penyenyapan *TLK1* juga meningkatkan kemo-sensitiviti terhadap dos sub-maut temozolimide 250 µM dan perencatan serangan dan migrasi sel kanser ($p<0.05$). Namun begitu, penyenyapan *TLK1* tidak mengakibatkan perubahan terhadap kebolehidupan, apoptosis, serangan dan migrasi sel normal astrocytes. Pemprofilan tapak jalan hiliran *TLK1* dikaji dengan menggunakan Mikro Atur Illumina Human HT12-12 v4 BeadChip. Analisis tapakjalan dengan WebGestalt terhadap 2,632 prob yang signifikan melebihi 1.1 FC telah mengenalpasti 20 tapakjalan yang terlibat dalam kanser. Di antaranya adalah tapak jalan replikasi DNA, kitar sel, perlekatan fokus, kitaran sel pada fasa-G1 kepada fasa-S, tapak jalan integrin-berperantara perlekatan sel dan tapak jalan yang terlibat dalam GBM. Analisis pengekspresan gen menggunakan PCR nyata-masa mendapati bahawa terdapat pengekspresan berbeza gen *THBS2, RAC2, FYN, PXN, COL4A2* dan *ROCK2*, yang berperanan dalam tapak jalan perlekatan fokus. *TLK1* dicadangkan sebagai pengatur proses serangan dan migrasi sel GBM melalui pengisyaratan protein pengikat GTP kecil, RAC2. Terdapat penindasan signifikan terhadap isyarat RAC2 di dalam sel titisan GBM yang telah mengalami penyenyapan sh-*TLK1* melalui asai pengaktifan RAC2. Penyenyapan *TLK1* mengakibatkan penurunan kadar pengekspresan fosforilasi p70S6 kinase. *In vivo xenocantum subkulitan* daripada sel titisan U87MG dengan penyenyapan sh-*TLK1* di dalam *balb/c* mencit gondola betina menunjukkan perbezaan yang signifikan ($p<0.05$) dalam potensi pertumbuhan tumor. Model 3D TLK1 yang dibina dariada peramalan struktur protein digunakan untuk penabiran celusan tinggi maya. Hasilnya, satu sebatian yang berkait di tapak mangkin model protein TLK1 telah ditemui dan dijangka mempunyai ciri yang sesuai sebagai ubat untuk merawat GBM. Kesimpulannya, penemuan komprehensif daripada kajian ini mendapati bahawa TLK1 dan tapak jalan berkaitannya mempunyai potensi besar untuk dijadikan sasaran sebagai terapi molekul untuk GBM.

CONTENTS

LIST OF TABLE

LIST OF ILLUSTRATION

LIST OF SYMBOLS

ºC	Degree celcius
Δ	Delta
≤	Less or equal than
<	Less than
>	More than
%	Percent
CT	Cycling threshold
g	Gravity
µg	Microgram
µg/mL	Microgram/millilitre
µL	Microliter
µM	Micromolar
hr	Hour
hrs	Hours
mg	Milligram
min	Minute
mL	Millilitre
ng	Nanogram
nm	Nanomol
ng/µL	Nanogram/microlitre
s	Second
v/v	Volume/volume

LIST OF ABBREVIATIONS

A2B5	Glial progenitor marker
ACTB	Beta-actin
AGM	Astrocyte growth medium
AIC	5-aminoimidazole-4-carboxamide
AKT1	v-akt murine thymoma viral oncogene homolog 1
AKT2	v-akt murine thymoma viral oncogene homolog 2
AKT3	v-akt murine thymoma viral oncogene homolog 3
ALK	Anaplastic Lymphoma Receptor Tyrosine Kinase
ALPK1	Alpha kinase 1
Arp 2/3	Actin related protein 2/3 complex
ARPC1B	Actin related protein 2/3 complex subunit 1B
ASF1	Anti-Silencing factor 1
ATP	Adenosine triphosphate
AURKA	Aurora kinase A
BAX	Bcl-2-associated X protein
BBB	Blood brain barrier
Bcl-xL	B-cell lymphoma-extra large
BER	Base Excision Repair
BrdU	Bromodeoxyuridine
CCND1	Cyclin D1
CCND2	Cyclin D2
CD133	Prominin-1
CD42	Glycoprotein Ib
CD44	Cell-surface glycoprotein
CDC2 or CDK1	Cyclin-dependent kinase 1
CDC25A	Cell division cycle 25A
CDK4	Cyclin-dependent kinase 4
CDK6	Cyclin-dependent kinase 6
CDKN2A	Cyclin-dependent kinase Inhibitor 2A
CDKN2B	Cyclin-dependent kinase Inhibitor 2B
CDKN2C	Cyclin-dependent kinase Inhibitor 2C
CHI3L1	Chitinase 3–like 1
CHK1	Checkpoint 1
CI	Confidence interval
c-MYC	v-myc avian myelocytomatosis viral oncogene homolog
CNS	Central nervous system
CO_2	Carbon dioxide
COL4A2	Collagen alpha-2(IV)
c-SRC	SRC proto-oncogene, non-receptor tyrosine kinase

CTBP1	C-terminal binding protein 1
CT-scan	Computerised tomography scan
DDX5	DEAD-box helicase 5
DEPTOR	DEP domain containing mTOR-interacting protein
DF1	Dharmafect 1
DMEM	Dulbecco's Modified Eagle's Medium
DNA	Deoxyribonucleic acid
DSB	Double strand breaks
E2F	E2F transcription factor 1
ECM	extracellular matrix
EDTA	Ethylenediaminetetraacetic acid
EGFR	Epidermal growth factor receptor
EGFRvIII	Epidermal growth factor receptor variant III
ELISA	Enzyme-link immunosorbance assay
EPR	Enhance permeability and retention
ERBB2	Erb-B2 receptor tyrosine kinase 2
ERK	Mitogen-activated protein kinase 1
ERα	Eostrogen receptor alpha
FBS	Fetal bovine serum
FDA	Food and Drug Administration
FGF	Fibroblast growth factor
FLT3,	Fms-like tyrosine kinase 3
FOXO	Forkhead box O
FOXO1	Forkhead box O1
FYN	FYN proto-oncogene, Src family tyrosine kinase
GABRA1	Gamma-aminobutyric acid type A receptor Alpha1subunit
GAS1	Growth arrest specific 1
GBM	Glioblastoma multiforme
GFP	Green flourescent protein
GLI2	GLI family zinc finger 2
GSEA	Gene set enrichment analysis
GSK3	Glycogen synthase kinase-3
GTP	Guanosine-5'-triphosphate
GβL	mTOR, mammalian LST8/G protein β-subunit–like protein
HEPES	4-(2-hydroxyethyl)-1-piperazineethanesulfonic acid
HPE	Histopathological examination
H-Ras	Harvey rat sarcoma viral oncogene homolog
HRP	Horse reddish peroxidase
IDH1	Isocitrate dehydrogenase (NADP(+)) 1, cytosolic
IDH2	Isocitrate dehydrogenase (NADP(+)) 2, cytosolic
IGF	Insulin growth factors

IL-11	Interleukin -11
IL-6	Interleukin -6
INCENP	Inner centromere protein
INK4a/*ARF*	Cyclin-dependent kinase inhibitor 2A
JAG1	Jagged 1
K-Ras	Kirsten rat sarcoma viral oncogene homolog
LFNG	O-fucosylpeptide 3-beta-N-acetylglucosaminyltransferase
LIMK	LIM domain kinase 1
LOH	Loss of heterozygosity
MAPK1	Mitogen-activated protein kinase 1
MDM2	MDM2 proto-oncogene
MDM4 or MDMX	MDM4 proto-oncogene
MEK	Mitogen-activated protein kinase kinase 7
MERTK	Proto-oncogene tyrosine-protein kinase MER
MET	MET proto-oncogene, receptor tyrosine kinase
MGMT	O-6-methylguanine-DNA methyltransferase
MGMT	O6-MG–DNA methyltransferase
MMP-2	Matrix metalloprotease 2
MMP-9	Matrix metallopeptidase 9
MMR	Mismatch Repair System
MRI	magnetic resonance imaging
MRP1	ATP binding cassette subfamily C member 1
MTIC	methyl)-1-triazen-1-yl-imidazole-4-carboxamide
mTOR	mechanistic target of rapamycin
mTORC1	mammalian target of rapamycin complex 1
mTORC2	mammalian target of rapamycin complex 2
MYCN	v-myc avian myelocytomatosis viral oncogene Neuroblastoma derived homolog
NADPH	Nicotinamide adenine dinucleotide phosphate
NEFL	Neurofilament, light polypeptide
NES	Nestin
NF1	Neurofibromatosis 1
NFkB	Nuclear Factor kappa B
NHA	Normal human astrocytes
NOTCH3	Notch 3
N-Ras	Neuroblastoma RAS viral oncogene homolog
O6-MG	O6-methylguanine
p70 S6K	p70S6 serine threonine kinase
PAK	p21 activated protein
PAK2	p21 activated protein 2
PAK3	p21 activated protein 3
PBS	Phosphate buffer saline

PDCD4	Programmed cell death 4
PDGFRA	Platelet derived growth factor receptor alpha
PGI_2	Prostaglandin 2
PGM2	Phosphoglucomutase 2
PI(3,4,5)P3	Phosphatidylinositol (3,4,5)-trisphosphate
PI(4,5)P2	Phosphatidylinositol 4,5-bisphosphate
PI3K	Phosphoinositide-3-Kinase phosphatidylinositol-4,5-bisphosphate 3-kinase
PI3KCA	Catalytic subunit alpha
PIK3R1	Phosphoinositide-3-Kinase, Regulatory Subunit 1
PIK3R2	Phosphoinositide-3-Kinase, Regulatory Subunit 2
PIK3R3	Phosphoinositide-3-Kinase, Regulatory Subunit 3
PKC	Protein kinase C
PLK1	Polo-like kinase 1
PRAS40	AKT1 substrate 1
PTEN	Phosphatase and tensin homolog
PUMA	BCL2 binding component 3
PVDF	Polyvinylidene difluoride
PXN	Paxillin
qPCR	Quantitative real time PCR
RAC2	Ras-related C3 botulinum toxin substrate 2 (rho family, small GTP binding protein Rac2)
RAD9	Chromatin-binding protein RAD9
RAF-1	Raf-1 proto-oncogene, serine/threonine kinase
Raptor	Regulatory-associated protein of mTOR
RAS	Human rat sarcoma
RFU	Relative fluorescence units
RHOA	Ras homolog family member A
RIOK1	RIO kinase 1
RIOK2	RIO kinase 2
RIPA	Radioimmunoprecipitation
RNA	Ribonucleic acid
ROCK2	Rho associated coiled-coil containing protein kinase 2
RTF	Reverse transfection
RTK	Receptor tyrosine kinase
SDS-PAGE	Sodium dodecyl sulfate polyacrylamide gel
SGK1	Serum/glucocorticoid regulated kinase 1
siRNA	Silencing RNA
SLC12A5	Solute carrier family 12 member 5
SLC12A5	Solute carrier family 12 member 5
SMO	Smoothened, frizzled class receptor
ssDNA	Single stranded DNA
SSEA-1	Stage-specific embryonic antigen 1
SSMD	Strictly standardized mean difference

STAT3	Signal transducer and activator of transcription 3
STMN1	Stathmin 1
SYT1	Synaptotagmin 1
TCGA	The Cancer Genome Atlas
TGF	Transforming growth factor
THBS2	Thrombospondin 2
TLK1	Tousled like kinase 1
TMZ	Temozolomide
TP53	Tumor protein p53
TRKA	CTGF that binds to tyrosine kinase receptor type A
TTK	TTK dual-specifity protein kinase
VEGF	Vascular endothelial growth factor
VEGFR	Vascular endothelial growth factor receptor
WEE1	WEE1 G2 checkpoint kinase
WHO	World Health Organization
WNT	Wingless-related integration site
ZEB-1	Zinc finger E-box binding homeobox 1

CHAPTER I

INTRODUCTION

1.1 BACKGROUND

Gliomas are the commonest brain tumours that arise from the astroglial cells that support the neurons and control the blood flow through many different fine processes which form close associations with both blood vessels and neurons (Allen & Barres 2009). World Health Organisation (WHO) classifies gliomas into four stages based on histological characteristics; i.e. grade I, II, III and IV (Ohgaki & Kleihues 2007). Glioblastoma multiforme (GBM), stage IV glioma or high-grade astrocytoma, is the most lethal human cancers which carries poor prognosis even after surgery and conventional therapy. Most of primary GBM arises *de novo* and develops progressively without recognisable symptoms or precursor lesions. Secondary GBM, which accounts only 5% of GBM, usually develops from low grade glioma and can only be detected later by neuroimaging or histological evaluation of less malignant glioma (Bleeker & Molenaar 2012; Ohgaki & Kleihues 2007). A major concern is the poor outcome of GBM at which the median survival is approximately 14 months despite advances in detection, radiation, chemotherapy, and surgery (Johnson & O'Neill 2012; Paw et al. 2015; Stupp et al. 2005).

The human kinome, compilation of 518 protein kinases, are the largest family of human enzymes. They are responsible for phosphorylation of tyrosine, threonine and serine residues in other proteins that activate or inhibit many important cellular functions through downstream signalling molecular pathways (G. Manning et al. 2010). Dysregulation of kinome functions will lead to diseases. Members of the

protein kinase family are amongst the most commonly mutated genes in human cancers, and both mutated and activated protein kinases have proved to be potential targets for the development of new anticancer therapies. Alterations at the kinome level by changes in expression, methylation, copy number alterations or mutations affect GBM downstream signalling pathways governing cellular proliferation, cellular survival, invasion, and angiogenesis (Bleeker et al. 2014). This intra-tumuoral heterogeneity in GBM causes difficulties in providing treatment to each patient.

The key study by The Cancer Genome Atlas (TCGA) identifies human glioblastoma genes which interconnect with core biological pathways such as metabolic, genetic and signal transduction pathways. Three major signalling pathways have been identified and they were altered in GBM patients including RTK/RAS/PI3K signalling pathway (88%), TP53 signalling pathway (87%) and RB signalling pathway (78%) (The Cancer Genome Atlas 2008). One of the important hallmarks of GBM is dysregulation of the cell cycle and enhanced GBM cell proliferation. Both occurs due to the inactivating mutations of the key tumour suppressor genes; namely the TP53 and RB pathways, primarily by governing the G1 to S phase transition. The absence of these cell cycle guardians renders tumours particularly susceptible to inappropriate cell division driven by constitutively active mitogenic signalling effectors, such as PI3K and MAP kinase (Ng et al. 2012).

In GBM, the inactivation of the TP53 pathway occurred in the form of *ARF* deletions (55%), amplifications of *MDM2* (11%) and *MDM4* (4%), in addition to mutations of *TP53* itself (The Cancer Genome Atlas 2008). As being the most vital checkpoint for DNA damage and apoptosis pathways, aberrant regulation in TP53 pathways will cause major breakdown in cellular homeostasis where cells are evading from apoptosis contributed by the downregulation of *BAX* and *PUMA* pro-apoptotic proteins (Haupt et al, 2003 and Ng et al, 2012). The RB pathway aberration in GBM occurs due to the homozygous deletion of the *CDKN2A* (55%), *CDKN2B* (53%) and *CDKN2C* (2%) locus on chromosome 9p21. This is followed by amplification of the *CDK4* locus (14%), amplification of *CCND2* (2%) and amplification of *CDK6* (1%). Genome wide association study (GWAS) also revealed that single nucleotide polymorphisms in the *CDKN2A* and *CDKN2B* have been identified as risk factors for

glioma development (Shete et al, 2009 and Wrensch et al, 2009). In cancerous events, amplification of cyclin dependant kinases will make cells insensitive to anti-growth signals, in this case, accumulation of phosphorylated RB proteins releases the E2F transcription or binding factor to activate transcription and trigger the onset of S-phase (Furnari et al. 2007a; Ng et al. 2012).

The RTK/RAS/PI3K signalling pathway alterations involved aberrations in at least two out of four types of Receptor Tyrosine Kinases (RTK) in GBM. The most frequent RTK aberrations involve mutation and amplification of the *EGFR* (41%), mutation in *ERBB2* (8%), amplification of *PDGFRA* (13%) and *MET* (4%). The downstream RTK components are also altered including 18% mutation and homozygous deletion of *NF1,* a negative regulator of the RAS transduction signalling pathway. The *PTEN* tumour suppressor, which inhibits the PI3K-AKT pathway, was reported to have 36% homozygous deletion and mutation. The *PI3K* and *AKT* were also found to be mutated by 15% and 2% respectively (The Cancer Genome Atlas 2008). Ultimately, *RTK* activating mutations transform the cell membrane into a catalytic surface populated with a high density of pro-mitotic signalling molecules, leading to cell proliferation. Concurrently, mutations of the *PTEN* prevent hydrolysis of PI(3,4,5)P3 into PI(4,5)P2 shutting off the RTK–PI3K pathway (Clarke & Dirks 2003; Soroceanu et al. 2013; Sugawa et al. 1990).

1.2 PROBLEM STATEMENT AND RESEARCH GAP

Highly proliferative and invasive cells are the key to the treatment failure in GBM patients. GBM tumour cells present two distinct features: highly invasive and highly proliferative and both are mutually exclusive by nature (Hatzikirou et al. 2012; Hatzikirou et al. 2005). Commonly, GBM tumours present with a bulky, proliferative, angiogenic tumour core, but they are also comprised of highly invasive penetrating tumour cells towards the normal brain parenchyma surroundings (Bonavia et al. 2011; Furnari et al. 2007). This condition becomes an infiltrative border and its removal by surgical resection is difficult, contributing to inadequate tumour removal and imminent tumour relapse mostly along the margins of the tumour incision (Huse & Holland 2010).

Glioma stem cells (GSC) are glioma cells with stem-cell like features and are postulated to be the major factor in GBM progression and resistance (Bao S. et al. 2006; Sampetrean & Saya 2013). GSC have the capability to self-renew without limit and have the ability to produce heterogeneous offspring that in the end transform into tumour bulk (Dietrich et al. 2008; Sampetrean & Saya 2013). They originate from a protected area with a unique environment known as a stem cell niche that is confined to the perivascular space and is oxygen-deprived conditions (Ignatova et al. 2002; Pointer et al. 2014; Thomas et al. 2014).

The complex surroundings of the glioma microenvironment are composed of various components of non-neoplastic stromal cells, including the vasculature, various infiltrating and resident immune cells, as well as other glial cells (microglia, satellite cells, Schwann cells, and oligodendroglia). It is also unique as it is encapsulated into anatomically distinct regions, referred to as tumour niches that in addition to tumour cells also foster GSC (Hambardzumyan & Bergers 2015). These niches do not merely harbour GSC but act as signalling or communication centres in which tumour cells and host cell populations dynamically interact through direct cellular contact or paracrine signalling to establish maintenance, growth, and protection of tumour cells and GSC from immune surveillance and therapeutic threats (Hambardzumyan & Bergers 2015; Hoelzinger et al. 2007). The interaction of the extracellular matrix (ECM) with cells is largely controlled by cell–integrin receptor interaction. Together with ECM-degrading proteases, the integrin family members are commonly known to orchestrate GBM cell invasion. These heterodimeric transmembrane adhesion receptors link the ECM bidirectionally along with the networks of intracellular signalling (Hynes 2002; Vehlow & Cordes 2013).

Specific inhibitors targeting EGFR, VEGFR and PI3K pathways have been used to treat GBM with conflicting results. Erlotinib, an EGFR inhibitor, has been successful in treating lung and breast cancers but not in GBM patients (Brandes et al. 2008). The poor efficacy in GBM is due to the different sites of *EGFR* mutations which occur at the extracellular domain whereas in lung cancers, the mutations are at the kinase domain (Vivanco et al. 2012). One of the major concerns of anti-angiogenic therapy is recurrent tumour cells are postulated to have tumour escape mechanism

making the cells more invasive and aggressive (Verhoeff et al. 2009). Despite binding of the inhibitor to the PI3K subunits, the GBM cells continue to proliferate due to the activation of RAS/MAPK/MEK alternative pathway (Foukas et al. 2010).

Although many inhibitors have been developed from time to time, there are still a need to identify novel targets to cure this deadly disease. With advanced biotechnology platforms as well as integrative analysis tools it will allow identification of novel kinome, which is a set of protein kinases in its genome pathways for GBM therapy. It may provide an implicative understanding to target this deadly disease in a very strategic manner. Findings from this study will hopefully benefit GBM patients which ultimately improve patients' survival.

1.3 HYPOTHESIS

Novel kinome targets for GBM can be identified using functional genomics approach. Identification of novel kinases that have significant roles in cancer pathways will provide efficient inhibition of GBM growth *in vitro* and *in vivo.* Subsequently, once its functional role is well understood, specific kinase inhibitors can be identified using bioinformatics approach.

1.4 STUDY OBJECTIVE

1.4.1 To investigate novel kinome pathways as potential targets for GBM therapy.

1.5 SPECIFIC OBJECTIVES

1. To identify upregulated kinases in GBM via meta-analysis from the Oncomine publicly available database and to identify potential novel kinases using RNA interference (RNAi) 'loss-of-function' screen.

2. To characterise molecular functions of selected kinase *in vitro* using functional assays and to characterise downstream pathways of selected kinase using microarray.

3. To determine the effect of the target kinase inhibition on the growth of subcutaneous glioblastoma xenografts.

4. To predict the 3D protein structure of the target kinase using comparative modelling and identify suitable small molecule inhibitors via receptor-ligand docking.

CHAPTER II

LITERATURE REVIEW

2.1 GLIOMAS

Gliomas are defined as any tumours having histological, immunohistochemical, and ultrastructural proof of glial cell differentiation which may arise from the brain or the spinal cord. These glial cells are usually mature cells that support and protect the neuronal cells by providing adequate supportive structure and blood supply (Allen & Barres 2009). The World Health Organization (WHO) classified gliomas into 4 grades, i.e. grade 1 to 4, based on their clinical and histopathological criteria according to the degree of tumour cell proliferation, cellular atypia, and microvascular proliferation (Louis et al. 2007). Grade I gliomas are usually benign, well-circumscribed, and seldom progress to more advanced stages. In contrast, grade II (diffuse astrocytoma), grade III (anaplastic astrocytoma), and grade IV gliomas (glioblastoma multiforme, GBM) are malignant and readily infiltrate into the brain parenchyma. Survival ranges from 3 to 10 years in grade II glioma, 2 to 5 years in grade III glioma, and about 1 year in grade IV gliomas (Louis et al. 2007; Tait et al. 2007).

Recently the 'International Society of Neuropathology-Haarlem Consensus Guidelines for Nervous System Tumour Classification and Grading' suggested that in order to accurately diagnose patients with glioma, integrated analyses by collecting patients' demographics data, molecular analysis of affected genes, radio images as well as tissue morphological analysis have to be performed. These involve the collection of all information regarding tissue samples, histological classification, WHO grade, as well as the molecular classification (Louis et al. 2014). Figure 2.1 shows the distribution of primary brain and central nervous system Gliomas by histological subtype in USA.

In Malaysia, brain tumour is the tenth to cancer occurring in men (Ministry of Health Malaysia 2007). A comprehensive study in the state of Sarawak reported that glioma was the second commonest adult brain tumour with 93 cases and high-grade glioma was the most common subtype which accounted for 39 cases (47.0%). GBM manifested at any age from neonates to the elderly (day 11 of life to 83 years old), and the highest incidence was in those aged 40–59 years (Goh et al. 2014).

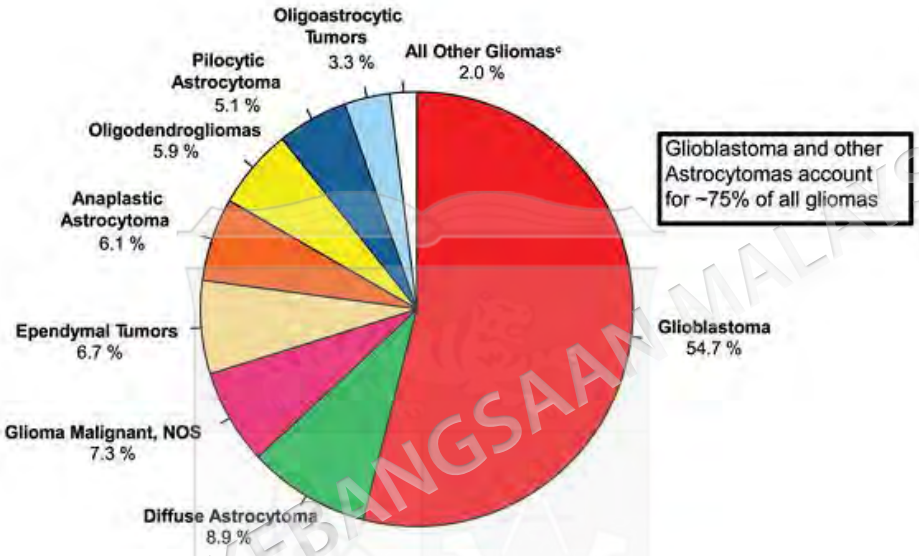

Figure 2.1 The distribution of primary brain and central nervous system Gliomas by histological subtype, taken from the Central Brain Tumour Registry, USA, from 2007 to 2011.

(Source: Ostrom et al. 2013)

2.1.1 Symptoms and Diagnosis

The common symptoms in patients with glioma are headaches, seizures, memory loss, and behavioural changes. Sometimes, cognitive impairment, language disability, and loss of sensation may also occur. Severe headache may occur depending on the tumour location which may affect normal brain function (Figure 2.2), and tumour expansion may increase intracranial pressure leading to nausea and vomiting (Sizoo et al. 2010).

Accurate diagnosis of glioma is made by computerised tomography scan (CT-scan) and magnetic resonance imaging (MRI) to determine the size of the tumour mass and location within the brain. Although both techniques deliver high-resolution images, MRI provides extensive information on oedema, mass effect, necrosis, and

haemorrhage at high tissue contrast. High-grade gliomas often present with necrosis of the central areas and more prominent peritumoral oedema compared with anaplastic gliomas (Cha 2005). Both MRI investigation and genetic analysis of tumour biopsy specimens are useful to ensure early diagnosis which will enable the provision of appropriate and adequate therapy as well as total surgical resection in primary and secondary high-grade glioma (Ideguchi et al. 2015).

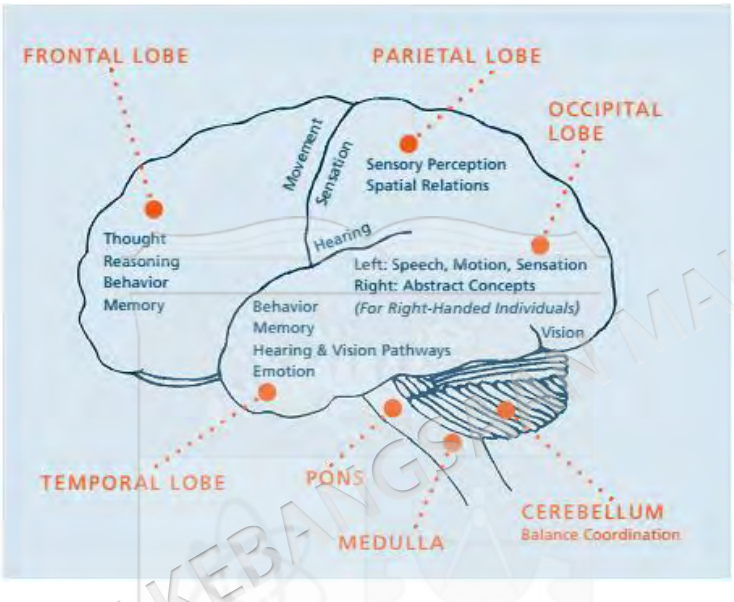

Figure 2.2 Functions of the brain lobes. Tumours at specific sites affect the brain functions and are associated with specific symptoms.

(Courtesy of www.abta.org)

2.2 GLIOBLASTOMA MULTIFORME

GBM is the most malignant astrocytoma, arising from poorly differentiated neoplastic astrocytes. It is the most frequent and aggressive type of primary brain tumour in humans, accounting for approximately 50% of all tumours of glial origin and 20% of all intracranial tumours (Bruce, 2005). Initially, the term 'glioblastoma multiforme' was used because of the heterogeneity of its histopathological macroscopic appearance which is particularly diverse; in Latin '*multi-forme*' or '*multiformis*' refers to 'many shapes' (Louis et al. 2007). Until recently, only the term 'glioblastoma' has been used because the disease is now considered less complicated as more research has been performed to reveal its unique molecular characteristics using current technology

platforms such as next-generation sequencing and proteomic array (Cerami et al. 2010; The Cancer Genome Atlas 2008).

Histologically, high-grade gliomas such as GBM exhibit morphological characteristics including nuclear pleomorphism, dense cellularity, vascular endothelial proliferation, and pseudopalisading necrosis (Huse & Holland 2010; Wen & Kesari 2008). Malignant gliomas appear as masses with irregular contours or irregular enhancing masses associated with oedema detected by MRI and CT-scan (Wen, & Kesari 2008). Despite advancements in technology and research strategies, the prognosis of GBM is still poor where maximal survival is only 15 months. The challenges in treatment include high vulnerability of the tissue where the tumour mass resides, diffuse invasiveness of tumour cells into the adjacent brain parenchyma, and recurrence of the disease by rapid growth of the infiltrating cells (Huse & Holland 2010; Sedo & Mentlein 2014).

The majority of GBM tumours are found in the frontal lobes of the supratentorial compartments. In addition, the tumour mass may be found in all cortical areas such as the brainstem, cerebellum, and spinal cord. The majority of malignant neoplastic cells are confined within the tumour bed and within the enhancing borders approximately 2 cm away. The migrating cells however can be found several centimetres from the tumour and even in the contralateral hemisphere of the brain (Adamson et al. 2009).

The aetiology of GBM is unknown. While the incidence of gliomas is increasing, the predisposing factors are still not well understood. Previous exposure to ionising radiation is the only verified environmental risk factor associated with gliomas in children that received prophylactic central nervous system irradiation for acute lymphoblastic leukaemia (Florian et al. 2013; Ohgaki & Kleihues 2005a). Other occupational exposure to chemical carcinogens such as rubber manufacturing, petroleum production, vinyl chloride, pesticides, cleaning services, as well as passive smoking exposure were initially thought to have a causal relationship with GBM. However, none of these factors have been recognised as an established cause of GBM (Fisher et al. 2007). Caucasians are more frequently affected than their Asian or African counterparts (Ohgaki & Kleihues 2005a; Parkin & Muir 1992; Wrensch et al. 2002).

GBM can manifest as a *de novo* lesion known as primary GBM occurring in more than of 90% cases or progress from less undifferentiated low-grade astrocytoma and is known as secondary GBM (Ohgaki & Kleihues 2007). Primary GBM usually develops in older adults as a highly aggressive and invasive *de novo* lesion devoid of any clinical or histological information of a less malignant precursor lesion. However, secondary GBM manifest in younger patients and develops through a progression from low-grade to high-grade astrocytoma of 5 to 10 years' duration. Although some cancer pathways are involved, primary and secondary GBM develop through distinct molecular pathways (Ohgaki & Kleihues 2005b, 2007, 2011) but their histological and clinical features are indistinguishable.

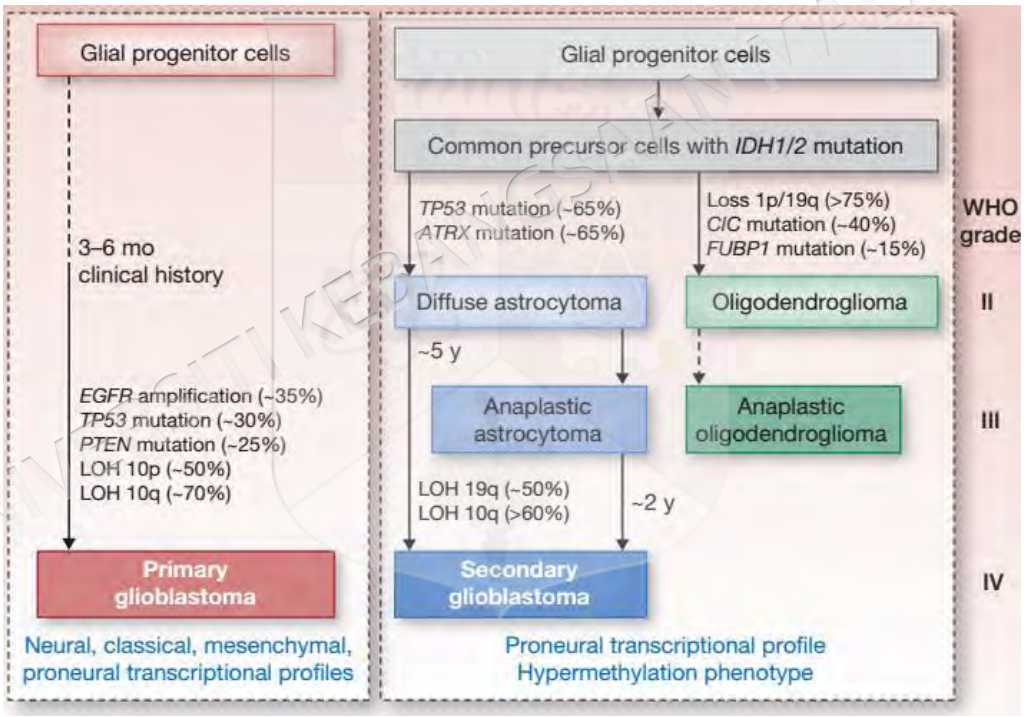

Figure 2.3 Genetic pathways which are involved in primary and secondary GBM. Different genetic mutations have been identified in primary and secondary GBM. Oligodendrogliomas share similar origins with secondary GBM through common precursor cells with *IDH1/2* mutation.

(Source: Ohgaki & Kleihues 2013)

2.2.1 Primary GBM

The majority of patients with primary or *de novo* glioblastomas manifest symptoms rapidly after a brief clinical history of less than 3 months and without evidence of a less malignant precursor lesion. Primary GBM occurs at the average age of 62 years. Primary GBM manifests in 70% of cases of loss of heterozygosity (LOH) at 10q, 36% with *EGFR* amplification, 31% with p16INK4a deletion, and 25% with *PTEN* mutation (Ohgaki & Kleihues 2007). Mutation of *P13KR1* and *P13KCA*, *NF1* alteration, loss of *INK4a*/*ARF*, and *MDM2*/*MDM4* amplification are also associated with primary GBM development. Primary GBM is also associated with absence of *IDH* mutation (Figure 2.3). However, none of these alterations reliably distinguishes the glioblastoma subtypes. This is because primary and secondary GBM are histologically largely indistinguishable molecular subtypes and have remained conceptual without being used for diagnostic or treatment decisions (Homma et al. 2006; Ohgaki & Kleihues 2013).

2.2.2 Secondary GBM

Secondary GBM is generally initiated from diffuse astrocytoma and occur in younger patients with an average age of 45 years. A common molecular lesion associated is *TP53* mutation (60%) which is associated with poor prognosis (Ohgaki & Kleihues 2005b, 2007; Ohgaki 2005). Partial LOH or full loss of the chromosome 10q arm but without the loss of 10p (Ohgaki 2005), overexpression of *PDGFR* as well as abnormalities in the p16 and RB signalling pathways (Wen & Kesari 2008) have been reported.

Through the Genome Wide Association Study (GWAS), Parsons and colleagues determined that the *IDH1* gene shows a somatic mutation predominantly at codon 132 (Parsons et al. 2008) in secondary GBM. *IDH1* mutations are the earliest detectable genetic alteration in low-grade diffuse astrocytoma precursor and in oligodendroglioma, indicating that these tumours are derived from different neural precursor cells dissimilar from those of primary GBM. In secondary GBM without *IDH1* mutation, the *IDH2* gene could be mutated. With a mutation frequency of 80%, it is important to note that

IDH1 and *IDH2* may play a key role in secondary GBM. This suggests the importance of their involvement in progression to high grade glioma. (Parsons et al. 2008).

Later, it was found that the *IDH1* gene, which encodes isocitrate dehydrogenase 1, catalyses the oxidative carboxylation of isocitrate to α-ketoglutarate (Narahara et al. 1985; Nobusawa et al. 2009). *IDH1* mutations dominantly inhibit the function of the enzyme by producing catalytically inactive heterodimers (Ichimura et al. 2009). *IDH2* is homologous to *IDH1*: both result in the production of NADPH in the Krebs cycle. Reduced glutathione regeneration requires the cofactor NADPH that regulates the mechanism for inhibiting oxidative damage. (Fu et al. 2010; Lee S.M. et al. 2002). In cancer, oxidative stress levels are increased in the brain compared with other organs.

Gain of the 7q arm is also commonly reported (21–50%) in diffuse astrocytoma, affecting the MET proto-oncogene, receptor tyrosine kinase (RTK) or *MET* gene located at 7q31.2 significantly and has also been reported to be related with poor prognosis in diffuse astrocytoma (Pierscianek et al. 2012). The MET protein kinase is comprised of an α-chain linked by a disulfide bridge to a β-chain (Birchmeier et al. 2003). The α-chain of MET kinase that imports the binding site for substrates is located at the extracellular kinase domain. Alternatively, the β-chain is involved in traversing the membrane by including the cytoplasmic kinase domain and the carboxy-terminal which is important in the regulation of the PI3K/AKT, RAS/MAPK, and STAT pathways (Birchmeier et al. 2003; Pierscianek et al. 2013). Other genetic alterations in secondary GBM include LOH at 9p, 19p, and 10q (Masui et al. 2012; Ohgaki & Kleihues 2007).

2.2.3 Molecular Subtypes of GBM

To accurately answer the issue of indistinguishable accurate molecular subtypes of GBM, large-scale profiling efforts such as those initiated by The Cancer Genome Atlas (TCGA) have attempted to catalogue and integrate the full spectrum of molecular abnormalities. The work involved large-scale gene expression analysis and has identified the molecular classification of GBM to four specific subtypes, namely proneural, neural, classic, and mesenchymal. This information was integrated with

multidimensional genomic data to establish patterns of somatic mutations and DNA copy number together with patient survival data (Verhaak et al. 2010). Through this initiative, the genotype to phenotype correlation in these cancers were elucidated for the first time.

Classic GBM refers to the subtype that frequently exhibits high *EGFR* alterations such as *EGFR* amplification and *EGFRvIII* mutations. Focal 9p21.3 homozygous deletion related to CDKN2A and other RB1-associated pathways such as CCND1 and CDK4 co-occurs with *EGFR* abnormalities. The expression of neural precursor and stem cell markers such as nestin (NES), Notch (NOTCH3, JAG1, and LFNG) and Sonic hedgehog (SMO, GAS1, and GLI2) is also high (Verhaak et al. 2010). From the same study, it was determined that 93% of the samples harboured chromosome 7 amplifications and chromosome 10 deletions with some abnormalities in the *NF1*, *TP53*, *IDH1*, or *PDGFRA* genes.

The mesenchymal subtype is characterised by overexpression of the chitinase 3–like 1 (*CHI3L1*) and *MET* genes (Phillips et al., 2006) which are the common mesenchymal markers. The consolidation of upregulation of CD44 and MERTK, which are mesenchymal and astrocytic markers, reflects the process of epithelial-to-mesenchymal transition that has been related to the dedifferentiation and transdifferentiation of tumours (Thiery 2002). The striking characteristic of this subtype is the strong association with the high frequency of *NF1* mutation or deletion and low levels of *NF1* mRNA expression. The high necrotic index is correlated with the expression signatures of genes from the wound healing process along with NF-κB signalling. In this GBM subtype, the rate of mutations of the *TP53* and *PTEN* genes is 32% (Verhaak et al. 2010).

The proneural subtype manifests with a high frequency of *TP53*, *IDH1*, as well as *PDGFRA* mutations, which all mimic secondary GBM characteristics. This subtype is associated with high survival and usually develops in younger patients (Verhaak et al. 2010).

The neural subtype is characterised by the expression of neuronal markers such as GABRA1, NEFL, SLC12A5, and SYT1 which mirror normal brain tissue samples. This is confirmed by the gene ontology (GO) categories which are correlated with neuronal projection, axonal and synaptic transmission, as well as neural, astrocytic, and oligodendrocytic gene signatures. The neural subtype has been confirmed as GBM by morphological examination and harbours DNA copy number variations together with gene mutations (Verhaak et al. 2010).

2.3 THE HUMAN KINOME AND SIGNALLING PATHWAYS

The human kinome is the set of protein kinases in human genome (G. Manning et al. 2002). Kinases are enzymatic proteins consisting of 518 kinase family members which reflects 1.7% of the human genome, suggesting the essential role of kinomes in cellular regulation (Manning G. et al. 2002). Since its completion, the Human Genome Project has aided the discovery of comprehensive novel human kinase genes. Reversible phosphorylation of proteins catalysed by kinases is a key component of many cellular signalling pathways involved in cellular growth, apoptosis, senescence, differentiation, proliferation, angiogenesis, cytoskeletal rearrangement, and metabolism (Matthews and Gerritsen, 2010). Kinases mediate phosphorylation by catalysing the transfer of a phosphate group from a high-energy donor, usually ATP, or to a lesser extent GTP, to proteins or lipids (Manning G. et al. 2002). The phosphate acceptor in the proteins is the hydroxyl group of either a serine, threonine, or tyrosine residue which can be located within a similar molecule, for example, auto-phosphorylation, or are proteins different or distinct from the kinase. This phosphorylation-dependent signalling can involve a complex cascade of networks which amplifies and regulates multiple cellular signalling outputs (Duong-Ly, & Peterson 2013).

Mutations in kinase genes or aberrant chromosomal structure can result in the activation of oncogenic kinases and hence cells lose the ability to control the cellular division and proliferation processes (Capra 2006). Parallel analysis of the kinase chromosomal map with known disease loci identified 164 kinases mapped to amplicons observed in tumours (Knuutila et al. 1998), and 80 kinases were mapped to loci involved in other diseases (Manning G. et al. 2002). Futreal et al. (2004) discovered that the

commonest protein domains encoded by cancer genes are domains belonging to protein kinases, where there are 27 out of 291 ‘cancer kinomes’, suggesting that protein kinases are crucial in driving cancer progression (Futreal et al. 2004).

Oncogenic kinases regulate many important aspects in oncogenesis hence serving as putative targets for cancer drug design (Patel et al. 2012; Workman et al. 2013). All oncogenic kinases as well as other related proteins participate in cellular functions that involve the transduction of signals from the extracellular environment through the membrane into the cytoplasm and towards the nucleus. In the nucleus, transcription is initiated to generate proteins that will finally contribute to the oncogenic phenotype (Tsatsanis & Spandidos 2000).

Signal transduction in the cell occurs in several processes. The most commonly described process is signalling from growth factors and cytokines via transmembrane receptors (Blume-Jensen & Hunter 2001; Tsatsanis & Spandidos 2000). The major family of transmembrane receptors are the RTKs. RTKs initiate oncogenesis by oligomerisation induced by ligand binding (Blume-Jensen, & Hunter 2001). Examples of ligands frequently associated with this process are epidermal growth factors (EGF) and insulin growth factors (IGF) (Voudouri et al. 2015) secreted into the surroundings by the tumour. Later, it leads to phosphorylation and intercellular signalling molecule recruitment (Tsatsanis & Spandidos 2000). Once signalling is initiated at the transmembrane receptors, it is transduced through cytoplasmic proteins via the cytoplasm into the nucleus. Structurally altered oncogenic kinases from serine/threonine kinase family members, for example AKT (Franke 2008) and non-RTKs such as c-SRC (Stettner et al. 2005), act as intracellular cytoplasmic proteins that activate signalling cascades into the nucleus. Cytoplasmic proteins are responsible for activating transcription factors, for example STAT3 (Kanno & Miyake 2015) and c-MYC (Zheng et al. 2008), by phosphorylation within the nucleus, leading to alterations of genetic expression. This will ultimately contribute to subsequent cancer progression by promoting the growth, apoptosis, invasion, and migration of cancer cells (Hanahan & Weinberg 2011).

2.3.1 Major Altered Signalling Pathways in GBM

The Cancer Genome Atlas (TCGA), which is the largest cancer genomics initiative working group, has comprehensively characterised and catalogued the genotypes and epigenetic events of more than 500 samples from 33 different tumour types mainly from kidney, brain, nervous system, breast, lung, blood, colorectal, uterus, ovary and head and neck cancer (The Cancer Genome Atlas 2008; Tomczak, Czerwińska & Wiznerowicz 2015). One of the earliest and hallmark findings was the characterisation of the signalling pathways involved in GBM (The Cancer Genome Atlas 2008). Initially, GBM was thought to evolve along a linear progression due to the accumulation of mutations. However, the findings from TCGA proposed that the evolution of GBM occurs along multiple pathways such as signalling pathways, metabolic pathways and genetic pathways as a feedback mechanism to various selective pressures to attain GBM cancer phenotypes (Ng et al. 2012; Verhaak et al. 2010). As shown in Figure 2.4, TCGA have identified a highly interconnected network of aberrations involving three major signalling pathways, namely the TP53 and RB1 tumour suppressor as well as the RTK/RAS/PI3K signalling pathways (Prados et al. 2015; The Cancer Genome Atlas 2008).

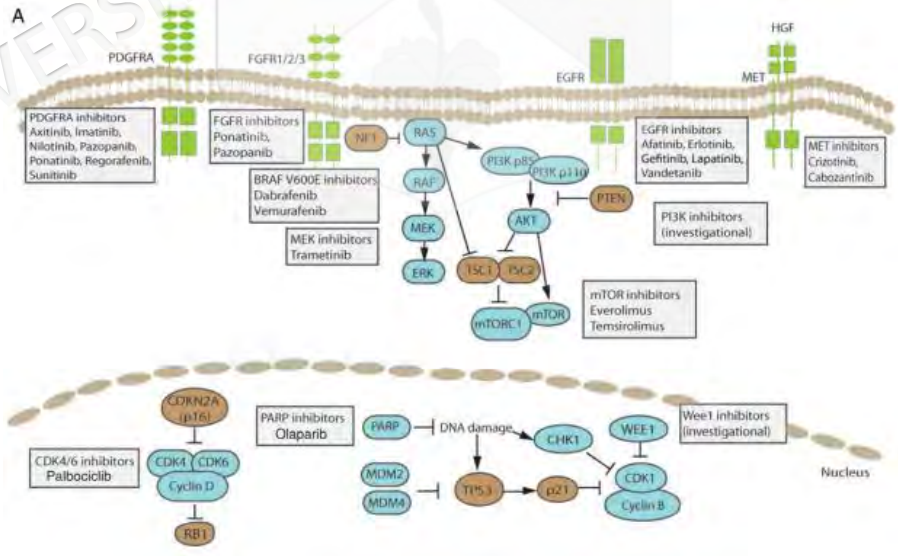

Figure 2.4 Significantly mutated kinases genes identified in the primary glioblastoma TCGA dataset. Pathway representation of three frequently altered pathways namely RTK/RAS/PI3K, TP53 and RB1 signalling pathways and their selected potential therapeutic agents.

(Source: Prados et al. 2015)

2.3.2 RTK/RAS/PI3K Signalling Pathway

The RTK/RAS/PI3K signalling pathway is an important aspect in normal cellular regulation, orchestrating several important processes in cancers including cellular proliferation, motility, apoptosis, and metabolism (Vanhaesebroeck et al. 2010). PI3K signalling pathway is regulated by various effectors as shown in Figure 2.5. The first and crucial intracellular members of this signalling pathway are growth factors which act as ligands, e.g. EGF, VEGF, and PDGF, in conjunction with their respective transmembrane receptors, mainly RTKs that include EGFR, VEGFR, and PDGFR. The binding of growth factors to the kinase receptors leads to the phosphorylation of PI3K subunits from phosphatidylinositol 4,5-biphosphate (PIP2) to phosphatidylinositol 3,4,5-triphosphate (PIP3). Subsequently this will recruit AKT through its pleckstrin homology domain to the membrane where AKT can be phosphorylated at Thr308 by 3-phosphoinositide–dependent protein kinase-1 (PDPK1) and at Ser473 by mTORC2/rapamycin-insensitive companion mTOR for full AKT activation (Sami & Karsy 2013). AKT activates mTOR that interconnects several upstream signals to effector actions on multiple downstream targets. These downstream targets play crucial roles in cellular proliferation, growth, and motility. This pathway is inhibited by the tumour suppressor protein PTEN (Mao H. et al. 2012; Zoncu et al. 2011). These RTKs also activate the downstream of the RAS signalling pathways by activating RAF1, MEK, and MAPK (Newton 2003).

Typically, from TCGA analysis of GBM, most of the genes encoding for RTKs, particularly *EGFR* and *PDGFR*, are either mutated or amplified, causing aberrant regulation of their signalling cascades. *EGFR* mutations in GBM cluster in the extracellular domain, including in-frame deletions of the 'variant III' (Furnari et al. 2007) and missense mutations (Lee J.C. et al. 2006). In lung cancer *EGFR* mutations localise in the intracellular kinase domain (Sharma S.V. et al. 2007). In GBM however, respond is different. The amplification of *EGFR* frequently overexpresses the receptor variant III commonly known as EGFRvIII (Gan et al. 2009; Sugawa et al. 1990) and characterised by a truncated extracellular domain with ligand-independent constitutive activity (Aldape et al. 2004; Frederick et al. 2000; Sugawa et

al. 1990; A. J. Wong et al. 1992) hinders the response towards EGFR inhibitors. Inhibitors namely erlotinib, gefitinib, and nimotuzumab have poorer GBM patients response compared with patients having lung cancer (Vivanco et al. 2012). In GBM, the amplification of *EGFR* frequently overexpresses the receptor variant III commonly known as EGFRvIII (Gan et al. 2009; Sugawa et al. 1990). This is characterised by a truncated extracellular domain with ligand-independent constitutive activity (Aldape et al. 2004; Frederick et al. 2000; Sugawa et al. 1990; A. J. Wong et al. 1992). Shinojima et al. (2003) determined that overexpression of EGFRvIII correlates with poor prognosis. In contrast, Montana et al (2011) found that EGFRvIII is associated with high survival rates in patients with GBM receiving surgery and radiotherapy or chemotherapy.

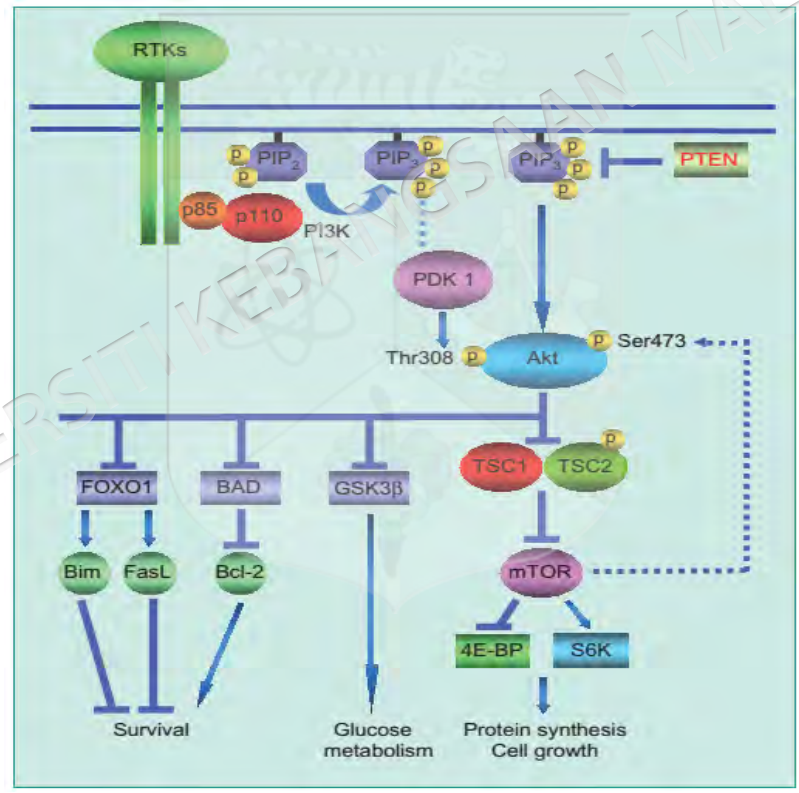

Figure 2.5 PI3K signalling pathway regulated by various effectors. PDK1 phosphorylates AKT and feedback loop involving the mTOR–Rictor complex causing activation of AKT and leading to the phosphorylation of many downstream substrates that critically control multiple cellular processes

(Source: Adapted from Cheng et al, 2009)

Activation downstream of RTK mostly by growth factors leads to activation of PI3K, a lipid kinase complex that stimulates the cellular proliferation, differentiation, metabolism, and survival processes. RTK alterations occur approximately in 70% of GBM cases either by amplification of RTKs (EGFR, VEGFR, or PDGFR) or deletion of the *PTEN* gene. A number of cancers show gain-of-function mutations in the PI3K catalytic gene *PIK3CA*, leading to constitutive kinase activity (Gymnopoulos et al. 2007). This lipid enzyme contains a 110-kDa catalytic subunit known as p110 and a p85 regulatory subunit complexed as a heterodimer. Class I PI3Ks are further subdivided into class IA and IB. In mammals, the class IA catalytic subunit consists of three isoforms: α, β, and σ. The p85 regulatory subunits are translated by three genes, namely *PIK3R1*, *PIK3R2*, and *PIK3R3*, which encode the p85α, p85β, and p55γ isoforms (Cheng et al. 2009). Essentially, p110β plays an important role in growth and metabolism, and p110γ and p110σ are crucial for controlling immunological functions. Uniquely, cancer cells have activated PI3K/AKT signalling and cells escape apoptosis by increasing their dependency on glucose metabolism via the PI3K/AKT/GSK downstream pathway and inhibiting BAX pro-apoptotic regulation in the presence of growth factor withdrawal (Rathmell et al. 2003).

Protein kinase B (PKB), commonly known as AKT, is a member of the serine/threonine kinase family and is conserved from primitive metazoans to humans (Chautard et al. 2014). Mammalian cells express three different isoforms, namely AKT1 or PKBα (62 kDa), AKT2 or PKBβ (56 kDa), and AKT3 or PKBγ (62 kDa), translated by genes located on chromosomes 14, 19, and 1 (Franke 2008). These isoforms are involved in cancer. AKT acts as a central node in the PI3K complex signalling cascade, with crosstalk and feedback loops influencing its governance. The N-terminal pleckstrin homology domain and C-terminal regulatory tail consist of a turn motif and hydrophobic motif as well as a hinge region connecting the pleckstrin homology domain to a kinase domain which are common structures that are shared by the AKT isoforms (Chautard et al. 2014; Franke 2008). These three isoforms are highly expressed and active in glioma cells especially in *PTEN*-null cells (Endersby et al. 2011). Active AKT phosphorylates multiple targets to mediate its effects on cellular function, including the Forkhead box class O (FOXO) factors, GSK3 isoforms, and tuberous sclerosis complex 2, as well as mTORC1 activity (Manning B.D. & Cantley 2007).

The mechanistic target of rapamycin (mTOR), which is commonly deregulated in many cancers in addition to GBM, is a critical effector of the AKT downstream pathways (Albert et al. 2009; Laplante & Sabatini 2012). The mTOR protein presents in two protein complexes, namely mTORC1 and mTORC2. MTORC1 is composed of Raptor (regulatory-associated protein of mTOR), mTOR, mammalian LST8/G protein β-subunit–like protein (GβL), DEPTOR (DEP domain containing mTOR-interacting protein), and PRAS40 (Hara et al. 2002). Meanwhile, mTORC2 is consists of the Rictor regulatory protein, mTOR, GβL, and mammalian stress–activated protein kinase interacting protein 1 (Sarbassov et al. 2004; Zoncu et al. 2011).

The activation of mTORC1 causes phosphorylation of the S6 kinases (S6K1 and S6K2) and eukaryotic initiation factor 4B that controls translation as well as programmed cell death 4 protein (PDCD4) (Dorrello et al. 2006; Jacinto et al. 2006; Volarević & Thomas 2001). It also phosphorylates the 4E binding proteins, which are a family of proteins involved in repressing the cap-dependent mRNA translation of cyclins, MYCN, Bcl-xL, S6, and PDCD4 (Benedetti & Graff 2004; Sonenberg, & Gingras 1998). The integration of various inputs including growth factors, energy status, oxygen, and amino acid levels to regulate cell growth by promoting the biosynthesis of proteins, lipids, and organelles as well as limiting catabolic autophagic activity are performed by this protein complex (Laplante & Sabatini 2012). Meanwhile, mTORC2 activation causes AKT, SGK1, and PKC phosphorylation, which are all involved in mediating cellular survival, proliferation, cytoskeletal organisation, and metabolism (Sami & Karsy 2013). Mutations upstream of mTORC1 and mTORC2, namely PI3K isoforms in cancer, lead to dysregulation of the mTOR pathway (Sarker et al. 2009). In GBM, hyperactivation of mTORC1 in mTOR signalling is common, which may develop in parallel with cells with *TP53* malfunction (Feng et al. 2005).

Phosphatase and tensin homologue (*PTEN*), located on chromosome 10, is a tumour suppressor gene, and *PTEN* mutations lead to the development of various cancers including GBM (Parsons et al. 2008; Salmena et al. 2008). *PTEN* regulates the PI3K/AKT pathway in a negative feedback manner by blocking AKT signalling by reducing intracellular levels of PIP3 (Franke 2008; Koul 2008). Hence, *PTEN* plays a critical role in regulating its downstream effectors including mTOR (Koul 2008).

Chromosome 10 LOH, which causes *PTEN* deletions or mutations, commonly occurs in GBM. Loss of *PTEN* expression by deletion, mutation, or methylation crucially mirrors activation of the AKT pathway due to the accumulation of PIP3, while retention of *PTEN* preserves the inactivation of AKT. There is conflict regarding the conclusion as to whether loss of *PTEN* is associated with poor prognosis. Carico et al. found that loss of *PTEN* was not correlated with poor overall survival in patients with newly diagnosed GBM who receive temozolomide (TMZ) treatment (Carico et al. 2012). McEllin et al. (2010) found that in *PTEN*-deficient glioma cell lines, the activation of repairs of DNA double-stranded breaks produced by TMZ adducts was not effective. Therefore, the loss of *PTEN* allows cells to undergo apoptosis without resistance to TMZ treatment.

The human rat sarcoma (*RAS*) gene is a transforming oncogene belonging to the G protein family that includes three highly related genes known as H-Ras, N-Ras, and K-Ras (Rajalingam et al. 2007). RAS encodes a monomeric G-protein that cycles between an active form bound to GTP and an inactive form that binds to GDP. The activation of RAS further activates RAF kinase by direct binding, which then regulates downstream signalling pathways including the MAPK pathway (Moodie et al. 1993; Steelman et al. 2011). The negative feedback mechanism of the RAS/MAPK pathway is controlled by the neurofibromatosis 1 protein encoded by the *NF1* gene that catalyses the exchange of GTP for GDP in RAS, consequently preventing cell proliferation (Cichowski et al. 2003). Inactivating mutations in *NF1* occurs in about 20% of GBM, causing *NF1* loss-of-function leading to increased cellular proliferation (Parsons et al. 2010; The Cancer Genome Atlas 2008). Defects in the RAS/MAPK pathway cause the dysregulation of cellular growth and the induction of other aberrant cellular processes such as invasion and evasion of apoptosis (Mao H. et al. 2012).

2.3.3 TP53 Signalling Pathway

TP53 is most well-known tumour suppressor and is commonly mutated in cancer. The TP53 pathway plays an important role in the development of secondary GBM compared with primary GBM (The Cancer Genome Atlas 2008). *TP53* mutations are the first detectable genetic alteration in 2/3 of low-grade diffuse astrocytoma precursor lesions

and the frequency is parallel to that in anaplastic astrocytomas and secondary glioblastomas. *TP53* mutations are present in primary glioblastomas, but at a lower frequency (30% of cases) (Ohgaki & Kleihues 2007). In secondary glioblastomas, 57% of *TP53* mutations have been reported to be located in the 2 hotspot codons 248 and 273; however, in primary glioblastomas, mutations are more equally distributed throughout all exons, with only 17% of mutations occurring at codons 248 and 273 (Ohgaki & Kleihues 2007; Brennan et al. 2009). The TP53 pathway reacts to DNA damage and various genotoxic and cytotoxic stresses by activating cell cycle arrest and apoptosis. Subsequently, after DNA damage, TP53 is activated and induces the transcription of genes such as *p21Waf1*/*Cip1* that function as regulators of cell cycle progression in the G1 phase. Synchronously, it is also an important transcription factor regulating more than 2,600 genes involved in cell development and invasion (Huang et al. 2007; Huse & Holland 2010).

Deactivation of *TP53* occurs by multiplication of the *MDM2* gene which subsequently activates the E3 ubiquitin ligase that targets TP53 for degradation, viral infection, deletion of the p14 *ARF* gene, and mislocalisation of TP53 into the cytoplasm (Vogelstein et al. 2000). The ARF/MDM2/MDM4/p53 pathway is disrupted in 78% of GBM cases, suggesting that this pathway is important in GBM tumours (The Cancer Genome Atlas 2008).

MDM2 is an E3 ubiquitin ligase that negatively regulates TP53 in two ways: first, via transcriptional inhibition through direct binding, and second by E3 ligase activity degradation (Itahana et al. 2007; Kubbutat et al. 1997). In all GBM, amplification of *MDM2* occurs in about 10% of cases but only in tumours without *TP53* mutation. This suggests that *MDM2* amplification may provide an alternative means for tumours to alter TP53-regulated growth control without having to alter *TP53* itself (Mao H. et al. 2012; Reifenberger et al. 1996). Another essential regulator of TP53 is *MDM4* or *MDMX*, found on 1q32 (Mu et al. 2003). MDM4 was originally discovered as a TP53-interacting protein through screening of a mouse embryo cDNA expression library (Shvarts et al. 1997) and is found to be overexpressed in glioma (Markus et al. 1999). Both *MDM2* and *MDM4* function as negative regulators of TP53 as shown in

Figure 2.6. However, they are also involved in TP53-independent activities, suggesting their important roles in tumorigenesis and tumour progression (Li & Lozano 2013).

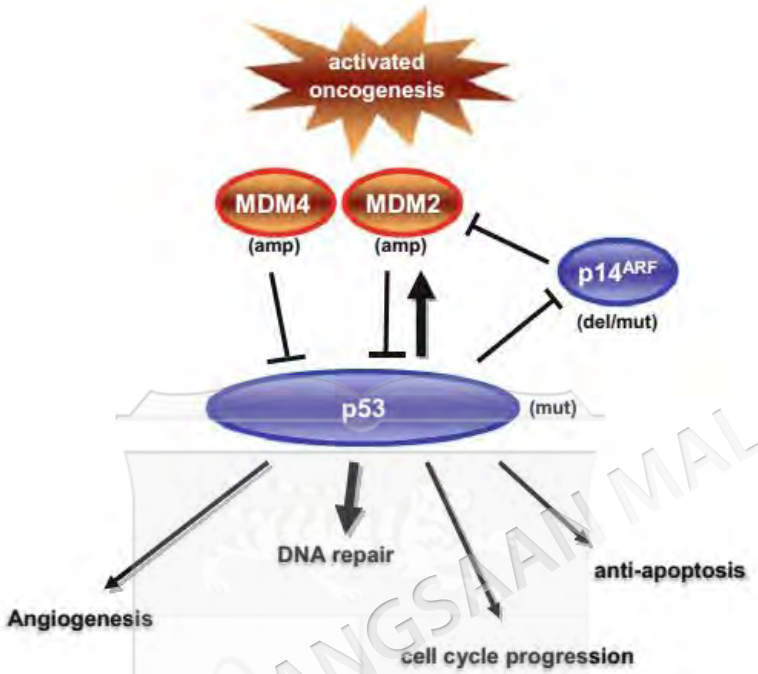

Figure 2.6 *MDM2* and *MDM4* are crucial negative regulators of TP53. In the normal state, p14ARF inhibits MDM2 activation of TP53. Activation of ATM and its downstream effectors CHK2 and TP53 occurs in the presence of DNA damage. In GBM, activating genetic alterations (red circles) and inactivating genetic alterations (blue circles) transform these genes to become oncogenic. Hence, the aberrantly expressed proteins will distort normal functional activities, promoting angiogenesis, DNA repair, cell cycle progression and anti-apoptosis.

(Source: Sedo, & Mentlein 2014)

Amongst the upstream regulators of the TP53 pathway is the tumour suppressor protein ARF (p14ARF) (Kamijo et al. 1998; H. Mao et al. 2012; Nakamura et al. 2001). TP53 transcriptional activities are regulated by ARF through direct binding to MDM2 leading to subsequent inhibition of its E3 ubiquitin ligase activity (Kamijo et al. 1998). In low-grade and high-grade gliomas, *ARF* inactivation or mutation is frequently reported (Nakamura et al. 2001). Both ARF and INK4a are encoded by the CDK2A locus (Solomon et al. 2008). They are critical regulators of the growth pathway in TP53 and RB1. Homozygous deletion of this locus (p16INK4a/p14ARF/p15INK4b) is amongst the commonly found mutations in GBM (Solomon et al. 2008). Co-deletion of

ARF and INK4a are found to be increased in parallel with tumour progression from low- to high-grade gliomas (Labuhn et al. 2001). This suggests that the locus containing ARF and INK4a is essential in GBM pathogenesis and that the deletion of this locus is fundamentally important (Solomon et al. 2008). Robertson et al. (2010) observed that the germline p16INK4A/p14ARF and TP53 mutations do not play a major role in familial glioma and are confined only in the context of Li-Fraumeni syndrome.

2.3.4 RB1 Signalling Pathway

The RB1 signalling pathway sends the anti-proliferative signals at the G1 phase of the cell cycle, signalling cells to enter into a transient quiescent (G0) state or into a post-mitotic, differentiated state. Typically, the RB protein is hyperphosphorylated in quiescent cells and blocks the E2F family of transcription factors. These alterations include mutations in *RB1*; amplifications of *CDK4*, *CDK6* (Costello et al. 1997), *CCND1*, or *CCND2*; and homozygous deletions of *CDKN2A*, *CDKN2B*, or *CDKN2C* (The Cancer Genome Atlas 2008). In normal cell cycle regulation, phosphorylation of RB1 occurs due to the activation of cyclin D1 and its associated cell cycle–dependent kinases CDK4 and CDK6 at G1–S transition. CDK4/6–cyclin D1 complex kinase activity is tightly regulated via complex signalling together with CDKNA, CDKN2B, and CDKN2C (Ng et al. 2012).

In GBM, 60–80% of RB1 pathway components are mutated, causing escape of anti-growth signals. It is noteworthy that from GWAS, single-nucleotide polymorphisms in *CDKN2A* and *CDKN2B* have been identified as the risk factors for glioma development (Shete et al. 2009; Wrensch et al. 2009). Hypermethylation-mediated silencing of the *RB1* promoter and *CDKN2A* has been frequently observed in secondary (43%) rather than primary GBM tissues (14%) (Wolter et al. 2001; Nakamura et al. 2012). As the RB1 pathway is inactivated by the kinase activity of the CDK4/CDK6/cyclin D1 complex, inhibition of CDK4/6 may be a novel chemotherapeutic treatment strategy in patietns with GBM with aberrantly expressed RB1. PD0332991 or palbociclib released by Pfizer appears to be an interesting drug for glioblastoma treatment and could be a valuable addition to the standard treatment of care. Raub et al. (2015) and Schröder & McDonald (2015) combined PD0332991, a

CDK4/6 inhibitor, with TMZ and reported significant efficacy. It was found that the pattern of RB1 pathway inhibition in patients with GBM with CDKN2A/CDKN2C co-deletion is similar to that of CDK4/6 inhibition in GBM (Wiedemeyer et al. 2010). Therefore, it is suggested that careful intervention of the inhibitor should be taken into consideration as a deficiency in RB1 may cause acquired CDK4/6 inhibitor resistance (James et al. 2014). Signalling mechanism of the RB1 pathway in regulation with the cell cycle are shown in Figure 2.7. The complete overview of integrated signalling pathways involved in GBM can be visualised via Figure 2.8.

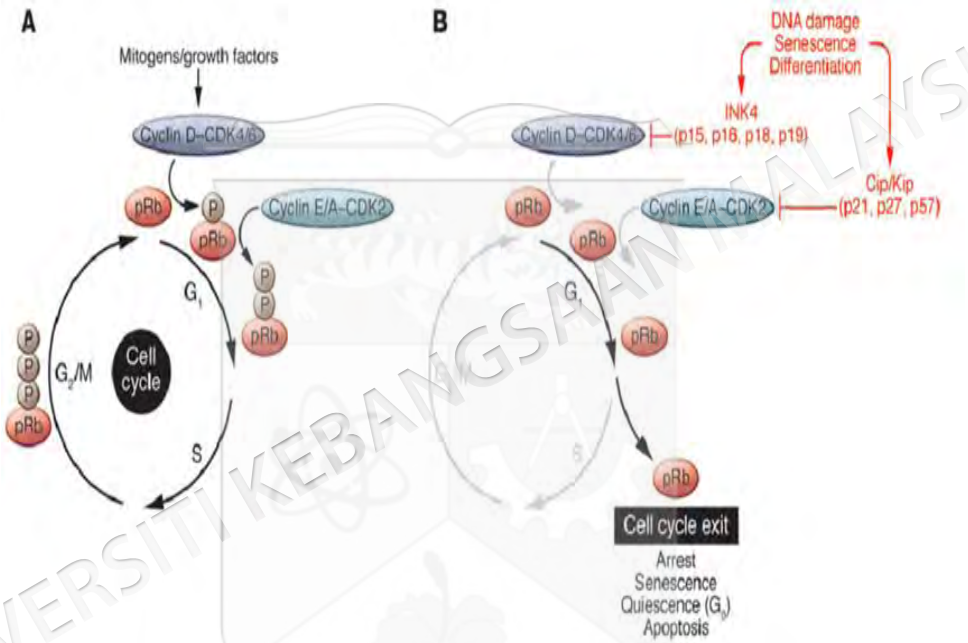

Figure 2.7 Signalling mechanism of the RB1 pathway in regulation with the cell cycle. (A) Cyclin D1–CDK4 complexes and later cyclin E–CDK2 complexes phosphorylate RB later in the G1 phase which will result in RB inactivation. Subsequently, this signals cells to proceed to the G1/S phase and DNA to undergo further replication in the S-phase. During G2/M, RB continues to be phosphorylated. When mitosis is complete, RB is dephosphorylated and becomes active again. (B) Anti-proliferative feedback mechanism of RB occurs when DNA damage, senescence, and differentiation are present, causing activation of CDK inhibitors such as INK4 and Cip/Kip family members, leading to the inhibition of the cyclin–CDK complexes. This signals RB to undergo G1 arrest as well as depart the cell cycle mechanism.

(Courtesy of Sachdeva et al, 2012)

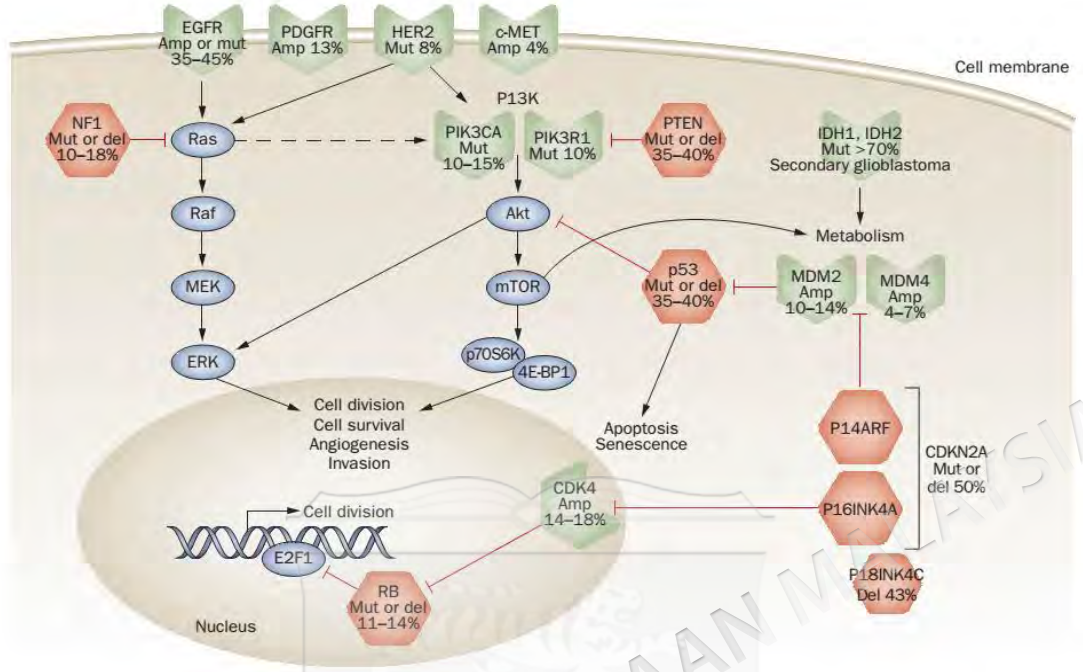

Figure 2.8 Complete overview of integrated signalling pathways involved in GBM.

(Source: Purow et al, 2009)

2.4 GBM TREATMENT MODALITIES

2.4.1 Surgery

Maximal resection of tumour by surgery is essential whenever possible to minimise tumour cell infiltration. Surgical debulking reduces the symptoms from the mass effect and provides tissue for histologic diagnosis and molecular studies. Visualisation of tumours includes MRI-guided neuronavigation, functional MRI, preoperative mapping, neuronavigation, and intraoperative MRI (Asthagiri et al. 2007). Fluorescence-guided surgery with 5-aminolevulinic acid for resection has improved the safety of surgery and has led to the improvement of progression-free survival (Stummer et al. 2006). Patients who undergo extensive surgical tumour removal may have a modest survival advantage. A significant survival advantage was associated with resection of 98% or more of the tumour volume, with a median survival of 13 months (95% confidence interval (CI)

11.4–14.6 months) as compared with 8.8 months (95% CI 7.4–10.2 months; p<0.0001) for resections of less than 98% (Lacroix et al. 2001). Stereotactic biopsies should be performed only in patients who have inoperable tumours that are located in critical areas (Wen et al, 2008).

2.4.2 Radiotherapy

Radiotherapy is an important component of GBM treatment. After standard radiotherapy, 90% of tumours recur at the original site. Waiting times before initiation of radiotherapy might not affect outcomes for patients with glioblastoma (Noel et al. 2012). Initially, surgical removal of radiation necrosis that may lead to secondary recurrence performed on patients that have received radiotherapy is advantageous. Unfortunately, Grossman et al. reported no significant impact on patient survival following resection of radiation necrosis in patients who developed true tumour recurrence (Grossman et al. 2016).

GBM in older patients, i.e. aged more than 70 years, is difficult to treat and such patients have worse prognosis compared to younger patients. Among such patients, radiotherapy confers a modest benefit with median survival of approximately 29.1 weeks as compared with supportive care, where median survival is 16.9 weeks (Keime-Guibert et al. 2007). Radiotherapy is not suitable for older patients as they cannot tolerate it well, hence a short course of radiotherapy or chemotherapy with the oral alkylating drug TMZ is considered advantageous (Glantz et al. 2003; Wen & Kesari 2008).

2.4.3 Chemotherapy

Alkylating agents such as procarbazine and dacarbazine are commonly used to treat GBM. Later, as part of a rationale drug development action plan in 1980, an imidazole derivative known as TMZ was developed and has become one of the most successful chemotherapeutic agents, achieving complete bioavailability after oral intake with good blood–brain barrier penetration (Newlands et al. 1997). TMZ was approved by the US FDA in 1999 for use in recurrent anaplastic astrocytoma based on its impressive patient

free survival of 46% in a phase II randomised clinical trial comparing oral procarbazine and TMZ (Wong E.T. et al. 1999). This prodrug undergoes spontaneous hydrolysis and is converted to the active metabolite 5-(3-methyl)-1-triazen-1-yl-imidazole-4-carboxamide (MTIC) in the bloodstream at physiological pH. Subsequently, MTIC is degraded to the methyldiazonium cation, which transfers the methyl group to DNA, and the final degradation product, 5-aminoimidazole-4-carboxamide (AIC), which is excreted via the kidneys (Baker et al. 1999; Newlands et al. 1997).

The conversion of TMZ to MTIC results in the formation of a reactive DNA-methylating agent with an affinity for transferring methyl to 3 sites of the DNA sequence nucleotides: N7-guanine, N3-adenine, and O6-guanine. The cytotoxic action of TMZ occurs via the O6-methylguanine (O6-MG) DNA adducts although the amount of the DNA lesion present is only 5%. These DNA lesions are sensed by the DNA mismatch repair (MMR) pathway which later promotes the DNA double-strand breaks and subsequently lead to cell death via apoptosis and/or autophagy (Kanzawa et al. 2003; Villano et al. 2009; Ziegler et al. 2008).

Resistance towards TMZ occurs when the O6-MG–DNA methyltransferase (MGMT) enzyme repairs the cytotoxic lesion by removing the O6-alkylguanine DNA adduct. Mechanistically, it occurs by covalent transfer of the alkyl group to the conserved active site cysteine and restores the guanine to normal, restoring the repair system in the DNA. Subsequently, MGMT receives the methyl group from O6-MG, leading to its inactivation and later to ubiquitin-mediated degradation (Garcia 2009). However, the reduction of MGMT by promoter hypermethylation or O6-MG or ineffective dosing schedules will result in increased TMZ cytotoxic effects. Recovery of MGMT is fast, i.e. a few hours by *de novo* synthesis, in human malignant brain tumours and peripheral blood cells (Soniya Sharma et al. 2009; Tolcher et al. 2003). Therefore, MGMT methylation predicts the clinical response of primary gliomas to first-line chemotherapy with the alkylating agent TMZ (Paz et al. 2004) and using MGMT inhibitors may enhance the cytotoxic effects of TMZ on tumour cells (Pegg 2000; Ramirez et al. 2013). By performing gene expression analysis, the response of patients towards TMZ treatment can be predicted (Yachi et al. 2008).

Additionally, the presence of DNA adducts produced by TMZ activity activates the TP53-dependent DNA damage pathway and suppresses MGMT activity post-TMZ exposure. Tumours harbouring wild-type *TP53* are TMZ-sensitive compared with tumours with mutant *TP53* (Blough et al. 2011; Martin et al. 2012). Therefore, the characterisation of *MGMT* expression and *TP53* status in GBM might assist in stratifying patients who will respond well or not to TMZ treatment (Hermisson et al. 2006).

Although they comprise 80% of the total methylation process, N7-methylguanine and N3-methyladenine are usually repaired by the base excision repair pathway and are generally not cytotoxic (Newlands et al. 1997). Generally, PARP inhibitors may halt the BER pathway, hence increasing the number of TMZ cytotoxic adducts (Villano et al. 2009). Mechanism of TMZ action for inducing tumour cell death is shown in Figure 2.9.

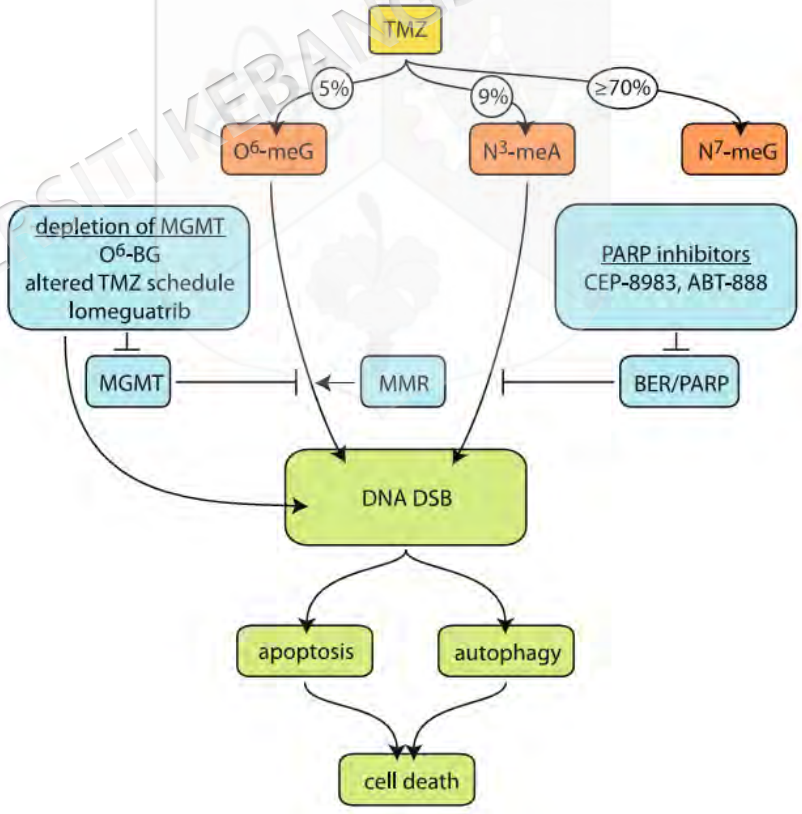

Figure 2.9 Mechanism of TMZ action for inducing tumour cell death.

(Adapted from Villano et al. 2009)

2.5 KEY PROBLEMS WITH GBM TREATMENT

2.5.1 Highly Proliferative and Invasive Cells

Unlike other solid tumours, GBM cells rarely metastasise outside the brain but are highly invasive within the perivascular or intracranial structure. Importantly, these cells do not depend on intravascular or lymphatic metastases to spread. They actively migrate throughout the tortuous extracellular spaces of the brain, subsequently forming distant satellite tumours (Lun et al. 2011). This phenomenon resembles normal brain cells during embryonic development, or adult stem cells in the mature brain, which both similarly migrate along extracellular routes, exploiting the brain vasculature, or after injury, the nerve bundle guides (Cuddapah et al. 2014).

Hatzikirou and colleagues (2005) initially proposed a unique principle that is involved in GBM progression called the 'Go–Grow' principle. Using a simple growth model and mathematical modelling, they demonstrated that only a short period of time is needed for relapse to occur subsequent to total removal of the tumour bulk. This indeed presented the premise that the mechanism of GBM progression cannot be based completely on a mutation-based concept. They proposed that the switch from the proliferative to invasive tumour phenotype can be explained based on the microscopic 'Go or Grow' mechanism or migration, alternatively presenting a different process of proliferation and migration in which oxygen deprivation status is the key factor (Hatzikirou et al. 2012; Hatzikirou et al. 2005).

The 'Go–Grow' principle as shown in Figure 2.10 suggests that GBM progression depends on two critical aspects: 1) rate of cell proliferation and 2) cell migration speed. Theoretically, proliferation and invasion are not permanent and both are mutually exclusive phenotypes. In this case, tumour cells that are highly invasive have lower proliferative speed. However, cells that are highly proliferative are less invasive. At macroscopic level, cell–cell interactions and microenvironmental factors are both essential for regulating the switching of the phenotypes. Meanwhile, chemotherapy, hypoxia, and ionising radiations can force tumour cells such as glioma stem cells into a 'go' phenotype (Hatzikirou et al. 2012; Huber et al. 2013; Stock &

Schwab 2009). However, tumour microenvironment factors such as angiogenesis, tumour extracellular matrix (ECM), and anaerobic glycolysis are responsible for boosting tumour cell repopulation and recurrent tumour development. This dynamic phenotypic change between the proliferative and invasive condition of single tumour cells determines the overall phenotype of tumour growth (Hatzikirou et al. 2012; Xie et al. 2014).

GBM tumour cells present two distinct features: highly invasive and highly proliferative and both are mutually exclusive by nature (Hatzikirou et al. 2012; Hatzikirou et al. 2005). Commonly, GBM tumours present with a bulky, proliferative, angiogenic tumour core, but they are also comprised of highly invasive penetrating tumour cells towards the normal brain parenchyma surroundings (Bonavia et al. 2011; Furnari et al. 2007). This condition becomes an infiltrative border and its removal by surgical resection is difficult, contributing to inadequate tumour removal and imminent tumour relapse mostly along the margins of the tumour incision (Huse & Holland 2010). Post–surgical removal, these invasive GBM cells residues adopt or change to a proliferative phenotype, but develop into a local recurrent tumour which is more aggressive. The programme switching between proliferation and invasion indicates tumour progression. The dynamicity and plasticity of the action of GBM cells by adapting with their surrounding environment leads to difficulty in providing accurate treatment for GBM (Xie et al. 2014).

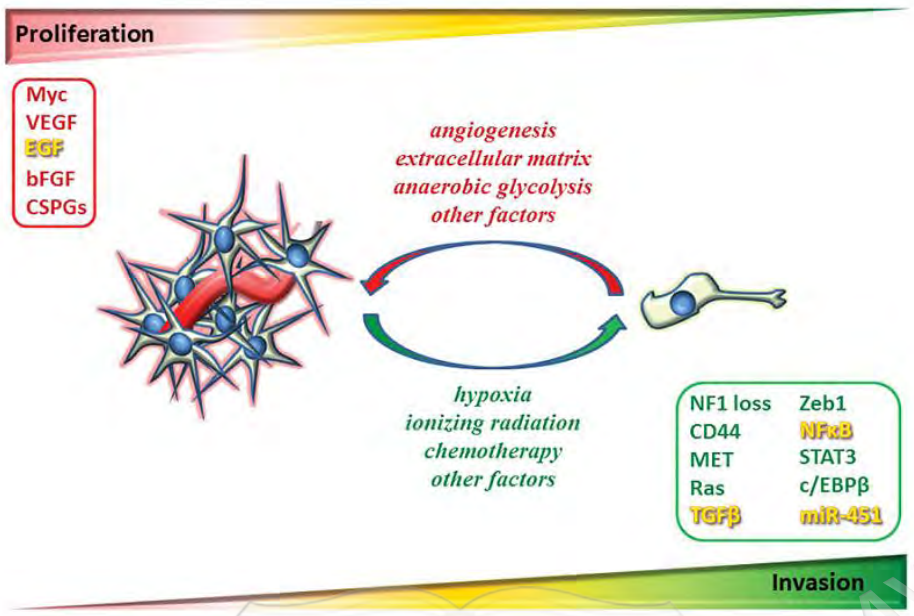

Figure 2.10 The 'Go–Grow' principle states that cell proliferation and invasion are two phenotypes that are mutually exclusive and are controlled by different genes and effectors. The switching of tumour phenotypes depends on tumour surroundings

(Source: Xie at al. 2014)

2.5.2 Glioma Stem Cells

Glioma stem cells (GSC) are glioma cells with stem-cell like features and are postulated to be the major factor in GBM progression and resistance (Bao S. et al. 2006; Sampetrean & Saya 2013). GSC have the capability to self-renew without limit and have the ability to produce heterogeneous offspring that in the end transform into tumour bulk (Dietrich et al. 2008; Sampetrean & Saya 2013). Only a small number of GSC is needed to commence and initiate local relapse. However, GSC do not need to be the initial tumour origin. They originate from a protected area with a unique environment known as a stem cell niche that is confined to the perivascular space and is oxygen-deprived conditions (Ignatova et al. 2002; Pointer et al. 2014; Thomas et al. 2014). This perivascular location is the perfect site for tumour cell interactions with the surrounding pericytes and endothelial cells together with tissue-specific components as a conservation process of the GSC population (Brooks et al. 2013).

Several markers of GSC have been proposed, including the hematopoietic stem cell marker CD133, and A2B5, a marker of glial progenitor cells, although no single

marker appears to correlate with the presence of GSC (Ogden et al. 2008). A carbohydrate adhesion molecule associated with glycoproteins and glycolipids whereby its expression is associated with neural stem cells, namely stage-specific embryonic antigen 1 (SSEA-1), was also suggested as a GSC marker (Germano, & Binello 2014; Mao X.G. et al. 2009). Phenotypically, GSC are capable of generating spheres in suspension, termed neurospheres (Ignatova et al. 2002).

GSC may become quiescent and enter the cell cycle only when the tumour mass decreases or signals the stem cells to proliferate (Yamada et al. 2011). Many signalling pathways are involved in the regulation of GSC-controlling embryonic pathways, such as the Notch, Hedgehog, and Wnt/β-catenin signalling pathways and hence have emerged as an attractive therapeutic approach (Germano & Binello 2014; Pointer et al. 2014). An example is targeting the Notch pathway, which can be accomplished by γ-secretase inhibitors, for example RO4929097. However, an unfavourable pharmacokinetic profile has been reported, halting the development of RO4929097 (Thomas et al. 2014). Figure 2.11 simplifies GSC characteristics and their targeting strategy.

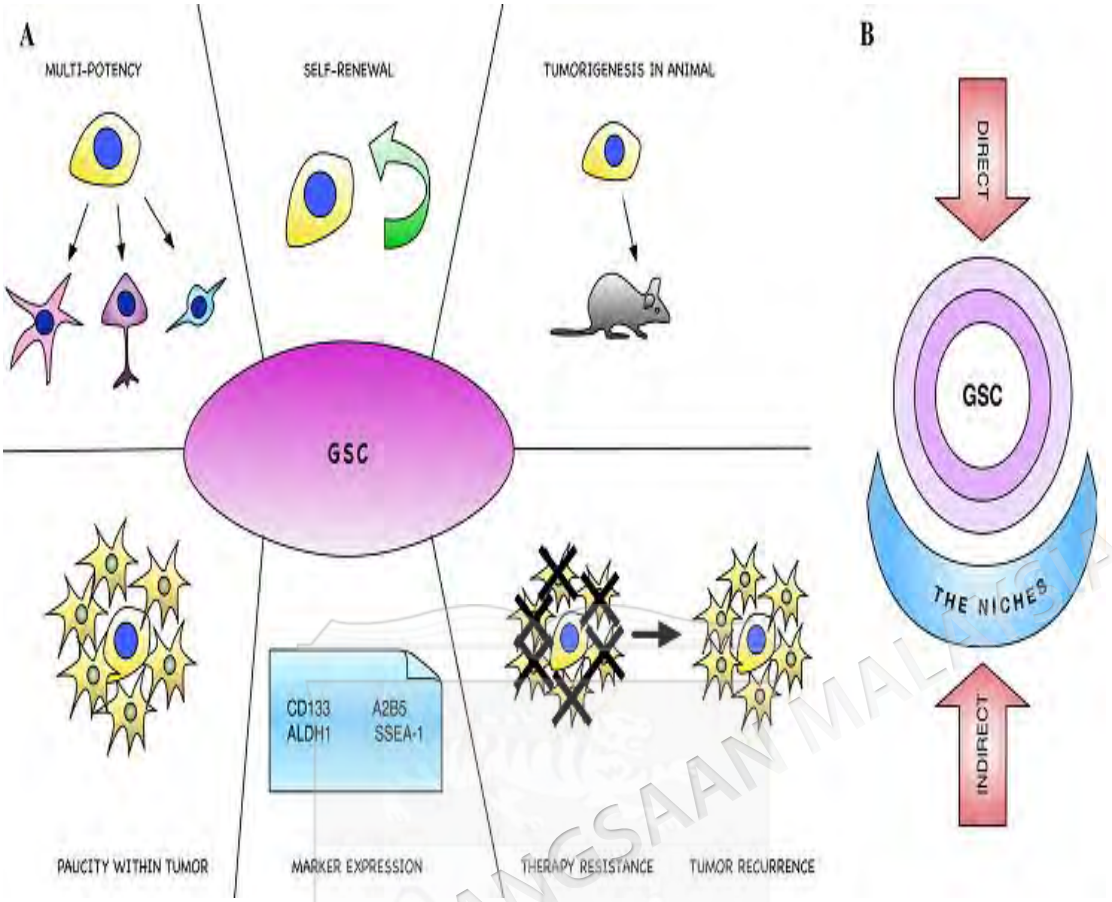

Figure 2.11 GSC characteristics and their targeting strategy. (A) GSC have fundamental properties of cancer stem cells, such as multipotency, self-renewal, and tumorigenesis. They also represent only a fraction of the tumour cell population, which may be characterised by certain markers, and are the major factor in causing resistance to conventional therapy. (B) Targeting GSC may be accomplished via direct and indirect strategies. The direct therapeutic strategies for overcoming GSC resistance to standard therapy (namely radiation and TMZ) can be achieved by blocking GSC function and inducing GSC differentiation. The indirect therapeutic strategies target the GSC niche or the microenvironment, namely the perivascular, hypoxic, and immune niches

(Source: Germano & Binello 2014)

2.5.3 Crosstalk between Tumour Cells and the Microenvironment

The GBM tumour microenvironments where GBM tumour cells develop and grow display heterogeneous phenotypes. The complex surroundings of the glioma microenvironment are composed of various components of non-neoplastic stromal cells, including the vasculature, various infiltrating and resident immune cells, as well as other glial cells (microglia, satellite cells, Schwann cells, and oligodendroglia). It is

also unique as it is encapsulated into anatomically distinct regions, referred to as tumour niches that in addition to tumour cells also foster GSC (Hambardzumyan & Bergers 2015). These niches do not merely harbour GSC but act as signalling or communication centres in which tumour cells and host cell populations dynamically interact through direct cellular contact or paracrine signalling to establish maintenance, growth, and protection of tumour cells and GSC from immune surveillance and therapeutic threats (Hambardzumyan & Bergers 2015; Hoelzinger et al. 2007).

The perivascular niche is an essential compartment wherein neural stem cells and GSC reside. The brain vasculature is an integral component of the major stem cell niches in the brain, specifically in the subventricular zone and subgranular zone, with a critical function of supporting stem cell proliferation and regeneration (Shen et al. 2008; Tavazoie et al. 2008). In GBM, considerable elevation of VEGF activity triggers robust and abnormal angiogenesis leading to disorganised and leaky blood vessels (Shideng Bao et al. 2006). This is in concert with other angiogenic factors such as FGF and PDGF, which are largely produced by tumour cells. This has severe consequences because they can cause disruption of the blood–brain barrier (Shideng Bao et al. 2006; Calabrese et al. 2007; Yancopoulos et al. 2000).

The irregular vascular phenotype and functions cause sluggish blood flow and irreconcilable oxygen delivery within the tumour. Due to this, it will lead to the development of local hypoxic regions, forming pseudopalisading necrosis (Hambardzumyan & Bergers 2015). The factors contributing to pseudopalisading necrosis in addition to obstructive vessels and collapse include vaso-occlusion from angiopoietin-2–mediated endothelial cell apoptosis, vascular regression, and intravascular thrombosis due to the activation of pro-coagulation factors (Brat et al. 2004; Hambardzumyan & Bergers 2015; Yancopoulos et al. 2000).

Exclusive paracrine interaction between astrocytes and glioma cells has been observed from co-culture experiments, demonstrating that astrocytes can enhance proliferation and matrix metalloprotease-2 (MMP-2)-dependent invasion of glioma cells *in vitro* (Gagliano et al. 2009). Reactive astrocytes in GBM also produce the connective tissue growth factor known as CTGF that binds to tyrosine kinase receptor

type A (TRKA) and integrin β1, forming the integrin β1–TRKA cell surface receptor complex which leads to NF-κB activation, induction of the transcriptional repressor ZEB-1, disruption of cell–cell contacts through loss of E-cadherin, and finally, glioma cell and GSC infiltration (Edwards et al. 2011).

2.5.4 Complex Tumour ECM Relationship Leading to GBM Invasion

The ECM is composed of a large collection of biochemically distinct components including proteins, glycoproteins, proteoglycans, and polysaccharides with different physical and biochemical properties (Whittaker et al. 2006). The dynamic functions of the ECM depend on its diversified biomechanical, biochemical, and physical features. Anchorage to the basement membrane is important for biological functions such as asymmetric cell division in stem cell biology and regulation of tissue polarity, cell proliferation, differentiation, motility, and tissue organisation, hence ECM dynamics deregulation is another hallmark of cancer (Hynes 2002; Lu et al. 2012). The interaction of the ECM with cells is largely controlled by cell–integrin receptor interaction. Together with ECM-degrading proteases, the integrin family members are commonly known to orchestrate GBM cell invasion. These heterodimeric transmembrane adhesion receptors link the ECM bidirectionally along with the networks of intracellular signalling (Hynes 2002; Vehlow & Cordes 2013). Integrins are comprised of 18 α-subunits and eight β-subunits that pair to form at least 24 different functional heterodimeric receptors that each bind to one or more ECM ligands. This specificity obliges integrin–ligand binding events to enforce distinct niches or boundaries, so that cells expressing only certain integrin heterodimers can pass within an ECM containing specific components such as laminin, collagen, vitronectin, or fibronectin (Hynes 2002; Seguin et al. 2015).

In parallel with the overexpression of promigratory ECM proteins, increased expression of specific integrin receptors has been identified in GBM tumour samples. Therefore, this stresses the importance of integrins throughout GBM development. The expression of several integrin subunits such as β1, β3, β4, or β8 in combination with α2, α3, α5, or αv is significantly increased in GBM tumours compared to the normal brain cells or in cell lines derived from GBM tumours (Paulus & Tonn 1995;

Riemenschneider M.J. et al. 2005; Rooprai et al. 1999). GBM cells and blood vessels in GBM tumours express high levels of integrins αvβ3 and αvβ5, which serve as adhesive receptors throughout GBM neoplasms and their periphery (Gingras et al. 1995; Schnell et al. 2008). Therefore, this indeed suggests a strong relationship with integrins, as GBM tumour grade histology correlates positively with their expression (Gingras et al. 1995; Schnell et al. 2008; Vehlow & Cordes 2013).

During the invasion process, GBM tumours secrete ECM-degrading membrane protease enzymes. One of the well-studied proteases is MMP-9. The interaction of integrin and tumour cells leads to the increased expression of MMP-9 together with urokinase-type plasminogen activator (uPAR) (Rao 2003). In addition, MMP-9 acts as a processing enzyme for CD44 cleavage. CD44 is a single-chain transmembrane glycoprotein that is widely expressed in physiological and pathological conditions. CD44 is implicated in cell–cell and cell–matrix adhesion, migration, and signalling and its expression is prominent in GBM tissue samples (Chetty et al. 2012; Veeravalli & Rao 2012). The downstream mechanism that occurs amid integrin receptor interaction is the activation of key signalling elements that mediate receptor-initiated signalling in the regulation of GBM invasion, namely the Rho family GTPases, including RAC, RHOA, and CDC42. These GTPases regulate cell morphology and actin dynamics and stimulate cell squeezing through the narrow extracellular spaces that are typical of the brain parenchyma (Burridge & Wennerberg 2004; Ellert-miklaszewska et al. 2013). GBM motility is a dynamic process and the cellular movement can change based on the interaction with the environment switch (Figure 2.12).

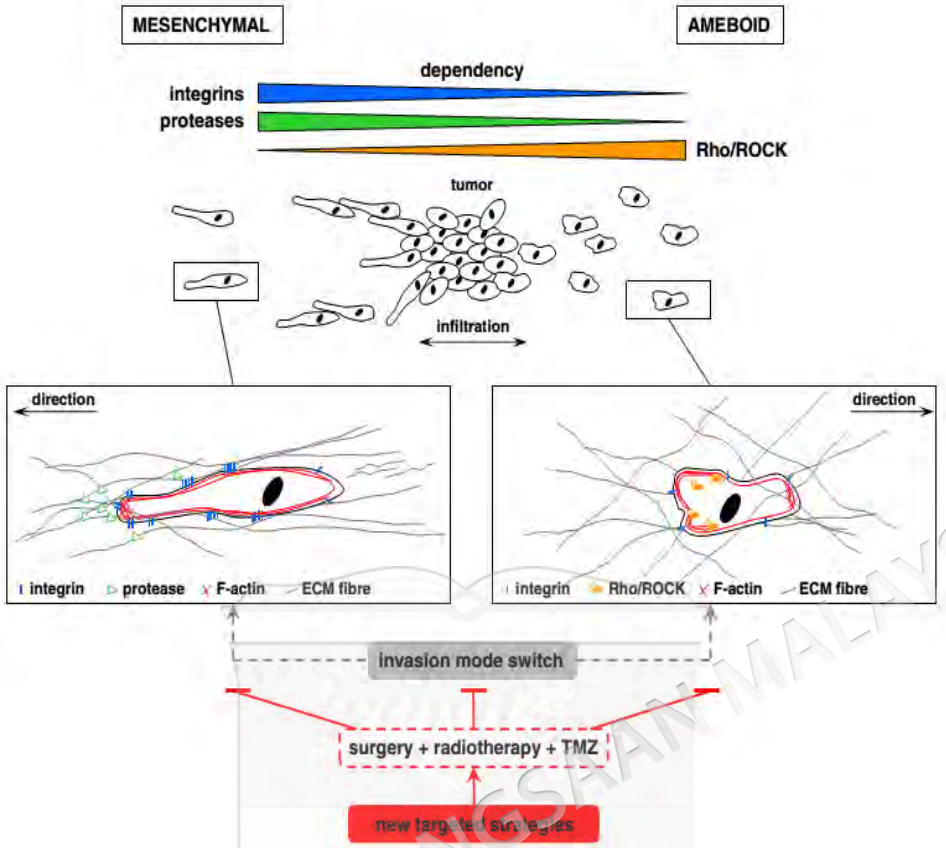

Figure 2.12 GBM motility is a dynamic process and the cellular movement can change based on the interaction with the environment switch. Commonly, mesenchymal invasion is activated in the presence of the upregulation of integrins and proteases. However, GBM cells can evolve when integrins and proteases are inhibited by specific drugs such as cilengitide. The activation of the alternative Rho/ROCK signalling pathway will be activated in this case, or activation of the integrin-independent invasion mechanism. This process is called amoeboid invasion whereby cells squeeze through the ECM meshwork utilising actomyosin contractility. Therefore, the switching of invasion mode will lead to therapeutic resistance

(Source: Vehlow & Cordes 2013).

2.5.5 Failure of Current Kinase Inhibitors Due to Activation of Rescue Signalling Pathways

The advancement in technology has provided routes for fast, efficient, and practical characterisation of molecular genetic tumour signatures. Indeed, the characterisation of specific tumour signatures can be tailored to personalised and precision medicine. Impressive high-throughput platforms have been developed, enabling the selection of specific treatment interventions for patients. Hindering the process however, is that the

tumour might undergo molecular changes or evolution during the same period. At the same time, monitoring treatment response will need frequent analysis of biopsy tissue before the appropriate treatment is selected (Tanaka et al. 2012). Many obstacles prevent the success of the current kinase inhibitors which target specific 'driver' kinases and its associated pathways during disease progression.

PI3K and mTOR are an important signalling node convergence points between multiple growth factor receptors and nutrient pathways and serve as an alternative strategy to block deregulated growth factor signalling in cancer (Nichol & Mellinghoff 2015). However, the current developed inhibitors fail to yield much benefit due to the complexity of aberrant kinase structure and function as well the ability of cellular evolution to occur (Logue & Morrison 2012). Failure of the downstream inhibition of P13K, namely that of mTOR, by rapamycin and its analogue inhibitors, or rapalogs, i.e. temsirolimus, everolimus, and ridaforolimus, occurs because it allosterically inhibits mTORC1-mediated S6K activation but does not inhibit mTORC2. Inhibition of the negative feedback loop between mTORC1 and the upstream pathway members and treatment with rapalogs can also cause complicated activation of the PI3K/AKT pathway. The promotion of cell survival occurs when an mTOR inhibitor fails to reduce phosphorylation of the oncogenic eukaryotic translation initiation factor 4E-BP1, a component downstream of the mTOR signalling pathways (Jhanwar-Uniyal et al. 2015).

The induction of AKT activation by rapamycin occurs through the loss of negative feedback, causing treatment resistance (Thoreen et al. 2009). PI3K hyperactivity and its downstream factors may result in increased signalling pathway activity, leading to many protumorigenic activations such as migration, self-renewal, growth, cell cycle, and proliferation. The activation of AKT by convergent pathways through the autocrine secretion of IGF-1 warrants multiple targeted therapies for the PI3K/AKT/mTOR signalling pathway (Westhoff et al. 2014; Willems et al. 2012).

The multicentre phase II clinical trial of PX-866, which is a pan-PI3K isoform inhibitor, also failed to identify a statistically significant association between clinical outcome and relevant molecular characteristics in patients with GBM. The study

however was well-designed whereby the investigators attempted to associate disease stabilisation with mutations that were hypothesised to aberrantly activate the PI3K pathway and precipitated the condition of pathway dependence. For example, loss-of-function mutations or deletions in *PTEN*, gain-of-function mutations in genes encoding the catalytic and regulatory subunit of PI3K namely *PIK3CA* and *PIK3R1*, and the oncogenic EGFRvIII mutant (Nichol & Mellinghoff 2015; Pitz et al. 2015), which have not been investigated by any clinical trials so far. This suggests that PX-866 may not effectively block PI3K signalling participants or that alternative pathways have been activated (Pitz et al. 2015).

EGFR has been consistently detected in the nuclei of cancer cells from primary tumour specimens and highly proliferative tissues. Four primary EGFR inhibitors, namely gefitinib, cetuximab, erlotinib, and panitumumab, have revealed negative feedback. Although these drugs received US FDA approval in less than 4 years to cure cancer from 2003 until 2006, the results show that intrinsic and acquired resistance to EGFR inhibitors hinders the eradication of GBM and that the inhibitors are not as successful in treating GBM as they are in eradicating lung cancer (Wheeler et al. 2010). Amongst the earliest studies that discovered the different effects of EGFR inhibitors between lung and brain cancer was that by Vivanco and colleagues. They indicated that therapeutic failure in GBM, particularly erlotinib, is due to the different conformational requirements of mutant *EGFR*, which may participate in the insufficient levels of EGFR inhibition (Vivanco et al. 2012).

Patients with GBM also have the propensity to display better response to treatment due to the mutated EGFRvIII or the amplified *EGFR* together with preserved *PTEN* function (Fan & Weiss 2010; Mellinghoff et al. 2005). Unfortunately, many variable results are seen in clinical trials. Interestingly, the mechanisms through which the EGFR-driven signalling network contributes to adaptation and treatment resistance warrant wider characterisation beyond the traditional ‘linear pathway’ but must be examined from the superior view as integrative interaction networks.

Another important aspect of acquired resistance is that GBM tumours coexpress both wild-type *EGFR* and the mutant *EGFRvIII* (Heimberger et al. 2005; Verhaak et al.

2010). The truncation of EGFRvIII resulting from an in-frame deletion of the coding sequence on exon 2–7 may lead to loss of the extracellular domain, thus preventing its ligand binding potential from function properly (Ekstrand et al. 1992; Wong A.J. et al. 1992). Apart from that, constitutive activation of *EGFRvIII* is reported because of reduction in ubiquitin-induced receptor degradation due to reduced interaction with the E3 ligase Cbl (Frederick et al. 2000; Wong A.J et al. 1987 and 1992).

Defects in the EGFR-driven signalling network result in hypo- or hyperactivation of multiple downstream pathways; such pathway cross-talk between the EGFR-driven signalling network and other RTK pathways will result in a robust mechanism for treatment resistance. This observation is based on the coactivation of the c-MET proto-oncogene and EGFR-induced signalling. When tumour cells are treated with EGFR inhibitors, c-MET maintains PI3K signalling and cellular survival by recruiting the GAB1–PI3K complex that is commonly associated with EGFR signalling (Stommel et al. 2007). This proposes the premise that the switching of oncogenic signalling is based on the existence of 'dominant' and 'secondary' RTK pathway activation (Xu & Huang 2010).

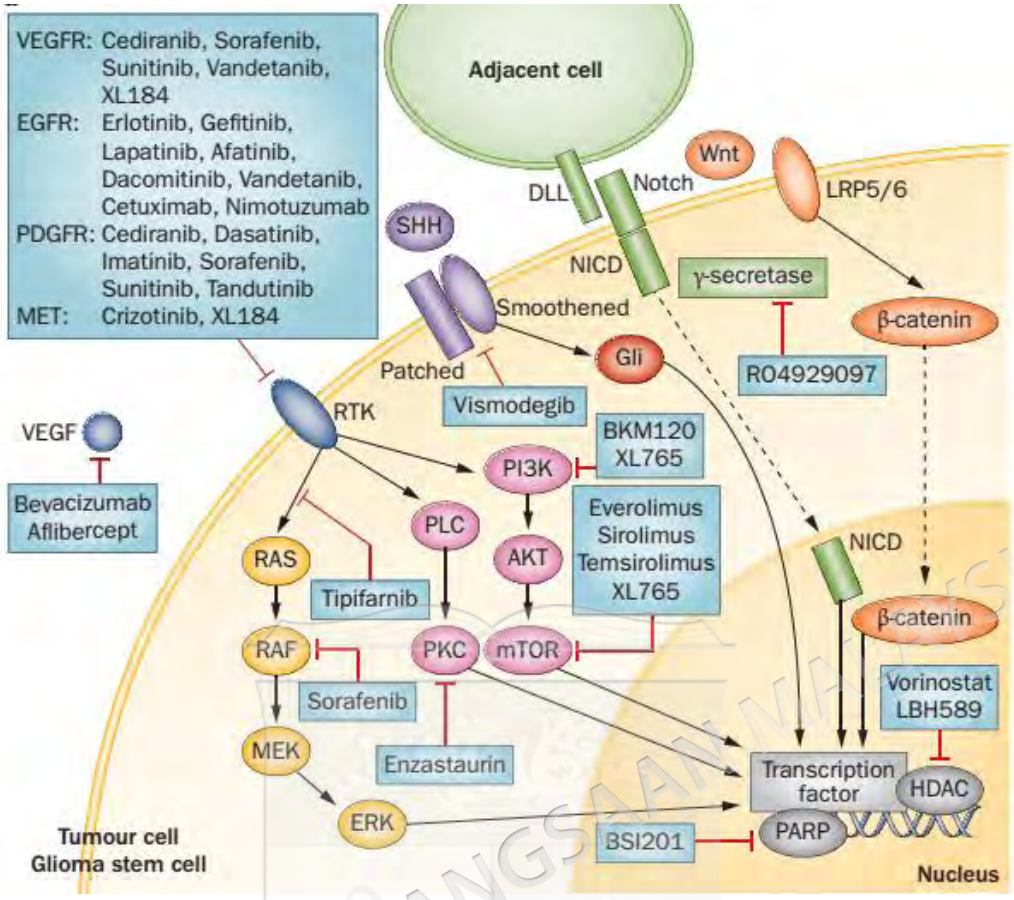

Figure 2.13 Novel molecular inhibitors developed to target GBM tumour cells and GSC signalling pathways.

(Source by: Tanaka et al. 2012)

2.6 NOVEL DRUGGABLE SIGNALLING PATHWAYS IN GBM

The concept of targeted therapy depends on the continued activity of specific activated or overexpressed oncogenes to maintain their malignant phenotype (Weinstein & Joe 2008). This is essential for *in vivo* and *in vitro* studies whereby knockdown expression experiments will aid in the validation of the hypothesis. In this study, we aimed to investigate at the less-established roles of kinases in signalling to prevent bias in identifying novel kinome targets. According to Fedorov et al., approximately 50% of kinases are not well characterised in terms of function and impact on the major signalling pathways. To overcome this, some of these kinases have been analysed using specificity screening platforms (Fedorov et al. 2010).

The characterisation of kinases as targets that are selective for tumour cell progression within the complex signalling networks and diverse mutational landscape might be successful when using the unbiased RNAi platform. This is also added to the data generated by genomic approaches such as large-scale deep sequencing, comparative genomic hybridisation, and microarray expression analysis. RNAi provides large-scale tools to suppress the expressed genes and allows functional analysis of gene suppression on specific cellular processes such as response to drugs. RNAi-based genetic screens allow the unbiased characterisation of essential genes that modulate drug responses. Therefore, the understanding of candidate genes that regulate GBM progression can also be explored (Berns & Bernards 2012; Thaker et al. 2009). Previous RNAi screening data have revealed that the dependence of cancer cell lines on specific kinases is highly diverse and have identified a large number of largely uncharacterised protein kinases essential for the proliferation and survival of cancer cell lines (Fedorov et al. 2010; Grueneberg et al. 2008; Manning B.D. 2009). As the concept of oncogene addiction is compelling for designing therapeutic strategies to treat cancer, the unbiased kinome-specific and genome-wide RNAi screens are revealing unexploited areas of potential therapeutic intervention (Manning B.D. 2009).

With the advancement of the functional genomics approach, the identification of novel and effective targets for GBM therapeutic intervention has rapidly increased significantly and at the same time has enabled rapid drug development in the clinical setting. Shahryar *et al*. analysed the kinase gene expression profiles of various tumour types on publicly available microarray data and revealed that the cell cycle kinases such as WEE1, TTK, CDC2, BUB1, and AURKA kinase are overexpressed in GBM. Functional validation showed that the WEE1 G2 checkpoint kinase is a major regulator of the G2 checkpoint in GBM cells. Inhibition of WEE1 by siRNA or small molecular compounds in cells exposed to DNA damaging agents such as TMZ resulted in abrogation of G2 arrest, inhibition of the DNA repair mechanism, and apoptosis. The results from *in vivo* experiments support the *in vitro* findings in which WEE1 knockdown sensitised GBM tumours to radiotherapy and therapeutic agents (Mir et al. 2010). Indeed, WEE1 is currently progressing to clinical trials (Do et al. 2013).

Integrative analysis from various aspects has also proven that the PI3K/PTEN/AKT pathway is essential as the centre for multiple regulators of cell migration. Seo et al. (2104) identified 91 cell migration–regulating genes via unbiased genome-wide functional shRNA and cDNA screen. Their network analysis suggested that cell migration determinants are highly dependent on the PI3K/PTEN/AKT pathway and on their downstream factors, namely FOXO1 and p70S6K1. Downstream validation identified ALK or RTK ALK, which was initially characterised as an oncogene in human anaplastic large cell lymphoma and neuroblastoma as one of the cell migration–promoting genes. It specifically utilises the p55γ regulatory subunit of PI3K to activate the PI3K/AKT pathway rather than the more common p85 subunit (Polgar et al. 2005; Roskoski 2013; Seo et al. 2014). This suggests that multiple inhibition of PI3K is needed to prevent rescue pathway activation (Palmer et al. 2009; Wasik et al. 2009).

Reed and colleagues performed an elegant study using a unique *Drosophila* glioblastoma model and kinome-wide genetic screen to identify new genes required for RTK- and PI3K-dependent neoplastic transformation. Interestingly, the atypical kinases RIOK1 and RIOK2 are overexpressed in GBM cells in an AKT-dependent manner and are involved with the downstream of PI3K mTORC2 components. *In vitro* validation in human GBM cells proved that RIOK1 and RIOK2 overexpression appeared to be correlated with RTK mutation/overexpression and/or *PTEN* loss in GBM tumour cells (Read et al. 2013), suggesting that the genetic heterogeneity in GBM results in different forms of neoplastic activation. As tumour heterogeneity remains the major obstacle in treating GBM, we were motivated to unveil novel kinome signalling pathways and their mechanisms in regulating neoplastic transformation using multiple integration of various experimental approaches.

CHAPTER III

MATERIALS AND METHODS

3.1 MATERIALS

3.1.1 Chemicals

Absolute methanol (Sigma, USA), Molecular biology grade absolute ethanol, (Fisher Bioreagents™, Fisher Scientific, UK), 1% Crystal violet solution (Sigma, Germany), Mini-PROTEAN TGX™ Precast Gels (Biorad laboratories, Singapore), RIPA buffer (Thermo Scientific, USA), 10x Tris/Glycine Buffer (#1610734EDU, Biorad laboratories, Singapore) 1 L, 10x premixed electrophoresis buffer, contains 25 mM Tris, 192 mM glycine, pH 8.3, 10x Tris Buffered Saline (#1706435EDU, Biorad laboratories, Singapore), Pierce ECLPlus chemiluminescence substrate (Pierce, USA).

A. Cell Culture Reagents

Dulbecco's Modified Eagle's Medium contains high glucose with 4500 mg/L glucose, L-glutamine, and sodium pyruvate (DMEM, #7777) (Sigma, USA), fetal bovine serum (FBS) (Gibco, USA), TrypLE (Gibco, USA), 1x Phosphate buffer saline (PBS), pH 7.4 (Gibco, USA). Clonetics™ AGM™ (Astrocyte growth medium) BulletKit (#CC-3187 & CC-4123) and ReagentPack™ (CC-5034) from Lonza, USA and sodium bicarbonate (Nacalai-Tesque, Japan).

B. RNAi Screening Reagents

Reverse transfection (RTF) Optimization Kit (Thermo Science- Dharmacon, USA) containing RTF optimization plates with DharmaFECT Cell Culture Reagent (DCCR;# B-004500-100) and DharmaFECT Transfection Reagent 1, 2, 3 or 4 (# T-2001, T-2002, T-2003, T-2004). ON-TARGETplus SMARTpool siRNA Custom RTF library containing 113 kinases genes of interest with 6.25 pmol per well, one (1) positive control, one (1) negative control (Thermo Science- Dharmacon, USA), ON-TARGETplus Non-Targeting pool siRNA (#001810-10-50, Dharmacon, USA), DharmaFECT 1 (DF1) transfection reagent (Thermo Scientific, Cat # T-2001-03), 5x siRNA buffer (# B-002000-UB, Thermo Scientific), PrestoBlue® Cell Viability reagent (Thermo Fischer Scientific, USA).

C. Antibodies

Primary antibody, mouse anti-human TLK1 (Santa Cruz, USA), Secondary antibody; Goat anti-mouse (Santa Cruz, USA). Control antibody; primary mouse anti-human B2M (Santa Cruz, USA) and secondary antibody; goat anti-mouse (Santa Cruz, USA).

3.1.2 Equipments and devices

Equipments and devices used in the experiments were, FACSAria II flowcytometer (BD Biosciences, USA), Varioskan Flash spectral scanning multimode reader (Thermo Scientific, Vantaa, Finland), ultrasonic bath (FB 15055, Fischer Scientific,USA), Bench Top Refrigerated Centrifuge (5810R, plate rotor, Eppendorf, German), Bench Top Refrigerated Centrifuge (Allegra X-12R, Mini-PROTEAN 3 (Bio-Rad Laboratories), Trans-Blot® SD Semi-Dry Electrophoretic Transfer Cell (Bio-Rad Laboratories), Confocal microscropy by Leica TCS SP5 II, (Germany), NanoDrop 1000 spectrophotometer (Thermo Scientific, USA), Rotor-Gene 6000 (QIAGEN, Germany), Applied Biosystems 7500 Fast Real Time PCR System (Applied Biosystems, USA), Heidolph MR 3001K magnetic stirring hotplate and vortex mixer (Germany), pH meter (Cyber pH-14L, Cyberlab, USA), shaker (IKA KS 260 basic, Germany), oven and water bath (Memmert, Germany), weighing machine

(Pioneer, OHAUS, USA), laminar airflow and Biological Safety Cabinet Class II (NuAire, USA), Olympus CKX41 inverted microscope (Japan), CO_2 incubator (RS Biotech dan New Brunswick, Eppendorf, Germany), and Chemi-Doc image documentation system (Bio-Rad Laboratories).

3.2 METHODS

3.2.1 Research Procedure

This research was divided into five major components. In the first phase, meta-analysis on GBM was performed using Oncomine cancer microarray datasets to identify significant upregulated kinome that would be used as candidate targets for synthetic lethality screening.

Second phase involved loss of function RNAi screening of the identified kinases targets using Custom siRNA Smartpool from Dharmacon.

After potential "hits" have been identified, the third phase involved *in vitro* functional validation on two different GBM cell lines; LN18 and U87MG using various functional assays such as cell viability assay, apoptosis assays, ELISA, proliferation assay, clonogenic assay, invasion and migration assays, cell adhesion assay as well as cell cycle assay. Since the identified kinase target is a novel target for GBM, we performed microarray on U87MG cells to identify the TLK1 downstream pathways.

To strengthen *in vitro* findings, the fourth phase is involving *in vivo* experiment on female *balb-c* nude mice. Transduced GBM cell lines were xenografted on the subcutaneous flank of the mice to understand the tumorigenic effects of the identified target.

Finally, to investigate if there are available inhibitors that can be used as potential targets for GBM, comparative modelling approach was performed as there were no available crystal structure of the identified kinase. Prior to that, high throughput virtual ligand docking screening were performed on the 3D model.

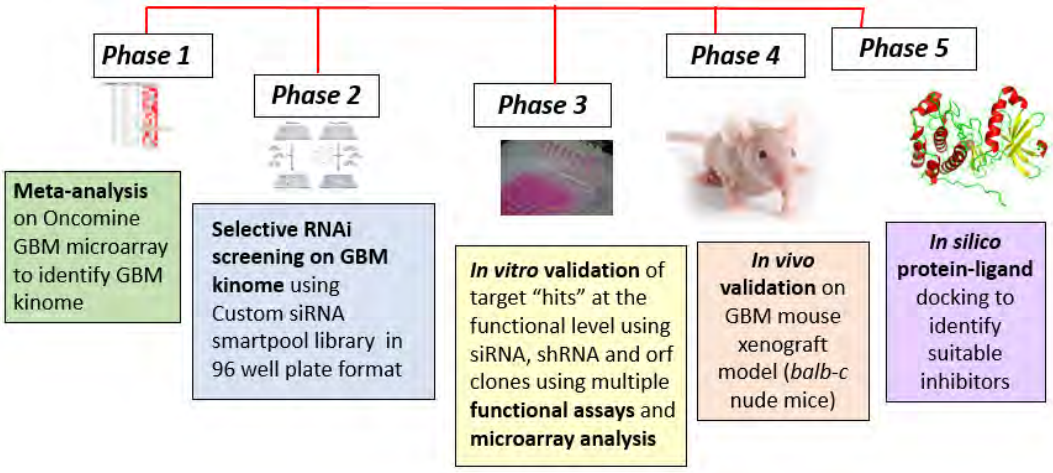

Figure 3.1 Research methodology chart

3.2.2 *In Silico* Analysis via Oncomine

Meta-analysis was performed to identify kinases that are involved in GBM using five different microarray datasets from Oncomine database, Research Edition (Rhodes et al. 2004). Analysis was performed on May 2011. Datasets were obtained from Bredel Brain (Bredel et al. 2005), Liang Brain (Liang et al. 2005), Shai Brain (Shai et al. 2003), Lee Brain (Lee et al. 2006) and Sun Brain (Sun et al. 2006). All significantly up-regulated kinases genes were selected based on their median rank and *p-value* of less than 0.05 (95% confidence interval). A less stringent p-value selection was used to ensure that all statistically significant and important kinases data were captured. All identified kinases were then compared with the "Human Kinome Database" (May, 2011) (www.kinase.com) (Manning et al. 2002) base on kinase gene nomenclature but not on their amino acid or nucleotide sequences. High throughput RNAi silencing of the selected kinases were performed to further determine functional status of these targets.

3.2.3 Cell Culture Condition

Human GBM cell lines LN18 and U87MG were obtained from the American Type Culture Collection (ATCC, Manassas, VA, USA). Cells were maintained in monolayer in Dulbecco's modified Eagle's medium (DMEM, Sigma-Aldrich, St. Louis, MO, USA) mixed with 10% FBS (Lonza Inc, Allendale, NJ, USA). The cell lines were routinely

maintained at 37°C in humidified 5% CO_2 atmosphere. Cells were harvested by removing media and cells were then washed with 5ml of 1X Dulbecco's Phosphate Buffered Saline (Gibco, USA) and trypsinised using 1X TrypPLE (Gibco, USA).

Normal human astrocytes (NHA) were obtained from Lonza, USA and maintained in monolayer using Astrocyte Basal Medium mixed with AGM™ BulletKit. The cell lines were also routinely maintained at 37°C in humidified 5% CO_2 atmosphere. Cells were harvested and washed using ReagentPack™ (CC-5034) containing Trypsin/EDTA, Trypsin neutralizing solution and HEPES Buffered Saline Solution

3.2.4 High Throughput RNAi Screening

RNA interference (RNAi) screening was performed on a custom library of 113 overexpressed human kinases genes using Dharmacon ON-TARGETplus SMARTpools™ siRNA RTF library with 6.25 pmol of lyophilized siRNA per well (Dharmacon, Lafayette, CO, USA) on a 96-well format plates. The U87MG and LN18 cell lines were wet-reverse transfected with 0.15 µl lipophilic base transfection reagent, Dharmafect 1 (DF1) (Dharmacon, Lafayette, CO, USA) giving a final concentration of 50 nM siRNA pool per target gene per well according to the manufacturer's protocol. Cells were then incubated at 37°C in a humidified 5% CO_2 atmosphere for 48hr to allow efficient RNA silencing. After 48hr of incubation, the cell culture medium was changed and the cell viability was measured at 96 hr by adding 1:10 ratio of resazurin based solution, PrestoBlue® cell viability assay with 10µl dropped onto each well (Invitrogen, Carlsbad, CA, USA). Cells mixture were incubated for 1 hr at 37ºC for one hour. Relative fluorescence units (RFU) were measured using VarioSkan Flash multimode plate reader (Thermo Scientific, Vantaa, Finland) at 560nm and 590nm of wavelengths. All experiments were performed in triplicates. Non-targeting siRNA was used as a negative control (Dharmacon, Lafayette, CO, USA) while Polo-like kinase 1 (PLK1) siRNA (Dharmacon, Lafayette, CO, USA) was included as a positive control.

A. Data Analysis for RNAi Silencing

Raw RFU data has been log-transformed and the Median Absolute Deviation (MAD) was used as "hits" identification analysis because it is resistant to outliers in the samples. It has been shown to identify weak hits in RNAi data efficiently compared with B-score, Z-score, standardized standard mean deviation (SSMD) or mean + k standard deviation (S.D) while still capturing the strong hits and controlling false positives hits (Birmingham et al. 2009; Chung et al. 2006). Rescaled MAD for RNAi screening suggested by Zhang is by the formula; MAD = 1.4826 median ($[x_i$-median(x)]) so that the data values is comparable with SD when the data is normally distributed making sure that it has greatest "power" to obtain true "hits" (Zhang X.D. et al. 2006). The strength of our "hits" was compared with SSMD and unpaired t-test against non-targeting control. This is important to ensure that the target of interest has significant role in cancer cell vulnerabilities.

3.2.5 RNA Extraction and qPCR

Transfected cells were harvested at 48hr and RNA extraction was performed using RNeasy Plus Mini kit (Qiagen, Hilden, Germany). Quantitative real time PCR (qPCR) was carried out using iTaq Universal SYBR green master mix (Bio-Rad Laboratories, USA) on Rotor Gene 6000 real time platform (Corbett Life Science, Sydney, Australia). The TLK1 primers were forward: 5'-CAGTGGAAGTTTGGAGGGGCCG-3' and reverse: 5'-CCGGATGGCGGCGT-GTGAT-3'. Beta-actin (ACTB) was used as a housekeeping gene and relative gene expression was determined using 2-ΔΔCt method (Livak & Schmittgen 2001). For microarray validation, qPCR was performed on *TTK, CDC2, MAPK1, RAC2, PI3KR1, ROCK2, DDX5, THBS2, FYN, PXN,* and *COL4A2* genes. Primers were listed in the appendices.

3.2.6 Protein Extraction and Western Blot

Cells were harvested by lysis with Radioimmunoprecipitation Assay (RIPA) buffer for protein extraction (Thermo Scientific, Rockville, IL, USA) supplemented with protease

cocktail inhibitor (Roche Diagnostics, GmbH, Germany), 25 µM of sodium fluoride (New England Biolabs, USA) and 25 µM of sodium orthovanadate (New England Biolabs, USA) followed by sonication for 1 minutes and centrifugation at 4°C for 30 minutes. Supernatant containing total protein lysate were collected in supernatant and protein concentration were measured using Bradford reagents (Bio-rad laboratories, Hercules, CA, USA).

30 µg of proteins were resolved by sodium dodecyl sulfate polyacrylamide gel (SDS-PAGE) on a MiniProtean Precast gels and 1x Tris-glycine buffer (Biorad technologies, USA) and transferred to polyvinylidene difluoride (PVDF) membrane (Biorad technologies, USA). Subsequently, the membranes were probed with primary antibody to confirm protein knockdown. Primary antibodies used for blotting were mouse anti human-TLK1 (#sc-100345, Santa-Cruz, USA) (1:200). Later, the membrane was washed for 4 times with 1x TBST (Thermo Fischer Scientific, USA) and blotted with goat anti-mouse antibody conjugated to horse reddish peroxidase (HRP) (#sc-2005, Santa Cruz, USA) with 1:2000 dilution using casein blocker (Biorad, USA) overnight at 4ºC. After incubation, the membrane was washed with 1x TBST (Thermo Fischer Scientific, USA) for 4x with 5 minutes of washing on the orbital shaker. Signals were measured using Pierce ECLPlus substrate (Pierce, USA) and viewed under Bio-Rad chemiluminescence imager (Bio-Rad laboratories, USA). Loading control used was mouse anti-human beta-actin (#sc-69879, Santa-Cruz, USA) whilst the secondary antibody was goat anti-mouse IgG-HRP (#sc-2005, Santa Cruz).

3.2.7 Pool TLK1 siRNA Transient Transfection

Resuspension of 20 nmol lyophilized ON-TARGETplus pool siRNA for TLK1 and pool non-targeting siRNA (#D-001810-10, Dharmacon, USA) was performed using 1x siRNA buffer to make 100 µM of stock. Prior reverse-transfection, 5 µM of siRNA solution in 1x siRNA buffer were prepared. For experiments requiring 96-well plates, reagents for transfection were prepared in separate tubes. In tube 1, 10 µl of siRNA in serum free media was added with 0.5 µl of 5 µM siRNA in 9.5 µl serum free media. In tube 2, 10 µl of diluted DF1 transfection reagent were prepared in serum free medium (0.1 µl of DF1 mixed with 9.85 µl of serum free media). Both tubes were gently mixed

and left for 5 minutes incubation at room temperature. Subsequently, content from tube 1 and 2 were mixed for 20 minutes at room temperature.

Total of 5,000 cells were plated on each 96-well plate and suspension were made with 80 µl of antibiotic free-complete DMEM/well. Cells suspension in antibiotic free medium were mixed later with previously prepared siRNA, serum free media and transfection reagent in each well plate. Cells were incubated for 48 hr (RNA) and 72 hr (protein) at 37ºC in 5% CO^2.

The ON-TARGET plus TLK1 siRNA (si -*TLK1*) sequences were; GAGUAUGCAAGAUCGAUUA, GAAGCUCGGUCUAUUGUAA, GCAAUGACUUGGAUUUCUA and GUUCAAAGA-UCACCCAACA.

3.2.8 orf Clones and shRNA Transduction

The Precision LentiORF lentiviral particles individual clones (#V13121301) and LentiORF RFP control (OHS5832) (Thermo scientific, Open Biosystems, Inc., USA) were used to overexpress *TLK1* in U87MG and LN18 cells as per manufacturer's recommended protocol. The GIPZ shRNA individual clones (#V3LHS_637461, #V3LHS_637455, #V3LHS_335655) and the GIPZ non-targeting shRNA control clones were purchased in viral particle format (Thermo scientific, Open Biosystems, Inc., USA) to knockdown U87MG and LN18 cells. The day before transduction, 5x 10^4 of U87MG and LN18 cells were seeded onto the 24-well tissue culture plate with their respective medium by not more than 40-50% confluent. The LentiORF control viral stock were diluted in a round bottom 96-well plate using serum-free medium using series of 5-fold dilutions to reach a final dilution of 390,625-fold. After dilution, the virus stock was pre-incubated for 5 minutes at room temperature.

Subsequently, the 24-well plate was labelled using one row for each replicate. The culture medium in the 24-well plate was removed from the cells. Then, 225 µL of serum-free medium was added to each well. Cells were transduced by adding 25 µL of diluted control LentiORF lentivirus from the original 96-well plate to a well on the 24-well destination plate containing the cells. Transduced cultures were incubated at 37 °C

for 4-6 hours. Subsequently, 1 mL of normal concentration DMEM was added and cells was left for 72 hours. The TurboGFP expressing cells or colonies of cells were counted to determine functional titre and relative transduction efficiency. Similar methods was used to perform shRNA transduction in both LN18 and U87MG cell lines. To determine successful knockdown and overexpression of the gene of interest, qPCR was also performed.

3.2.9 Cell Viability Assay

The U87MG and LN18 cells were reverse transfected with 25 nM *TLK1* siRNA in 6 well plate.100µl of Presto Blue Cell Viability reagent (Invitrogen, USA) was added into each well plate. After an hour of incubation, reading were taken using a microplate reader SkanIt RE for Varioskan Flash 2.4 (Thermo Scientific, Vantaa, Finland) at excitement/emission 560/590 nm. Subsequently, reading was taken at 24, 48, 72 and 96 hrs time points. Experiment was performed in three replicates.

3.2.10 Functional Microarray Experiment

Total RNA from U87MG cells was isolated using the RNeasy Plus Mini kit (Qiagen, Hilden, Germany). A total of 150 ng of purified RNA was further amplified using Illumina Total Prep RNA amplification kit (Life Technologies, Carlsbad, USA). Biotin labelled cRNA were directly hybridized on the Illumina Human HT-12 v4 Expression Beadchip arrays kit (Illumina Inc, San Diego, CA, USA) according to the manufacturer's protocol. Microarray beadchips were scanned using the iScan array scanner (Illumina Inc, San Diego, CA, USA) and the intensity data were then processed using Genome Studio version 2008.1 (Illumina Inc, San Diego, CA, USA). Data were then further analysed using GeneSpring GX 12.6 (Agilent Technologies, Santa Clara, CA, USA).

A. Data Analysis

Fluorescent intensities were log transformed, quantile normalized and prefiltered to remove low quality data. Principal component analysis (PCA) was used to assess quality

control of the data. Moderated unpaired t-test was used to determine underlying pathways involved after TLK1 knockdown in U87MG cells. P-value computation was asymptomatic whilst multiple testing correction applied was Benjamini-Hochberg. A significant gene list was obtained where $p<0.05$ and fold change of more than 1.1 were chosen for pathway analysis. Clustering heat map of differentially expressed genes were performed using hierarchical base on Euclidean similarity measure and complete linkage. Gene set enrichment analysis (GSEA) was performed using filtered probes signals with q-value <0.3. Pathway analysis was performed using WebGestalt (Wang et al. 2013) and Pathway Studio 8.0 software (Adriane Genomic, Rockville, MD, USA).

3.2.11 Apoptosis Assays

Apoptosis assays that includes ssDNA assay, Annexin V and Caspase 3-7 were performed to understand the role of *TLK1* silencing in modulating the apoptosis pathway.

A. Single Stranded DNA Assay

Cells were seeded in 96 well plate ($3x10^3$ cells/well) and transfected with si-*TLK1*. After 48hrs, apoptotic activity assay was carried out using ssDNA apoptosis Enzyme-link immunosorbance assay (ELISA) kit (Chemicon International, CA, USA) according to the manufacturer's protocol. Presence of single stranded DNA (ssDNA) in apoptotic cells were detected with a mixture of primary and peroxidase labelled secondary antibodies. Colorimetric reading was taken at 405 nm wavelength using VarioSkan Flash multimode plate reader (Thermo Scientific, Vantaa, Finland).

B. Annexin V Fluorescence Assay

The Annexin-V assay was performed using Annexin-V-FLUOS staining kit (#11988549001, Roche, Germany). The 20 µl Annexin-V-Fluos were pre-diluted in 1 ml incubation buffer and 20 µl propidium iodide solution were added. Transfected cells were washed with PBS and centrifuged at 200 × g for 5 minutes. The cell pellet were suspended in 100 µl of Annexin-VFLUOS labelling solution which have been pre-

mixed earlier. Suspension were incubated for 10 to 15 minutes at 15 to 25°C. Analysis was made using Tali® Image Cytometer (Thermo Fischer Scientific, USA).

C. Caspase-3 and Caspase-7 Assay

The CellEvent™ Caspase-3/7 Green Detection Reagent (#C10423, Invitrogen, Carlsbad, CA, USA) was added on the transfected cells at a final concentration of 3 µM to the sample. Cells were later incubated for 30 minutes at 37°C. Cells were imaged using confocal microscope by Leica TCS SP5 II, (Leica, Germany) on the appropriate filter for FITC and the Alexa Fluor® 488 dye. The excitation/emission for the CellEvent™ Caspase-3/7 Green Detection Reagent was 502/530 nm.

3.2.12 Cell Cycle Assay

Cell cycle assay was performed using 1 x 10^6 LN18 and U87MG cells that have been transfected with siTLK1 or non-targeting siRNA. Cells were harvested using a standard protocol as mentioned in the CycleTEST™ PLUS DNA Reagent Kit protocol (BD Biosciences, Ontario, Canada). Subsequently, cells were washed three times with wash buffer. Cells were then suspended in solution A containing trypsin. Then, solution B with trypsin inhibitor and RNase was added into the cell suspension. Finally, solution C which contains propidium iodide (PI) was added. Flow cytometric analysis was performed using BD FACSAria™ (BectonDickinson, New Jersey, USA). Data was analysed using ModFit LT software (Verity Software House, USA). The percentage of arrested cells was measured by the percentage of hypodiploid cells accumulated at the G0/G1, S, G2/M checkpoints of the cell cycle. Experiments was performed in triplicates.

3.2.13 Colony Formation Assay

Cells were initially transfected with si*RNA* for 48 hr in T45 flask prior assessment of cells colony formation in monolayer. After change of media, sub-lethal dose of temozolomide (250 µM) was added to determine chemo-sensitization effect of *TLK1* inhibition. At 96 hrs, 100 cells were counted and seeded on 6-well plates. Colonies

were allowed to grow for 14 days. Later, DMEM were removed and cells were washed gently with PBS before being fixed with 50% methanol for 10 minutes and stained with 0.5% crystal violet diluted in 50% methanol for an hour. After that, stain was removed and cells were washed with distilled water. Colony containing more than 50 cells were counted to as one single colony. Images of the colonies were captured using Chemi-Doc Imager (Bio-Rad Laboratories, USA). Experiment was performed in triplicates.

3.2.14 BrdU Proliferation Assay

Proliferation assay was performed using bromodeoxyuridine (BrdU) (#2750, Milipore, Massachusetts, USA). Transfected cells were cultured for 24 hrs in the present of BrdU which was incorporated into newly synthesized DNA strand of the proliferating cells. The cells were then fixed, and incubated with anti–BrdU monoclonal antibody for 1 hour. Goat anti-mouse IgG peroxidase was added onto the well. Incorporation of BrdU in the proliferating cells leads to colorimetric changes from clear to blue which was measured using VarioSkan Flash multimode plate reader at 450 nm wavelength (Thermo Scientific, Vantaa, Finland).

3.2.15 Invasion And Migration Assays

A. Transwell Cell Invasion and Migration Assay

The QCM™ 24-Well Cell Invasion Assay kit (#ECM554, Milipore, Massachusetts USA) and QCM™ 24-Well Cell Migration kit (#ECM509; Chemicon) were used to assess the migration and invasion properties of the siRNA, shRNA and orf-transfected GBM cells through the extracellular matrix. The siRNA transfected in normal human astrocytes were also assessed. Each kit contains a polycarbonate membrane coated with a thin layer of extracellular matrix with 8 µm pore size.

Cells were initially transfected in T45 flask. Subsequently, cells were harvested when it reaches 80% confluency. Cells were later mixed with serum free-DMEM and let grown for 24 hours in order to starve the cells. Subsequently, these cells were harvested and counted. Each insert contains 1.5 x 10^3 of cells suspended in 250 µl

DMEM-serum free media. Prior to this, 500 µl of DMEM-with serum were aliquoted at the bottom of the insert by ensuring absence of air bubbles in between. Plates were covered and incubated for 48 hr at 37°C in a 5% CO_2 incubator.

Migrated and invaded cells were detached from the lower fragment of the insert using cell detachment solution by incubation for 30 minutes at 37ºC. Sufficient lysis buffer/dye solution were prepared for all samples. CyQuant GR Dye was diluted with 4x Lysis Buffer 1:74. About 75 µL of this lysis buffer/dye solution was aliquoted to each of the well containing 225 µL cell detachment solution with the cells that invaded through the ECMatrix™ coated membrane and incubated for 15 minutes at room temperature. About 200 µL of the mixture was transferred to a 96-well plate suitable for fluorescence measurement. Reading was taken using VarioSkan Flash multimode plate reader (Thermo Scientific, Vantaa, Finland) using 480/520 nm filter set. Experiment was performed in triplicates.

B. Wound Healing Assay

Lentiviral transduced GBM cells with TLK1 shRNA and orf clones were cultured in six well plate containing DMEM with 10% FBS. After cells were cultured for 24 hours, medium was replaced with FBS-free media until it reach its 90% final confluency. Monolayer of cells were scratched using a sterile 200 µl yellow micropipette tip. The well was rinsed carefully to remove dislodged cells and grown in FBS-free media for 24 hour and 48 hours. The wounds were examined and photographed using a phase contrast microscope (Olympus, Tokyo, Japan) immediately after scratches were created at 24 hour and 48 hours later. The distance of cells migration was calculated by substracting the distance between edges at 24 hour and 48 hours from the distance measured at 0 hour. Experiments were performed in triplicates.

C. Cell Adhesion Assay

The ECM adhesion plates were allowed to warm up at room temperature under sterile condition for 10 minutes. Cell suspension containing 0.1-1.0 x 10^6 cells/ml were prepared in serum free media. A total of 150 µL of the cell suspension was added to the

inside of each well (BSA-coated wells are provided as a negative control). Plate was later incubated in a cell culture incubator for 30-90 minutes. Media from each well was discarded and ensure that the wells were not allowed to dry. Each well were gently washed 4 to 5x with 250 µL PBS. PBS were aspirated from each well and 200 µL of cell stain solution was added. Then, incubation was performed for 10 minutes at room temperature. Cell stain solution was discarded from the wells and wells were washes 4 to 5x with 500 µL deionized water. Solution was discarded and air dried the wells for 20 minutes. About 200 µL of extraction solution were added per well, and then incubated for 10 minutes on an orbital shaker. A total of 150 µL suspension from each extracted sample were transferred to a 96-well microtiter plate. Reading was measured using colorimetric measurement using OD of 560nm by using VarioSkan Flash multimode plate reader (Thermo Scientific, Vantaa, Finland).

3.2.16 ELISA Based Assays

ELISA based assays were performed to validate TLK1 downstream pathways findings at the protein level. Few protein assays were chosen based on its relevancy from the functional microarray analysis.

A. Total/phosphorylated TP53, Erk/AKT/p70 S6K Activation Assay

Total/phosphorylated TP53, Erk/AKT/p70 S6K activation assay was performed using InstantOne™ ELISA (#85-86018 and # 85-86123, eBioscience, Inc., San Diego, USA). Media from the transfected cells were removed and cells were gently washed with PBS. Cells were lysed with 100 µl of freshly prepared Cell Lysis Buffer Mix (1x) and were shaken at 300 rpm using shaker at room temperature for 10 minutes. 50 µl/well cells lysate was prepared and added to each of the InstantOne assay wells. 50 µl/well of cells lysis mix (1x) which serves as negative control were added. The same amount of positive control cell lysate were also added to separate wells as assay control. Freshly prepared antibody cocktail 50 µl/well was aliquoted to each of the testing wells. The microplate was covered with adhesive seal and left for incubation for 1 hour at room temperature on a microplate shaker at 300 rpm. Wells were washed with 200 µl/well of wash buffer (1x) for three times. The final wash was performed by inverting on a lint-

free paper towel to remove remaining wash solution. About 100 µl/well of the detection reagent was added to each of the wells and incubated for 30 minutes with shaking at 300 rpm. The reaction was halted by adding 100 µl/well of stop solution to each well. Colorimetric measurement was taken using VarioSkan Flash multimode plate reader (Thermo Scientific, Vantaa, Finland) set at 450 nm.

B. CDC42 and RAC Activation Assay

The GTP-bound levels of RAC and CDC42 were analysed with modified ELISA kit that specifically detects Small GTPase associated protein called G-LISA activation assay biochemistry kit (#BK127 and #BK125 Cytoskeleton, Denver, CO, USA) according to the manufacturer's instructions. LN18 and U87MG cells were seeded at 150×10^3 cells per well in a 6-well plate and allowed for three days for attachment. Immediately after washing twice with ice-cold PBS, the cells were harvested by scraping in lysis buffer and cells were processed rapidly on ice. The lysates were centrifuged at 17,800 g at 4°C for 2 minutes. Protein concentration was determined according to the manufacturer's protocol using Precision RedTM Advanced Protein Assay (#Part GL50, Cytoskeleton, USA), and the cell extracts were adjusted to 0.25 mg/mL for CDC42 assay and RAC assay. Cell lysates were incubated in RAC or CDC42-GTP affinity plate for 15 minutes and washed. The detection of bound CDC42-GTP or RAC was through specific antibody recognition and HRP colorimetric detection system. Colorimetric measurement was taken using VarioSkan Flash multimode plate reader (Thermo Scientific, Vantaa, Finland) set at 490 nm.

3.2.17 Xenograft Mice Model

Fourty-two immune-deficient nude mice (BALB/c-nu; 6 weeks old; 16–18 g) obtained from BioLASCO, Taiwan were randomly divided into 7 groups and maintained in pathogen-free environments. All animal experiments carried out in this study were complied with the international guidelines for the care and treatment of laboratory animals. This study have been approved by the UKM Animal Ethics Committee with ethics registration number; UMBI/2014/ROSLAN/24-SEPT./607-SEPT.-2014-DEC.-2014.

Injection of overexpressed and knocked down TLK1 in U87MG were performed using equal numbers of U87MG-pGIPZ-nontargeting control, U87MG-pGIPZ-shTLK1-455, U87MG-shTLK1-461, U87MG-pLOC-RFP control, and U87MG-pLORF-TLK1-301 cells (3×10^7) in logarithmic growth phase. These cells were harvested, washed in PBS, and suspended in 200 µl of PBS. The cell suspension will be injected subcutaneously into the right sub-dorsal flank tissue of nude mice to establish subcutaneous xenograft models. Over 40-days observation period, nude mice were monitored daily, and the sizes of transplanted tumours will be measured by slide calliper every 7 days. A growth curve for transplanted tumour was plotted after calculating the tumour volume.

Experiment was terminated at day 47 due to completion of observation. Mice were sacrificed and all tumour formed subcutaneously were weighed using weighing machine (Pioneer, OHAUS, USA). Tissue as well as adjacent tumour tissue were snap frozen and kept in liquid nitrogen for future study.

3.2.18 Statistical Analysis

For *in vitro* functional experiments all data were expressed as mean ± standard deviation and analysis of significance was performed using the Student's t-test (Microsoft Office Excel). The p-values < 0.05 (95% confidence interval) was considered significant.

Statistical analysis for *in vivo* experiment, comparisons among all groups were performed using one-way analysis of variance (ANOVA). Then, the Mann-Whitney test was used for comparison of differences between the two groups by ANOVA. Values of $p<0.05$ was considered statistically significant in all cases.

3.3 Template identification and comparative modelling

The amino acid sequence of human TLK1 was retrieved from UniProt with the accession number: Q9UKI8 at http://www.uniprot.org/. The sequence was submitted to the I-TASSER (Iterative Threading ASSEmbly Refinement) at the http://zhanglab.ccmb.med.umich.edu/ITASSER (October, 2016) server to identify

acquired templates based on threading approach from the protein data bank (Yang et al. 2015). All parameters of modelling were remained as default. The values of C-score as implemented in the I-TASSER server were used to select the best PDB structure ligand docking simulation using MTi OpenScreen server (Rey et al. 2015).

3.3.1 Validation of modelled structure

The best 3D model suggested by I-TASSER was used for further investigation. The latest version of PDBsum at http://www.ebi.ac.uk/thornton-srv/databases/pdbsum/ (October, 2016) provides further information on protein function prediction, structural topology, PROCHECK and cleft analysis. We also used ProSA which displays scores and energy plots that highlight potential problems spotted in protein structures (Wiederstein, & Sippl 2007).

3.3.2 Virtual screening and ligand-docking analysis

Suitable ligand binding site as suggested from ITASSER was used for further virtual screening. To confirm the presence of protein cavities during molecular dynamics trajectories, the fpocket online server (Guilloux, Schmidtke & Tuffery 2009) is use as it is a very fast open source protein pocket (cavity) detection algorithm based on Voronoi tessellation at http://bioserv.rpbs.univ-paris-diderot.fr/services/fpocket/ (October, 2016).

Later, virtual screening of chemical compounds using MTiOpenScreen, allows performing docking into a user-defined binding site or blind docking using automated virtual screening with AutoDock Vina (Rey et al. 2015). MTiOpenScreen contains two in-house prepared drug-like chemical libraries containing 150, 000 PubChem compounds from the Diverse-lib database containing diverse molecules and the iPPI-lib enriched in which these molecules are likely to inhibit protein–protein interactions.

3.3.3 Visualization of protein-ligand interaction

The three-dimensional and two-dimensional visualisation of ligand-protein interaction were performed using the Accelrys' Discovery Studio 4.0 Visualizer, Accelrys Software Inc., USA.

3.3.4 *In silico* bioavailability study

Lead molecules identified from the high throughput ligand-docking screening were subjected to further *in silico* filtering to identify drugs with the best pharmacokinetic properties in terms of their absorption, distribution, metabolism, excretion and toxicity (ADME-Tox) of the compound. This was done using the FAF-Drugs3 (version 3 June 2015 edition) filtering tool (Lagorce et al. 2015). This step will ensure the suitability of lead molecules based on toxicity for future *in vivo* applications. The logP parameter for the analysis is based on XlogP3 algorithm (Rey et al. 2015). We applied Central Nervous System (CNS) drugs physicochemical criteria (Frattini et al. 2013; Pajouhesh, & Lenz 2005), which includes selection of compounds having (1) molecular mass 135 Da until 582 Da, (2) partition coefficient (logP) of -0.2 until 6.1, (3) hydrogen bond donors less or equal to three, (4) hydrogen bond acceptors less or equal to five and (5) topological surface area (tPSA) within 3 until 118. We also included filtering of undesirable substructures moieties and retrieving covalent inhibitors as well as filter for Pan Assay Interference Compounds (PAINS).

CHAPTER IV

RESULTS

4.1 IDENTIFICATION OF UPREGULATED KINASES IN GBM MICROARRAY DATASETS

Meta-analysis on five Oncomine microarray gene expression datasets had identified 113 kinases out of 7000 upregulated genes that were significantly upregulated in GBM. To validate these kinases, these data were compared to "The Human Kinome Database" (www.kinase.com) (Manning et al. 2002). The kinases were evaluated and grouped into their respective kinase groups. Ninety out of 113 kinases were pure human kinase enzymes whilst others were kinase related genes. *CDK2, CDK4, CCND2, MAK, MARCKS, MAP2K3, MOBKL1B, CDK6, AKAP13, PLAU* and *STK17A* were amongst the top highly expressed kinases. Functional clustering analysis using the **D**atabase for **A**nnotation, **V**isualization and **I**ntegrated **D**iscovery (DAVID) revealed that the kinases involved in the cell cycle pathway (21 out of 113) and focal adhesion kinases as the main key players in GBM. Table 4.1 and table 4.2 show diverse distribution of kinases within the kinases groups.

Table 4.1 The number of upregulated kinases identified in each kinase group

Kinase group	Number of kinases identified
STE Ser/Thr Protein Kinases class	8
CMGC Group (including cyclin-dependent kinases (CDKs), mitogen-activated protein kinases (MAP kinases), glycogen synthase kinases (GSK) and CDK-like kinases)	9
AGC group - ROCK and ETA subfamily	7
Atypical group – DNAPK, ROCK & RIO3	5
Tyrosine Kinase group	7
Casein (CK1) group	11
Tyrosine Kinase Like group	5
Cytidylate monophosphate kinase (CAMK) group	17
Other group	20
Total	**113**

Table 4.2 List of upregulated kinases identified from meta-analysis on five Oncomine microarray datasets comparing GBM and normal brain ($p<0.05$).

Kinase	NCBI ID	Full name
ADPGK	83440	ADP-dependent glucokinase
AK2	204	adenylate kinase 2
AKAP13	11214	A kinase (PRKA) anchor protein 13
AKAP2	11217	A kinase (PRKA) anchor protein 2
ALPK1	80216	alpha-kinase 1
ALPK3	57538	alpha-kinase 3
AURKA	603072	aurora kinase A
BMP2K	55589	BMP2 inducible kinase
BTK	695	bruton agammaglobulinemia tyrosine kinase
CASK	8573	calcium/calmodulin-dependent serine protein kinase (MAGUK family)
CCND2	894	cyclin D2
CDK1	983	cyclin-dependent kinase 1
CDK13	8621	cyclin-dependent kinase 13
CDK2	1017	cyclin-dependent kinase 2
CDK2AP1	8099	cyclin-dependent kinase 2 associated protein 1
CDK4	1019	cyclin-dependent kinase 4
CDK6	1021	cyclin-dependent kinase 6
CDKN1	1026	cyclin-dependent kinase inhibitor 1A (p21, Cip1)
CDKN2C	1031	cyclin-dependent kinase inhibitor 2C (p18, inhibits CDK4)
CDKN3	1033	cyclin-dependent kinase inhibitor 3
CERKL	375298	ceramide kinase-like
CK1	1452	casein kinase 1, alpha 1, CSNK1A1
CKS1B	1163	CDC28 protein kinase regulatory subunit 1B, NB4 apoptosis/differentiation related protein

to be continued…

…continuation

CKS2	1164	CDC28 protein kinase regulatory subunit 1B
CLK2	1196	CDC-like kinase 2
CSK	1445	c-src tyrosine kinase
CSNK2A1	CSNK2A1	casein kinase 2, alpha 1 polypeptide
DAPK3	1613	death-associated protein kinase 3
DCLK2	166614	doublecortin-like kinase 2
DDR2	4921	discoidin domain receptor tyrosine kinase 2
DNAPK	5591	protein kinase, DNA-activated, catalytic polypeptide, PRKDC
DOK1	1796	docking protein 1, 62kDa (downstream of tyrosine kinase 1)
DRAK	9262	STK 17B - DAP kinase-related apoptosis-inducing protein kinase 2, serine/threonine kinase 17b
DTYMK	1841	deoxythymidylate kinase (thymidylate kinase)
DYRK3	8444	dual-specificity tyrosine-(Y)-phosphorylation regulated kinase 3
EIF2AK1	27102	eukaryotic translation initiation factor 2-alpha kinase 1
FASTK	10922	Fas-activated serine/threonine kinase
FLT3	2322	fms-related tyrosine kinase 3
GK	2710	glycerol kinase
HIPK1	204851	homeodomain interacting protein kinase 1
HK2	HK2	hexokinase 2
ILK	3611	integrin-linked kinase
IP6K2	51447	inositol hexakisphosphate kinase 2
IRAK3	11213	interleukin-1 receptor-associated kinase 3
IRAK4	51135	interleukin-1 receptor-associated kinase 4
ITK	3702	IL2-inducible T-cell kinase
ITPKB	3707	ITPKB inositol-trisphosphate 3-kinase B

to be continued…

…continuation

KDR	3791	kinase insert domain receptor (a type III receptor tyrosine kinase)
KIF7	374654	kinesin family member 7
LIMK2	3985	LIM domain kinase 2
LOK	6793	serine/threonine kinase 10 , STK-10
MAK	4117	male germ cell-associated kinase
MAP2K3	5606	mitogen-activated protein kinase kinase 3, MEK3
MAP3K1	4214	mitogen-activated protein kinase kinase kinase 1, MAP/ERK kinase kinase 1
MAP3K14	9020	NIK, mitogen-activated protein kinase kinase kinase 14, MAP3K14
MAP3K2	10746	mitogen-activated protein kinase kinase kinase 2, MEKK2
MAP3K6	9064	mitogen-activated protein kinase kinase kinase 6, MEKK6
MAP3K7	6885	mitogen-activated protein kinase kinase kinase 7, MEKK7, TGF-beta activated kinase 1
MAPK1	5594	ERK2, mitogen-activated protein kinase 1
MAPK7	5598	mitogen-activated protein kinase 7, BMK1; ERK4; ERK5
MAPKAP1	79109	mitogen-activated protein kinase associated protein 1
MARCKS	4082	myristoylated alanine-rich protein kinase C substrate
MARK3	4140	MAP/microtubule affinity-regulating kinase 3
MELK	9833	maternal embryonic leucine zipper kinase
MERTK	10461	c-mer proto-oncogene tyrosine kinase
MOBKL1B	55233	MOB1, Mps One Binder kinase activator-like 1B (yeast)
MOBKL2A	126308	MOB1, Mps One Binder kinase activator-like 2A (yeast)
MST1	4485	macrophage stimulating 1 (hepatocyte growth factor-like)
MTOR	2475	mechanistic target of rapamycin (serine/threonine kinase)
NEK11	79858	NIMA (never in mitosis gene a)- related kinase 11

to be continued…

…continuation

NEK2	4751	NIMA (never in mitosis gene a)-related kinase 2
NEK8	284086	NIMA (never in mitosis gene a)- related kinase 8
NTRK2	4915	neurotrophic tyrosine kinase, receptor, type 2
PBK	55872	PDZ binding kinase TOPK
PFKFB3	5209	6-phosphofructo-2-kinase/fructose-2,6-biphosphatase 3
PFKFB4	5210	6-phosphofructo-2-kinase/fructose-2,6-biphosphatase 4
PHKA1	5255	phosphorylase kinase, alpha 1
PHKB	5257	phosphorylase kinase, beta
PHKG1	5260	phosphorylase kinase, gamma 1 (muscle)
PI4K2B	55300	phosphatidylinositol 4-kinase type 2 beta
PIK3R5	23533	phosphoinositide-3-kinase, regulatory subunit 5
PKN2	5586	protein kinase N2
PKN3	29941	protein kinase N3
PLAU	5328	plasminogen activator, urokinase
PLAUR	5329	plasminogen activator, urokinase receptor
PRKAB2	5565	protein kinase, AMP-activated, beta 2 non-catalytic subunit
PRKCE	5581	protein kinase C, epsilon
PRKD1	5587	protein kinase D1
PRKD2	25865	protein kinase D2
PRKRA	8575	protein kinase, interferon-inducible double stranded RNA dependent activator
PRKRIR	5612	PRKRIR protein-kinase, interferon-inducible double stranded RNA dependent inhibitor, repressor of (P58 repressor), DAP4
PSKH1	5681	protein serine kinase H1
RIOK3	8780	RIO kinase 3
RIPK1	8737	receptor (TNFRSF)-interacting serine-threonine kinase 1

to be continued…

…continuation

ROCK1	6093	Rho-associated, coiled-coil containing protein kinase 1
RPS6KB1	6198	ribosomal protein S6 kinase, 70kDa, polypeptide 1
SKAP2	8935	src kinase associated phosphoprotein 2
SNRK	54861	SNF related kinase
STK17A	9263	DAP kinase-related apoptosis-inducing protein kinase 1, DRAK1
STK33	65975	serine/threonine kinase 33
STK36	27148	serine/threonine kinase 36
STK38	11329	serine/threonine kinase 38, NDR1
STK38L	23012	serine/threonine kinase 38 like
SYK	6850	spleen tyrosine kinase
TK1	7083	thymidine kinase 1, soluble
TLK1	9874	tousled-like kinase 1
TP53RK	112858	TP53 regulating kinase
TTK	7272	TTK protein kinase
TYK2	7297	tyrosine kinase 2
TYROBP	7305	TYRO protein tyrosine kinase binding protein
WNK4	65266	WNK lysine deficient protein kinase 4
YANK2	55351	STK32B, serine/threonine kinase 32B
ZAK	51776	sterile alpha motif and leucine zipper containing kinase AZK

4.2 HIGH-THROUGHPUT RNAi SCREEN IN LN18 AND U87MG GBM CELL LINES

Prior to the RNAi screening experiment, appropriate optimization was performed to ensure the robustness of the assay. RNAi screenings were performed on two different GBM cell lines harbouring two different mutations. The LN18 cells harbour TP53 mutation and wild type PTEN whilst U87MG cells have wild type TP53 and mutant PTEN. The presence of these associated genotype it serve as good representative model of highly proliferative GBM. Filtered 113 upregulated kinases genes were screened with pooled siRNA targeting each genes. Loss of cellular function following gene silencing was determined by measuring cell viability using resazurin based assay. The kinases were silenced using ONTARGETPlus SMARTpool siRNA library, targeting four different sites on each gene. A gene would only be considered to be a potential therapeutic target if the value fell below the cut-off point that was calculated by kMedian Absolute Deviation (+ or - kMAD). Different from z-score or SSMD, the cut off values were generated from normalisation between inter-plate variations. In this study, -kMAD was used for statistical calculation instead of +kMAD to identify potential "hits" with decreased activity.

To assess cell viability, Presto Blue resazurin base reagent were added in each 96-well plate after 96 hrs of incubation. Mixture was incubated for 1 hrs at 37C. Fluorescence signal were determined using ELISA plate reader. The –kMAD score of each cell line were calculated and sorted using scatter plots (Figure 4.1 and Figure 4.2). Visualisation of –kMAD by scatter plots clearly shows PLK1 consistently have the lowest –kMAD value and this was expected because siRNA for PLK1 is a positive control for each experimental plates. RNAi screening on LN18 identified 20 potential hits of which mostly involved in cell cycle and checkpoint control regulation namely *AURKA, CDKN1A, CDC2, NEK2, NEK8* and *TLK1* (Figure 4.1). In U87MG however, 22 potential hits were identified that plays critical role in various cellular pathways. Only *CDC2, STK33, TLK1, CLK2* and *CDKN3* are related to cell cycle and mitosis regulation (Figure 4.2).

To identify relevant kinase target for further functional investigations, “hits” list identified from previous statistical analysis were overlapped using Venn diagram (Figure 4.3A). Four kinases namely, *CDC2, TLK1, FLT3* and *LAK* were found to be overlapped in both cell lines. Other kinases list that was not overlapped are suggested to be cell line specific (Figure 4.3B). Further validation were performed on *CDC2, TLK1, FLT3* and *LAK* on a small scale basis. Figure 4.3C shows that only silencing *TLK1* significantly reduced the number of viable cells of which reduction is in between 10% to 40% ($p<0.05$). This leads to the selection of *TLK1* as potential investigative target for this project. *TLK1* was also selected because its functional role in GBM is not yet established.

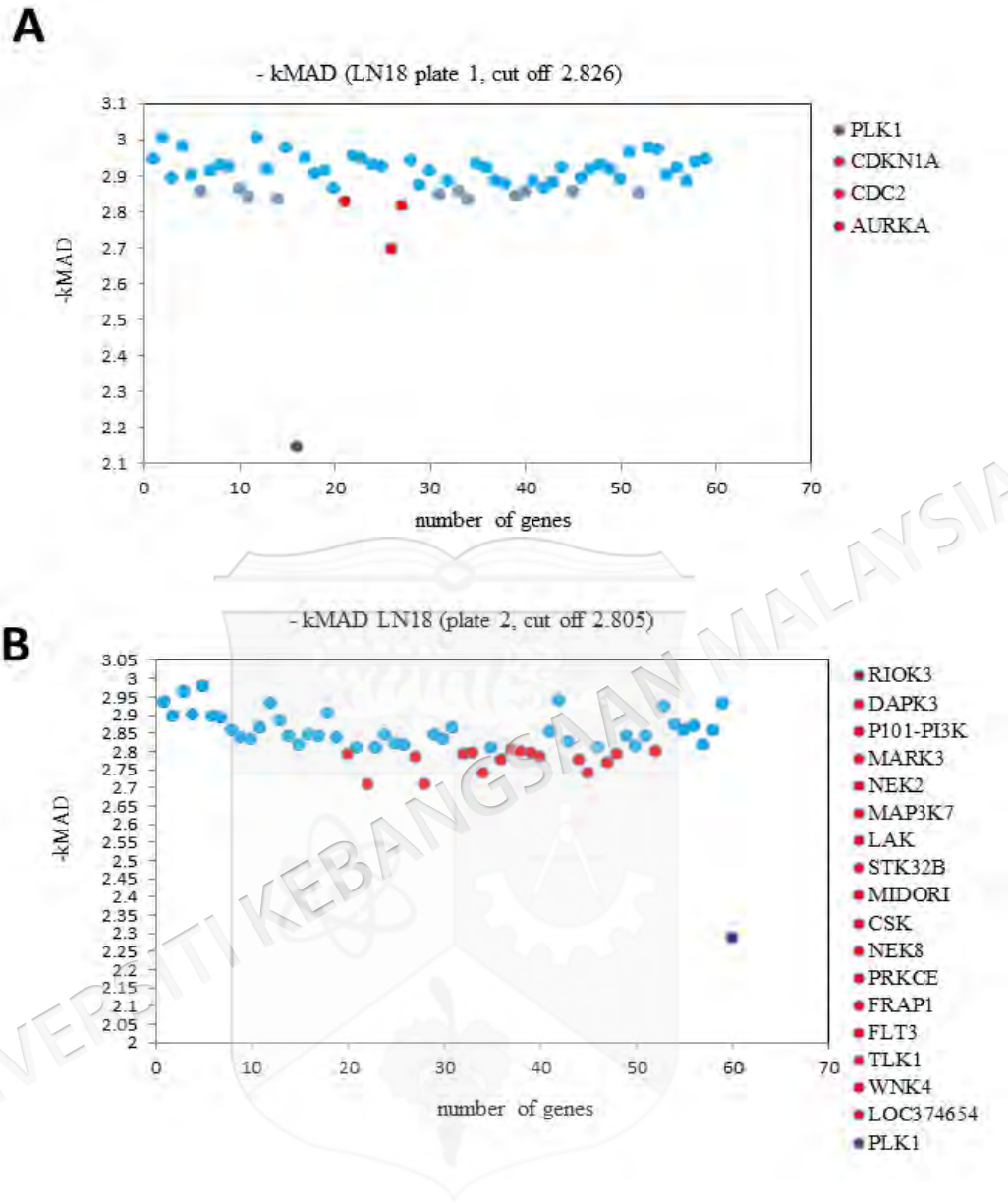

Figure 4.1 Visualization of RNAi screening -kMAD scatter plots in LN18 cells. Two different sets of 96-well plates were used for screening 113 kinase genes and different pools of siRNAs were coated inside each well. Calculation was made and each plate had their respective cut-off points. A) Plate 1 with cut-off point of 2.826 had three potential hits, namely *CDKN1A*, *CDC2* and *AURKA* (in red). PLK1 had the lowest value suggesting a robust positive control for the assay. B) Plate 2 had cut-off point of 2.805, with 17 hits with PLK1 also in the list suggesting a robust assay.

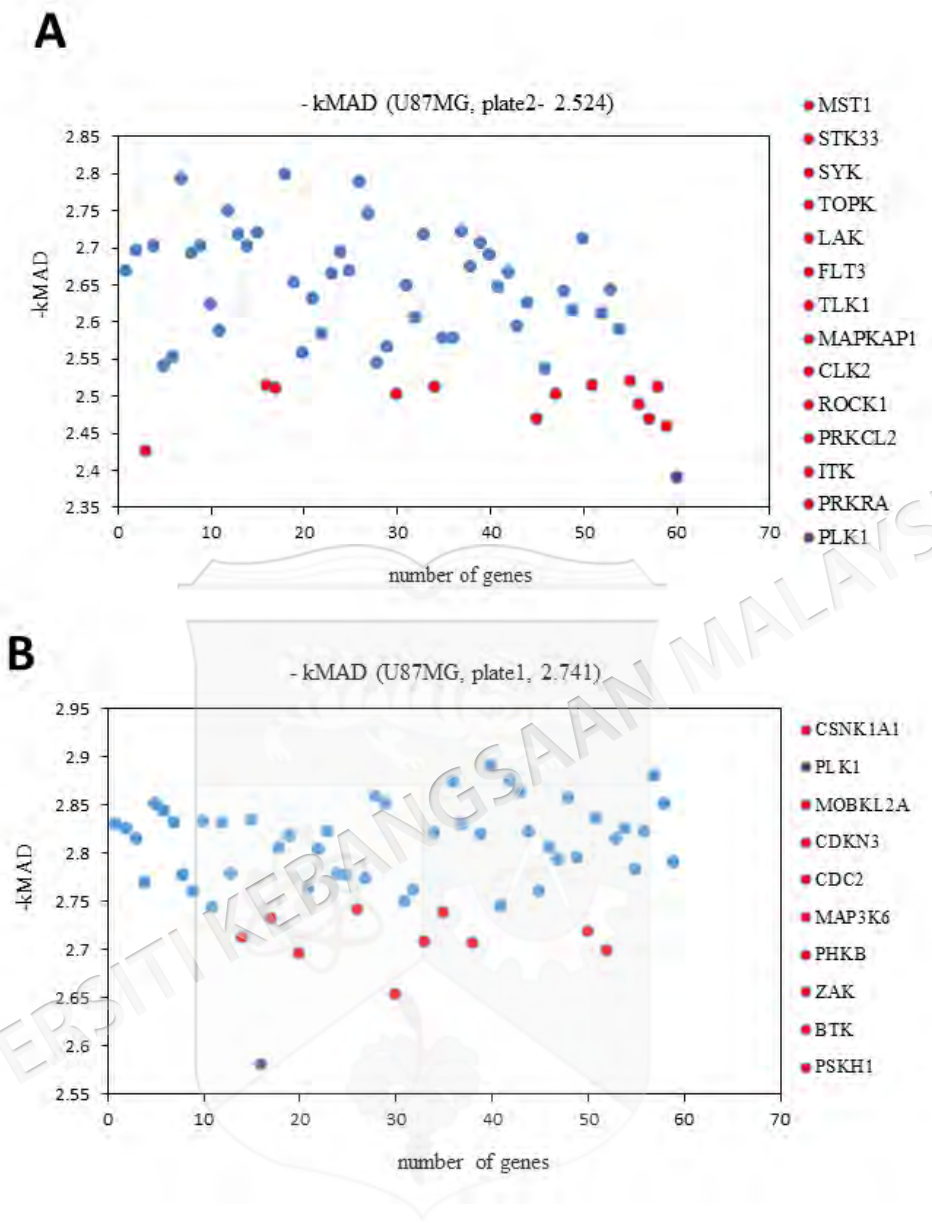

Figure 4.2 Visualization of RNAi screening -kMAD scatter plots in U87MG cells. Two different sets of 96-well plates were used for screening 113 genes and different pools of siRNAs were coated inside each well. Calculation was made and each plate had their respective cut-off points. A) Plate 1 with cut-off point of 2.525 had 13 potential hits labelled in red dots. PLK1 in purple dot had the lowest value suggesting a robust positive control for the assay. B) The second plate had cut-off point of 2.741, with nine hits in red dots with PLK1 (purple dot) also in the list suggesting robustness of this assay.

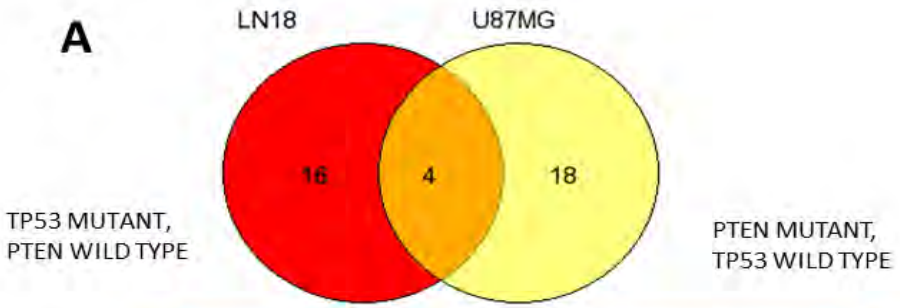

B

LN18	BOTH	U87MG
AURKA	CDC2	BTK
CDKN1A	FLT3	CDKN3
CSK	LAK	CLK2
DAPK3	TLK1	CSNK1A1
FRAP1		ITK
LOC374584		MAP3K6
MAP3K7		MAPKAP1
MARK3		MOBKL2A
MIDORI		MST1
NEK2		PHKB
NEK8		PRKCL2
P101-PI3K		PRKRA
PRKCE		PSKH1
RIOK3		ROCK1
STK32B		STK33
WNK4		SYK
		TOPK
		ZAK

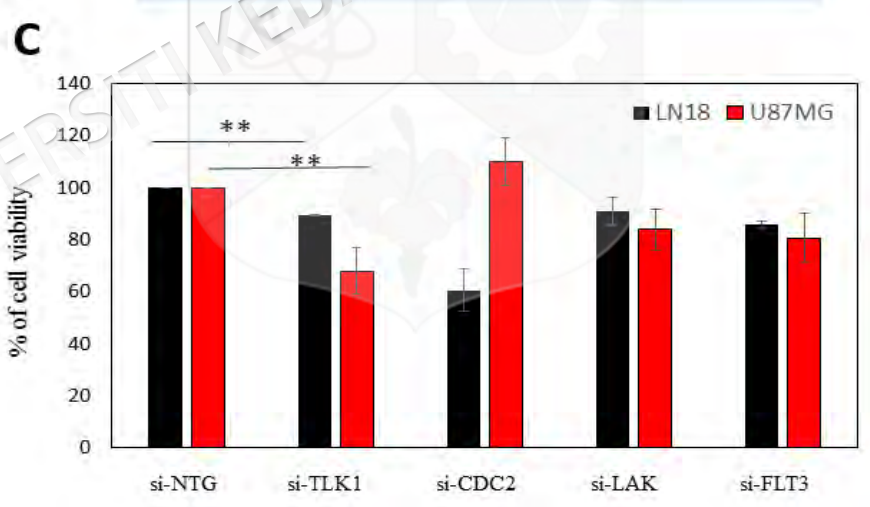

Figure 4.3 Identified potential hit genes from RNAi screen targeting the GBM kinome in LN18 and U87MG cell lines. Cells were transfected with 452 siRNA library targeting 113 kinases. Identification of hits was obtained from robust kMAD statistical analysis. A) Venn-diagram of genes identified from the analysis; 16 genes were identified in LN18 cells whilst U87MG had 18 potential hits. Four genes were consistently present in both cell line namely *CDC2*, *TLK1*, *FLT3* and *LAK*. B) The complete list of genes identified from RNAi screen C) Validation of four genes identified from RNAi screen.

4.3 EXPRESSION OF *TLK1* IN GBM CELL LINES

TLK1 expression was assessed in three different GBM cell lines namely U87MG, A172 and LN18. *TLK1* was highly expressed in U87MG (nine –fold), A172 (six –fold) and LN18 (four –fold), higher than normal human astrocytes. These results were also supported by bioinformatics data from European Bioinformatics Institute (EMBL-EBI) database in which *TLK1* was overexpressed in the proliferative subtype of GBM ($p<0.01$) as shown in Figure 4.4. For further experimental work, A172 is not being used because it is not tumorigenic although it contains *CDKN2A* and *PTEN* mutations.

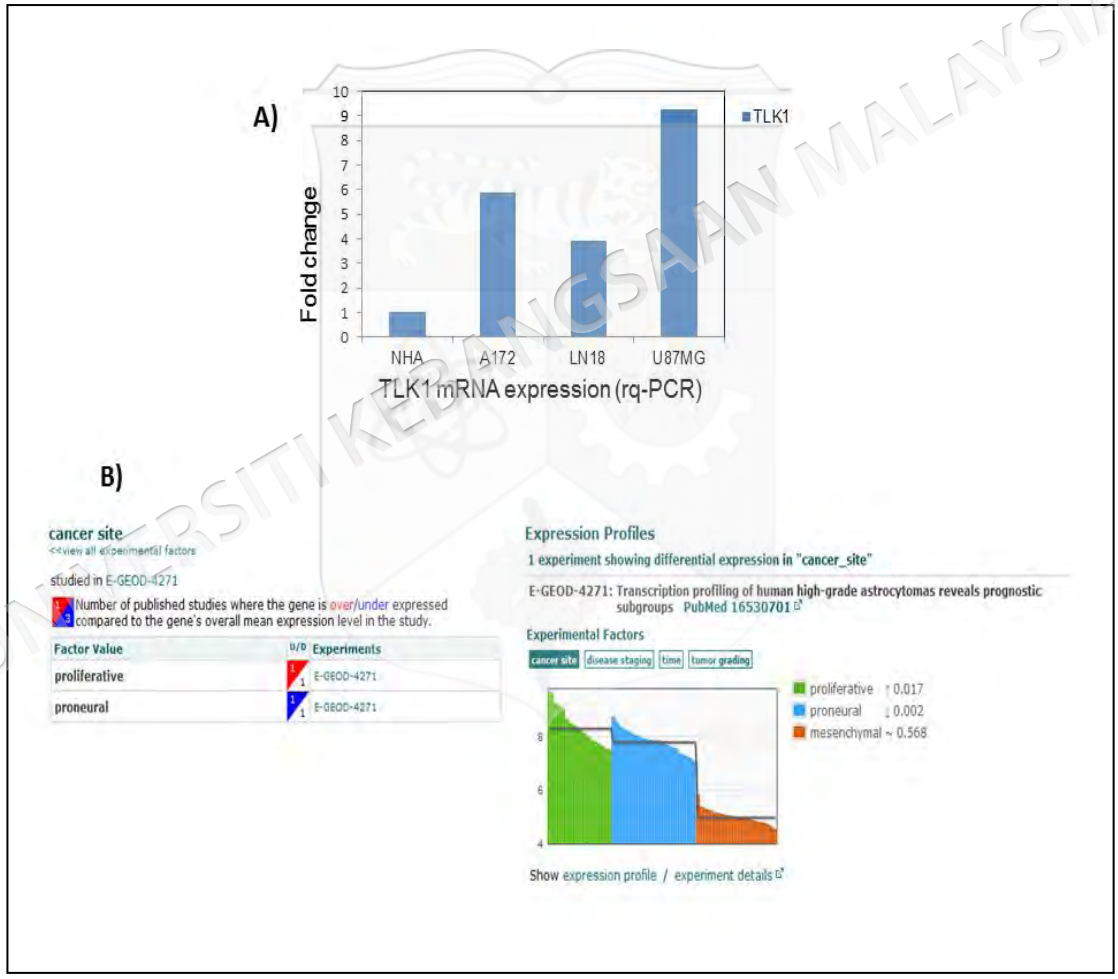

Figure 4.4 Expression of *TLK1* in GBM. A) qPCR identification of *TLK1* mRNA expression. *TLK1 i*s over-expressed in GBM compared to control cell lines (NHA= normal human astrocytes). B) The EMBL-EBI gene expression database showed that *TLK1* is overexpressed in the proliferative subtype of GBM.

4.4 ROLE OF TLK1 IN MODULATION OF SURVIVAL AND APOPTOSIS PATHWAYS

To test the functional effects of *TLK1*knockdown and overexpression in modulation of cell survival and apoptosis pathways, U87MG and LN18 cells were transfected with siRNA or shRNA transduced with pGIPZ lentivirus targeting *TLK1*. *TLK1* was also overexpressed in U87MG and LN18 cells using pLOC-orf-clones via viral transduction. Later, cell functions were investigated using several assays including Presto Blue resazurin based assay, Brdu proliferation assay, and ssdna apoptosis pathway.

4.4.1 Cell Viability Analysis

In order to analyse the impact of *TLK1* on GBM tumour cell survival, knockdown strategy using transient transfection of specific si-*TLK1* on U87MG and LN18. As shown in Figure 4.5A, *TLK1* mRNA level decreased by more than 80% and *TLK1* protein expression decreased significantly in si-*TLK1* transfected GBM cell lines. This resulted in morphological changes in both cell lines by presence of cell shrinkage, pyknotic and fragmented nuclei. This observation was supported by quantitative measurement of percentage of viable cells whereby si-*TLK1* cells have reduced number of viable cells significantly compared with non-targeting control (NTG) after 72hrs of incubation (Figure 4.5B).

To ensure the results obtained was not due to the off-target effects in siRNA, we also used shRNA by stably transducing it into GBM cells using pGIPZ lentivirus. Two different sequences of shRNA was used namely sh-TLK1-461 and sh-TLK1-455. Transduction efficiency of *TLK1* mRNA shows more than 40% knockdown (Figure 4.6A). Fluorescence imaging of GFP transduced GBM cells shows green fluorescence protein (GFP) signals were present by up to 70% each field (Figure 4.6B). Measurement of GFP signals by flow cytometer also shows successful transduction in both GBM cell lines especially those transduced with sh-*TLK1*-461 (Figure 4.6C). Two shRNA were also used to determine the effect at cell viability level (Please refer to Appendix E).

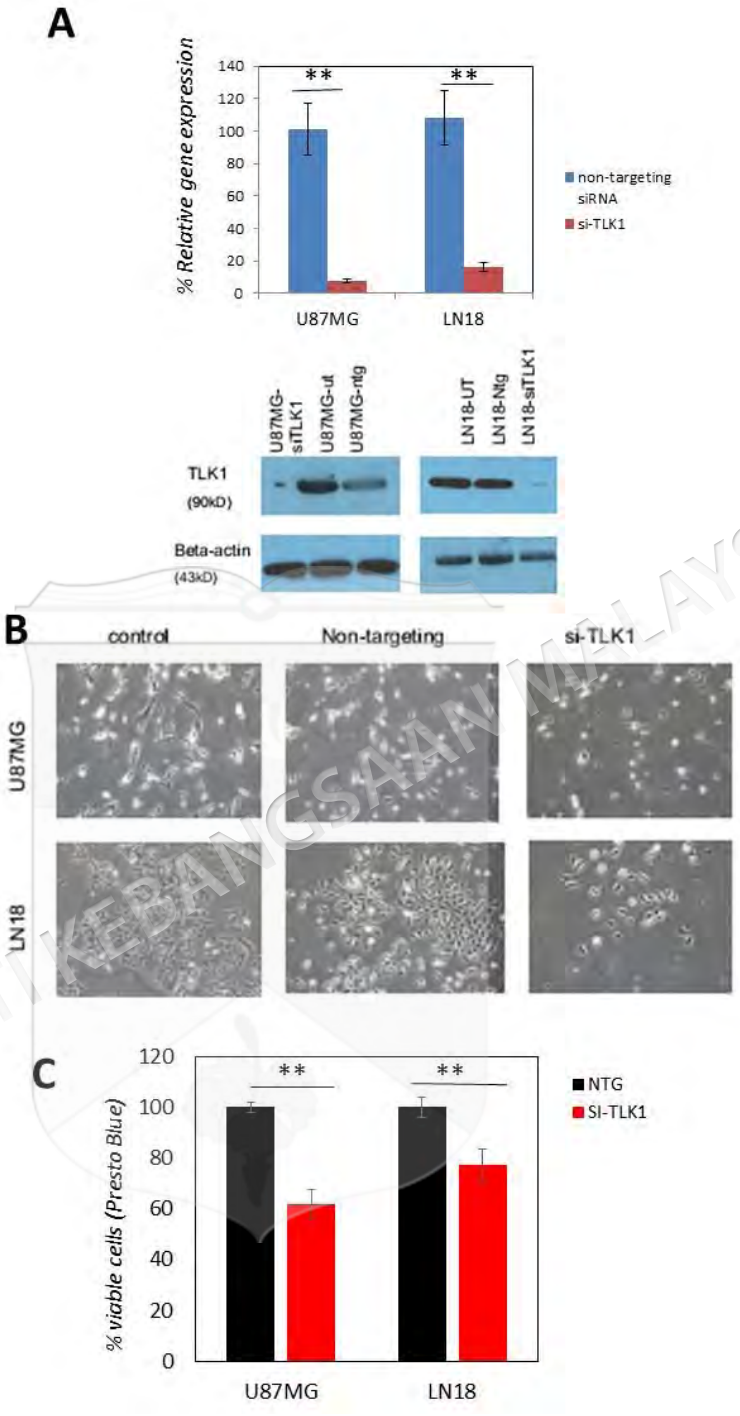

Figure 4.5 Silencing *TLK1* in GBM cells reduced cell viability. A) Transfection efficiency was determined by using qPCR. Silencing *TLK1* in both cell lines were effective with >80% of transfection efficiency. Western blot analysis shows successful knockdown at protein level at 72 hrs. B) Morphological changes seen through light microscopy after 72 hrs of transfection in both cell lines whereby number of live cells were reduced. C) Validation of *TLK1* silencing using ONTARGET Plus TLK-siRNA reveals significant reduction of U87MG and LN18 cells by 40% and 20% respectively at 72 hrs.

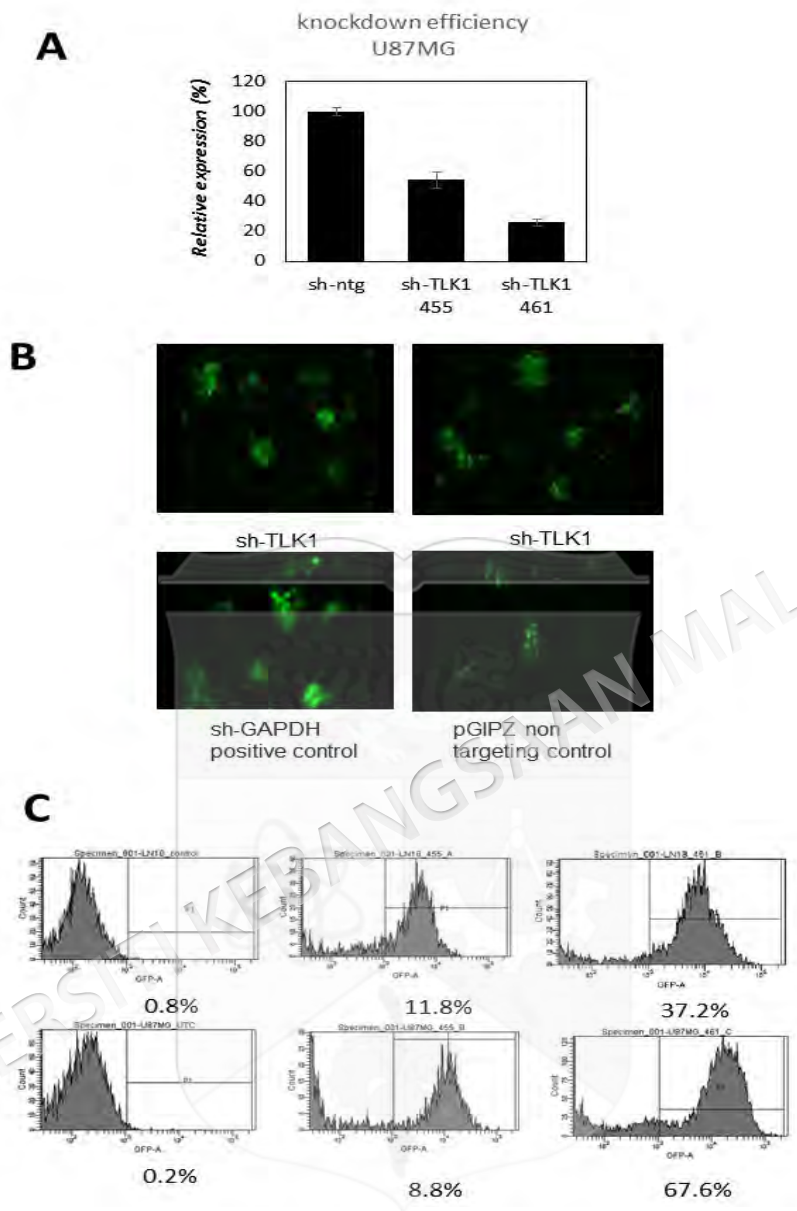

Figure 4.6 TLK1 knockdown via transduction of pGIPZ-shTLK1 lentiviral delivery. A) Knockdown efficiency was determined by qPCR where sh-TLK1-461 had a better efficiency compared with sh-TLK1-455. B) Fluorescence images of GFP in U87MG cells indicating successful transduction. GFP signals reached up to 70% in each microscopic field. Results of transduced sh-TLK1 was comparable with pGIPZ positive GAPDH control and non-targeting control. C) GFP signals from transduced LN18 (top) and U87MG (bottom).

4.4.2 Apoptosis and Proliferation Analysis

To validate the mechanism involved causing reduced number of viable cells due to *TLK1* knockdown, apoptosis and proliferation assay were performed. Si-*TLK1* caused increased in ssDNA apoptosis signals by 0.2 in LN18 and 0.4 in U87MG cell line (Figure 4.7A) in comparison with their respective non-targeting controls. As shown in Figure 4.7B, silencing TLK1 consistently increased by 50% in U87MG cells and this is in line with known targets namely TTK and MAPK1 that when silenced will increased apoptosis signals in GBM cells. Proliferative capability characterised by DNA synthesis inhibition was significantly inhibited in U87MG transduced with sh-TLK1-461 only but not in others (Figure 4.7C). Hence, this may suggest activation of a particular rescue pathway mechanism.

Since apoptosis signals were observed in both GBM cell lines using ssDNA apoptosis assays, characterization of specific caspases activation was performed using caspase 3-7 activation assay. Qualitative fluorescence imaging using confocal microscopy shows increased in DEVD-complex formation by presence of green dots as shown in Figure 4.8.

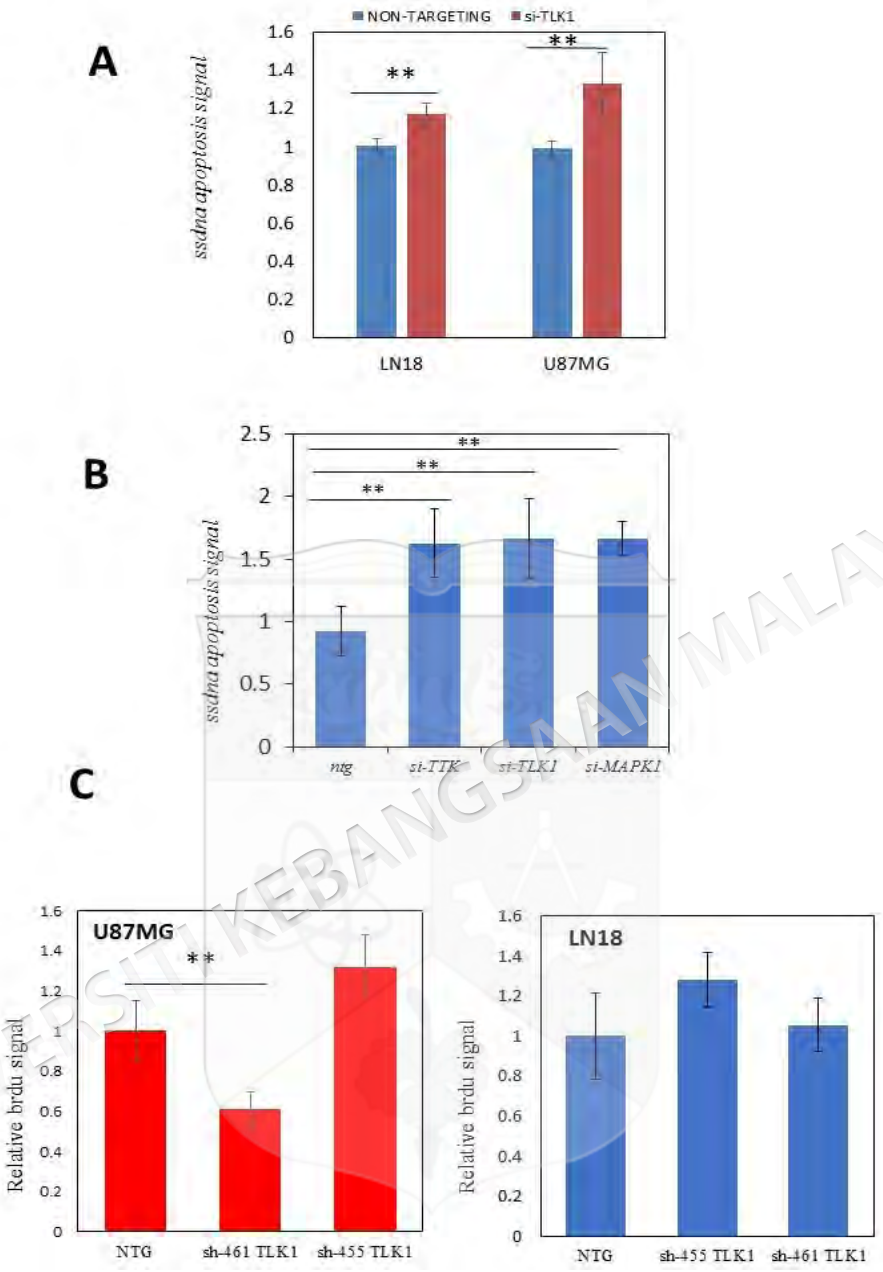

Figure 4.7 Apoptosis effect due to TLK1 silencing in GBM cells. A) Cells were transfected for 48 hrs and later apoptosis signals were detected using single stranded apoptosis ELISA base assay (Chemicon, USA). Each data was normalised with non-targeting siRNA control. Significant increase in ssdna signal in U87MG cells was observed compared to LN18 (**p<0.05). B) *TLK1* knockdown showed significant increase in apoptosis signal similar with the two previously reported potential cancer targets, *MAPK1* and *TTK* kinase in U87MG (**p<0.05). C) To assess proliferative capability of GBM cells, BrdU proliferation assay (Chemicon, USA) was performed at 24 hrs on GBM cells that had been transduced with GIPZ sh-TLK1 and TLK1-lentiorf clones. Significant reduction in BrdU signal was seen in U87MG treated with sh-TLK1-461 only compared to sh-NTG (**p<0.05).

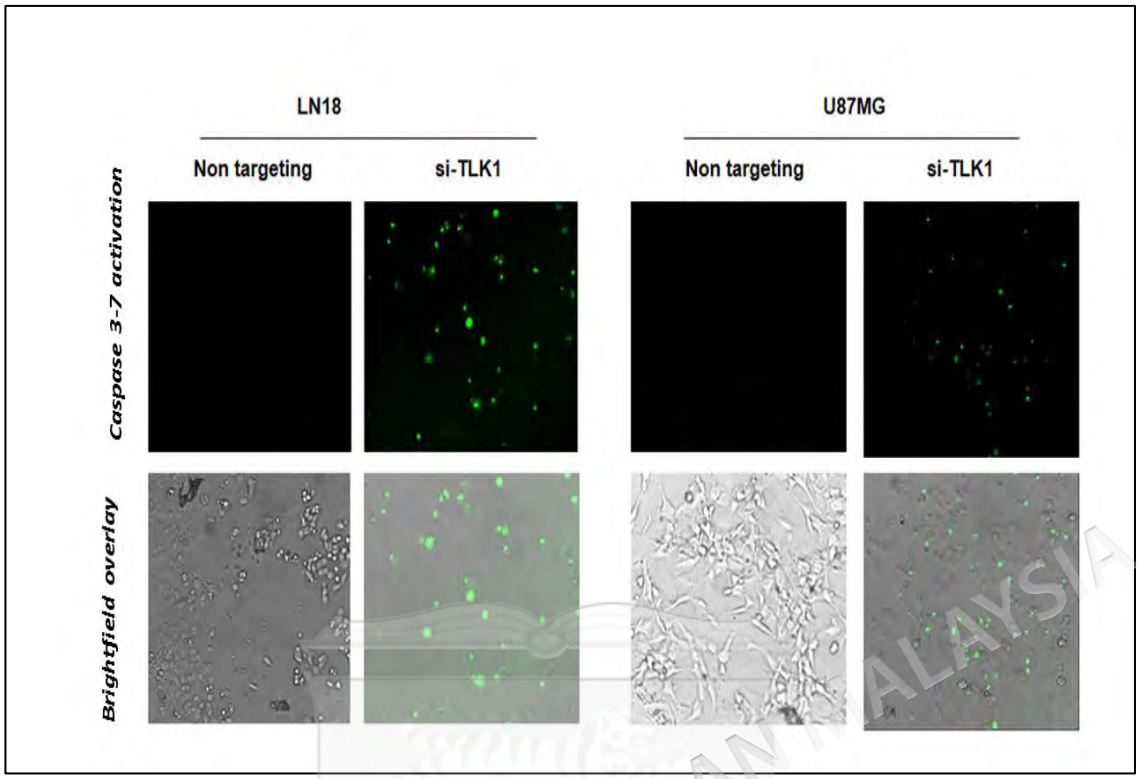

Figure 4.8 Confirmation of the caspase 3-7 apoptotic pathway involvement due to TLK1 silencing by qualitative analysis observed in LN18 and U87MG cells. Results has been taken from confocal microscopy analysis (Leica, Germany). Note that green dots represent the formation of DEVD-complex due to caspase 3-7 activation.

4.4.3 Chemosensitization Effect of TLK1 Silencing with TMZ

Silencing of *TLK1* has been previously reported as a suitable chemosensitising agent in cholangiocarcinoma (Takayama et al. 2010). To test if the effect of silencing *TLK1* as a sensitising agent towards conventional chemotherapy such as TMZ is similar in GBM, U87MG cells were treated with sub-lethal dose of TMZ 250 µM and 25 nM of si-*TLK1*. Silencing of *TLK1* in combination with sublethal dose of TMZ in GBM cell lines especially in U87MG showed chemo-sensitisation effect compared with silencing *TLK1* alone (Figure 4.9A). Prior to this experiment, the sub-lethal dosage of TMZ which is 1:10 of TMZ IC50 dose in both U87MG and LN18 cell lines was determined by performing TMZ titration assay as mentioned in Appendix I.

Assessment of colony formation in cells treated with TMZ and si-TLK1 in both U87MG and LN18 cells showed significant sensitization effect when combined with TMZ by significant reduction of colony growth after 14 days of incubation (**$p<0.05$) (Figure 4.9B). Note that this experiment data was normalized with their appropriate controls. This finding is consistent with Takayama et al. (2010) suggesting that TLK1 might be a potential sensitising agent for cancer therapy.

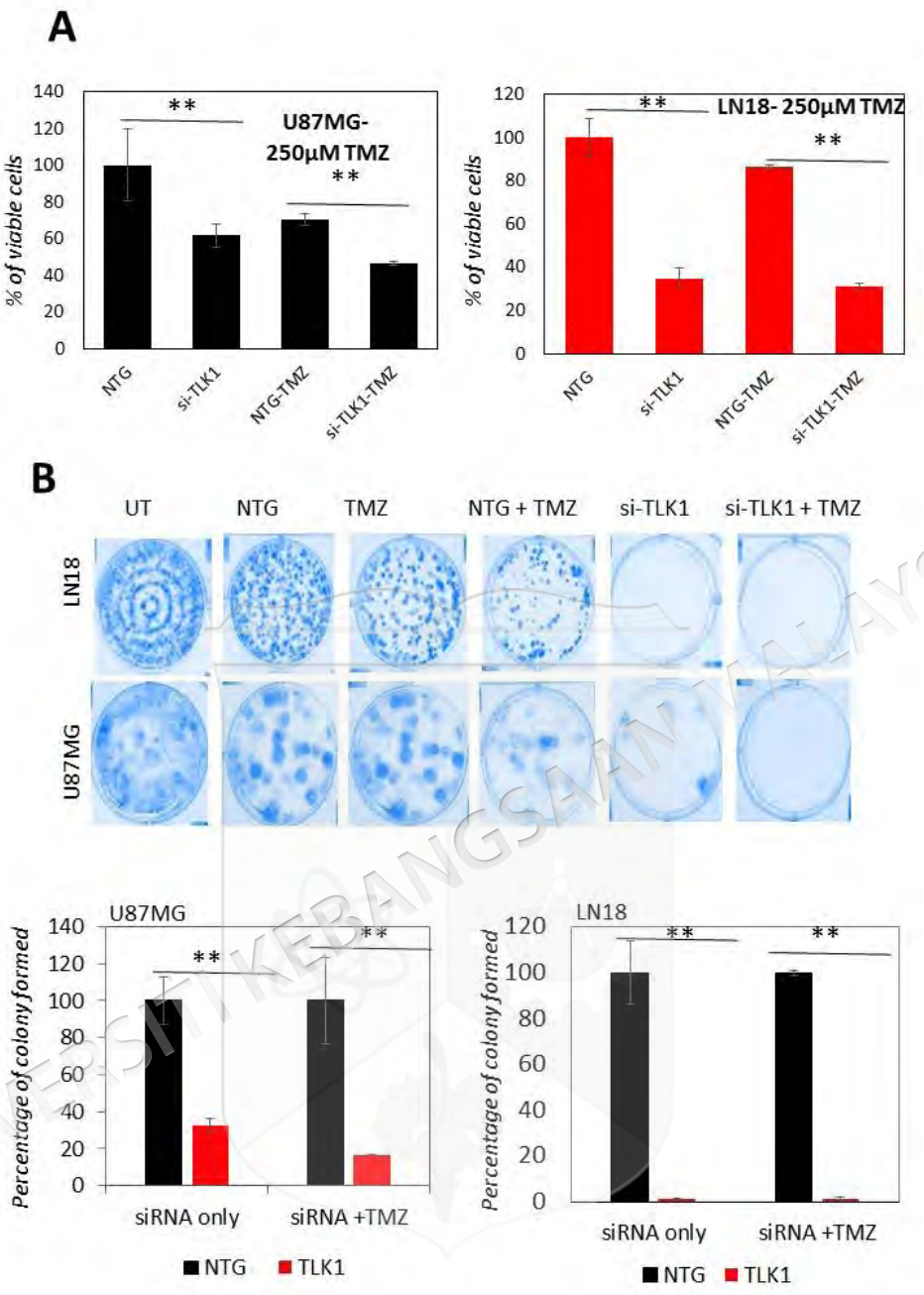

Figure 4.9 *TLK1* silencing sensitizes GBM cells to TMZ. A) GBM cells were transfected with pool TLK1 siRNA for 48 hrs. Cells were later treated with sub-lethal dose of TMZ (250 µM) for the next 48 hrs and the percentage for viable cells were measured using cell viability reagent. Chemosensitization effect were measured by normalizing si-*TLK1* vs. si-*TLK1* combined with TMZ (250 µM). U87MG and LN18 cells showed significant sensitization effect (**p<0.05). B) Colony formation assessment on GBM cells treated with si-*TLK1* and si-*TLK1* combined with TMZ. After 96 hrs, cells were harvested and were counted. Each 6-well plate contained 100 cells. Cells were left to grow for 14 days and was later stained with 0.5% crystal violet. From colony assay it was also shown that silencing TLK1 sensitised GBM cells to TMZ (**p<0.05).

4.4.4 Effects of TLK1 Overexpression in GBM Cells

Knockdown of TLK1 has been shown to reduce cell proliferation and apoptosis in GBM cells. To test the effect of TLK1 overexpression in U87MG cells, the expression of TLK1 was increased using pLOC-orf-clones by lentiviral delivery. Analysis using qPCR was performed after 96 hrs of transduction and showed that *TLK1* expression increased up to 20 fold compared to U87MG empty-RFP-vector control as shown in Figure 4.10A. Indeed, transduction efficiency of TLK1 orf-clones was successfully observed by presence of GFP signals via fluorescence imaging (Figure 4.10A).

In cells overexpressing *TLK1*, cell proliferation was increased (Figure 4.10C) characterised by increased of cell viability by 40% compared to non-targeting control and increased in the clonogenic potential (Figure 4.10C and Figure 4.10D) as well as resistance towards apoptosis by decreased in annexin-V signal (Figure 4.10E) when cells were treated with 2.5 mM of TMZ promoting resistance. The increased Brdu signal suggests that the capacity of DNA synthesis was significantly high in cells overexpressing *TLK1* (Figure 4.10F). Although from mRNA expression analysis LN18 shows lower TLK1 expression compared with U87MG, this cell line is phenotypically highly proliferative compared with U87MG. Hence this gives difficulty for us to perform transduction of orf clones since LN18 gets confluence fast. U87MG was chosen for overexpression also because in knockdown experiment, most of the important functional assays was performed using U87MG. This would allow validation of functional consequences in the same cell line.

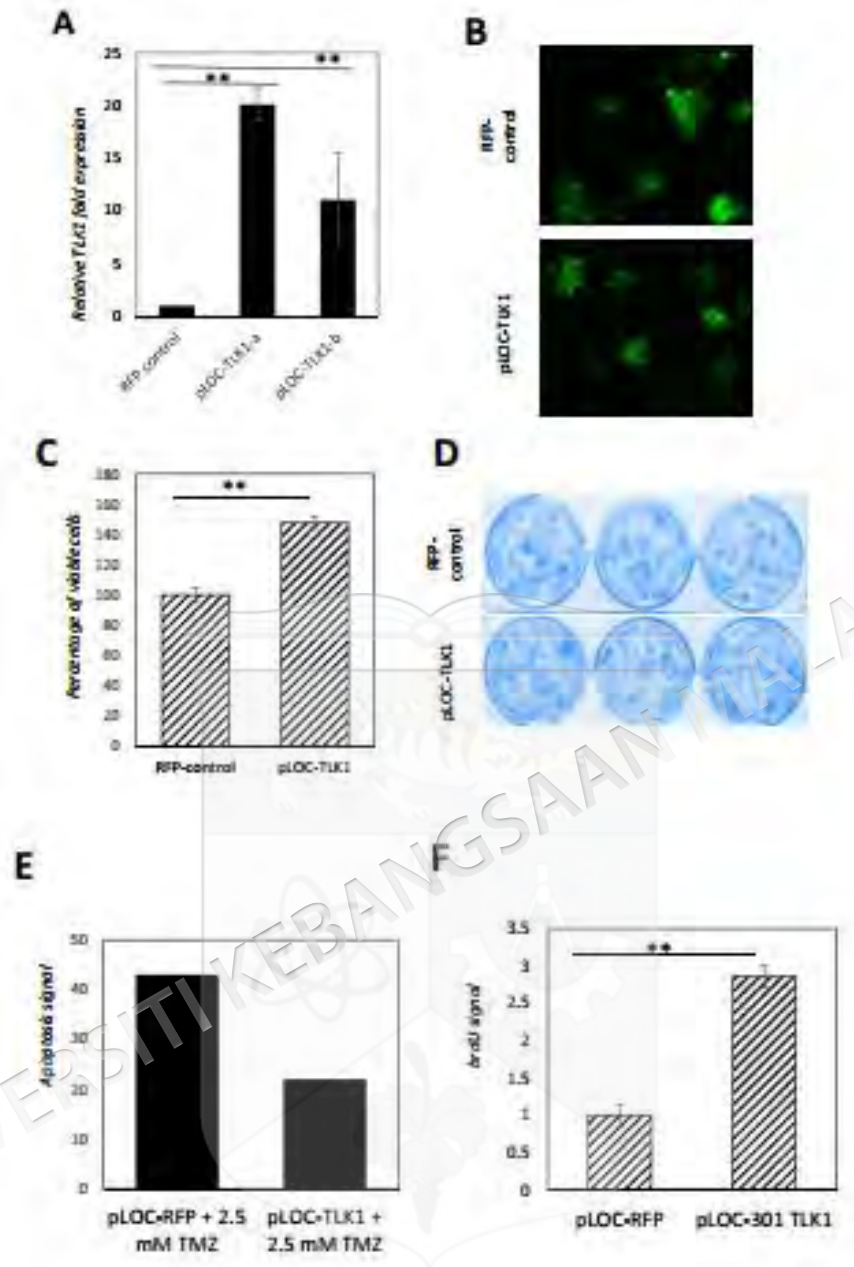

Figure 4.10 Effects of pLOC-TLK1 orf clones transduction in U87MG. A) Expression of TLK1 mRNA after it had been transduced with pLOC-TLK1 orf clones. TLK1 expression increased by almost 20 folds. B) Successful transduced cells were monitored using Nikon Fluorescence microscopy by observing presence of GFP signals in each cells. C) Overexpression of TLK1 in the transduced U87MG cells leads to increased number of viable cells by 40%. D) Proliferative capability of U87MG-pLOC-TLK1 clones have increased as shown by an increase in the number of clones in the six-well plates. GBM cells clones were stained with 0.5% crystal violet after 14 days of incubation. E) Apoptosis signal decreased by 50% in U87MG transduced cells. Apoptosis signal was detected using Annexin-V stain (Roche, Germany) and measured using TALI Fluorescence Imager (Life Technologies, USA). F) Increased of Brdu signal in TLK1 overexpressing cells.

4.4.5 Cell Cycle Analysis

Cell cycle analysis using fluorescence base flow cytometry allows determination of specific cell cycle which have been arrested during *TLK1* knockdown in GBM cells. Findings were validated using siRNA and shRNA as well as open reading frame clones for overexpression. TLK1 knockdown by siRNA and shRNA significantly increased the S-phase cells population in U87MG (Figure 4.11A and Figure 4.12C) However, in LN18, although S-phase was increased when silenced with siRNA (Figure 4.11B), in shRNA knockdown LN18 cells, only G0G1 cycle was increased (Figure 4.12A).

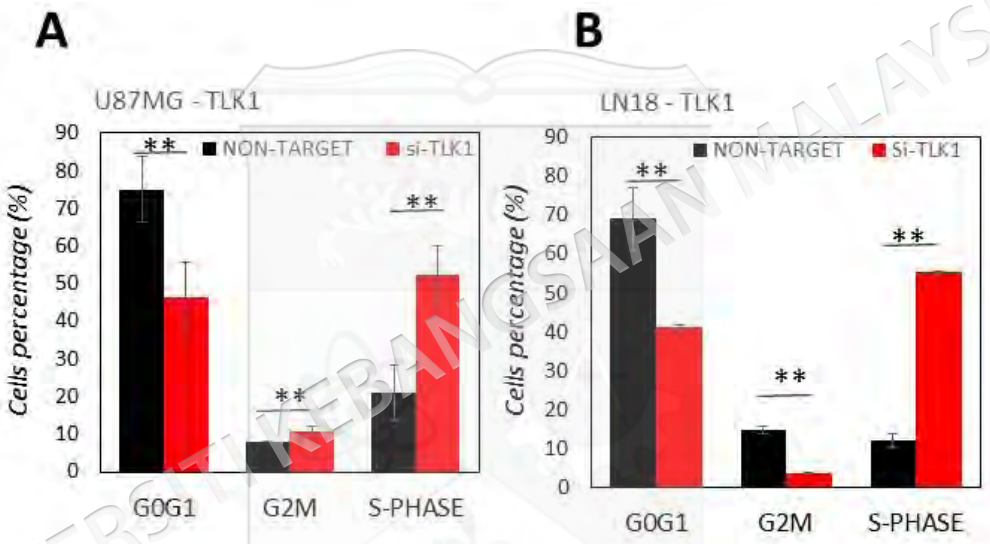

Figure 4.11 Cell cycle analysis on transiently transfected GBM cells. A) U87MG was transfected using SMARTPool si-TLK1and after 48hrs of transfection, cell cycle analysis was performed using BD-cell cycle analysis kit. There was significant increase in the number of cells ($p<0.05$) at S-phase, G2M phase as well as G0G1 phase. B) LN18 was transfected with si-TLK1 and similar analysis was performed. There was markedly increased in S-pahse cells and decrease significantly ($p<0.05$) in G0G1 cells. Contradict with U87MG, LN18 cells shows significant decreased ($p<0.05$) of cells at G2M phase. All experiments were performed in triplicates and results were compared with non-targeting siRNA control.

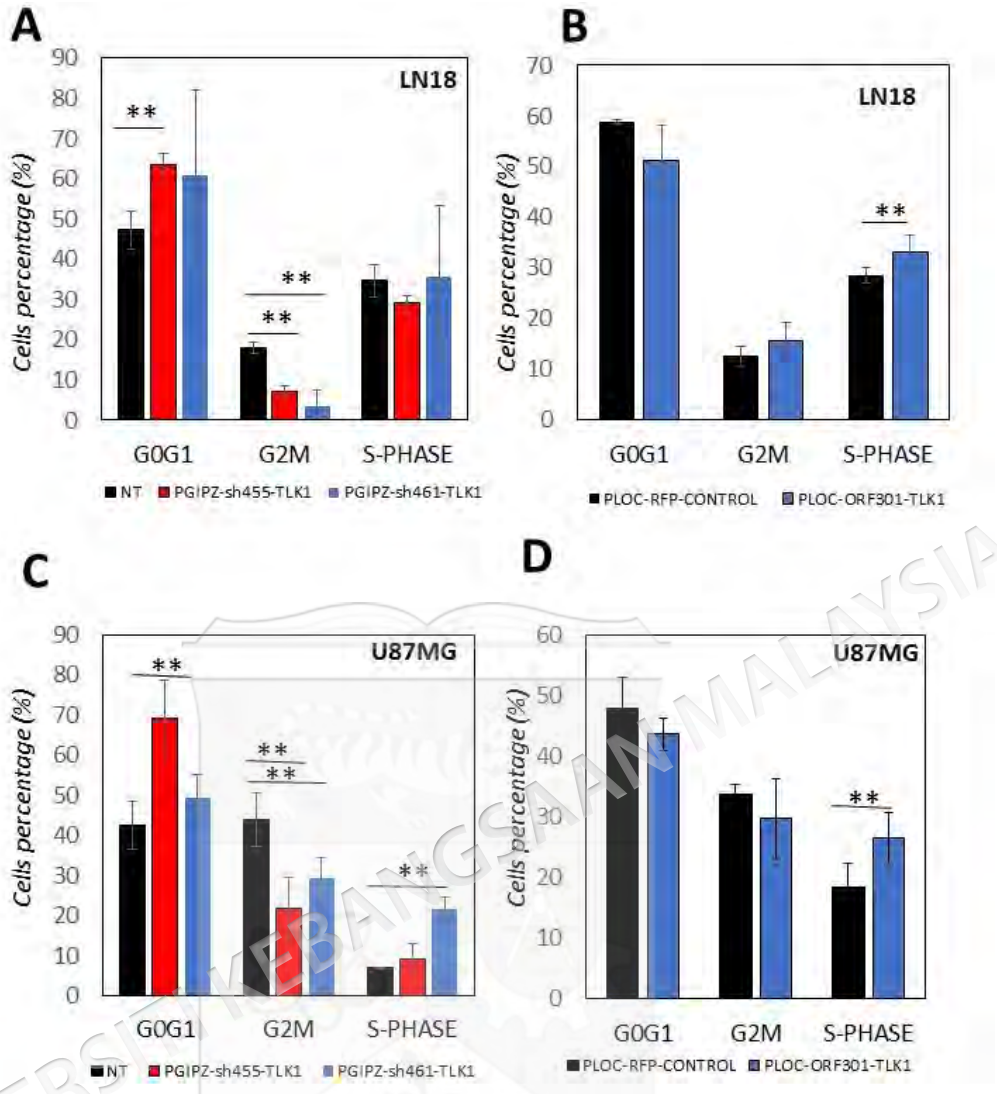

Figure 4.12 Cell cycle analysis on tansduced GBM cells with sh-*TLK1* and orf clones. GBM cells were transduced and after 96 hrs, cell cycle analysis was performed using ModFit LT. A) TLK1 knockdown by sh-TLK1-455 in LN18 cells causes significant increase of G0G1 cells ($p<0.05$). Significant decrease in the number of cells at G2M phase was observed in both sh-*TLK1*-455 and sh-*TLK1*-461. B) LN18 cells that have been transduced with orf-clones shows minor increase of cells at S-phase ($p<0.05$) by 4.68% . C) U87MG cells that was knocked down with sh-*TLK1*-455 and sh-TLK1-461 show significant increase ($p<0.05$) of signals at G2M phase and S-phase. However, only sh-*TLK1*-455 shows significant increase ($p<0.05$) in GOG1 signal. D) Results from U87MG transduced with orf-clones was in concordant with LN18 cells whereby significant increase in the number of cells was observed. Experiments were performed in triplicates and results were compared with their respective controls.

4.5 TLK1 IN REGULATION OF INVASION AND MIGRATION PATHWAYS

GBM cells have the ability to aggressively infiltrate or invade into the normal brain tissues and along the vascular tracks, which hinders complete resection of all malignant cells and limits the effect of localized radiotherapy while sparing normal tissue. Although anti-angiogenic treatment exerts anti-edematic effect in GBM, unfortunately, tumours progress with acquired increased invasiveness. Therefore, it is an important task to gain a deeper understanding of the intrinsic and post-treatment invasive phenotypes of GBM in hopes that the gained knowledge would lead to novel GBM treatments that are more effective and less toxic.

In this study, the roles of *TLK1* in GBM cancer invasion and migration were investigated. Hence, to test functional role of *TLK1* knockdown and overexpressing cells in GBM cell invasion and cell motility, transwell invasion and migration assay as well as wound healing assay were performed.

4.5.1 Effects of TLK1 Silencing on Migration and Invasion

Transfected si-*TLK1* LN18 cells had more reduction of cell migration (30%) compared with si-*TLK1* U87MG cells (20%). However, in migration assay, 50% of U87MG cells were inhibited compared with only 20% in LN18 cells (Figure 4.13 A). Validation on transduced U87MG cells with sh-*TLK1* resulted in almost 50% reduction in cell invasion and migration. However, in *TLK1* overexpressing cells, there was significant increase in cell migration and invasion by 20% and 50% respectively (Figure 4.13 B).

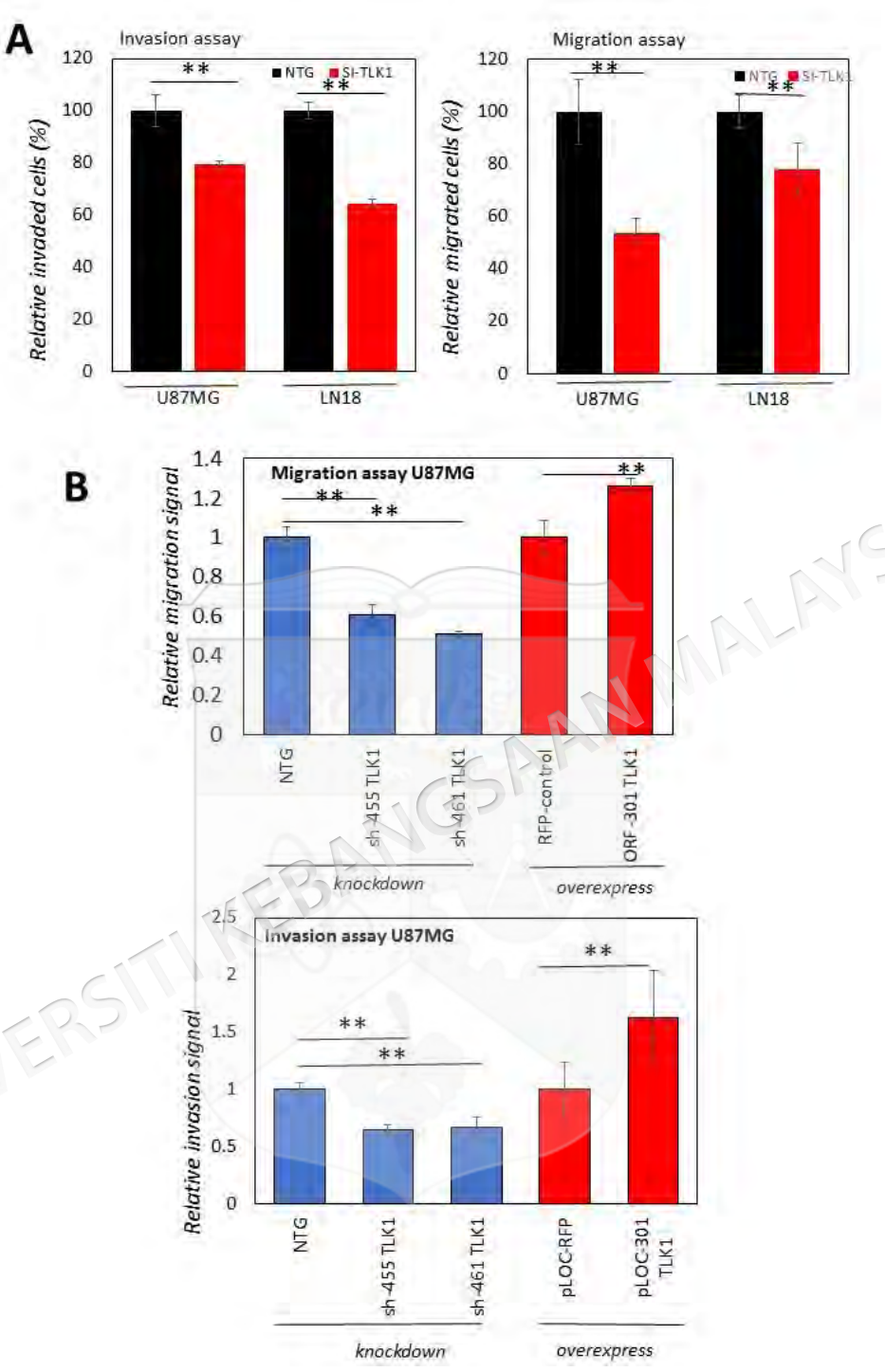

Figure 4.13 Effects of TLK1 silencing on GBM invasion using flourometric based invasion andmigration assay. A) Transfection of si-TLK1 in LN18 and U87MG cells reduces the invasion signals significantly ($p<0.05$) compared with non-targeting control. B) Parental U87MG cells transduced with pGIPZ-sh-TLK1 and pLOC-TLK1-orf clones. Invasion and migration of U87MG cells were inhibited significantly, whilst cells overexpressed with orf clones showed significant increase in their invasion and migratory capacity within the extracellular matrix.

4.5.2 Wound Healing Analysis

Cellular motility as measured by qualitative wound healing assay was performed on LN18 cells but not U87MG cells. This was because when U87MG cells reached their confluence level, they became spheres, hence difficult to perform scratching experiment with the pipette (please refer Appendix E, page 180). Photomicrographs show that the wound closures in knockdown TLK1 cells were slower than non-targeting control and untreated control cells at 24 hrs and 48 hrs (Figure 4.14). However, in TLK1 overexpressing cells, the wound closure was much aggressive compared with pLOC-RFP-vector control and untreated cells (Figure 4.15). Reduced invasion and migration in GBM cells are not affected by 'off-target' effect due to the reduction in cell viability induced by increased in apoptosis signal. GBM cells were grown to reach 80% confluency and after that all non-viable cells were centrifuged and removed during washing. Residual cells were later grown in serum free media for 24 hrs. Therefore, cells harvested after the culture are purely invasive cells in nature and not highly proliferative cells of which their cells might be affected by sirna and shrna knockdown.

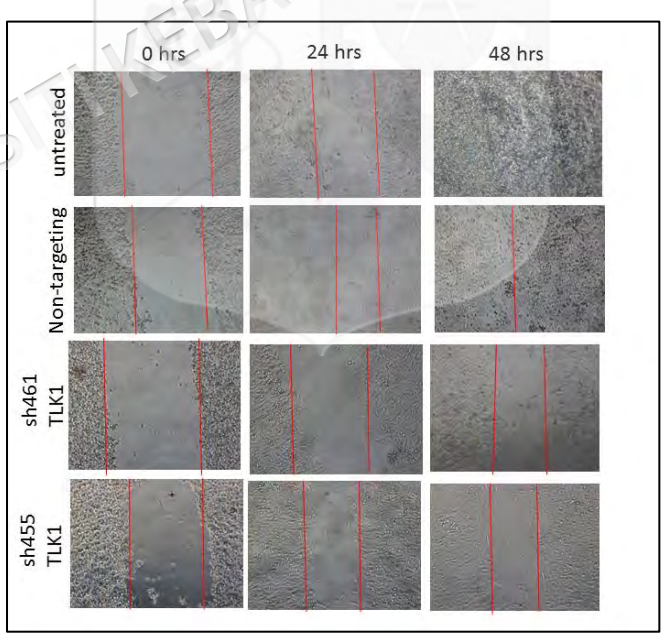

Figure 4.14 Effect of TLK1 knockdown in LN18 cells in wound healing. Stably transduced GIPZ sh-TLK1 LN18 cells were scratched with 200 µl pipette tip at 0 hr. Observations on wound closure were made at 24 hrs and 48 hrs. At each time point, wound closure was photographed under a phase contrast microscope. Wound was still maintained during 48 hrs observation.

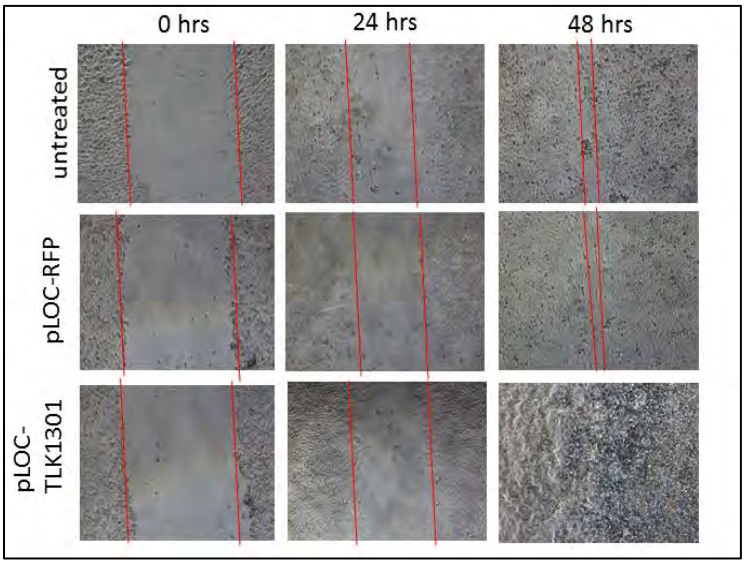

Figure 4.15 Effect of lentiorf TLK1 overexpression in LN18 cells. Stably transduced TLK1-lentiorf clones LN18 cells were scratched with 200 µl pipette tip at 0 hr. Observations on wound closure were made at 24 hrs and 48 hrs. At each time point, wound closure was photographed under a phase contrast microscope. Overexpressed TLK1 cells wound was completely closed during 48 hrs observation compared with pLOC-RFP control cells and untreated LN18 cells.

4.5.3 Analysis on Cell Adhesion

An important aspect of cancer invasion is the involvement of cell adhesion complexed with various type of extracellular matrix commonly named as fibronection, collagen 1, collagen 4, laminin, and fibrinogen. Knockdown of TLK1 using siRNA caused significant increase in U87MG cells to collagen 1 and laminin adhesion (Figure 4.16). This was consistently shown in stable TLK1 knockdown U87MG and LN18 cells whereby adhesion of cells to laminin was increased significantly. However, in TLK1 overexpressing U87MG cells, adhesion of cells to laminin was decreased significantly (Figure 4.17). Although cell adhesion to laminin was reduced in TLK1 overexpressing LN18 cells, this result was not statistically significant.

TLK1 knockdown U87MG and LN18 cells were consistently showing similar binding patterns to fibronectin whereby cell adhesion to fibronectin was increased in TLK1 knockdown cells but decreased in TLK1 overexpressing U87MG and LN18 cells (Figure 4.17).

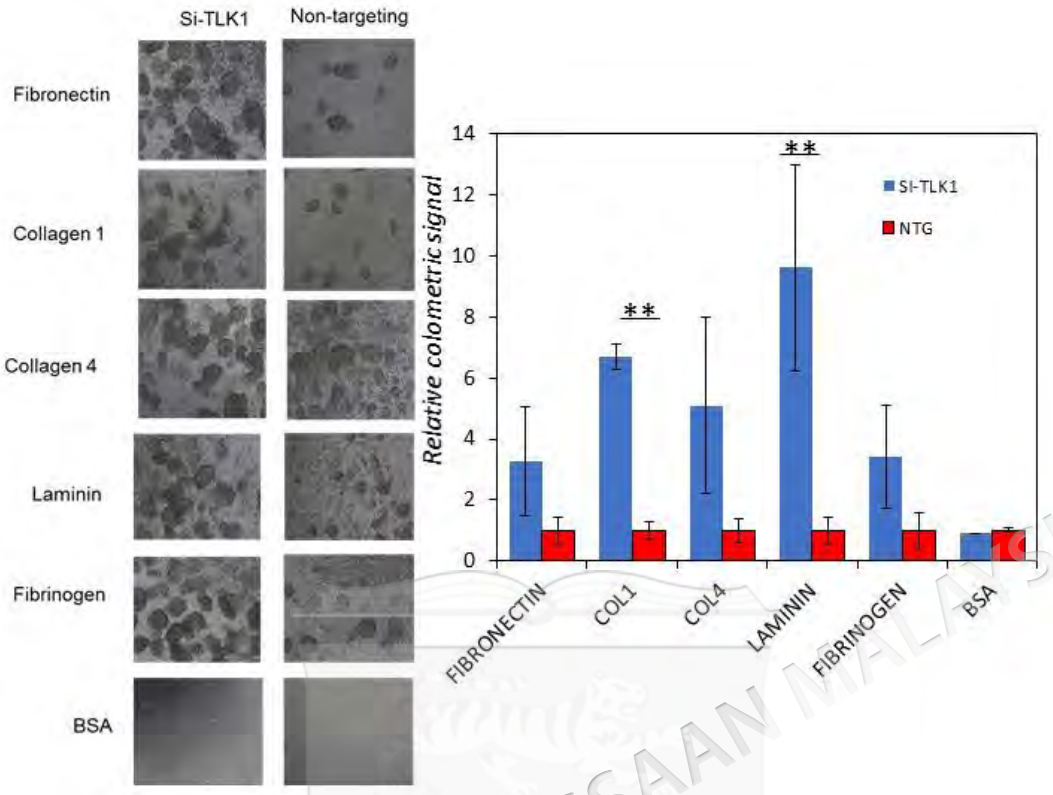

Figure 4.16 Effect of TLK1 knockdown using siRNA in U87MG cells on cell adhesion in the ECM-array (Cell Biolabs, USA). On the left was the representative micrographs of U87MG transfected cells on ECM-array containing fibronection, collagen I, collagen IV, laminin, and fibrinogen. Cell adhesion effect analysis is shown on the right. Knockdown of TLK1 increases binding of U87MG cells to collagen 1 by seven fold and laminin by almost nine fold. Statistical analysis was performed using Student's unpaired t-test (**$p<0.05$) and the experiment was performed in triplicates.

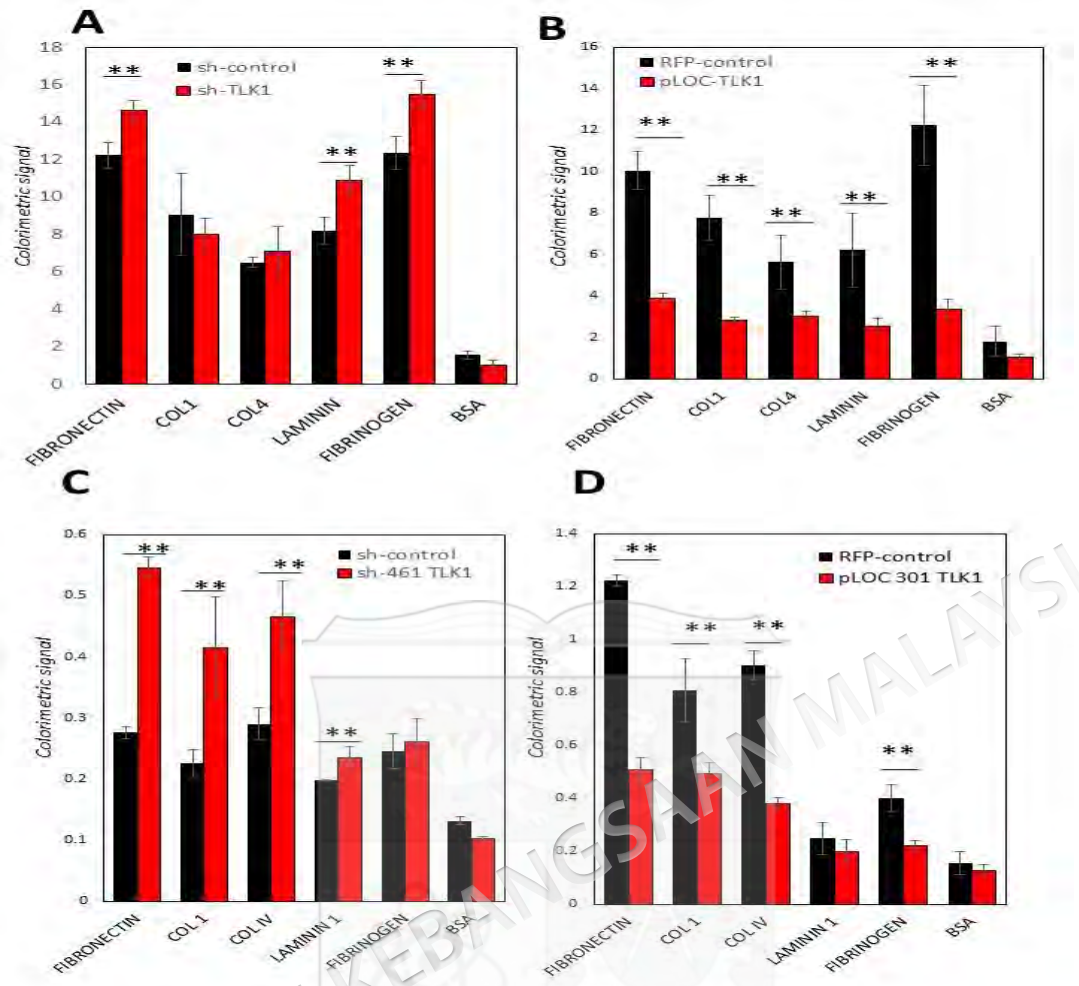

Figure 4.17 Cell adhesion analysis on GBM cells transduced with pGIPZ TLK1 sh-RNA and pLOC-TLK1 orf clones. A) U87MG cells with TLK1 knockdown show significant increased in the capacity of cells adhered to fibronection, laminin and fibrinogen. B) In overexpressed TLK1 U87MG cells, however, show significant decreased in cell adhesion towards fibronectin, collagen I, collagen IV, laminin and fibrinogen. C) LN18 cells with TLK1 knockdown shows significant increased in fibronectin, collagen I, collagen IV and laminin. D) However in overexpressed TLK1 LN18 cells, significant decreased of cell adhesion signals towards fibronectin, collagen I, collagen IV and fibrinogen were observed. Results were compared with their respective controls, and BSA were considered as negative controls in this assay. No significant difference was observed in cells treated with BSA. Experiments were performed in triplicates. ** indicates significant difference, $p<0.05$ by t-test between transduced cells with their controls.

4.5.4 Morphological Changes

Silencing of TLK1 was shown previously to inhibit invasion and migration of GBM cells. This effects might be due to inhibition of certain important elements that regulate cell motility. Morphological changes were also observed in terms of cellular structures of GBM cells. This suggests that silencing TLK1 might inhibit the formation of lamellipodia, fillopodia and invadopodia of GBM cells. However, this is quite uncertain since more characterisations have to be made to confirm this hypothesis.

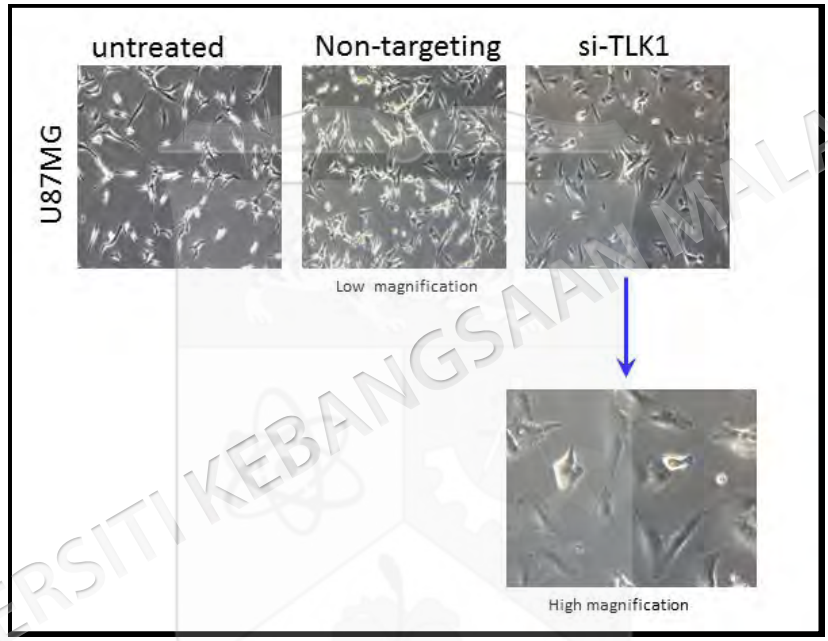

Figure 4.18 Knockdown of TLK1 alters cell morphology of U87MG cells. Representive micrographs of U87MG cells in 4x low magnification and 10x high magnification. U87MG cell morphology were altered after transfected with si-TLK1. These changes were observed during 96 hrs post-transfection. Cells became large, flatter and more rounded upon TLK1 knockdown. Pictures were taken using Olympus FX microscope.

4.6 MICROARRAY ANALYSIS OF SI-*TLK1* TRANSFECTED U87MG CELLS IDENTIFIED DOWNSTREAM PATHWAYS OF TLK1

As potential druggable target for cancer, it is essential to characterise the genome-wide impact of TLK1 inhibition and to identify cancer cell phenotypes targeted by modulation of TLK1 levels. To investigate the global effects of TLK1 depletion on U87MG cell gene expression, changes in the transcript levels were determined by functional microarray analysis on the cells treated with si-TLK1 and non-targeting siRNA. There were 527 genes having 1.5 fold changes (p-value < 0.05) with 300 upregulated genes and 227 downregulated genes and 2,632 genes having 1.1 fold changes (p-value <0.05) with 1281 upregulated and 351 downregulated genes (Figure 4.19).

Pathway analysis enrichment analysis was performed using WebGestalt server. Cell cycle related pathways including cell cycle, DNA replication and G1 to S cell cycle control were significantly sensitive to TLK1 knockdown. Interestingly, most of the identified pathways were mostly involved in cancer progression (Table 4.3).

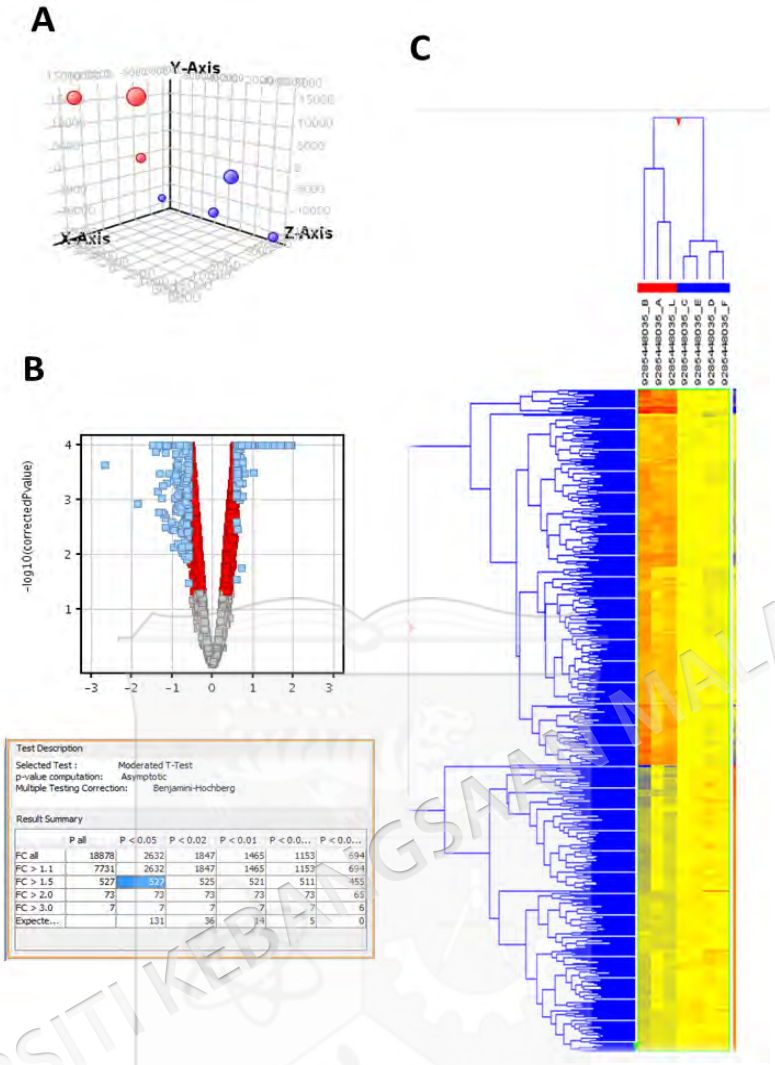

Figure 4.19 Global transcriptome changes in U87MG cells following knockdown of *TLK1*. A) Principle component analysis of *TLK1* knockdown cells compared with non-targeting control cells. Each group was clustered in their respective group. Red group refers to si-*TLK1* cells while blue group refers to non-targeting control cells. B) Volcano plot shows distribution of differentially expressed genes after it was analysed using Benjamini-Hochberg multiple testing correction and moderate t-test. There were 527 genes having 1.5 fold changes (p-value < 0.05; 300 up-regulated genes and 227 down-regulated genes) and 2,632 genes having 1.1 fold changes (p-value <0.05). C) Hierarchiecal clustering analysis based on Euclidean similarity measure and complete linkage heat map of differentially expressed genes. Analysis identified *TLK1* gene expression was amongst the top 20 down-regulated genes confirming the robustness of this microarray experiment.

Table 4.3 Functional pathway analysis identified statistically significant pathways affected by TLK1 knockdown in U87MG cells. Pathway analysis was performed using WebGestalt server on 2,632 differentially expressed genes (1.1 fold change).

Pathway Name	#Gene	Statistics
Cell cycle	39	2.70e-31
DNA Replication	27	7.26e-31
G1 to S cell cycle control	26	1.78e-20
DNA damage response	17	5.30e-11
TGF beta Signaling Pathway	19	1.63e-07
TSH signaling pathway	10	0.0001
Wnt Signaling Pathway	8	0.0003
Focal Adhesion	16	0.0003
Parkin-Ubiquitin Proteasomal System pathway	9	0.0006
TOR signaling	6	0.0013
Wnt Signaling Pathway and Pluripotency	10	0.0013
Interleukin-11 Signaling Pathway	7	0.0013
Integrin-mediated cell adhesion	10	0.0013
Signaling Pathways in Glioblastoma	9	0.0016
Sphingolipid Metabolism	5	0.0016
Mismatch repair	4	0.0016
TNF alpha Signaling Pathway	10	0.0019
Apoptosis	9	0.0026
Regulation of Actin Cytoskeleton	12	0.0035
MAPK signaling pathway	12	0.0051

4.6.1 Focal Adhesion Pathways

Amongst the identified pathways altered by *TLK1* knockdown, focal adhesion pathways have become the major interest in relation to the involvement of *TLK1* in GBM cell invasion and migration (Figure 4.20). Focal adhesion was chosen because it is less reported and novel in the field of cancer biology compared with TGF-beta pathway. This was also motivated by previous functional results whereby knockdown of *TLK1* inhibited GBM cell invasion and migration. Integrin-mediated cell adhesion pathway is a sub-pathway in focal adhesion pathways. This pathway was selected for further validation as it has important function in the regulation of cancer invasion (Figure 4.21).

Eight genes in focal adhesion pathway were further validated in si-*TLK1* transfected U87MG cells using qPCR (Table 4.4). Seven out of eight genes show concordant with microarray expression. Similar downregulations of *RAC2, ROCK2, PXN* and *FYN* were found in si-*TLK1* transfected LN18 cells (Figure 4.22). This suggests that these genes play important interactions with *TLK1*.

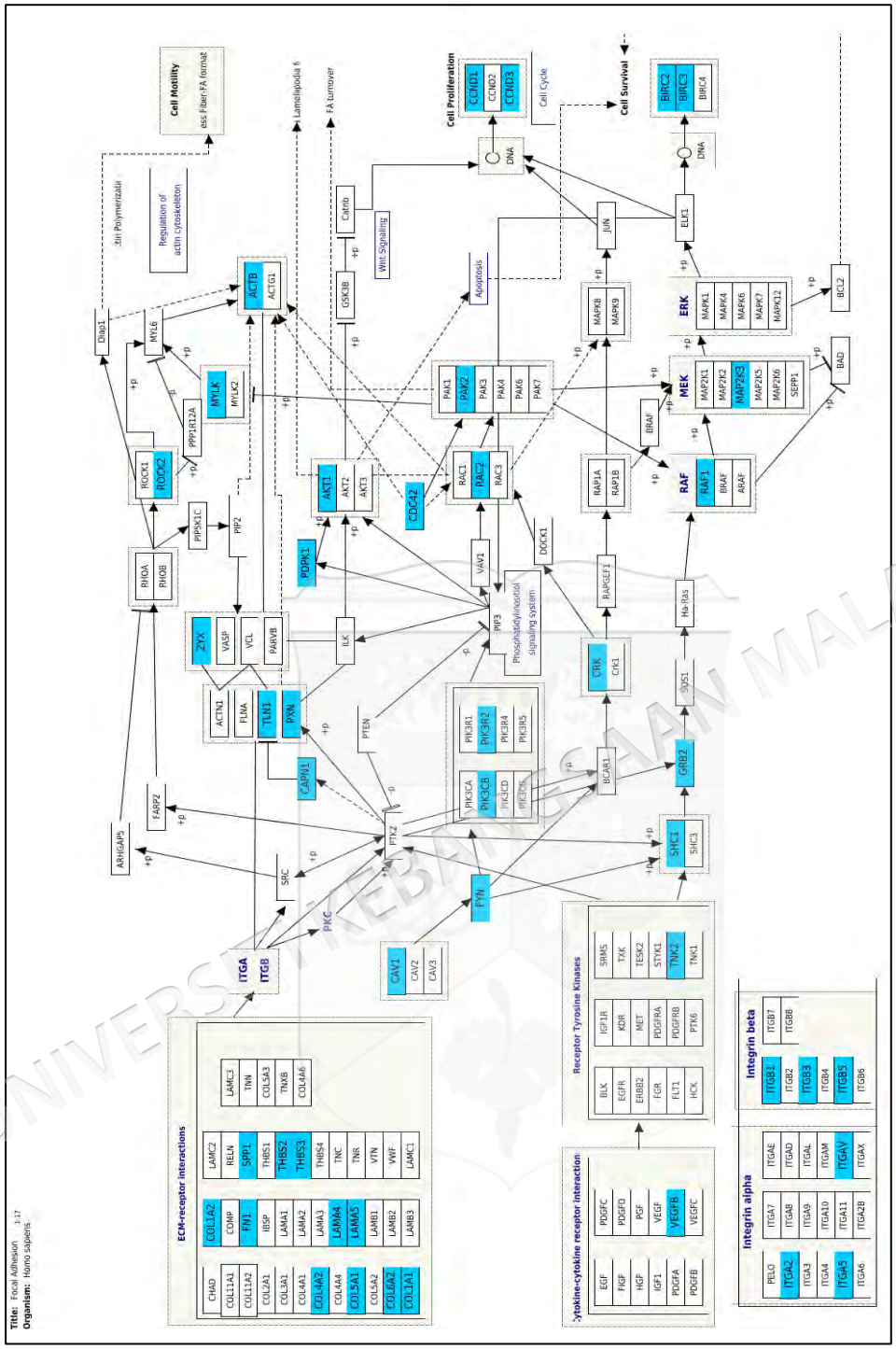

Figure 4.20 Focal adhesion pathways are affected by TLK1 knockdown in U87MG cells by microarray study.

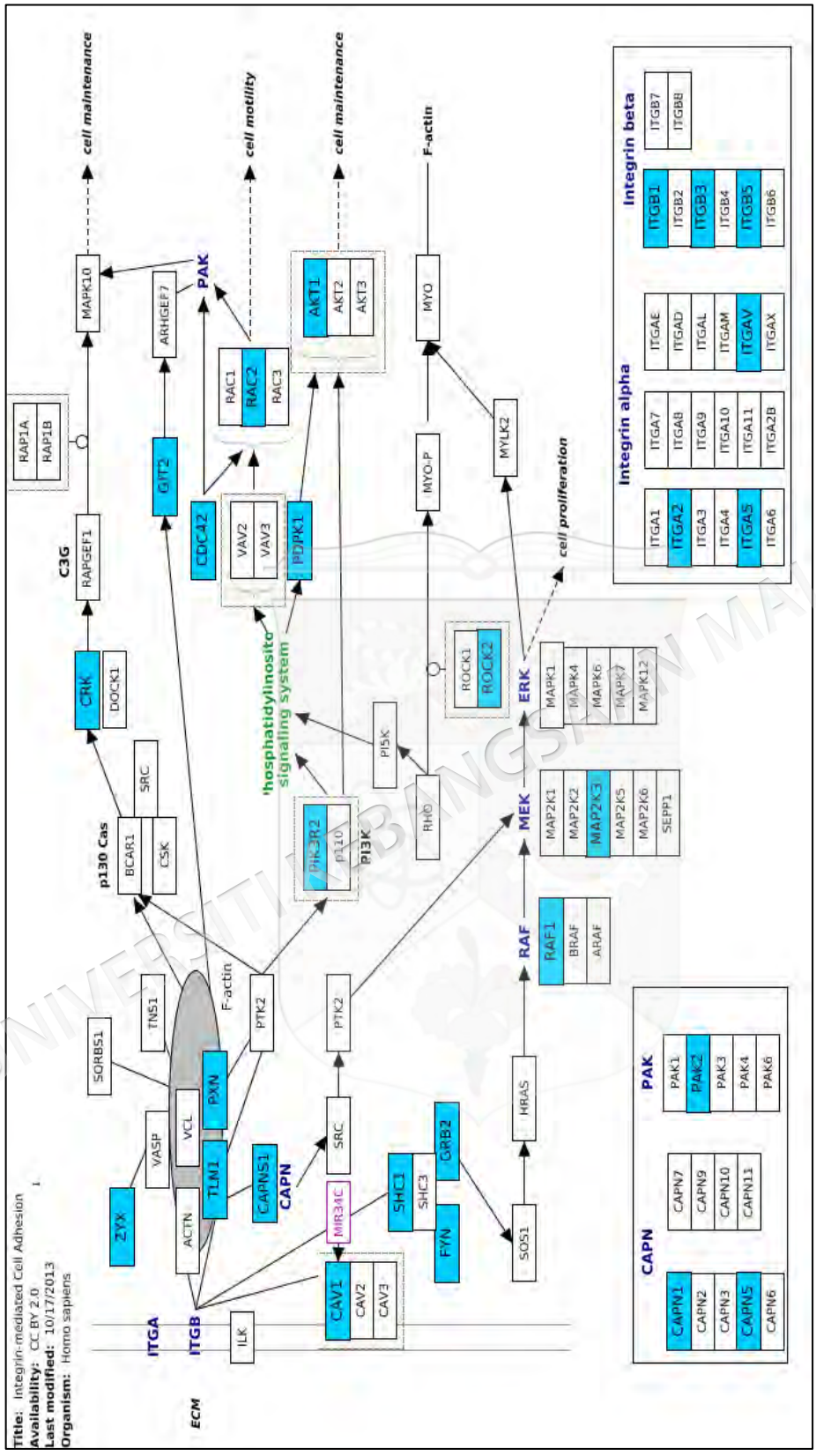

Figure 4.21 Integrin-mediated cell adhesion pathway is a sub-pathway in focal adhesion pathways. This pathway was selected for validation as it has important function in the regulation of cancer invasion.

Table 4.4: Validation of microarray profiling by SYBR green-based rq-PCR on eight selected genes involved in the integrin-mediated cell adhesion pathway. Only *ARPC1B* gene expression did not concur with microarray mRNA expression.

Gene	Microarray	rq-PCR
TLK1	-2.295	0.082
RAC2	-3.887	0.173
ROCK2	-1.36	0.616
PXN	-1.53	0.436
COL4A2	-1.2	0.617
THBS2	-1.66	0.633
FYN	-1.42	0.581
ARPC1B	2.01	0.539

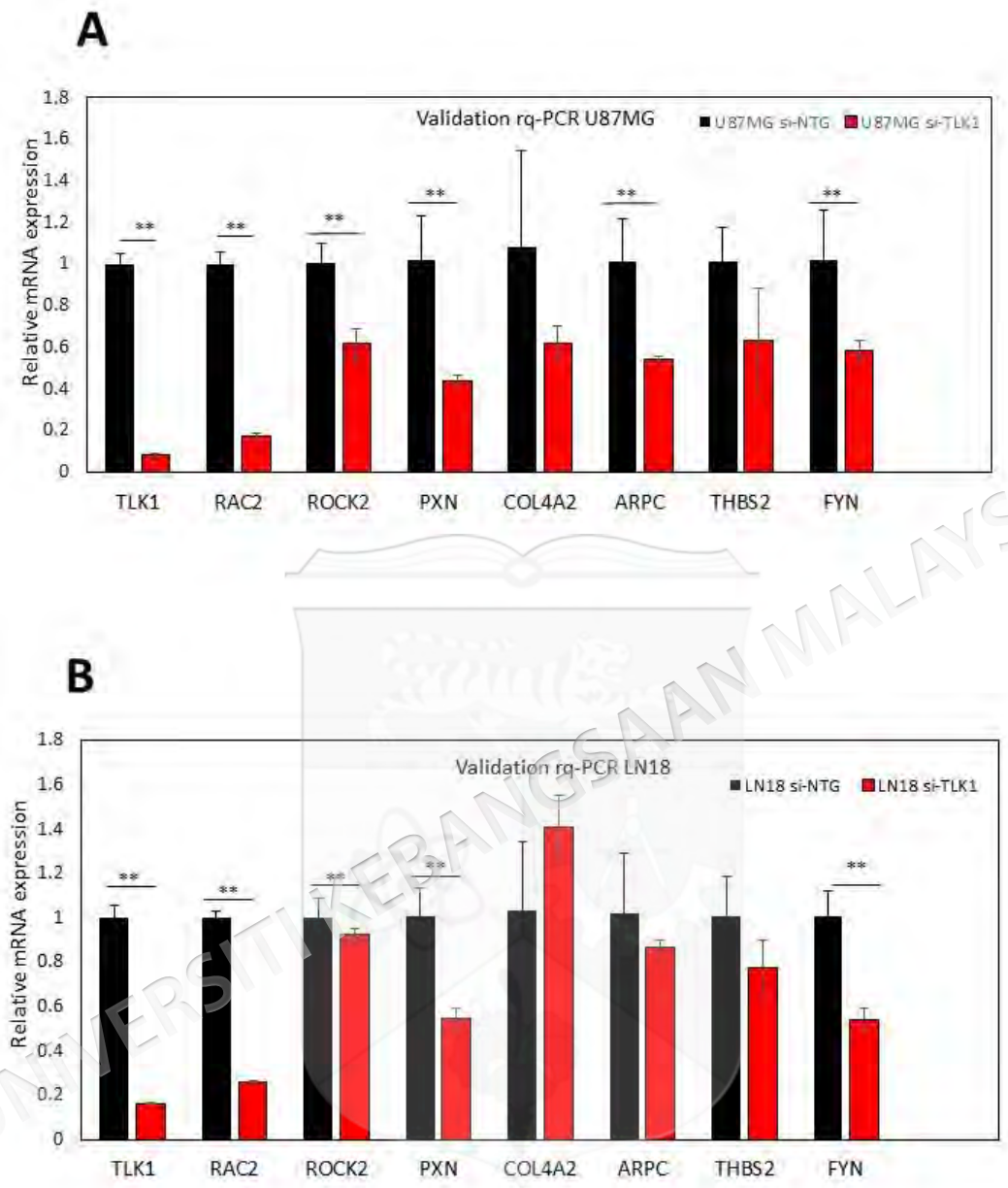

Figure 4.22 Validation of eight important genes from microarray analysis that were found to be the downstream genes of *TLK1* and were hypothesised to interact with the focal adhesion pathway in GBM cells. A) U87MG cells were transfected with si-*TLK1*. After 48 hrs of post-transfection, cells were harvested and mRNA was extracted. Genes of interest were amplified using iTaq Universal SYBR green master mix in an ABI rq-PCR systems. The *TLK1, RAC2, ROCK2, PXN* and *FYN* expression show significant reduction ($p<0.05$) compared with non-targeting siRNA control. B) LN18 cells were also transfected with si-*TLK1*. Gene expression analysis was performed 48 hrs post-transfection. Only *TLK1, RAC2, ROCK2, FYN* and *PXN* expression were downregulated and this result was in concordant with the si-*TLK1* transfected U87MG cells.

4.7 TLK1 MAY HAVE ROLE IN INTEGRIN MEDIATED CELL ADHESION PATHWAY SIGNALLING

RAC2 and *PXN* are known to be major player in focal adhesion turnover. Since the decreased of *RAC2* was in concordant with TLK1 and it is statistically significant, the mRNA expression of *RAC2* and *PXN* in untreated GBM cells were investigated. *RAC2* expression in GBM cells was very high by more than 20 fold change compared with *PXN* expression (Figure 4.24). Hence, it was hypothesized that TLK1 signalling might be via the CAV1-FYN-PI3K-RAC2/CDC42 pathway which is part of the integrin mediated cell adhesion pathway.

To validate this hypothetical pathway, several ELISA based assays were performed by InstantOne kit (Ebiosciences, USA) and G-LISA kit (Cytoskeleton, USA).

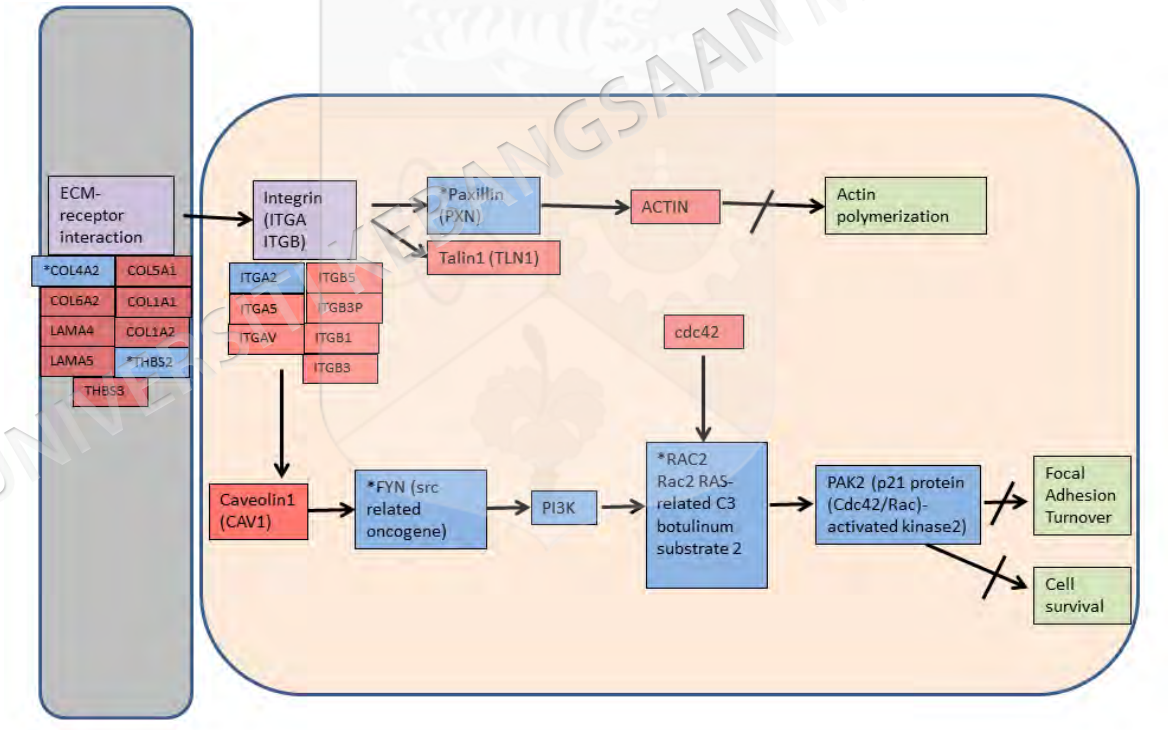

Figure 4.23 Functional microarray functional profiling suggests that inhibition of GBM cell migration and invasion might be due to inhibition of the integrin mediated cell/focal adhesion pathway. Mechanisms involved inhibition of actin polymerization and focal adhesion turnover.

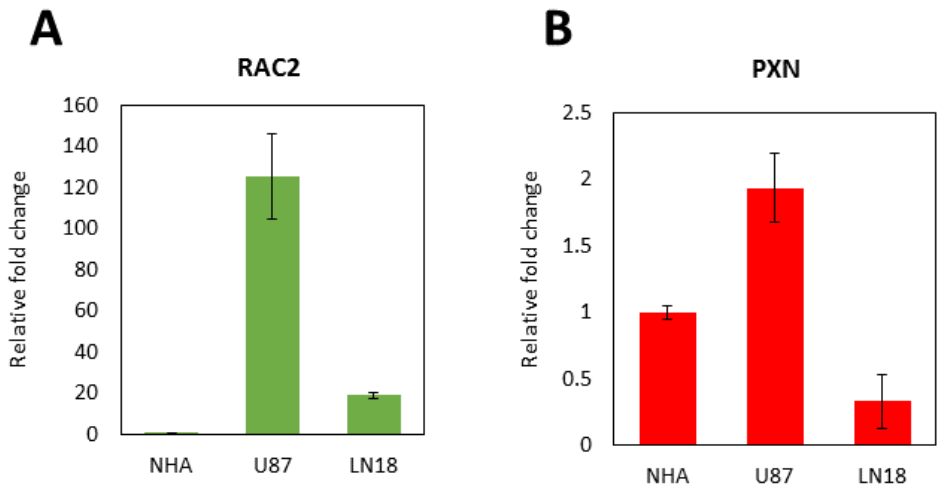

Figure 4.24 Gene expression analysis on two important genes involved in focal adhesionpathway. mRNA was extracted from U87MG and LN18 using RNAEasy kit (Qiagen, Germany) and its expression was amplified using iTaq SYBR green Universal Master Mix (Biorad, USA). A) *RAC2* expression was 120 fold higher in U87MG cells compared with normal human astrocytes. *RAC2* expression in LN18 was 20 fold higher than normal human astrocytes. B) *PXN* expression was found to be increased by two fold compared with normal human astrocytes. However, *PXN* expression was down regulated in LN18 cells.

4.7.1 Downstream Pathway Validation using ELISA Assays

To validate the downstream functional activation of TLK1, selected few protein markers namely TP53, AKT1/2/3, p70 S6K, ERK 1/2/3, RAC2 and CDC-42 activation were selected. Analysis from transduced U87MG cells showed that, in depleted TLK1 cells, phosphorylated TP53 was increased in U87MG (1.64) compared with total TP53 (1.564). P70 S6K signal decreased significantly to 0.39 and 0.38 from 1.0 sh-non-targeting control. There was probably an alternative pathway activation when there was significant increase in AKT signal in sh-TLK1-455 (0.5) and increase of ERK 1/2/3 by 0.2 unit in both sh-TLK1 sequences compared with their respective sh-non targeting control (Figure 4.25).

Interestingly, in LN18 TLK1 depleted cells, similar pattern of increased in AKT and ERK was observed. No obvious change was seen in total/phospho TP53/P70 S6K was observed (Figure 4.25). Increased in phosphorylation of ERK1/2/3 in both knockdown and overexpression of TLK1 is due to the alternative pathways activation that is associated or closely related with ERK1/2/3.

In this study, RAC2 was hypothesised to be involved in the regulation of GBM cell invasiveness. Hence, to confirm RAC2 activation at the protein level, an ELISA based assay was performed. RAC2 activation was significantly reduced by more than two fold in TLK1 depleted U87MG and LN18 cells (Figure 4.25).

Prior RAC2 activation, RAC2 will bind to CDC-42 and PAK2-complex to activate downstream signalling. In this study, CDC-42 activation was significantly increased in TLK1 depleted U87MG cells but not in TLK1 depleted LN18 cells whereby CDC-42 activation was decreased. In overexpressing TLK1 LN18 cells, RAC2 and CDC-42 signal was significantly high suggesting an important involvement of both molecules in GBM invasive behaviour. U87MG cells, however, had lower RAC2 and CDC-42 signals (Figure 4.26).

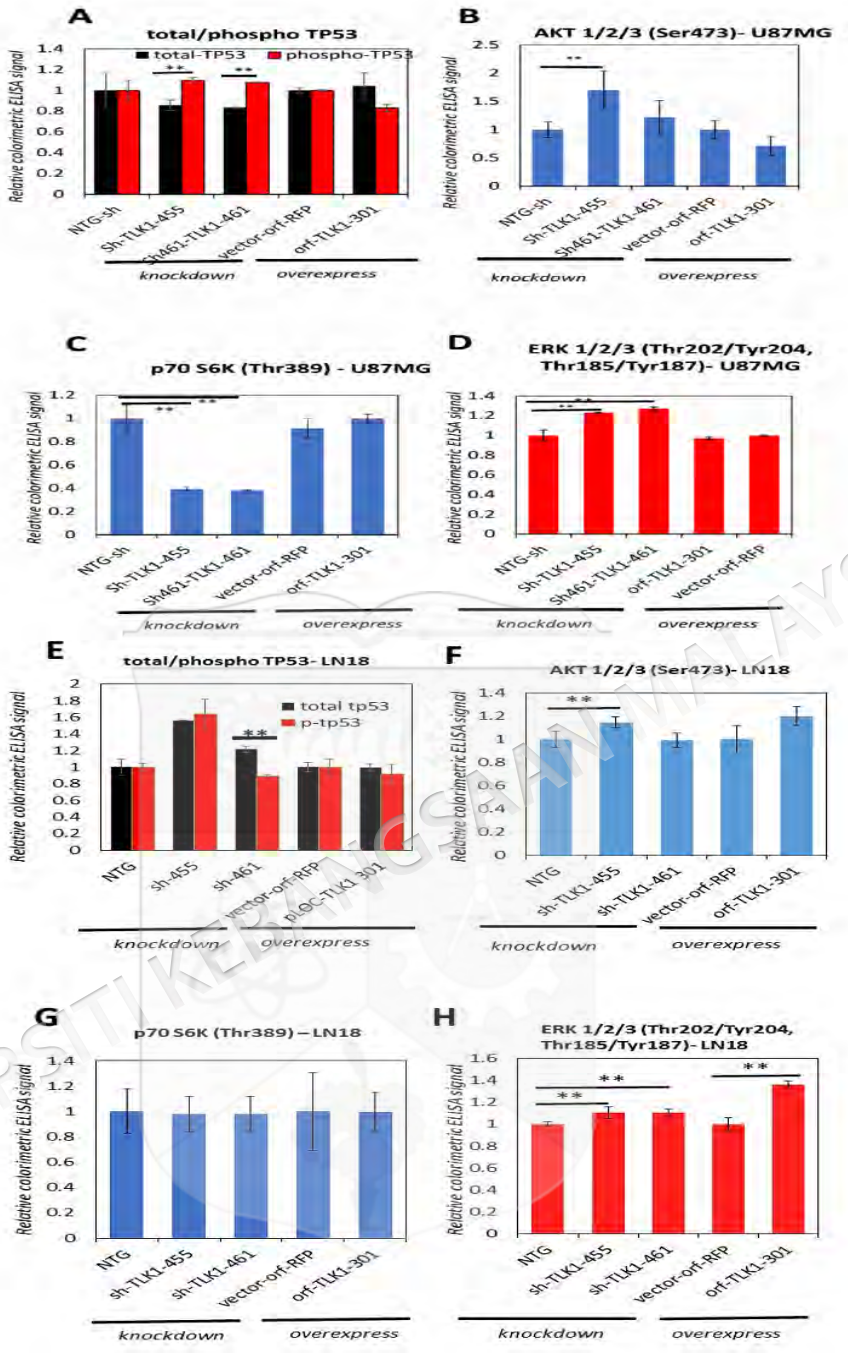

Figure 4.25 Understanding potential role of TLK1 downstream kinome signalling using ELISA based assay in U87MG and LN18 cells. Both cell lines were transduced with GIPZ shRNA and lentiorf clones. Cell lysates were later extracted after 72 hrs and respective kinase levels were measured. A) Phosphorylated TP53 increased significantly in TLK1 knockdown U87MG (**p<0.05). B) significant activation of AKT 1/2/3 in sh-TLK1-455 U87MG only (**p<0.05). C) significant reduction in p70s6k activation seen in knockdown TLK1 U87MG (**p<0.05) D) significant increase in ERK activation seen in both sh-TLK1 sequences U87MG (**p<0.05). E) Phosphorylated TP53 decreased in TLK1 knockdown LN18 sh-TLK1-461 (**p<0.05). F) significant activation of AKT 1/2/3 in sh-TLK1-455 LN18 only (**p<0.05). G) no significant p70s6k activation seen in LN18 H) significant increase in ERK activation seen in both sh-TLK1 and orf clones (**p<0.05).

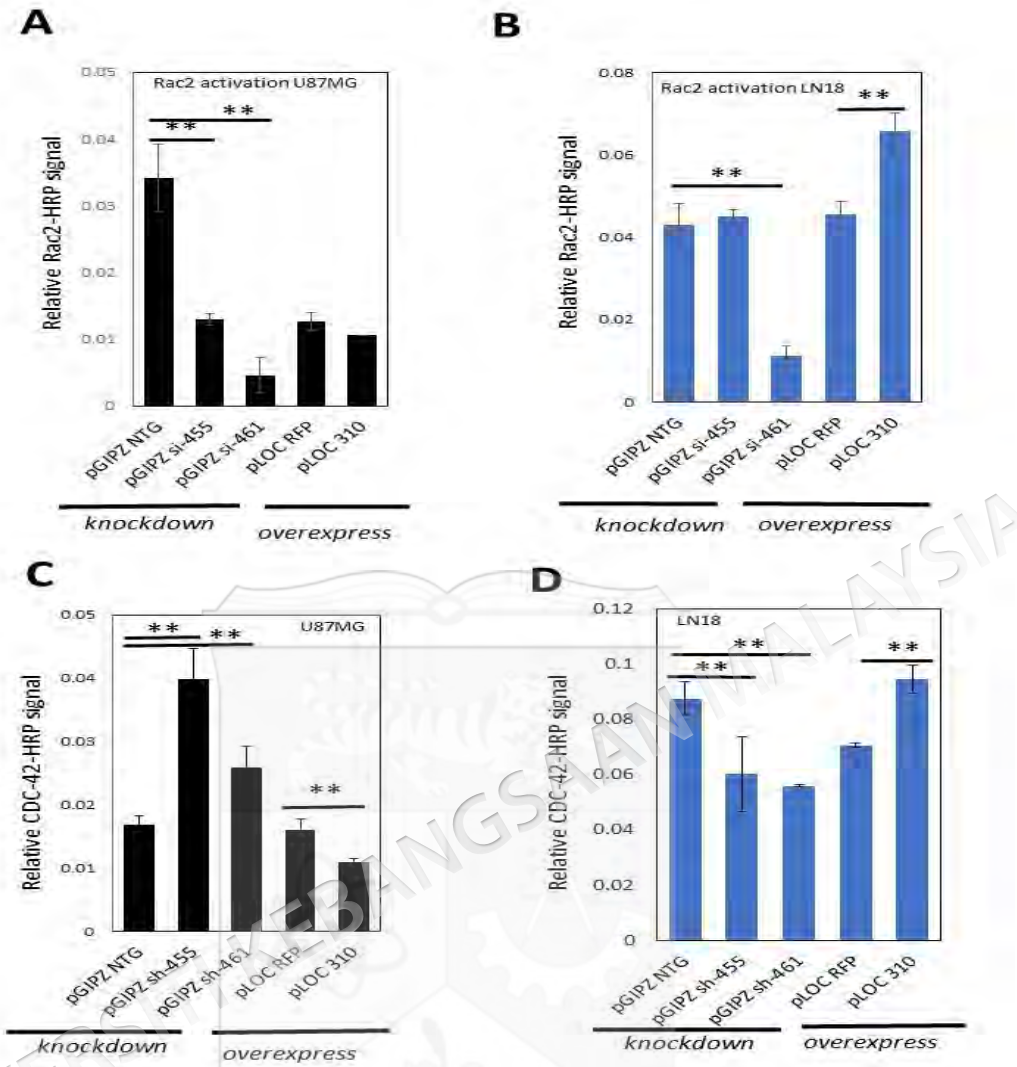

Figure 4.26 Modulation of RAC2 and CDC42 in TLK1 knockdown and overexpressing GBM cells A) U87MG cells were transduced with pGIPZ-sh-TLK1. Significant decreased ($p<0.05$) in relative RAC2-HRP signal was observed in both shRNAs (sh-TLK1-461 and sh-TLK1-455) by more than three fold change. However, in overexpressed TLK1 in U87MG by induction of pLOC-TLK1-orf-clones, no significant difference was observed. B) Relative RAC2-HRP signal was significantly decreased ($p<0.05$) in LN18 knockdown with sh-TLK1-461 only. However, in overexpressed LN18 cells, RAC2 activity was significantly increased ($p<0.05$). C) CDC42 activity was markedly increased in U87MG cells treated with sh-TLK1-455 and sh-TLK1-461. In contrast CDC42 activity decreased in LN18 cells transduced with pLOC-TLK1-orf clones ($p<0.05$) D) CDC42 activity was significantly decreased in both LN18 cells transduced with shRNAs. Significant decreased in CDC42 acivity ($p<0.05$) was observed in in overexpressed TLK1 LN18 cells.

4.8 FUNCTIONAL ANALYSIS ON SI-TLK1 KNOCKDOWN NORMAL HUMAN ASTROCYTES

The most important aspect of determining specific cancer target is that to be able to characterise whether a particular target is specific only to cancer cells but not neighbouring normal cells. To determine the specificity of TLK1 as potential target for brain cancer, the effect of TLK1 silencing in normal human astrocytes was studied. Silencing TLK1 did not cause significant changes in the normal human astrocyte NHA cell viability, morphology or activating any apoptosis effects (Figure 4.27A, B, C and D). The inhibition also did not cause any significant changes towards invasion and migration signals (Figure 4.27E and Figure 4.27F).

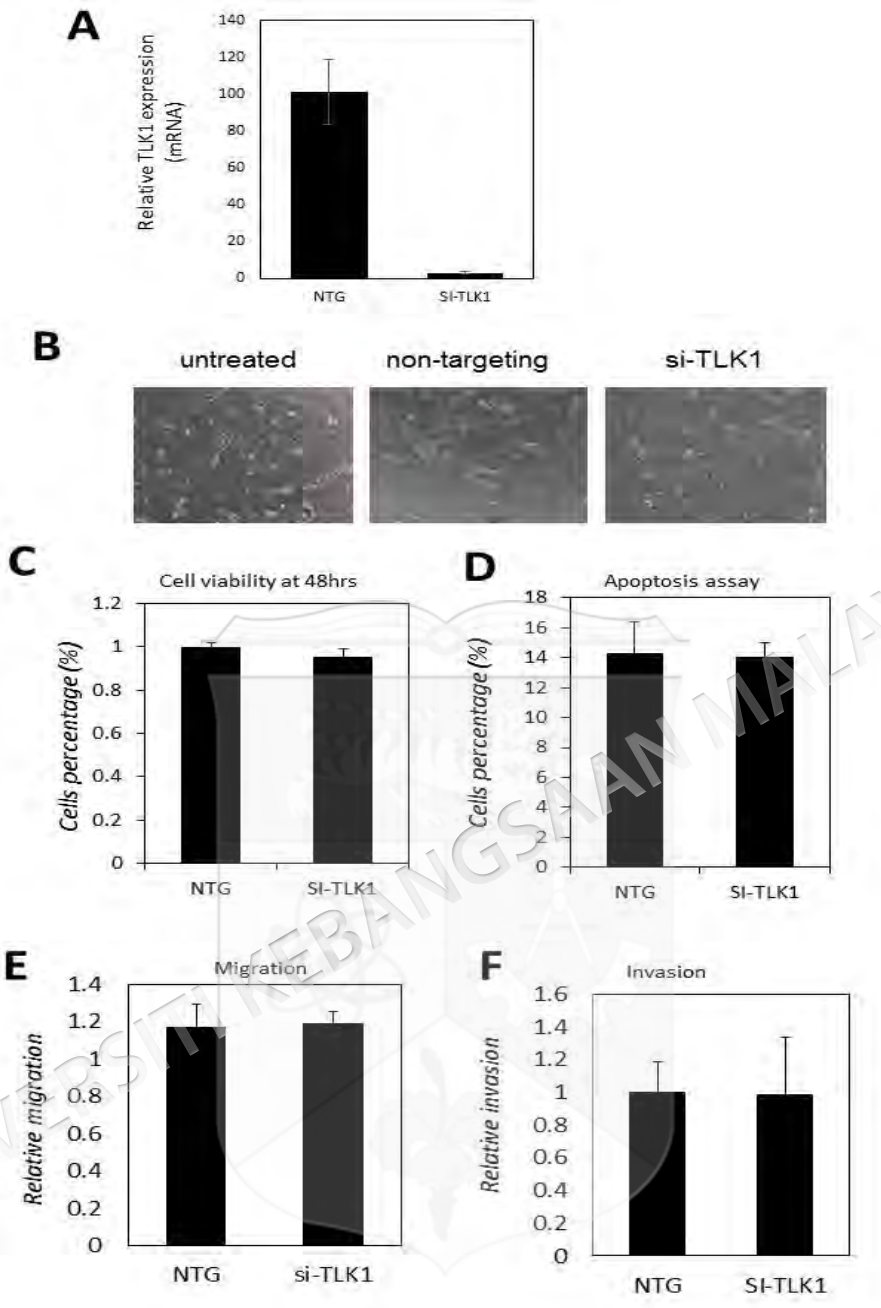

Figure 4.27 Functional analysis on transiently transfected NHA with TLK1 siRNA. A) Transfection of si-TLK1 in normal human astrocytes was more than 90% efficient. mRNA was extracted from NHA after 48 hrs of transfection and subjected to qqPCR. B) Morphological observation showed that si-TLK1 did not affect cellular changes and viability (10x magnification). C) No significant difference in cell viability was observed at 48 hrs post-transfection. Analysis was performed using Presto Blue reagent (Life technologies, USA). D) No significant apoptosis difference was observed during Annexin-V staining (Roche diagnostic, German) suggesting NHA cells were not affected by gene knockdown. E) When TLK1 was inhibited in NHA cells, no significant difference in the cell migration was observed. F) No significant results were observed in NHA treated with si-TLK1.

4.9 *IN VIVO* ANALYSIS OF U87MG TLK1 KNOCKDOWN AND TLK1 OVEREXPRESSING XENOGRAFT MODEL

TLK1 knockdown can efficiently inhibit cell proliferation, induce the S-phase cell cycle arrest and suppress the migration and invasion of U87MG cells *in vitro*. To verify whether the effect of TLK1 RNAi on growth of GBM cells is also observed *in vivo*, parental U87MG-sh-non-targeting control cells, or U87MG-sh-TLK1-455, or sh-TLK1-461 were injected into nude mice to develop subcutaneous GBM xenografts. Tumour volume was delayed significantly for mice injected with U87MG-sh-TLK1-455, or sh-TLK1-461 cells observed at day 21, 28 and 35 only ($p<0.05$). However, at day 42, results were not significant (Figure 4.28A). At day 47, the mice were sacrificed and the weights of the tumours were recorded. The mean tumour weight of the U87MG-sh-455 and U87MG-sh-461 group was prominently reduced compared to the U87MG-sh-non-targeting cells ($p<0.05$) as shown in Figure 4.28B and Figure 4.28C.

The effects of TLK1 overexpressing U87MG cells in subcutaneous xenograft model were also studied. Results showed no obvious statistically significant difference between control U87MG-RFP cells with U87MG-pLOC-TLK1 cells (Figure 4.29).

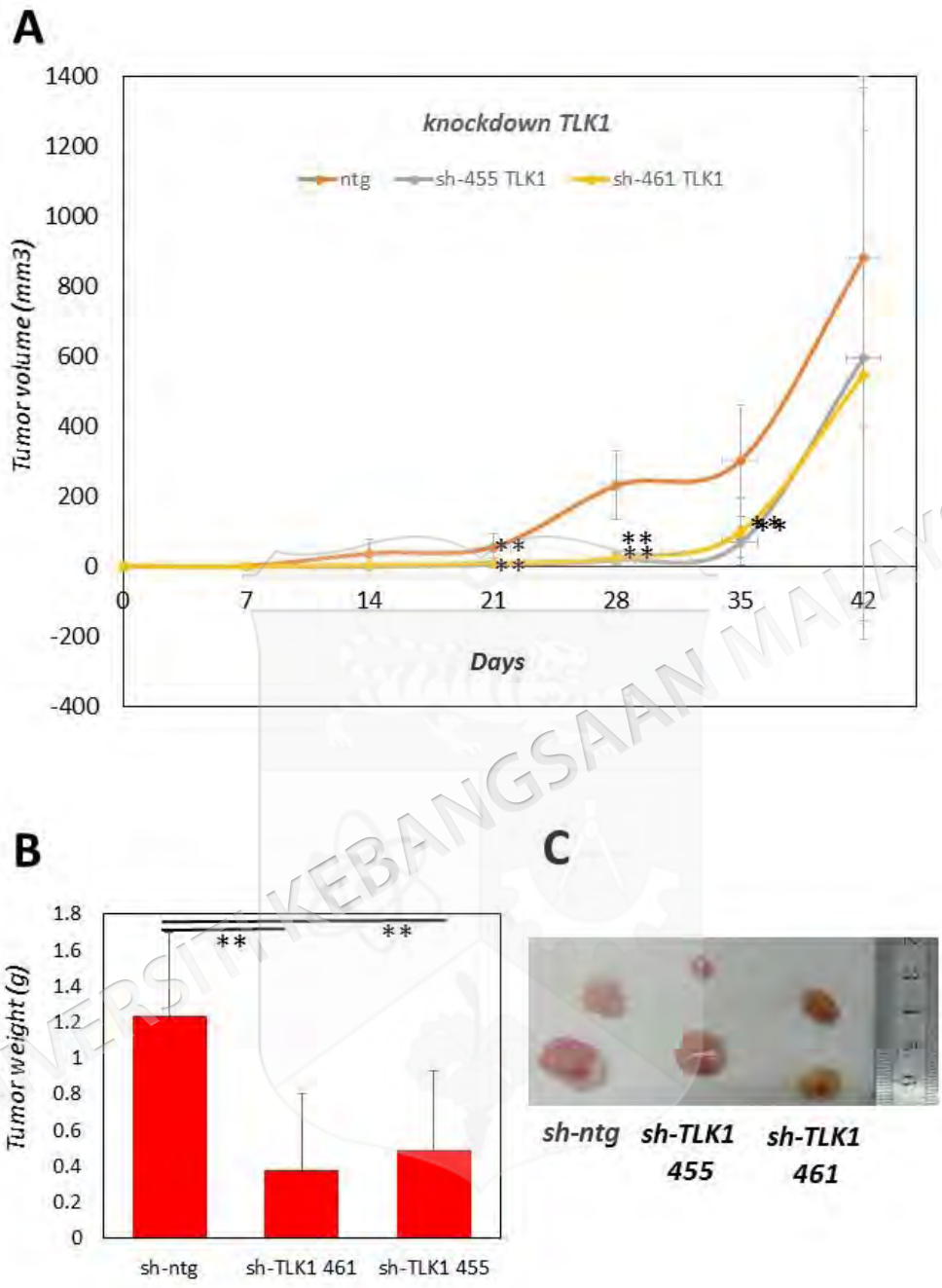

Figure 4.28 TLK1 knockdown decreases tumorigenicity in nude mice. A) *BALB/c-nu* mice were injected subcutaneously with 3×10^7 of U87MG control cells; or U87MG-sh-*TLK1*-455 or sh-*TLK1*-461 knockdown cells. Tumour sizes were determined by measuring the tumour volume every five days from 7 to 42 days after injection. B) Average tumour weights of mice 40 days after injection are shown. Values represent means ± SD obtained from 5 independent samples. C) Representative tumour formation was photographed 47 days after injection.

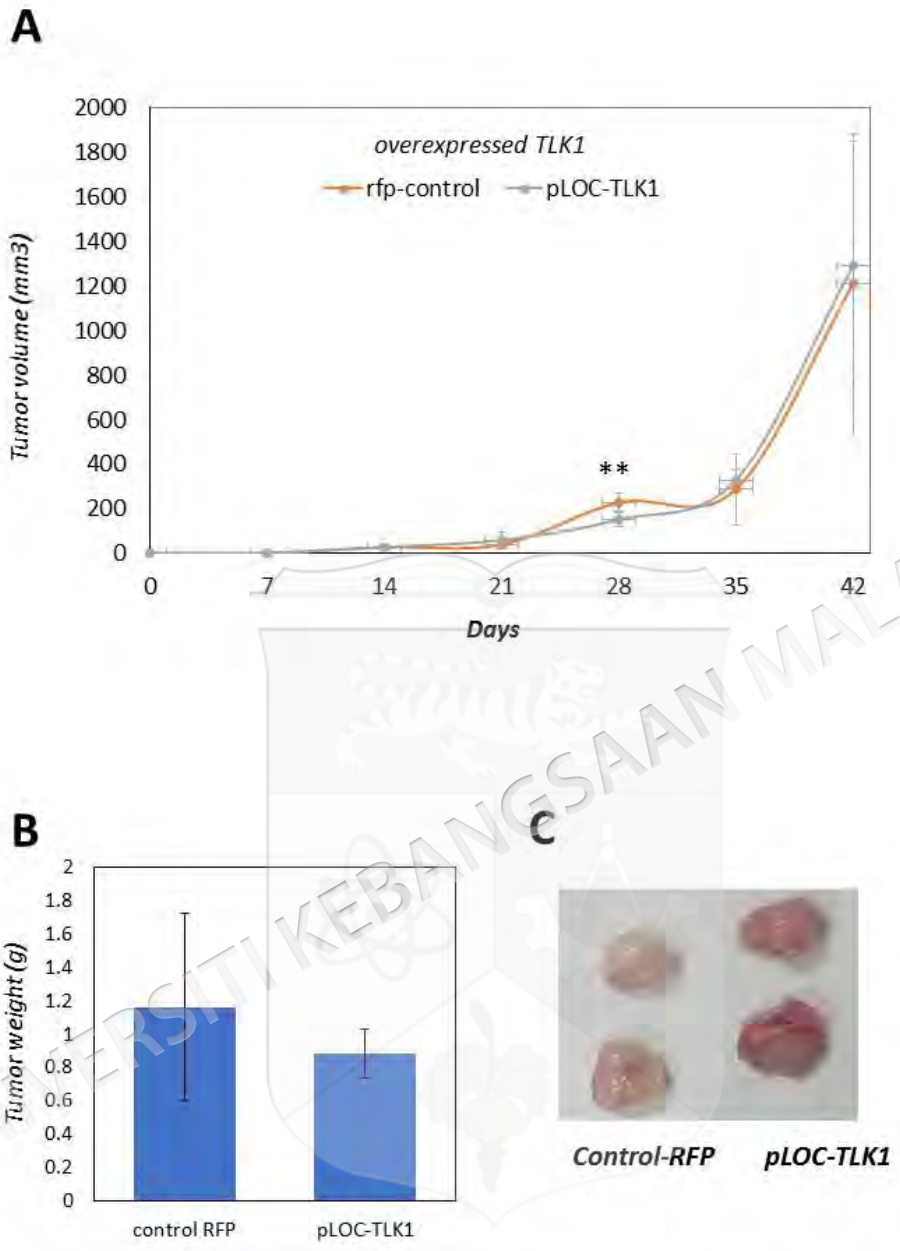

Figure 4.29 TLK1 overexpression by pLOC-TLK1 did not show significant difference in nude mice compared with RFP-control cells. A) *BALB/c-nu* mice were injected subcutaneously with 3×10^7 of U87MG RFP-control cells; or U87MG-pLOC-TLK1 orf clones. Tumour sizes were determined by measuring the tumour volume every five days from 7 to 42 days after injection. B) Average tumour weights of mice 47 days after injection are shown. Values represent means ± SD obtained from five samples. C) Representative tumor formation was photographed 47 days after injection experiments.

4.10 COMPARATIVE MODELLING OF TLK1 USING I-TASSER

Submission of TLK1 amino acid sequence to the I-TASSER server generated multiple threads using a representative PDB structure library to search for the possible folds by Profile- Profile Alignment (PPA), Hidden Markov Model, PSIBLAST profiles, Needleman-Wunch and Smith-Waterman alignment algorithms. This generated 10 best templates selected from thLOMETS threading programs used by the the ITASSER server. This is shown in Figure 4.30 which shows top 10 templates close to the original TLK1 sequence.

Figure 4.31 shows top 3 predicted models. Model 1 was the best model determined by its C-Score of -0.11 was selected with estimated accuracy of 0.70±0.12 (TM-Score) and 8.5±4.5Å (RMSD) (Figure. 2A). C-score is a confidence score for estimating the quality of predicted models by I-TASSER. It is calculated based on the significance of threading template alignments and the convergence parameters of the structure assembly simulations. The PDB ID: 5dzcA had the best TM-score and was selected for modelling of TLK1 3D structure (Table 4.5). The PDB ID: 5dzcA is a Crystal Structure of PVX_084705 (Plasmodium Vivax) in complex with AMP-PNP with a resolution of 2.3 Å.

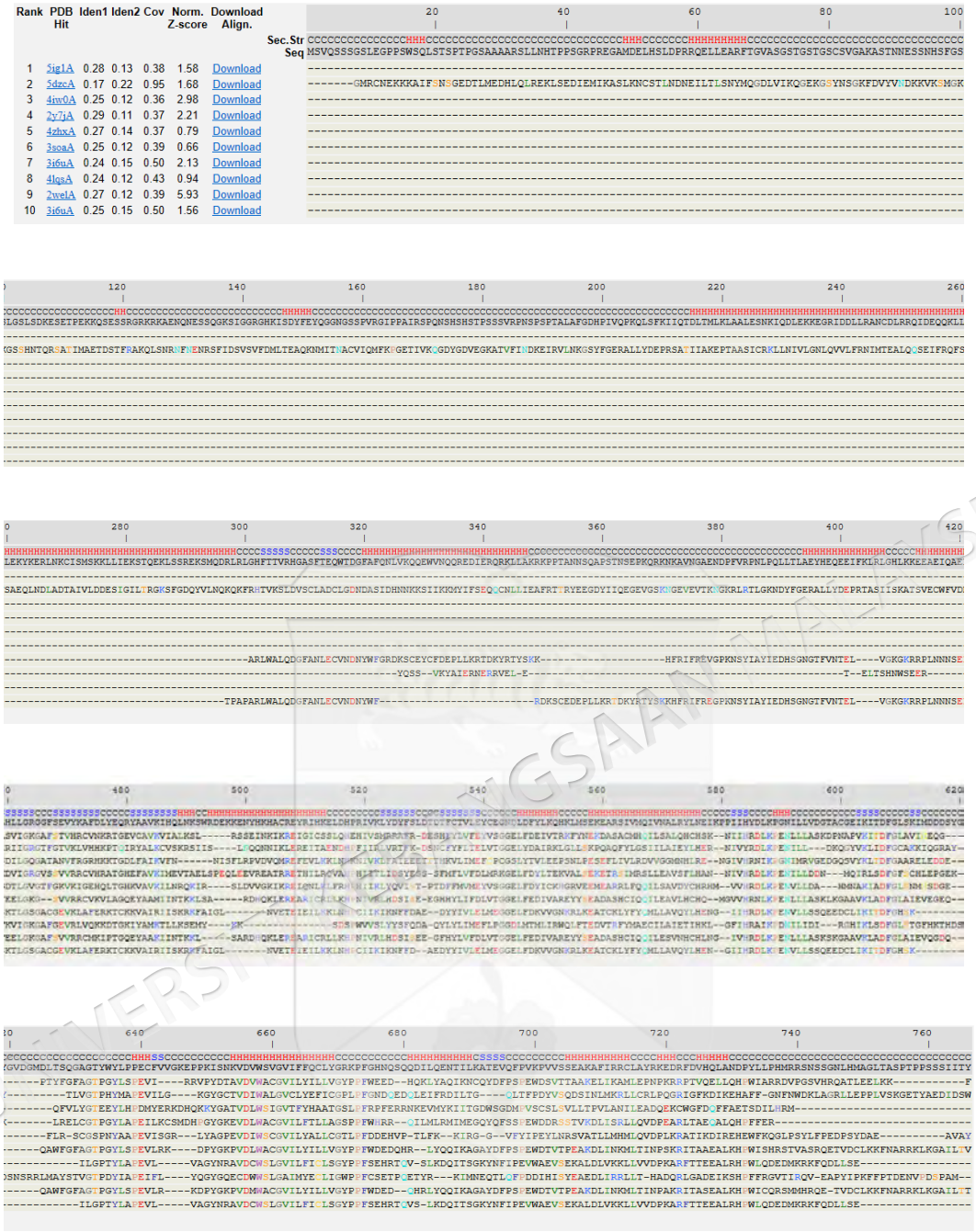

Figure 4.30: Top 10 threads generated from the ITASSER (analysis performed on 17 October, 2016). Full results can be obtained from http://zhanglab.ccmb.med.umich.edu/I-TASSER/output/S294083/.

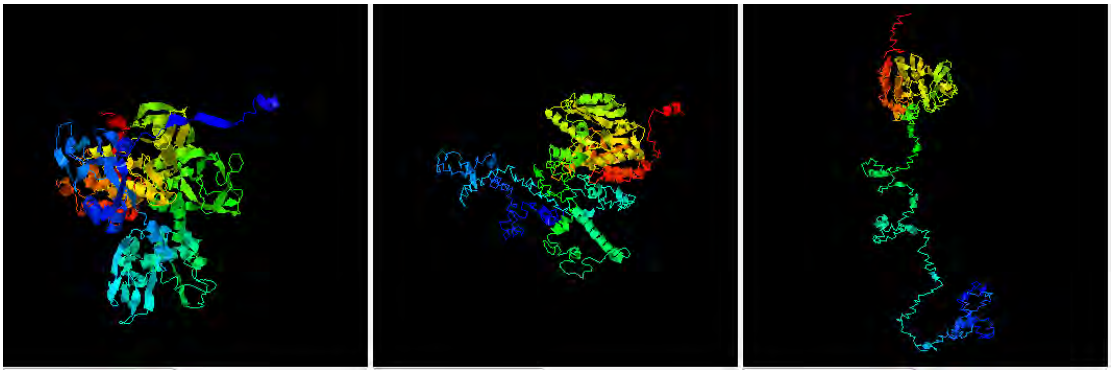

A **B** **C**

Figure 4.31: Top 3 final models predicted by I-TASSER. A) Model 1, is the best 3D model having C-score of -0.11, with estimated TM-score of 0.70±0.12 and estimated RMSD of 8.5±4.5Å (Model 1). B) Model 2 structure having C-score of -3.94 C) Model 3 structure having C-score of -3.91.

Table 4.5: Top identified structural analogs in PDB Used by ITasser to create TLK1 3D model protein structure.

Ranking	PDB Hit	TM-score	RMSD[a]	IDEN[a]	Cov
1	5dzcA	0.928	1.54	0.160	0.948
2	3c4wB	0.406	4.01	0.171	0.452
3	3nynA	0.402	4.08	0.139	0.449
4	4yhjA	0.400	3.92	0.159	0.444
5	2acxA	0.397	3.80	0.149	0.437
6	3krxA	0.395	4.36	0.148	0.447
7	4tnbA	0.395	3.69	0.150	0.435
8	3c4yB	0.378	3.82	0.167	0.420
9	2vo0A	0.370	2.62	0.232	0.389
10	2fo0A	0.369	4.26	0.168	0.424

(a) Ranking of proteins is based on TM-score of the structural alignment between the query structure and known structures in the PDB library. (b) RMSDa is the RMSD between residues that are structurally aligned by TM-align. (c) IDENa is the percentage sequence identity in the structurally aligned region. (e) Cov-represents the coverage of the alignment by TM-align and is equal to the number of structurally aligned residues divided by length of the query protein.

4.10.1 Model validation

We chose model 1 as TLK1 3D model for downstream analysis as it has the highest C-score. Validation of the model was performed including the geometric properties of the backbone conformations, and analysed using structure evaluation programs. Ramachandran plot calculations were calculated with PROCHECK program. Ramachandran plot of model 1 was shown in Figure 4.32. TLK1 3D model indicated that 81.3% of the residues in the most favourable region, 14.7% in the allowed region, 2.4% in the generously allowed region and 1.6% in the disallowed region (Table 4.6).

The 3D model of TLK1 was also assessed using ProSA Z-score. The program Protein Structure Analysis (ProSA) (https://prosa.services.came.sbg.ac.at/prosa.phpis) (October, 2016) an established tool which has a large user base and is frequently employed in the refinement and validation of experimental protein structures and in structure prediction and modelling. the quality scores of a protein are displayed in the context of all known protein structures and problematic parts of a structure are shown and highlighted in a 3D molecule viewer. ProSA addresses the needs encountered in the validation of protein structures obtained from X-ray analysis, NMR spectroscopy and theoretical calculations. TLK1 3D model overall Z-score quality was -5.58 suggesting a good quality 3D model compared with the available structure from NMR and X-ray (Figure 4.33A). Figure 4.33B shows the energy plot of the model quality by plotting energies as a function of amino acid sequence position. Usually, positive values correspond to problematic or erroneous parts of a model. ERRAT overall quality factor is 88.195% and at least more than 65% of the amino acids have scores more than or equal to 0.2 in the 3D/1D profile by VERIFY3D analysis at http://services.mbi.ucla.edu/SAVES/T/?job=208882 (October, 2016). Pro-Motif analysis from the same web server showed that the 3D model has 766 amino acids with 10 beta buldges, 16 helices, 39 helix-helix interacts, 66 beta turn and 8 gammas turn.

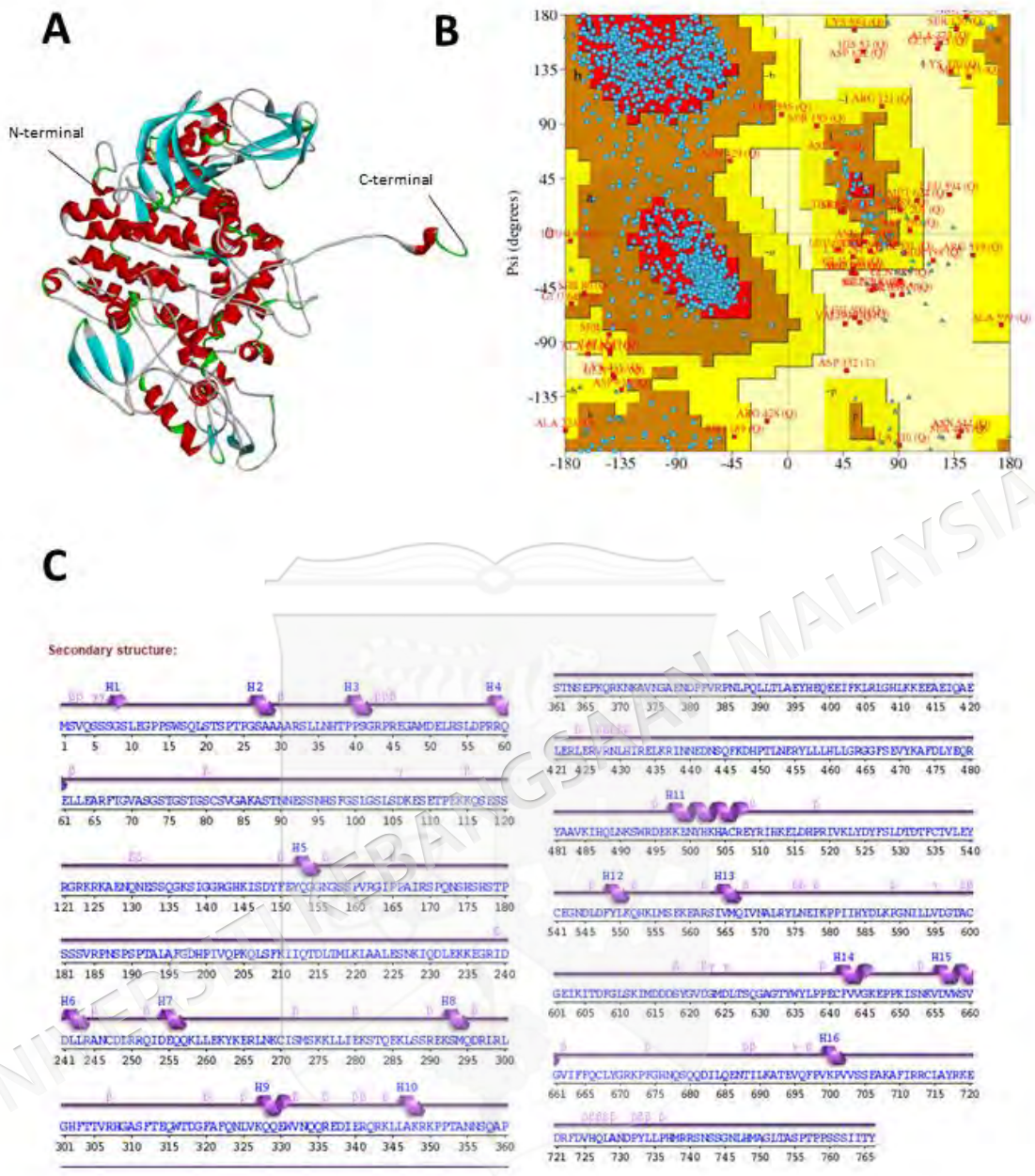

Figure 4.32: Model chosen was close with PDB 5DZC structure having the highest TM-score. A) Structure of protein visualized using Accelrys Discovery Studio. B) Ramachandran plot of the TLK1 3D model C) Secondary structure of TLK1 3D model analysed from PDBSum.

Table 4.6: Detailed Ramachandran plot statistics of TLK1 3D model structure obtained from PROCHECK analysis.

Parameter	Value in percentage (%)
Most favoured region	81.3
Additional allowed region	14.7
Generously allowed region	2.4
Disallowed region	1.6
Non-glycine and non-proline residues	100

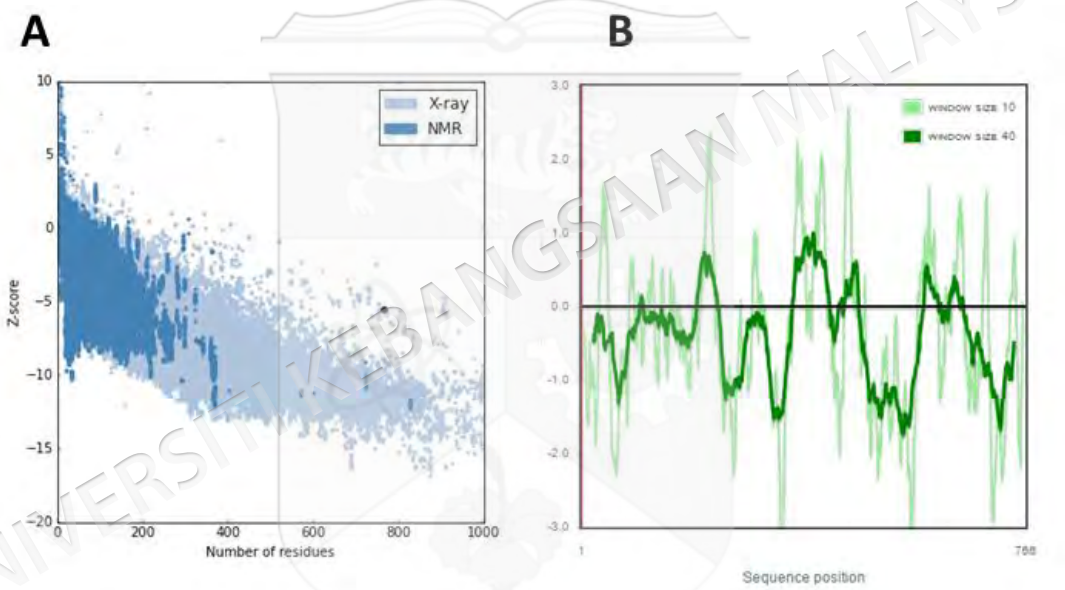

Figure 4.33: ProSA web analysis of TLK1 3D model. ProSA-web Z score of all protein chains in PDB determined by X- ray crystallography (light blue) or NMR-spectroscopy (dark blue) with respect to their length. The z-score of TLK1 3D model is highlighted as large dots. B) The energy plot of TLK1 3D model.

4.10.2 Preparation of receptor 3D model for ligand binding site

Characterization of candidate pockets and cavity detection on protein surfaces in protein structures is a very essential in ligand screening. Fpocket software was used for validation and preparation of the protein ligand binding site that was previously identified by ITasser server using COACH algorithm (Figure 4.34A). Fpocket is an open source pocket detection package based on Voronoi tessellation which determines

region of an atom coincides with the region of centers of all possible contact spheres that contact the atom (Guilloux et al. 2009). Figure 4.34B shows the region that is suitable as pocket binding for the 3D model structure which have been refined by fpocket that will be used for subsequent virtual screening analysis.

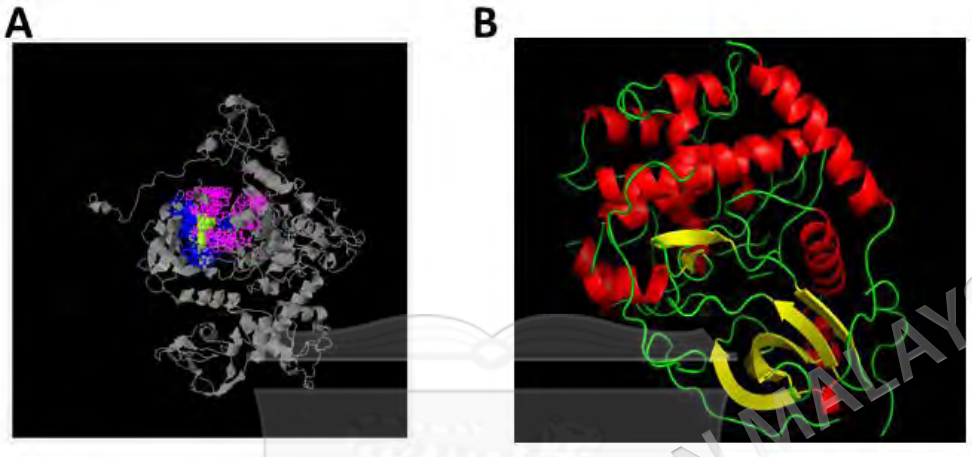

Figure 4.34: Predicted binding site of ADP in TLK1 3D model identified by COACH and verified by fpocket analysis A) The ligand binding site residues at 462,463,464,465,467,468,470,483,485,521,538,539,540,541,545,590,593,606,607 amino acid which binds ligand of ADP identified by COACH server. This binding site was chosen as it has highest C-score of 0.60. This ligand binding site for TLK1 3D model was homologous to PDB structure of 4IB3A. B) 3D structure refined by fpocket analysis and visualised using Pymol.

4.10.3 Virtual screening and docking using MTiOpenScreen

The protein structure from TLK1 3D model analogous to 4IB3A was uploaded in PDB format in the MTiOpenScreen server (http://bioserv.rpbs.univ-paris-diderot.fr/services/MTiOpenScreen/) (October, 2016) which later cleaned and preprocessed automatically. All hetero-atoms are removed and hydrogen atoms are added to the structure (Rey et al. 2015). The 3D structure contains information about list of residues defining the binding site for docking purposes. The chemical compound collection (iPPI-lib) to target protein-protein interactions containing 384,372 molecules were uploaded for the server to perform virtual screening. The predicted binding energies of the three best-scored poses of the 1000 top ranked compounds and physico-chemical properties of ligands were downloaded. Table 4.7 shows top 20 results of structure-based virtual screening with TLK1 3D model (4IB3A) as a protein receptor.

Table 4.7: Virtual Screening Results Using MTiOpeen-Screen

Compound	Energy	nRot	Library	Is Lead Like?	HBA	HBD	LogP	MW	TPSA
24270660_Intermediate	-11.3	3	iPPI-lib	Yes	7	1	2.75	383.4	102.58
124894369_Intermediate	-10.7	2	iPPI-lib	Yes	4	2	3.07	322.4	90.46
49671666_Intermediate	-10.7	5	iPPI-lib	Yes	4	2	3.87	347.5	49.33
26514148_Intermediate	-10.7	2	iPPI-lib	Yes	6	0	3.6	308.7	69.38
96021300_Accepted	-10.6	4	iPPI-lib	Yes	4	1	3.86	312.4	50.7
26615709_Accepted	-10.6	5	iPPI-lib	Yes	6	0	3.31	403.5	64.43
26538610_Intermediate	-10.5	3	iPPI-lib	Yes	8	2	2.15	324.3	120.67
29216696_Intermediate	-10.5	4	iPPI-lib	Yes	5	1	4.69	357.4	67.49
847663_Intermediate	-10.4	1	iPPI-lib	Yes	5	1	2.48	296.3	54.71
24305702_Accepted	-10.3	2	iPPI-lib	Yes	5	1	4.31	323.8	55.96
24373223_Intermediate	-10.3	6	iPPI-lib	Yes	7	2	1.59	352.3	106.61
22402861_Intermediate	-10.2	3	iPPI-lib	Yes	4	0	4.42	294.3	58.71
26626142_Accepted	-10.2	3	iPPI-lib	Yes	5	1	2.28	291.3	67.75
862479_Intermediate	-10.1	5	iPPI-lib	Yes	5	1	4.87	333.4	71.08
87349769_Intermediate	-10.1	6	iPPI-lib	Yes	5	3	3.2	368.4	106.03
14730674_Intermediate	-10.1	4	iPPI-lib	Yes	3	0	5.27	415.7	49.57
24312174_Intermediate	-10.1	2	iPPI-lib	Yes	3	2	4.57	277.3	49.33
26614386_Intermediate	-10.1	4	iPPI-lib	Yes	8	1	1.34	364.4	92.49
49818336_Intermediate	-10	6	iPPI-lib	Yes	6	2	2.28	385.4	100.11

Legends: nRot - number of rotatablc bonds, HBA – Hydrogen bond accetor, HBD -Hydrogen bond donor, LogP - partition coefficient of a molecule between an aqueous and lipophilic phase, MW-Molecular Weight, TPSA - Total Polar Surface Area

4.10.4 *In silico* pharmacokinetic analysis

All 1000 best ranked molecules were uploaded to the http://fafdrugs3.mti.univ-paris diderot.fr. (October, 2016), to filter and analysed molecules using predefined physicochemical filters as well as with several simple pharmacokinetic ADMET (absorption, distribution, metabolism, excretion and toxicity) principles. Analysis identified 221 compounds that meets selected fafdrugs3 filtering criteria. Final selection of the best predicted compound that can potentially binds to TLK1 3D model with less toxicity effects were chosen manually base on the Pfizer 3/75 Rule Positioning (Hughes et al. 2008) and Golden Triangle Rule (Johnson, Dress & Edwards 2009). Final filtering identified only one compound ID26626142 known as, 2-[2-(1H-Imidazol-4-yl)-ethyl]-benzo[de]isoquinoline-1,3-dione met the best selection criteria. The chemical structure, IUPAC names, the radar plot of physicochemical analysis, oral absorption estimation data and the Pfizer 3/75 Rule Positioning plot, which estimating drug-like molecule that are likely to cause toxicity and experimental promiscuity, are presented in Figure 4.35**.**

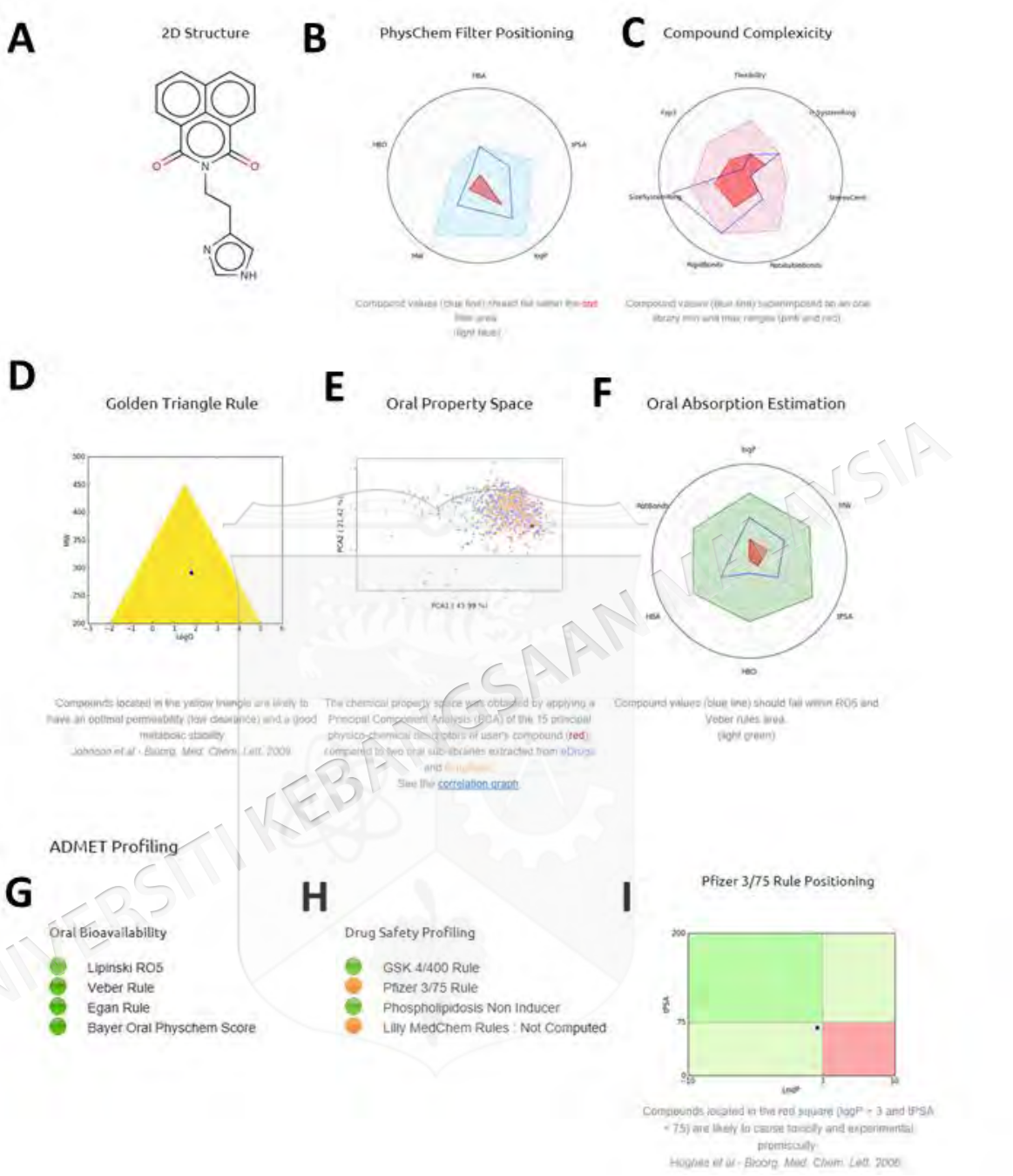

Figure 4.35: Overall pharmacological characteristics of ID26626142 shows excellent property **(A)** Chemical structure of identified compound ID26626142 known as, 2-[2-(1H-Imidazol-4-yl)-ethyl]-benzo[de]isoquinoline-1,3-dione **(B)** Physical chemical filter positioning showed that dark blue line referring to ID26626142 compound values falls into CNS light blue filter area **(C)** Calculation for compound complexity **(D)** Base on Johnson et al, 2009, compound ID26626142 falls within the yellow triangle that indicated compound have optimal permeability and good metabolic stability (**E)** Oral property space shows compound (red) falls within accepted range **(F)** Oral absorption estimation fall within acceptable Lipinski rule of five and Veber rule **(G)** ADMET profiling of ID26626142 shows good oral bioavailability **(H)** Drug safety profiling shows compound ID26626142 have adequate criteria for CNS drug that will be able to penetrate through the BBB adequately **(I)** Pfizer 3/75 shows Compound ID26626142 (blue dot) have high oral bioavailability profile.

Analysis from Table 4.8 shows that identified compound follows Lipinski rule of five which is known as the major principle to evaluate druglikeness of a compound with pharmacological activity that make it orally active drug in humans.

Table 4.8: Physiochemical properties of ligands from the docking study that passes ADME-TOX Lipinski Rule of Five and CNS filtering.

Parameters	**ID26626142**
Molecular weight	291.304
partition coefficient (logP)	2.48
solubility of the drug in water (logSw)	1.78
Total Polar Surface Area (tPSA)	67.750
Rotatable bonds	3
Rigid Bonds	22
Flexibility	0.12
Hydrogen Bond Donors	1
Hydrogen Bond Acceptors	5
Hydrogen Bond Donors_ Hydrogen Bond Acceptors	6
Number of system ring	2
Max Size System Ring	13
Charge	0
Total charge	0
Heavy atoms	22
Carbon atoms	17
Heteroatoms	5
Ratio Hydrogen/Carbon	0.294118
Lipinski violation	0
Solubility mg/ml	9809.105
Solubility forecast index	Reduced Solubility
Phospholipidosis	Non-Inducer
Status	Accepted

4.10.5 Molecular interaction mode analysis of protein–ligand

The molecular docking results showed compound ID26626142 showed good binding affinity with TLK1 3D model. It was observed that the binding energy between compound and receptor is -10.2 kcal/mol respectively. Hydrogen bonding and hydrophobic interactions play an important role to fit the ligands into the active site of the target site of the 3D TLK1 model as shown in Figure 4.36.

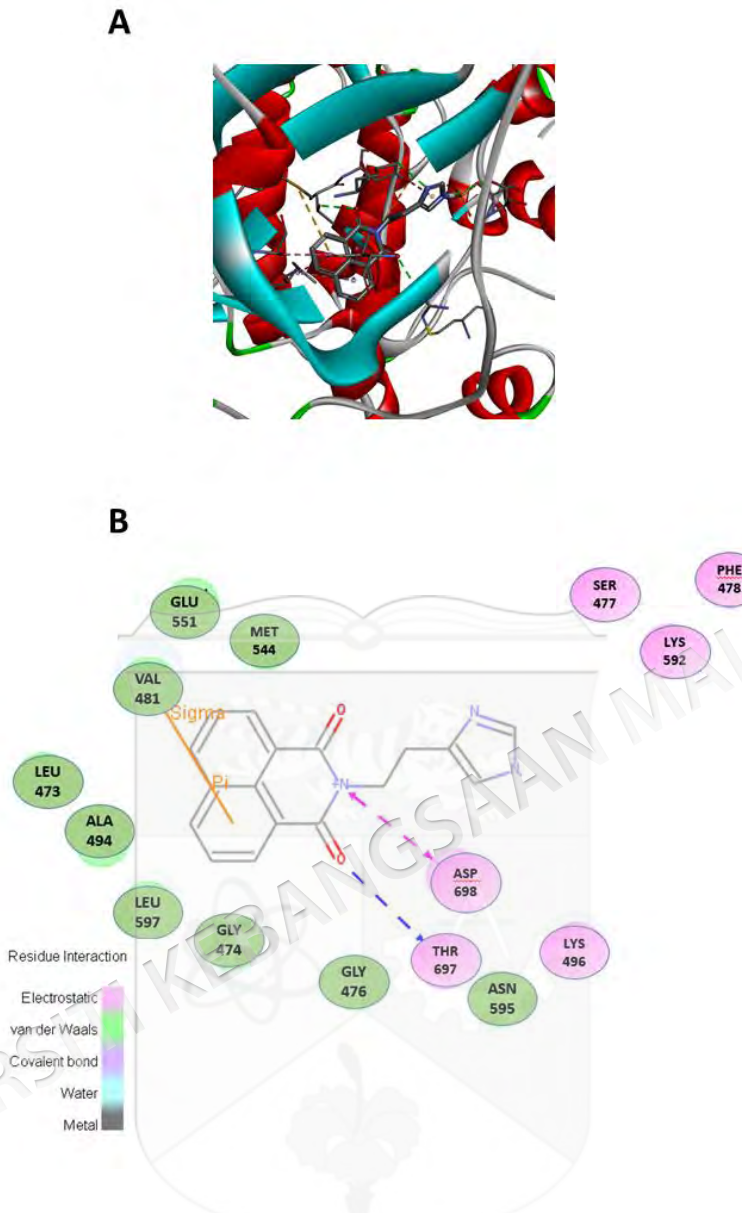

Figure 4.36: Ligand-3D protein model interaction A) Ligand ID26626142 in the predicted binding site of the TLK1 3D model. B) 2D ligand interaction diagram showing presence of hydrophobic interactions between the ligand and LEU473, GLY476, GLY474, ALA494, LYS496, MET544, GLU551, ASN595, and LEU597. Pi-Pi interaction occurs at VAL481, whilst hydrogen bond interaction at THR697. The three-dimensional and two-dimensional visualisation of ligand-protein interaction were performed using Accelrys' Discovery Studio 4.0 Visualizer, Accelrys Software Inc., USA.

CHAPTER V

DISCUSSION

5.1 IDENTIFICATION OF NOVEL TARGETS BY INTEGRATION OF THE *IN SILICO* ANALYSIS AND FUNCTIONAL GENOMICS APPROACH

Four targets were identified; *CDC2, FLT3, LAK* and *TLK1* in the high throughput RNAi 'loss-of-function' screen. These hits are overexpressed in gliomas particularly GBM (Rhodes et al. 2004). Less commonly reported kinase related genes were also identified as positive "hits" because the commonly reported well established kinases such as *EGFR, PDGFR*, and *MAPK1* were purposely not included for RNAi screen during the selection of candidate targets since the major aim is to identify novel kinase targets for GBM.

CDC2 or CDK1 is a key player in cell cycle regulation and highly conserved protein that functions as a serine/threonine kinase. CDC2 initiates its protein kinase activity by constructing a complex with cyclin A, cylin B, and p13suc1 (Draetta et al. 1987; Nigg 1995). Recently, RNAi-based screen in malignant pleural mesothelioma (MPM) revealed that CDK1 was found to be a suitable target with additional ability to sensitise MPM cells to cisplatin (Linton et al. 2014). Overexpression of CDC2 promotes oncogenesis and progression of human gliomas and *CDC2* knockdown reduces cells proliferation by causing an increase in the number of G2M cell cycle arrest (Chen et al. 2008).

LAK or lymphocytes alpha-protein kinase or regularly known as ALPK1 or alpha kinase 1 comes from the family atypical kinases. The alpha-kinase family has been reported to be mutated in various cancers (Greenman et al. 2009). ALPK1 has

been implicated in epithelial cell polarity and exocytic vesicular transport towards the apical plasma membrane (Middelbeek et al. 2010). ALPK1 resides on golgi-derived vesicles where it phosphorylates myosin IA, an apical vesicle transport motor protein that regulates the delivery of vesicles to the plasma-membrane (Middelbeek et al. 2010).

FLT3 or fms-like tyrosine kinase 3, a class 3 of receptor tyrosine kinase, has an important role in the regulation of normal haematopoiesis. It was found to be relatively in highly abundance in astrocytic tumours but without detection of any activating FLT3 mutations involved (Eßbach et al. 2013). Activating mutations in FLT3, especially involving internal tandem duplications in the juxta membrane domain, are detected in approximately 30% of adult and 15% of childhood AMLs (Duheir et al, 2000 and Kottaridis et al, 2001) suggesting that the types of FLT3 abnormalities in GBM differ from leukemia. Recently, Bleeker et al. (2014) identified that FLT3 was one of the frequent gene that contained somatic mutations in GBM. On the other hand, the FLT3LG or the fms-like tyrosine kinase 3 receptor ligand, stimulates the maturation and proliferation of immune regulatory cells, dendritic cells and natural killer cells (Bleeker et al. 2014). Overexpression of FLT3LG in GBM cells may provide a positive advantage in activating the anti-tumour immune response (Ali et al. 2005). King et al. (2008) showed that combination therapy with adenoviral Flt3L and adenoviral thymidine kinase therapy had successfully eradicated multifocal brain tumour disease in a syngeneic, intracranial GBM model (King et al. 2008). Previous studies also have demonstrated successful stimulation of the immune system against glioma xenografts in animal models (Ali et al. 2005; King et al. 2008; Muhammad et al. 2009).

When revalidation was performed on the four candidate targets, Tousled-like kinase 1 (TLK1) showed consistent significant reduction in cellular viability. TLK1 was therefore selected for further evaluation of its cellular functions that yet to be fully characterised. TLK1 is a serine/threonine kinase homologous to the Tousled gene in *Arabidopsis thaliana* which is needed for normal flower and leaf development (Roe et al. 1997; Roe et al. 1993). There are two types of TLKs, namely TLK1 and TLK2, that are highly conserved in mammals (Shalom, & Don 1999). TLK1 is a potential novel therapeutic target for GBM and this gene essentially controls growth and survival of GBM cells. TLK1 activity is a cell cycle dependant and

it regulates chromatin dynamics including DNA replication, DNA repair, transcription, and chromosome segregation (De Benedetti 2012). TLK is absent in yeast suggesting that homologs of TLK only present in higher forms of eukaryotes (Carrera et al. 2003). A massive screening of 125 serine threonine kinases (STKs) identifies frequently altered STKs in different types of tumours (Capra 2006). However, due to lack of glioblastoma samples, Capra et al. were unable to identify the significance of TLK1.

5.2 EXPRESSION OF *TLK1* IN DISEASES

Expression of *TLK1* is upregulated in three different GBM cells and the expression is high in the proliferative subtype suggesting that its expression may differ in other GBM subtypes (Kolesnikov et al. 2015). To support these findings an independent microarray dataset GSE36425 was analysed using GEO2R and found that TLK1 expression was significantly higher ($p < 0.05$) in GBM patients with IDH mutation. According to the Cancer Genome Atlas database (c-Bioportal), 3% of GBM patients were found to have TLK1 alterations (Gao et al. 2013). Dysregulation of TLK1 expression is predicted to be related with calcium overload diseases such as glaucoma and Alzheimer's disease (Zhang Y. et al. 2015).

5.3 TLK1-RAC2-CDC42-PAK2 MODEL PATHWAY

From this study, a hypothetical pathway was postulated to explain the TLK1-RAC2-CDC42-PAK2 pathway in GBM cells. TLK1 is a cell cycle kinase which controls DNA transcription. Inhibition of its machinery affects translation of downstream effectors RAC2 and PAK2. Without proper balance or ratio of RAC2/CDC42, it will cause abnormal cellular survival, invasion and migration (Fife et al. 2014; Mulloy et al. 2013). The downstream critical kinase in these processes is the PAK2. Evidence from the microarray analysis identified that most of group 1 PAK substrates were significantly downregulated namely; *LIMK, STMN1, PLK1, AURKA, RAF1, CTBP1, ERα, PXN, AKT1,* and *PGM2*. This suggests strong relationship between TLK1 and PAK2.

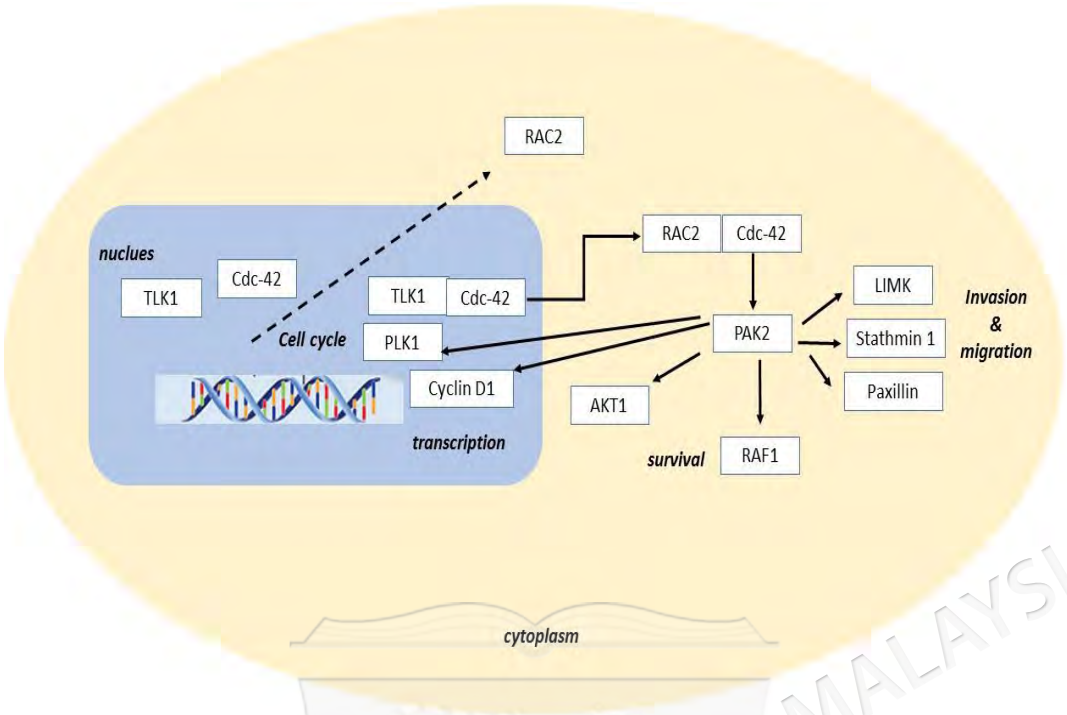

Figure 5.1 Hypothetical TLK1-RAC2-CDC42-PAK2 regulation pathways in GBM. CDC42 is localized within the nucleus together with TLK1. CDC42, being a small Ras GTP-binding protein may bind to TLK1 and might be a substrate for TLK1. Activated CDC42 in the nucleus binds or interact with activated TLK1 protein kinase to emit signals to the other CDC42 binding protein that is localized in the cytoplasm to bind with activated RAC2. In other cases, activated CDC42 may bind to activated TLK1 and later would be released into the cytoplasm to emit signal while binding with RAC2. In an adequate ratio or balance, CDC42 and RAC2 will bind to p21 protein which becomes activated PAK2 and emits signals for other downstream molecules. PAK2 signals AKT1 and RAF1 for the regulation of survival pathways. PAKs signals or interacts with LIMK, stathmin 1 and paxillin to initiate cells invasion and migration by activating important components of cell motility such as invadopodia, lamellipodia or fillopodia. Through this mechanism also, downstream of TLK1, which is PAK2, regulates cell cycle activity with PLK1 and cyclin D1 for initiation of transcriptional machinery. This figure is partially adapted from Baker et al. 2014.

5.4 MECHANISMS OF GBM CELL SURVIVAL REGULATED BY *TLK1*

Knockdown of *TLK1* in GBM cells caused significant reduction in cell viability and cell proliferation as shown by reduction in the clonogenicity potential and DNA synthesis. Subsequently, the latter process induced downstream activation of caspase -3 and caspase-7 intrinsic apoptosis pathway. This is in concordant with previous findings from Carrera et al. (2003), whereby *TLK1* activity was altered in the loss-of-function mutation induced in *Drosophila*, causing nuclear division arrest at interphase accompanied by apoptosis. Alternatively, it may activate a different novel form of

programmed cell death that is independent from caspase activation (Zhang Y. et al. 2015).

Interestingly, NHA was not affected by *TLK1* knockdown by siRNA suggesting that *TLK1* inhibition maybe specific only to the TLK1 over expressing cancer cells and will not disturb the growth and survival of these adjacent normal cells. However, the effect of *TLK1* inhibition by shRNA was unable to be demonstrated because of the difficulties in maintaining NHA cell line. In addition it was also difficult to get enough numbers of cells for further experiments. Although Polo-like kinase 1 (PLK1) was observed to be a better "hit" target to reduce GBM survival, it was reported that inhibition of PLK1 caused normal cell death (Arora et al. 2010). Hence, it was recommended to use *PLK1* as a positive reference target for the RNAi screening to ensure robustness of the assay (Arora et al. 2010; Azorsa et al. 2009; Echeverri & Perrimon 2006). Major problem associated with the current PLK1 inhibitor is manifestation of painful and debilitating peripheral neuropathy and off-target effects with other PLK such as PLK2 and PLK3 apart from being able to activate apoptosis pathway (Strebhardt et al. 2014).

TLK1 was reported to have important roles in the regulation of mitosis and cytokinesis in cells (Li Z., Gourguechon & Wang 2007; Li Z., Umeyama & Wang 2008). Inhibition of *TLK1* by shRNA decreases the number of cells undergoing mitosis by reduction of the cells at G2/M phase. The mechanisms are slightly different between U87MG and LN18 cells, U87MG cells were more sensitive to *TLK1* knockdown with increased G1/G0 cells, decreased G2/M cells and increased S-phase arrest. This was supported by decreased expression of *CDC2* and *TTK* cell cycle checkpoint kinases. However, increased in S-phase arrest was not observed in LN18 but there were increased expression of *CDC2* and *TTK* cell cycle checkpoint kinases. These findings were supported by *TLK1* knockdown in fibroblast cell line (BSF) which caused depletion of spindle formation and chromosome segregation (Li Z. et al. 2008), but not in cells with *TLK2* knockdown (Li Z. et al. 2007). Wang et al. (2004) suggested that TP53 status influences response of patients. They have shown that in TP53 wild type cells, CDC2 phosphorylation was disrupted in a TP53 dependant manner. Another possible indicator for mitotic catastrophe is that the inhibitions of the sister chromatid

cohesion in mitotic cells and DBS repair are due to the downregulation of *RAD21* (1.6 fold change) known as the double-strand-break repair protein rad21 homolog.

A previous study found that *CDC2* was overexpressed and the mean of pThr161-CDC2 positive cells in GBM was 2.8-fold and 5.6-fold higher than oligodendrogliomas and ependymomas respectively indicating active mitosis activation in these cells (Otero & Tihan 2011). CDC2 controls G2 to M transition by post-translation phosphorylation and if targeted, mitosis will be inhibited. Hence, *CDC2* serves as suitable target for GBM sensitisation as other alkylating agents such as temozolomide also induces G2 to M cell cycle arrest (Otero & Tihan 2011). Several issues have been reported with CDK1 inhibitors compared with CDK4/5 (Aarts et al. 2013; Belden et al. 2012; Lindqvist et al. 2009).

In *C. elegans*, TLK1 is reportedly phosphorylated by Aurora B, which later triggers TLK1 to further activates Aurora B kinase activity in an INCENP-dependent manner (Han et al. 2005). TLK1 is also required for Aurora B localisation to the spindle mid zone microtubules during late mitosis (Yeh et al. 2010). Interestingly, this study showed significant down-regulation of *AURKA-A*, *AURKA-B* and *INCENP* suggesting inhibition of both Aurora kinase activities as well as initiation of mitotic catastrophe due to *TLK1* inhibition.

TLK1 overexpression in GBM cells increased cellular survival, proliferation and resistant to apoptosis. This is in line with previous findings that overexpression of *TLK1* in breast and prostate cancers resulted in radiotherapy resistance (Ronald et al. 2011). However, Zhang et al. (2015) observed that overexpression of TLK1 in *Drosphila* eyes induced cell death and the loss of pigmentation. This may suggest that different role of TLK1 in eye development and chromatin regulation (Zhang Y. et al. 2015).

5.4.1 Regulation of Downstream TLK1 Survival Pathways

Different key kinases are implicated in U87MG and LN18 cells. Being TP53 wild type and PTEN mutant cell line, p70 S6 kinase (Thr389) was significantly down regulated and deactivated following TLK1 knock down in U87MG cells. The 70-kDa ribosomal

protein S6 kinase (p70S6k), a serine/threonine kinase, is a downstream target of PI3K/mTOR pathway which regulates cell growth by inducing protein synthesis components (Hanks & Hunter 1995; Ip et al. 2011). p70S6K is commonly reported to be upregulated in breast cancers and GBM (Heinonen et al. 2008; Pelloski et al. 2006). Harada et al. (2001) showed that function of p70s6k is far beyond protein synthesis and growth maintenance. The IGF-1 cytokines signals the p70s6k to control cell survival by inhibiting pro-apoptotic BAD through phosphorylation. Hence, deficient of p70s6k activates pro-apoptotic BAD vice versa (Harada et al. 2001).

Phosphorylated-TP53 were increased confirming that the mechanism of apoptosis occurs via TP53 dependant pathway. At the same time, increased activation of CDC42 (Rho GTPase) in knockdown *TLK1* cells indicates activation of apoptosis signalling pathway. Thomas et al. (2000) suggested that TP53 apoptosis cell death dependant activation did not only occur by *BAX* induction, but also in the presence of upregulation of actively membrane bound CDC42 in the wild type *TP53* cells (Thomas et al. 2000). In contrast, Tu and colleague (2001), suggested that CDC42 is actually a substrate for caspase which cause Fas-induced apoptosis via NFkB pathway (Tu & Cerione 2001). Alternatively, decreased CDC42 activity in overexpressed TLK1 cells resulted in cellular over growth which is in concordant with Warner et al. findings (Warner S.J. et al. 2010).

Mutations that affect *TP53*, an important guardian of the genome, significantly cause changes to the cellular feedback mechanisms. In LN18 cell line with mutant *TP53* and wild type *PTEN*, the cells showed different response to *TLK1* knockdown and overexpression. Knockdown of *TLK1* did not affect p70s6k activation, with decreased phosphorylated TP53 and decreased in CDC42 activation. The mode of apoptosis in LN18 cells identified earlier is through CDC42-PTEN-dependant mediated cell death pathway (Deevi et al. 2011). In overexpress TLK1 cells, the increased of CDC42 activation may suggest its role of LN18 aggressiveness compared with U87MG.

5.5 CHEMOSENSITISATION OF GBM CELLS BY TLK1 SILENCING

Activation of MGMT repair enzyme, the O6-methylguanine-DNA methyltransferase that repairs TMZ-generated O6-methylguanine-DNA adducts, is one factor that cause TMZ-resistance in GBM cells. Presence of the enzymes inherently activates the Base Excision Repair (BER) and Mismatch Repair System (MMR). Synthetic lethality identifies few genes such as MRP1 and WEE1 that increase chemo-sensitisation towards TMZ (Pokorny et al. 2015; Tivnan et al. 2015). Although MGMT is known to be a regular factor for TMZ resistance, current knowledge identifies that miRNA contributes an important factor in TMZ resistance (Hiddingh et al. 2014). In this study, *TLK1* would be an important target for sensitizing GBM cells towards TMZ. *TLK1* is also involved in the DNA damage and DNA repair whereby the kinase activity of *TLK1* decreases in response to genotoxic stress, such as ionizing radiation or treatment with hydroxyurea (Groth et al. 2003; Krause et al. 2003).

Overexpression of TLK1B, a spliced variant of the TLK1 mRNA increases resistance to ionizing radiation and doxorubicin, most likely due to changes in chromatin remodelling. Formation of TLK1-RAD9 complex activates DNA double stranded breaks (DSB). The repair mechanism occurs when RAD9 exchanges with ASF1 to promote nucleosomes eviction at the DSB and access to promote DNA repair (Sunavala-Dossabhoy & De Benedetti 2009). Knockdown of TLK1 inhibits phosphorylation of TLK-mediated phosphorylation of RAD9 (Ser-328) and chromatin assembly ASF1A and ASF1B, leading to impaired checkpoint recovery and inhibition of double stranded break (DSB) repair (Sillje & Nigg 2001; Sunavala-Dossabhoy & De Benedetti 2009). In the microarray data, similar pattern was observed whereby the expression of ASF1B was significantly downregulated by 1.62 fold change. Signature of DNA damage activation was observed by significant downregulation of CHK1 and CDC25A (Pires et al. 2015).

Takayama et al. (2010) demonstrated that *TLK1* knockdown induced sensitisation of a platinum-based cytotoxic compound cisplatin in cholangiocarcinoma cells. Ronald et al. (2011) showed that knockdown of *TLK1* sensitised DU45 prostate cancer cells to radiation significantly. Silencing of *TLK1*

sensitised GBM cells to TMZ especially in U87MG cells which have *PTEN* mutants but wild-type *TP53*. TMZ induces DNA damage by formation of DNA adducts and promotes G2 and S phase cell cycle arrest (Cui et al. 2010). Glioma cells with wild type *TP53* expression have the capability to sensitise cells to drugs and this supports the evidence that silencing *TLK1* sensitises U87MG cells to TMZ (Hermisson et al. 2006; Roos et al. 2007; Martin et al. 2012). However in cells with mutant *TP53*, GBM cells are resistant to TMZ (Blough et al. 2011). Simultaneous inhibition of *TLK1* may cause "global" and enhanced cell cycle arrest at both G2 to M and S-phase, synergizing the effect of TMZ on GBM growth inhibition. Nevertheless, not all chemotherapeutic agents are suitable for sensitisation with *TLK1* (Takayama et al. 2010).

5.6 REGULATION OF INVASION AND MIGRATION PATHWAYS BY TOUSLED-LIKE KINASE 1 IN GLIOBLASTOMA MULTIFORME

Targeting only apoptosis and survival signalling pathways is inadequate to stop cancer progression because this approach can rescues subpopulation of cancer cells from lethal DNA damage (Krakstad & Chekenya 2010). Hence, testing new molecular targets would require many strategies and one of them is to understand their roles in the invasion and migration pathways. Unique from other types of solid tumours, GBM cells rarely metastasise outside the brain but exhibit highly invasive behaviour. The GBM tumour cells infiltrate normal brain tissue which are phenotypically glial within the CNS (Dwyer & Matthews 2011). The invasion of GBM cells towards adjacent normal astrocytes occurs due to the disruption of the balance between the normal neural extracellular microenvironment inhibition to cellular reorganisation (Dwyer & Matthews 2011; Galtrey & Fawcett 2007). The neural ECM is quite complex unlike other peripheral matrices whereby they exhibit low levels of fibrillary proteins such as collagen, laminin and fibronectin (Ruoslahti 1996) which are localised at the substructures of CNS like subpial space, blood vessels, basement membranes and white matter tracts (Dwyer & Matthews 2011). However, the backbone of neural ECM is hyaluronic acid (HA) and majority of HA binding proteins are lectican family members of chondroitin sulfate proteoglycans like versican, aggrecan, brevican and brain-specific neurocan (Bandtlow & Zimmermann 2000).

GBM cells, when transfected with si-*TLK1* or sh-*TLK1*, had significantly reduced cell migration and invasion as observed by functional trans-well migration and invasion assay. This suggests that *TLK1* has an important role in the regulation of GBM cell invasion and migration. *TLK1* knockdown inhibits polar cells of *Drosophila* ovary to initiate collective movements of motile and non-motile which is an essential process for cellular invasion that may drive metastatic process (Xiang et al. 2015).

Interesting characteristics of *TLK1* inhibition observed in this study are the changes in the cell morphology seen in U87MG cells which are much more differentiated in its structure compared with LN18. The epithelial like astrocytic GBM cells become larger and flatter. This finding suggests that the formation of lamellipodia, fillopodia and invadopodia of GBM cells are inhibited. The mechanism involved in this process is still unknown. Functional microarray of *TLK1* knockdown in U87MG cells, was performed to identify downstream molecular pathways of *TLK1*. Several key pathways that regulate cellular motility and invasion were identified. The canonical pathways were found to be downregulated including TGF-beta, WNT, focal adhesion, mTOR, parkin-ubiquitination proteosomal system, and integrin mediated cell adhesion and regulation of actin cytoskeleton signalling pathways. In addition , there was also significant activation of IL-11 signalling pathway which has been reported as an emerging cytokine to mediate tumour promoting signals together with IL-6 (Ernst & Putoczki 2014).

The hypothesis is that TLK1 mediates invasion pathway through the integrin mediated focal adhesion pathway and RAC2 is the substrate for TLK1 to modulate downstream signalling. Components of the integrin mediated pathway including *RAC2, PXN, ROCK2* and *FYN* were observed to be significantly downregulated in both microarray and gene expression data analysis. Functional microarray analysis showed that *TLK1* silencing reduced src related oncogene *FYN* expression and hence inhibited PI3K signalling leading to suppression of *PAK2*. The p21 protein is an activated form of CDC42-RAC2-complex which finally inhibits focal adhesion turnover and cell survival (Szczepanowska 2009). *RAC2* expression is significantly upregulated in GBM cells especially U87MG but it is not expressed in any part of normal human brain cells (Uhlen et al. 2015). In line with the gene expression findings, *RAC2* was found to be

deactivated in *TLK1* knockdown GBM cells via ELISA-based assay. Uniquely, CDC42 activation was reduced in LN18 cells but increased in U87MG cells.

RAC2 gene is encoded for RAC2 which is RAS-related C3 botulinum toxin substrate 2, a small GTP binding protein in the RAC subfamily of the RAS superfamily together with RAC1, RAC3, and RhoG binding proteins (Pulgar et al. 2005). RAS protein is essential in the lamellipodial protrusions during mesenchymal migration and amoeboid migration of RAS transformed cells (Friedl & Wolf 2003). The loss of U87MG structure might be due to the reduction of RAC2 expression. Macrophages with RAC2-/- have reduced F-actin levels and completely lack podosomes, the integrin-based adhesion sites (Wheeler A.P. et al. 2006), which are related to invadopodia implicated for cancer cell invasion by matrix degradation (Seals et al. 2005). These findings was in concordant with recent findings by Joshi et al. in an *in vivo* mice study where mice lacking Rac2 displayed marked defect in tumour growth, angiogenesis and metastases (Joshi et al. 2014). In glioblastoma stem cells, RAC2 proteins are also involved in STAT3 and ERK activation, and regulates GSC marker expression such as CD133, SOX2 and HIF-2α to maintain its glioblastoma stem-cells like feature (Lai et al. 2015). In normal development circumstances, RAC2 is required for postnatal anti-angiogenic response involving wound healing (De et al. 2009).

CDC42 is also being part of the Rho-GTPase family proteins which have two functions; one regulates cell polarity and secondly it orchestrate cell cycle progression (Vega & Ridley 2008). CDC42 plays an essential role in controlling the direction of cell migration by determining the cell membrane localisation of lamellipodia, and by moving the microtubule-organising centre and Golgi apparatus in front of the nucleus and towards the leading edge of the cell. Overexpression of CDC42 in an orthotopic xenograft model showed enhancement of glioma cell invasion and migration (Okura et al. 2015).

The p21 activated kinases (PAK) is a serine/threonine kinases that are critical effectors that connect Rho GTPases to cytoskeleton reorganisation and nuclear signalling. It act as targets for the small GTP binding proteins, CDC42 and RAC, and have been implicated in a wide range of biological activities. It is presence in six

isoforms namely; PAK 1-6. PAK 1 – 3 belongs to the PAK I family, whilst PAK 4-6 belongs to PAK II family (Radu et al. 2014; Rane & Minden 2014). PAK 1 family proteins maybe viable targets for Ras-driven cancers as it is link as Ras effector signalling (Baker N.M. et al. 2014). PAK facilitates cross-talk with both RAF and PI3K effector signalling networks and enhances ERK signalling by phosphorylation of RAF-1 (Ser-338) and MEK1 (Ser-298) (Chaudhary et al. 2000; Coles & Shaw 2002; Eblen et al. 2002; Sun et al. 2000) as well as influencing transcription of genes that promote cell-cycle progression and cell survival by phosphorylating b-catenin (Arias-Romero et al. 2013; Zhu et al. 2012). *PAK2* is downregulated and appears to be significant within the microarray analysis. Marlin et al. (2009) described that conditional activation of full length PAK2 stimulated loss of contact inhibition and anchorage-independent in Hs578T cells. PAK2 also inhibits cell death of Hs578T cells during cisplatin induction and downregulates activation of caspase-3 and its own caspase cleavage to the proapoptotic PAK-2p34 fragment (Marlin et al. 2009). Activated PAK2 phosphorylates c-Jun at five threonine sites (Thr-2, Thr-8, Thr-89, Thr-93, and Thr-286) and displays an important role in EGF-induced cell proliferation and transformation (Li et al. 2011). PAK2 is overexpressed in breast cancer cell lines and phosphorylation of caspase-7 by PAK2 at Ser-30, Thr-173, and Ser-239 residues prevents doxorobuxin-induced apoptosis in breast cancer cell lines (Li et al. 2011). PAK2 is also reported to be hyperactivated or upregulated in colorectal, thyroid, pancreatic and ovarian cancers (Kumar et al. 2006). The activity of PAK2 depends on the dominant type of extracellular matrix. In this case they found that under collagen 1 in ovarian cancer, the PAK2 activity is higher to stimulate ovarian cell motility comparing with growing cells under fibronectin (Flate & Stalvey 2014).

Invadopodia are actin-based protrusions of tumour cells that modulate ECM proteolysis like fibronectin, laminin, and collagens. Inhibition of invadopodia may be observed by reduction of the number of components for actin assembly namely, Arp2/3 actin nucleation complex, neural Wiskott Aldrich Syndrome protein N-WASP-actin and contarctin (Winograd-Katz et al. 2014). In U87MG with *TLK1* inhibition, *ARPC1B* mRNA expression encodes one of the seven subunits of the human Arp2/3 protein that are downregulated.

Using functional microarray data on the global mRNA profiling of *TLK1* inhibition, the mechanisms involved in TLK1 related GBM invasion and migration was identified. Although adhesion of cells towards ECM components namely laminin and fibronectin were increased, there were absence of any upregulation of proteosomal enzymes. The process may actually activates formation of podosomes. Podosomes, commonly misunderstood as invadopodia, are present in normal differentiated cells (Murphy & Courtneidge 2011; Tarone et al. 1985). Podosomes exert adhesive and ECM degradation functions but do not have protrusive activity (Tarone et al. 1985). This have been confirmed by microarray data that absence of protease related genes or markers for example *MMPs* that were significantly dysregulated. Although some studies suggest that podosome forming "normal" cells may activate the invasion of tumour cells if alternative pathway activation occurs, for example *EGF* and *CSF-1* is increased (Hideki et al. 2006), our microarray data showed that these genes were not significantly differentially expressed. Hence, TLK1 knockdown may restore the podosomes of normal astrocyte function.

5.7 *IN VIVO* VALIDATION OF TLK1 IN SUBCUTANEOUS U87MG XENOGRAFT MODEL

The functional role of TLK1 in regulating GBM tumour growth in *balb-c* female nude mice was investigated. Although subcutaneous xenograft of knocked-down TLK1 cells showed significant decreased in growth rate, overexpressed TLK1 subcutaneous xenograft failed to show any effect on tumour growth. This might be due to the fact that the control cell line and overexpressed TLK1 cells are both already very aggressive in nature. Histopathological examination on tumour tissue could confirm this hypothesis. There was no significant tumour growth between control and knockdown cells at 42 days because tumour growth become irregular hence will be the study outliers. In the future, performing such experiment using low-grade glioma cell line could identify mechanistic behaviour of overexpressed TLK1 induced cells. Ronald and colleagues performed prostate cancer grade 3 (PC-3) xenograft model study in SCID/bg mice to test the *in vivo* effects of TLK1 inhibitor namely anti-psychotics thioridazine. Interestingly, oral administration of thioridazine inhibits tumour growth significantly (Ronald et al. 2013). Their study however only looked at the effects of TLK1 inhibition

or sensitisation effects towards the tumour xenograft rather than understanding functional role of the kinase in cancer progression.

5.8 COMPARATIVE MODELLING AND IDENTIFICATION OF TOUSLED-LIKE KINASE 1 INHIBITORS FOR GLIOBLASTOMA THERAPY VIA HIGH THROUGHPUT VIRTUAL SCREENING PROTEIN-LIGAND DOCKING

GBM remains as the solid tumour with the poorest survival in adults since the past few decades. The search for the right molecular target is still ongoing and one of the many approaches is by using computer-aided drug discovery tools. Our recent *in vitro* study identified TLK1 as a potential target for glioblastoma. We found *TLK1* to be overexpressed and the knockdown of *TLK1* reduced cellular proliferation and invasion (Ibrahim et al. 2013). An auto-phosphorylated chemical inhibition screen on recombinant TLK1B, which is a known splice variant, has been performed by Ronald et al, using more than 6,000 compounds. This study identified four inhibitors belonging to the class of phenothiazine antipsychotics that are structurally and chemically similar. The same study also showed that thioridazine was able to sensitize prostate cancer cells when used with doxorubixin (Ronald et al. 2013). Although chemical library screening for drug discovery seems promising, it is very expensive and time consuming. A study using the ChemBL database and Kinase SaRfari application identified 74 “hits” compounds that can potentially bind to TLK1 (Bento et al. 2014). However, no details were reported on the specific biding sites and the specific TLK1 structure that were used for the screen. In this study we used a computational approach to identify suitable TLK1 inhibitors based on a homology model that has been created.

One of the major challenges for optimal therapeutic intervention for glioblastoma and other types of brain tumor is to achieve maximal penetration across the blood brain barrier (BBB). The BBB is a structure composed of endothelial cells which is associated with perivascular neurons, pericytes and astrocytic end-feet processes. The endothelial cells connected by tight junctions form an almost impenetrable barrier to all compounds except highly lipidized small molecules of less than 400 Da (Nathanson, & Mischel 2011). Although many studies have identified drug-like molecules from high throughput virtual screening, most only follow the

Lipinski's rule of five and have neglected the probability calculations for the molecules to cross the BBB. This eventually led to dismal results in *in vivo* studies (Pardridge 1998; J. Wang et al. 2011). We used the recent version of the free pharmacokinetic and pharmacology identification software faf-drug3 combined with ADME-TOX software and utilized the CNS filter to identify drug-like molecules that are able to cross the BBB. After filtering 226 compounds identified from MTiopenscreen, we have characterized that 2-[2-(1H-Imidazol-5-yl)ethyl]-1H-benzo[de]isoquinoline-1,3(2H)-dione as the only best compound that fulfilled the CNS criteria. We observed that more than 60% of the interactions involved between receptor and ligands are hydrophobic. Identified compound is a hybrid between imidazole and isoquinoline derivatives.

The derivatives isoquinoline and imidazole a compound has been reported to be as an important component to inhibit molecular structures involved in cancer. Isoquinoline derivatives are abundant in natural products which have the ability to inhibit tumor cell growth and have low toxicity to normal cells (Yang et al. 2015). They have been identified as bioactive ingredients in many natural product-based therapeutics (Bentley 2006; Kitson, Millemaggi & Taylor 2009). To improve the solubility and selective delivery into tumour cells, Yang et al (2015) developed delivery of these compounds in tumour-cell targeted liposomes. Isoquinoline derivative named EDL-291 having molecular weight less than 200kD exhibits anti-glioblastoma effects both in vitro and in vivo (X. Wang et al. 2012). The quinoline alkaloids ring compounds show antiproliferative activity on a broad spectrum of different tumors, as they can target many different signaling and enzymatic pathways. Quinoline-based inhibitors against any of these pathways can potentially be effective anticancer drugs. Furthermore, several researchers have shown that quinoline-based compounds have the potential of being a very efficient drug with differential cell killing effects against malignant tumors. This important property of quinoline can be utilized further by studying the mechanism of action for each promising quinoline compound. Targeting selective cancer-specific signalling or enzymatic pathways by a quinoline compound will be extremely important for the development of effective and safe anticancer therapeutics. To further optimize the full potential of quinoline compounds, the structure based relationship-based study will likely continue to play an important role. It is highly likely that optimized quinoline compounds with excellent potency and little side effects will continue to be created.

Since quinoline compounds can substantially sensitize cell killing by other anticancer drugs in a cancer-specific manner, they can be very effective sensitizers for conventional cancer therapeutics (Viswas, & Lee 2011).

Imidazole a five member nitrogenous heterocycle constitutes the part of many essential amino acids histidine, bovine and vitamin B12 (Anderson, & Long 2010; Bellina, Cauteruccio & Rossi 2007). Imidazoles and their derivatives have attracted the attention of scientists due to their significant importance for designing the targeted molecules of medicinal importance which is closely related to the presence of polar imidazole ring, with two nitrogen atoms separated with a methylene, hydrogen bonds in which one amino hydrogen behaves as the donor while the other amino nitrogen as the acceptor (Anderson, & Long 2010). Imidazole and their derivatives are important scaffolds used in the treatment of many diseases like HIV-AIDS, cancer, tuberculosis and hepatitis C (Mumtaz et al. 2016). The substitution on different positions gives several compounds of interest. Thus, imidazole compounds have been an interesting source for researchers for more than a century. Structure activity relationship were reduced from biological results and will be used in further design of new active compound (Baroniya et al. 2010). Using multicomponent reaction, researchers manage to produce a series of 2,4,5-trisubstituted and 1,2,4,5-tetrasubstituted imidazole derivatives. Their anti-cancer potential was further evaluated against the panel of 60 National Cancer Institute cancer cell lines. Compound labelled as NSC 771432 displayed significant cytotoxic potential across the NCI 60 cell line panel. Further, in vitro studies confirmed that the NSC 771432 affects proliferation, migration, and anchorage independent growth of lung cancer cells by inducing cellular senescence. Taken together, the current study significantly highlights the potential of imidazole based molecules to develop novel anti-cancer agents (Sharma et al. 2014).

Findings from this study were based on a theoretical investigation of TLK1 3D model inhibition at the catalytic ADP site. However, the non-catalytic component of a particular kinase may also play a significant role in the regulation of cellular functions (Romano & Kolch 2011). Allosteric inhibition is possible if the TLK-ligand complex structure is further studied.

CHAPTER VI

CONCLUSIONS

Combination of *in silico* meta-analysis and selective RNAi screening allows identification of novel kinome pathways as potential targets for GBM therapy. *In silico* meta-analysis of microarray datasets had identified 113 upregulated kinases in GBM. Further robust statistical analysis of the custom loss-of-function RNAi screen identified four kinases namely *CDC2, FLT3, TLK1* and *ALPK1* as potential therapeutic targets for GBM. However, only Tousled-like kinase 1 (*TLK1*), a serine-threonine kinase commonly localised in the nucleus, was selected for further validation as its molecular functions in cancer particularly in GBM have not been widely studied.

In vitro functional analyses have been performed extensively to understand the roles of *TLK1* in GBM. Gene expression analysis has revealed that *TLK1* was overexpressed in U87MG and LN18 cell lines. TLK1 functions specifically in regulating GBM survival pathways and invasion-migration pathways were investigated. *TLK1* knockdown using siRNA and shRNA reduced cell viability and suppressed clonogenic potential of GBM cells. Further investigation identified the mechanisms involved were cell cycle arrest at G2M and G0G1 phases and induction of apoptosis signals through caspase-3 and caspase-7 intrinsic pathway activation. *In vitro* overexpression of TLK1 increased clonogenic potential and the GBM cells became resistant to apoptosis towards treatment with TMZ. There was also an increase in proliferative capacity as observed by cell viability and BrdU proliferation assays. Interestingly, TLK1 knockdown sensitised GBM cells towards TMZ suggesting that *TLK1* plays pivotal role for the repair of TMZ-induced DNA damage. The downstream GBM survival pathways affected by the *TLK1* inhibition were different between U87MG and LN18 cell lines. In LN18 cells, harbouring *TP53* mutant and *PTEN* wild

type, inhibition of *TLK1* decreased phosphorylated TP53 but did not increase phosphorylation of p70 S6K. Concurrently, CDC42 activation was also decreased. In contrast, knockdown of *TLK1* in U87MG cells (*PTEN* mutant, *TP53* wild type) decreased p70 S6K (mTOR/PI3K) activation and increased phosphorylation of TP53 and CDC42 (Rho GTPase) activation. These findings suggest that the mechanism of cell death in U87MG is typically via *TP53* dependent pathway.

Knockdown of *TLK1* significantly inhibited invasion and migration capacities of both U87MG and LN18 cells. Overexpression of *TLK1* increased invasion and migration of GBM cells. These results suggest that *TLK1* also regulates GBM cell invasion and migration. Morphological changes resulting from *TLK1* knockdown are probably due to inhibition of lamellipodia, fillopodia and invadopodia formations in GBM cells. *TLK1* knockdown with siRNA showed increased adhesion of GBM cells to collagen 1 and laminin suggesting activation of podosome rather than invadopodia formation. These results represent a valuable starting point for further approaches to determine *TLK1* downstream regulatory network. Silencing *TLK1* in normal human astrocyte (NHA) did not affect NHA cell viability or causing apoptosis as well as it did not affect GBM cell invasion and migration suggesting the effects of *TLK1* inhibition only occur in GBM cancer cells.

Functional microarray analysis identified global changes in U87MG cell transcriptome following knockdown of *TLK1* expression. Amongst important pathways involved in the invasion and migration of GBM cells were focal adhesion, integrin mediated cell adhesion and regulation of actin cytoskeleton pathways. Integrin-mediated cell adhesion pathway was further chosen for validation as one of its regulatory components, *RAC2* that encodes a Rho GTPase protein, was amongst the top significantly downregulated genes following *TLK1* knockdown. Gene expression analysis confirmed the involvement of RAC2-CDC42-PAK2 signalling pathway. RAC2 is important in regulating the lamellipodia formation during cell migration. *RAC2* was highly expressed in GBM cells particularly in U87MG cell line. Interestingly, ELISA based assay showed similar pattern of protein activation in U87MG in comparison with microarray findings. RAC2 activation was inhibited significantly whilst CDC42 activation was increased. Unfortunately, due to time and

funding limitation, PAK2 expression level was unable to be characterised. This leads to a working model whereby activated CDC42 in the nucleus binds or interacts with activated TLK1 protein kinase and activate RAC2. In other cases, activated CDC42 may bind to activated *TLK1* and later would be released in to the cytoplasm to emit signal while binding with RAC2. In an adequate ratio or balance; CDC42 and RAC2 will bind to p21 activated kinase 2 (PAK2) and emit signals for cellular invasion and migration activity. From this study, using *in vivo* female *balb-c* subcutaneous xenograft mice, it was shown that *TLK1* knockdown reduced GBM cell tumourigenic potential.

Finally, a 3D model for the catalytic domain of TLK1 model protein was successfully predicted to be a potential molecular target for GBM. Vigorous analysis was performed to determine its suitability and stability of the modelled structure through various structural bioinformatics platform. ID26626142 known as 2-[2-(1H-Imidazol-5-yl)ethyl]-1H-benzo[de]isoquinoline-1,3(2H)-dione was identified as the candidate compounds that potentially bind to TLK1 3D model. Further *in vitro* and *in vivo* studies is indeed needed to validate the therapeutic value of identified compound for GBM. Testing compound using multiple GBM cell lines will allow better understanding regarding functional inhibition of TLK1. For *in vivo* study, testing compound using orthotopic tumour mice model will provide accurate characterization of compound in inhibiting GBM from being more aggressive.

6.1 STUDY LIMITATIONS

GBM is a very heterogeneous disease and many key genes were involved which might be mutated or overexpressed. In this study the in vitro model used was only *TP53* wild type or mutant and *PTEN* wild type or mutant. Hence, results obtained might be bias to only specific mutations.

6.2 FUTURE STUDIES

Characterisation of TLK1 expression using IHC in Malaysian GBM patients' should be performed to determine its relevancy in this population. The major study limitation was that determination of the *TLK1* expression of in the Malaysian patients' using

immunohistochemistry cannot be performed. It is contributed to the low incidence of GBM in the population. Hence, future characterisation of TLK1 expression using IHC in Malaysian GBM patients' should be performed to determine its relevancy in this population.

In depth study on the role of TLK1 regulating the CDC2-RAC2-PAK2 pathway is warranted in order to confirm our initial findings. Measurement of actin cytoskeletal distribution by F-actin staining in *TLK1* knockdown and overexpress cells will be useful to validate the involvement of *TLK1* in regulating actin cytoskeleton reorganization and regulation of GBM cancer cell motility downstream of *TLK1*.

Testing the identified *TLK1* inhibitor, 2-[2-(1H-Imidazol-5-yl)ethyl]-1H-benzo[de]isoquinoline-1,3(2H)-dione in an *in vivo* system will determine whether they are suitable for future clinical use to reduce GBM tumour burden. They may be tested together with other FDA approved inhibitors such as the third generation PI3K inhibitors or the EGFR inhibitors.

This study has unveiled the downstream pathways of *TLK1* from functional microarray analysis. However, to provide accurate understanding of downstream phospho-signalling mechanisms involved in *TLK1* regulation, SILAC-phosphoprotemics technology will be advantageous. This high throughput proteomics technology has been proven to characterise many unidentified signalling pathways in cancer. Mining exact protein-protein interactions is also needed to understand TLK1 specific substrates that activate relevant cancer pathways. The most essential work that needs to be done is to purify and crystallize the protein structure of TLK1 so that characterization of TLK1 structure and function can be performed accurately.

REFERENCES

Aarts, M., Linardopoulos, S. & Turner, N. C. 2013. Tumour selective targeting of cell cycle kinases for cancer treatment. *Current Opinion in Pharmacology*, *1*, 1–7.

Adamson, C., Kanu, O. O., Mehta, A. I., Di, C., Lin, N., Mattox, A. K. & Bigner, D. D. 2009. Glioblastoma multiforme: a review of where we have been and where we are going. *Expert Opinion On Investigational Drugs*, *18*(8), 1061–1083.

Albert, L., Karsy, M., Murali, R. & Jhanwar-Uniyal, M. 2009. Inhibition of mTOR activates the MAPK pathway in glioblastoma multiforme. *Cancer Genomics and Proteomics*, *6*(5), 255–261.

Aldape, K. D., Ballman, K., Furth, A., Buckner, J. C., Giannini, C., Burger, P. C., Scheithauer, B. W. et al. 2004. Immunohistochemical detection of EGFRvIII in high malignancy grade astrocytomas and evaluation of prognostic significance. *Journal Of Neuropathology And Experimental Neurology 63*(7): 700–707.

Ali, S., King, G., Curtin, J., Candolfi, M., Xiong, W., Liu, C., Puntel, M. et al. 2005. Combined immunostimulation and conditional cytotoxic gene therapy provide long-term survival in a large glioma model. *Cancer Research 65*(16): 7194–7204.

Allen, N. J. & Barres, B. A. 2009. Glia — more than just brain glue. *Nature 457*(February):675–677.

Arias-Romero, L. E., Villamar-Cruz, O., Huang, M., Hoeflich, K. P. & Chernoff, J. 2013. Pak1 kinase links ErbB2 to β-catenin in transformation of breast epithelial cells. *Cancer Research 73*(12): 3671–3682.

Arora, S., Gonzales, I.M., Hagelstrom, R.T., Beaudry, C., Choudhary, A., Sima, C., Tibes, R., Mousses, S. and Azorsa, D.O., 2010. RNAi phenotype profiling of kinases identifies potential therapeutic targets in Ewing's sarcoma. *Molecular Cancer 9*(1): 1

Asthagiri, A. R., Pouratian, N., Sherman, J., Ahmed, G. & Shaffrey, M. E. 2007. Advances in Brain Tumor Surgery. *Neurologic Clinics 25*(4):975–1003.

Azorsa, D.O., Gonzales, I.M., Basu, G.D., Choudhary, A., Arora, S., Bisanz, K.M., Kiefer, J.A., Henderson, M.C., Trent, J.M., Von Hoff, D.D. and Mousses, S., 2009. Synthetic lethal RNAi screening identifies sensitizing targets for gemcitabine therapy in pancreatic cancer. *J Transl Med 7*(43)

Baker, N.M., Chow, H.Y., Chernoff, J. and Der, C.J., 2014. Molecular Pathways: Targeting RAC–p21-Activated Serine–Threonine Kinase Signaling in RAS-Driven Cancers. *Clinical Cancer Research 20*(18): 4740-4746.

Baker, S.D., Wirth, M., Statkevich, P., Reidenberg, P., Alton, K., Sartorius, S.E., Dugan, M., Cutler, D., Batra, V., Grochow, L.B. and Donehower, R.C., 1999. Absorption, metabolism, and excretion of 14C-temozolomide following oral

administration to patients with advanced cancer. *Clinical Cancer Research 5*(2): 309-317.

Bandtlow, C. E. & Zimmermann, D. R. 2000. Proteoglycans in the developing brain: new conceptual insights for old proteins. *Physiological Reviews 80*(4): 1267–1290.

Bao, S., Wu, Q., McLendon, R. E., Hao, Y., Shi, Q., Hjelmeland, A. B., Dewhirst, M. W. et al. 2006. Glioma stem cells promote radioresistance by preferential activation of the DNA damage response. *Nature 444*(7120): 756–760.

Bao, S., Wu, Q., Sathornsumetee, S., Hao, Y., Li, Z., Hjelmeland, A. B., Shi, Q. et al. 2006. Stem cell-like glioma cells promote tumor angiogenesis through vascular endothelial growth factor. *Cancer Research 66*(16): 7843–7848.

Baroniya, S., Anwer, Z., Sharma, P. K., Dudhe, R. & Kumar, N. 2010. Recent advancement in imidazole as anti cancer agents : A review. *Der Pharmacia Sinica*, *1*(3), 172–182.

Belden, C.J., Valdes, P.A., Ran, C., Pastel, D.A., Harris, B.T., Fadul, C.E., Israel, M.A., Paulsen, K. and Roberts, D.W., 2011. Genetics of glioblastoma: a window into its imaging and histopathologic variability. *Radiographics 31*(6): 1717-1740.

Bellina, F., Cauteruccio, S. & Rossi, R. 2007. Synthesis and biological activity of vicinal diaryl-substituted 1 H -imidazoles. *Tetrahedron 63*(799), 4571–4624.

De Benedetti, A. and Graff, J.R., 2004. eIF-4E expression and its role in malignancies and metastases. *Oncogene 23*(18): 3189-3199.

Bentley, K. W. 2006. b -Phenylethylamines and the isoquinoline alkaloids *Natural Product Reports* 444–463.

Bento, A. P., Gaulton, A., Hersey, A., Bellis, L. J., Chambers, J., Davies, M., Krüger, F. A. et al. 2014. The ChEMBL bioactivity database: an update. *Nucleic Acids Research 42*(Database issue): D1083–90.

Berns, K. & Bernards, R. 2012. Understanding resistance to targeted cancer drugs through loss of function genetic screens. *Drug Resistance Updates 15*(5-6): 268–275.

Birchmeier, C., Birchmeier, W., Gherardi, E. & Vande Woude, G. F. 2003. Met, metastasis, motility and more. *Nature Reviews. Molecular Cell Biology 4*(12): 915–925.

Birmingham, A., Selfors, L. M., Forster, T., Wrobel, D., Kennedy, C. J., Shanks, E., Santoyo-Lopez, J. et al. 2009. Statistical methods for analysis of high-throughput RNA interference screens. *Nature Methods 6*(8): 569–575.

Bleeker, F. E., Lamba, S., Zanon, C., Molenaar, R. J., Hulsebos, T. J. M., Troost, D., van Tilborg, A. A. et al. 2014. Mutational profiling of kinases in glioblastoma. *BMC Cancer 14*: 718.

Bleeker, F.E., Molenaar, R.J. and Leenstra, S., 2012. Recent advances in the molecular understanding of glioblastoma. *Journal of neuro-oncology 108*(1): 11-27

Blough, M. D., Beauchamp, D. C., Westgate, M. R., Kelly, J. J. & Cairncross, J. G. 2011. Effect of aberrant p53 function on temozolomide sensitivity of glioma cell lines and brain tumor initiating cells from glioblastoma. *Journal Of Neuro-Oncology 102*(1): 1–7.

Blume-Jensen, P. & Hunter, T. 2001. Oncogenic kinase signalling. *Nature 411*(6835):355–65.

Bonavia, R., Inda, M. -d.-M., Cavenee, W. K. & Furnari, F. B. 2011. Heterogeneity Maintenance in Glioblastoma: A Social Network. *Cancer Research 71*(12): 4055–4060.

Brandes, A. A., Franceschi, E., Tosoni, A., Hegi, M. E. & Stupp, R. 2008. Epidermal growth factor receptor inhibitors in neuro-oncology: hopes and disappointments. *Clinical Cancer Research 14*(4): 957–960.

Brat, D. J., Castellano-Sanchez, A. A., Hunter, S. B., Pecot, M., Cohen, C., Hammond, E. H., Devi, S. N. et al. 2004. Pseudopalisades in glioblastoma are hypoxic, express extracellular matrix proteases, and are formed by an actively migrating cell population. *Cancer Research 64*(3): 920–927.

Bredel, M., Bredel, C., Juric, D., Harsh, G. R., Vogel, H., Recht, L. D. & Sikic, B. I. 2005. Functional network analysis reveals extended gliomagenesis pathway maps and three novel MYC-interacting genes in human gliomas. *Cancer Research 65*(19): 8679–8689.

Brooks, M. D., Sengupta, R., Snyder, S. C. & Rubin, J. B. 2013. Hitting Them Where They Live: Targeting the Glioblastoma Perivascular Stem Cell Niche. *Curr Pathobiol Rep 1*(2): 101–110.

Burridge, K. & Wennerberg, K. 2004. Rho and Rac Take Center Stage. *Cell 116*(2): 167–179.

Calabrese, C., Poppleton, H., Kocak, M., Hogg, T. L., Fuller, C., Hamner, B., Oh, E. Y. et al. 2007. A Perivascular Niche for Brain Tumor Stem Cells. *Cancer Cell 11*(1): 69–82.

Capra, M. 2006. Frequent Alterations in the Expression of Serine/Threonine Kinases in Human Cancers. *Cancer Research 66*(16): 8147–8154.

Carico, C., Nuño, M., Mukherjee, D., Elramsisy, A., Dantis, J., Hu, J., Rudnick, J. et al. 2012. Loss of PTEN is not associated with poor survival in newly diagnosed

glioblastoma patients of the temozolomide era *PLoS ONE*, *7*(3): 1–8.

Carrera, P., Moshkin, Y. M., Gronke, S., Sillje, H. H. W., Nigg, E. A., Jackle, H. & Karch, F. 2003. Tousled-like kinase functions with the chromatin assembly pathway regulating nuclear divisions. *Genes & Development 17*(20): 2578–2590.

Cerami, E., Demir, E., Schultz, N., Taylor, B.S. and Sander, C., 2010. Automated network analysis identifies core pathways in glioblastoma. *PloS one 5*(2): e8918

Cha, S. 2005. Update on brain tumor imaging. *Current Neurology and Neuroscience Reports 5*: 169–177.

Chamberlain, M. C. 2011. Bevacizumab for the treatment of recurrent glioblastoma. *Clinical Medicine Insights Oncology*, *5*: 117–129.

Chaudhary, A., King, W. G., Mattaliano, M. D., Frost, J. A., Diaz, B., Morrison, D. K., Cobb, M. H. et al. 2000. Phosphatidylinositol 3-kinase regulates Raf1 through Pak phosphorylation of serine 338. *Current Biology CB*, *10*(9): 551–554.

Chautard, E., Ouédraogo, Z. G., Biau, J. & Verrelle, P. 2014. Role of Akt in human malignant glioma: From oncogenesis to tumor aggressiveness. *Journal of Neuro-Oncology 117*(2): 205–215.

Chen, H., Huang, Q., Dong, J., Zhai, D. & Wang, A. 2008. *BMC Cancer 11*: 1–11.

Cheng, C.K., Fan, Q.W. and Weiss, W.A., 2009. PI3K signaling in glioma—animal models and therapeutic challenges. *Brain Pathology 19*(1): 112-120.

Chetty, C., Vanamala, S. K., Gondi, C. S., Dinh, D. H., Gujrati, M. & Rao, J. S. 2012. MMP-9 induces CD44 cleavage and CD44 mediated cell migration in glioblastoma xenograft cells. *Cellular Signalling 24*(2): 549–559.

Chung, N., Zhang, X. D., Kreamer, A., Locco, L., Kuan, P.-F., Bartz, S., Linsley, P. S. et al. 2006. Revealing the world of RNA interference. *Journal Of Biomolecular Screening 13*(4): 497–509.

Cichowski, K., Santiago, S., Jardim, M., Johnson, B. W. & Jacks, T. 2003. Dynamic regulation of the Ras pathway via proteolysis of the NF1 tumor suppressor. *Genes & Development 17*(4): 449–454.

Clarke, I. D. & Dirks, P. B. 2003. A human brain tumor-derived PDGFR-alpha deletion mutant is transforming. *Oncogene 22*(5): 722–733.

Coles, L. C. & Shaw, P. E. 2002. PAK1 primes MEK1 for phosphorylation by Raf-1 kinase during cross-cascade activation of the ERK pathway. *Oncogene 21*(14): 2236–2244.

Costello, J. F., Plass, C., Arap, W., Chapman, V. M., Held, W. A., Berger, M. S., Su Huang, H. J. et al. 1997. Cyclin-dependent kinase 6 (CDK6) amplification in

human gliomas identified using two-dimensional separation of genomic DNA. *Cancer Research 57*(7): 1250–1254.

Cuddapah, V.A., Robel, S., Watkins, S. and Sontheimer, H., 2014. A neurocentric perspective on glioma invasion. *Nature Reviews Neuroscience 15*(7): 455-465.

Cui, B., Johnson, S.P., Bullock, N., Ali-Osman, F., Bigner, D.D. and Friedman, H.S., 2010. Decoupling of DNA damage response signaling from DNA damages underlies temozolomide resistance in glioblastoma cells. *Journal of Biomedical Research 24*(6): 424-435.

De, P., Peng, Q., Traktuev, D. O., Traktuevc, D. O., Li, W., Yoder, M. C., March, K. L. et al. 2009. Expression of RAC2 in endothelial cells is required for the postnatal neovascular response. *Experimental cell research*, *315*(2), 248–263.

De Benedetti, A. 2012. The Tousled-like kinases as guardians of genome integrity. *ISRN Molecular Biology 2012*.

Deei, R., Fatehullah, a, Jagan, I., Nagaraju, M., Bingham, V. & Campbell, F. C. 2011. PTEN regulates colorectal epithelial apoptosis through Cdc42 signalling. *British Journal Of Cancer 105*(9): 1313–21.

Dietich, J., Imitola, J. & Kesari, S. 2008. Mechanisms of Disease: the role of stem cells in the biology and treatment of gliomas. *Nature Clinical Practice. Oncology 5*(7): 393–404.

Do, K., Doroshow, J. & Kummar, S. 2013. Wee 1 Kinase as a target for cancer therapy. *Cell Cycle 12*(19): 3159–64.

Dorrello, N. V., Peschiaroli, A., Guardavaccaro, D., Colburn, N. H., Sherman, N. E. & Pagano, M. 2006. S6K1- and betaTRCP-mediated degradation of PDCD4 promotes protein translation and cell growth. *Science 314*(5798): 467–471.

Draetta, G., Brizuela, L., Potashkin, J. & Beach, D. 1987. Identification of p34 and p13, human homologs of the cell cycle regulators of fission yeast encoded by cdc2+ and suc1+. *Cell 50*(2): 319–325.

Duong-Ly, K. C. & Peterson, J. R. 2013. The human kinome and kinase inhibition. *Current Protocols in Pharmacology* (SUPPL.60): 1–14.

Dwyer, C.A. and Matthews, R.T., 2011. The neural extracellular matrix, cell adhesion molecules and proteolysis in glioma invasion and tumorigenicity. INTECH Open Access Publisher. *Molecular Targets of CNS Tumors* : 239–264.

Eblen, S. T., Slack, J. K., Weber, M. J. & Catling, A. D. 2002. Rac-PAK signaling stimulates extracellular signal-regulated kinase (ERK) activation by regulating formation of MEK1-ERK complexes. *Molecular and Cellular Biology*, *22*(17): 6023–6033.

Echeverri, C.J. and Perrimon, N., 2006. High-throughput RNAi screening in cultured cells: a user's guide. *Nature Reviews Genetics 7*(5): 373-384.

Edwards, L. A., Woolard, K., Son, M. J., Li, A., Lee, J., Ene, C., Mantey, S. A. et al. 2011. Effect of brain- and tumor-derived connective tissue growth factor on glioma invasion. *Journal of the National Cancer Institute 103*(15): 1162–1178.

Ekstrand, A. J., Sugawa, N., James, C. D. & Collins, V. P. 1992. Amplified and rearranged epidermal growth factor receptor genes in human glioblastomas reveal deletions of sequences encoding portions of the N- and/or C-terminal tails. *Proceedings of the National Academy of Sciences of the United States of America 89*(10): 4309–4313.

Ellert-miklaszewska, A., Ciechomska, I. & Kaminska, B. 2013. Glioma Signaling. *Advances in Experimental Medicine and Biology* 986: 209–220.

Endersby, R., Zhu, X., Hay, N., Ellison, D. W. & Baker, S. J. 2011. Nonredundant functions for Akt isoforms in astrocyte growth and gliomagenesis in an orthotopic transplantation model. *Cancer Research 71*(12): 4106–4116.

Ernst, M. & Putoczki, T. L. 2014. Molecular Pathways: IL11 as a Tumor-Promoting Cytokine-Translational Implications for Cancers. *Clinical cancer research* (6): 5579–5589.

Eßbach, C., Andrae, N., Pachow, D., Warnke, J.P., Wilisch-Neumann, A., Kirches, E. and Mawrin, C., 2013. Abundance of Flt3 and its ligand in astrocytic tumors. *OncoTargets and therapy 6*: 555–561.

Fan, Q.W. and Weiss, W.A., 2010. Targeting the RTK-PI3K-mTOR axis in malignant glioma: overcoming resistance. In *Phosphoinositide 3-kinase in Health and Disease* (279-296). Springer Berlin Heidelberg.

Fedorov, O., Müller, S. & Knapp, S. 2010. The (un)targeted cancer kinome. *Nature Chemical Biology 6*(3): 166–169.

Feng, Z., Zhang, H., Levine, A. J. & Jin, S. 2005. The coordinate regulation of the p53 and mTOR pathways in cells. *Proceedings of the National Academy of Sciences of the United States of America 102*(23): 8204–8209.

Fife, C. M., McCarroll, J. A. & Kavallaris, M. 2014. Movers and shakers: Cell cytoskeleton in cancer metastasis. *British Journal of Pharmacology 171*(24): 5507–5523.

Fisher, J. L., Schwartzbaum, J. A., Wrensch, M. & Wiemels, J. L. 2007. Epidemiology of brain tumors. *Neurologic Clinics 25*(4): 867–90

Flate, E. & Stalvey, J. 2014. Motility of select ovarian cancer cell lines: Effect of extracellular matrix proteins and the involvement of PAK2. *International Journal of Oncology* (9): 1401–1411.

Florian, I. S., Ungureanu, G. & Berce, C. 2013. Risk factors for gliomas. An extensive review. *Romanian Neurosurgery 20*(1): 5–21.

Franke, T. F. 2008. PI3K/Akt: getting it right matters. *Oncogene 27*(50): 6473–6488.

Frattini, V., Trifonov, V., Chan, J. M., Castano, A., Lia, M., Abate, F., Keir, S. T. et al. 2013. The integrated landscape of driver genomic alterations in glioblastoma. *Nature Genetics*, *45*(10), 1141–1149

Frederick, L., Wang, X. Y., Eley, G. & James, C. D. 2000. Diversity and frequency of epidermal growth factor receptor mutations in human glioblastomas. *Cancer Research 60*(5): 1383–1387.

Friedl, P. & Wolf, K. 2003. Tumour-cell invasion and migration: diversity and escape mechanisms. *Nature Reviews. Cancer 3*(5): 362–374.

Fu, Y., Huang, R., Du, J., Yang, R., An, N. & Liang, A. 2010. Glioma-derived mutations in IDH: From mechanism to potential therapy. *Biochemical and Biophysical Research Communications 397*(2): 127–130.

Furnari, F. B., Fenton, T., Bachoo, R. M., Mukasa, A., Stommel, J. M., Stegh, A., Hahn, W. C. et al. 2007. Malignant astrocytic glioma: Genetics, biology, and paths to treatment. *Genes & Development 21*(21): 2683–2710.

Futreal, P. A., Coin, L., Marshall, M., Down, T., Hubbard, T., Wooster, R., Rahman, N. et al. 2004. A census of human cancer genes. *Nature Reviews. Cancer 4*(3): 177–183.

Gagliano, N., Costa, F., Cossetti, C., Pettinari, L., Bassi, R., Chiriva-Internati, M., Cobos, E. et al. 2009. Glioma-astrocyte interaction modifies the astrocyte phenotype in a co-culture experimental model. *Oncology Reports 22*(6): 1349–1356.

Galtrey, C. M. & Fawcett, J. W. 2007. The role of chondroitin sulfate proteoglycans in regeneration and plasticity in the central nervous system. *Brain Research Reviews 54*(1): 1–18.

Gan, H. K., Kaye, A. H. & Luwor, R. B. 2009. The EGFRvIII variant in glioblastoma multiforme. *Journal of Clinical Neuroscience 16*(6): 748–754.

Gao, J., Aksoy, B. A., Dogrusoz, U., Dresdner, G., Gross, B., Sumer, S. O., Sun, Y. et al. 2013. Integrative Analysis of Complex Cancer Genomics and Clinical Profiles Using the cBioPortal. *Science Signaling 6*(269): pl1

Germano, I. M. & Binello, E. 2014. Stem cells and gliomas: past, present, and future. *Journal of Neuro-Oncology 119*(3): 547–555.

Gingras, M., Roussel, E., Bruner, J. M., Branch, C. D. & Moser, richard P. 1995. Comparison of cell adhesion molecule expression between glioblastoma

multiforme and autologous normal brain tissue. *Journal of Neuroimmunology*, *57*(1-2), 143–153.

Glantz, M., Chamberlain, M., Liu, Q., Litofsky, N. S. & Recht, L. D. 2003. Temozolomide as an alternative to irradiation for elderly patients with newly diagnosed malignant gliomas. *Cancer 97*(9): 2262–2266.

Goh, C. H., Lu, Y. Y., Lau, B. L., Wong, J. O. L., Lee, H. K., Liew, D. N. S. & Wong, A. S. H. 2014. Brain and spinal tumour. *Medical Journal of Malaysia 69*(6): 261–267.

Greenman, C., Stephens, P., Smith, R., Dalgliesh, G.L., Hunter, C., Bignell, G., Davies, H., Teague, J., Butler, A., Stevens, C. and Edkins, S., 2007. Patterns of somatic mutation in human cancer genomes. *Nature 446*(7132): 153-158.

Grossman, R., Shimony, N., Hadelsberg, U., Soffer, D., Sitt, R., Strauss, N., Corn, B. W. et al. 2016. The impact of resecting radiation necrosis and pseudoprogression on survival of patients with glioblastoma. *World Neurosurgery 89*: 37–41.

Groth, A., Lukas, J., Nigg, E. a., Silljé, H. H. W., Wernstedt, C., Bartek, J. & Hansen, K. 2003. Human Tousled like kinases are targeted by an ATM- and Chk1-dependent DNA damage checkpoint. *EMBO Journal 22*(7): 1676–1687.

Grueneberg, D. A., Degot, S., Pearlberg, J., Li, W., Davies, J. E., Baldwin, A., Endege, W. et al. 2008. Kinase requirements in human cells: I. Comparing kinase requirements across various cell types. *Proceedings of the National Academy of Sciences of the United States of America 105*(43): 16472–7.

Guilloux, V. Le, Schmidtke, P. & Tuffery, P. 2009. Fpocket : An open source platform for ligand pocket detection *BMC Bioinformatics 11*, 1–11.

Gymnopoulos, M., Elsliger, M.-A. & Vogt, P. K. 2007. Rare cancer-specific mutations in PIK3CA show gain of function. *Proceedings of the National Academy of Sciences of the United States of America 104*(13): 5569–74.

Hambardzumyan, D. & Bergers, G. 2015. Glioblastoma: Defining Tumor Niches. *Trends in Cancer 1*(4): 252–265.

Han, Z., Riefler, G. M., Saam, J. R., Mango, S. E. & Schumacher, J. M. 2005. The C. elegans Tousled-like Kinase Contributes to Chromosome Segregation as a Substrate and Regulator of the Aurora B Kinase. *Current Biology 15*(10): 894–904.

Hanahan, D. & Weinberg, R. A. 2011. Review Hallmarks of Cancer : The Next Generation. *Cell 144*(5): 646–674.

Hanks, S.K. and Hunter, T., 1995. Protein kinases 6. The eukaryotic protein kinase superfamily: kinase (catalytic) domain structure and classification.*The FASEB Journal 9*(8): 576-596

Hara, K., Maruki, Y., Long, X., Yoshino, K., Oshiro, N., Hidayat, S., Tokunaga, C. et al. 2002. Raptor, a binding partner of target of rapamycin (TOR), mediates TOR action. *Cell 110*(2): 177–189.

Harada, H., Andersen, J. S., Mann, M., Terada, N., & Korsmeyer, S. J. 2001. p70S6 kinase signals cell survival as well as growth, inactivating the pro-apoptotic molecule BAD. *Proceedings of the National Academy of Sciences 98*(17): 9666-9670.

Hatzikirou, H., Basanta, D., Simon, M., Schaller, K. & Deutsch, A. 2012. "Go or grow": The key to the emergence of invasion in tumour progression? *Mathematical Medicine and Biology 29*(1): 49–65.

Hatzikirou, H., Deutsch, A., Schaller, C., Simon, M. & Swanson, K. 2005. Mathematical Modelling of Glioblastoma Tumour Development: a Review. *Mathematical Models and Methods in Applied Sciences 15*(11): 1779–1794.

Heimberger, A. B., Hlatky, R., Suki, D., Yang, D., Weinberg, J., Gilbert, M., Sawaya, R. et al. 2005. Prognostic effect of epidermal growth factor receptor and EGFRvIII in glioblastoma multiforme patients. *Clinical cancer Research 11*(4): 1462–1466.

Heinonen, H., Nieminen, A., Saarela, M., Kallioniemi, A., Klefström, J., Hautaniemi, S. & Monni, O. 2008. Deciphering downstream gene targets of PI3K/mTOR/p70S6K pathway in breast cancer. *BMC Genomics 9*: 348.

Hermisson, M., Klumpp, A., Wick, W., Wischhusen, J., Nagel, G., Roos, W., Kaina, B. et al. 2006. O6-methylguanine DNA methyltransferase and p53 status predict temozolomide sensitivity in human malignant glioma cells. *Journal Of Neurochemistry 96*(3): 766–776.

Hiddingh, L., Raktoe, R.S., Jeuken, J., Hulleman, E., Noske, D.P., Kaspers, G.J., Vandertop, W.P., Wesseling, P. and Wurdinger, T., 2014. Identification of temozolomide resistance factors in glioblastoma via integrative miRNA/mRNA regulatory network analysis. *Scientific Reports* :*4*.

Hideki, Y., Fiona, P. & Condeelis, J. 2006. Invadopodia and podosomes in tumor invasion. *European Journal of Cell Biology 85*(3-4): 213–218.

Hoelzinger, D. B., Demuth, T. & Berens, M. E. 2007. Autocrine factors that sustain glioma invasion and paracrine biology in the brain microenvironment. *Journal of the National Cancer Institute 99*(21): 1583–1593.

Homma, T., Fukushima, T., Vaccarella, S., Yonekawa, Y., Di Patre, P. L., Franceschi, S. & Ohgaki, H. 2006. Correlation among pathology, genotype, and patient outcomes in glioblastoma. *Journal Of Neuropathology and Experimental Neurology 65*(9): 846–854.

Huang, P. H., Cavenee, W. K., Furnari, F. B. & White, F. M. 2007. Uncovering

therapeutic targets for glioblastoma: A systems biology approach. *Cell Cycle 6*(22): 2750–2754.

Huber, S. M., Butz, L., Stegen, B., Klumpp, D., Braun, N., Ruth, P. & Eckert, F. 2013. Ionizing radiation, ion transports, and radioresistance of cancer cells. *Frontiers in Physiology 4* (August): 1–14.

Hughes, J. D., Blagg, J., Price, D. A., Bailey, S., Decrescenzo, G. A., Devraj, R. V, Ellsworth, E. et al. 2008. Physiochemical drug properties associated with in vivo toxicological outcomes *Bioorganic & Medicinal Chemistry Letters 18*, 4872–4875.

Huse, J. T. & Holland, E. C. 2010. Targeting brain cancer: advances in the molecular pathology of malignant glioma and medulloblastoma. *Nature Reviews. Cancer 10*(5): 319–331.

Hynes, R. O. 2002. Integrins: Bidirectional, allosteric signaling machines. *Cell 110*(6): 673–687.

Ibrahim, K., Mat, F. C., Harun, R., Ngah, W. Z. W., Mokhtar, N. M. & Jamal, R. 2013. Silencing of Tousled-like Kinase 1 (TLK1) Reduces Survival, Migration and Invasion of Glioblastoma multiforme cells. *Asia Pacific Journal of Molecular Medicine*, *41* (1st National Conference for Cancer Research 5th Regional Conference on Molecular Medicine RCMM).

Ichimura, K., Pearson, D. M., Kocialkowski, S., Backlund, L. M., Chan, R., Jones, D. T. W. & Collins, V. P. 2009. IDH1 mutations are present in the majority of common adult gliomas but rare in primary glioblastomas. *Neuro-Oncology 11*(4): 341–347.

Ideguchi, M., Kajiwara, K., Goto, H., Sugimoto, K., Nomura, S., Ikeda, E. & Suzuki, M. 2015. MRI findings and pathological features in early-stage glioblastoma. *Journal of Neuro-Oncology 123*(2): 289–297.

Ignatova, T. N., Kukekov, V. G., Laywell, E. D., Suslov, O. N., Vrionis, F. D. & Steindler, D. A. 2002. Human cortical glial tumors contain neural stem-like cells expressing astroglial and neuronal markers in vitro. *Glia 39*(3): 193–206.

Ip, C. K. M., Cheung, A. N. Y., Ngan, H. Y. S. & Wong, A. S. T. 2011. p70 S6 kinase in the control of actin cytoskeleton dynamics and directed migration of ovarian cancer cells. *Oncogene 30*(21): 2420–2432

Itahana, K., Mao, H., Jin, A., Itahana, Y., Clegg, H. V, Lindström, M. S., Bhat, K. P. et al. 2007. Targeted inactivation of Mdm2 RING finger E3 ubiquitin ligase activity in the mouse reveals mechanistic insights into p53 regulation. *Cancer Cell 12*(4): 355–366.

Jacinto, E., Facchinetti, V., Liu, D., Soto, N., Wei, S., Jung, S. Y., Huang, Q. et al. 2006. SIN1/MIP1 maintains rictor-mTOR complex integrity and regulates Akt

phosphorylation and substrate specificity. *Cell 127*(1): 125–137.

James, C. D., Lu, Y.-J., Ozawa, T., Prados, M. D. & Waldman, T. 2014. RB1 Suppression is responsible for acquired CDK4/6 inhibitor resistance in glioblastoma. *Neuro-Oncology 16*(suppl 3): iii33–iii34.

Jhanwar-Uniyal, M., Gillick, J. L., Neil, J., Tobias, M., Thwing, Z. E. & Murali, R. 2015. Distinct signaling mechanisms of mTORC1 and mTORC2 in glioblastoma multiforme: A tale of two complexes. *Advances in Biological Regulation 57*: 64–74.

Johnson, D. R. & O'Neill, B. P. 2012. Glioblastoma survival in the United States before and during the temozolomide era. *Journal of Neuro-Oncology 107*(2): 359–364.

Johnson, T. W., Dress, K. R. & Edwards, M. 2009. Bioorganic & Medicinal Chemistry Letters Using the Golden Triangle to optimize clearance and oral absorption. *Bioorganic & Medicinal Chemistry Letters*, *19*(19), 5560–5564.

Joshi, S., Singh, A. R., Zulcic, M., Bao, L., Messer, K., Ideker, T., Dutkowski, J. et al. 2014. Rac2 controls tumor growth, metastasis and M1-M2 macrophage differentiation in vivo. *PloS one 9*(4): e95893.

Kamijo, T., Weber, J. D., Zambetti, G., Zindy, F., Roussel, M. F. & Sherr, C. J. 1998. Functional and physical interactions of the ARF tumor suppressor with p53 and Mdm2. *Proceedings of the National Academy of Sciences of the United States of America 95*(14): 8292–8297.

Kanno, H., Miyake, S., & Nakanowatari, S. 2015. Signaling pathways in glioblastoma cancer stem cells: a role of Stat3 as a potential therapeutic target. *Austin J Cancer Clin Res 2*(2): 1030.

Kanzawa, T., Bedwell, J., Kondo, Y., Kondo, S. & Germano, I. M. 2003. Inhibition of DNA repair for sensitizing resistant glioma cells to temozolomide. *Journal of Neurosurgery 99*(6): 1047–1052.

Keime-Guibert, F., Chinot, O., Taillandier, L., Cartalat-Carel, S., Frenay, M., Kantor, G., Guillamo, J.-S. et al. 2007. Radiotherapy for glioblastoma in the elderly. *The New England Journal of Medicine 356*(15): 1527–1535.

Kelly, R. & Davey, S. K. 2013. Tousled-like kinase-dependent phosphorylation of Rad9 plays a role in cell cycle progression and G2/M checkpoint exit. *PloS one 8*(12): e85859.

King, G. D., Muhammad, a K. M. G., Curtin, J. F., Barcia, C., Puntel, M., Liu, C., Honig, S. B. et al. 2008. Flt3L and TK gene therapy eradicate multifocal glioma in a syngeneic glioblastoma model. *Neuro-Oncology 10*(1): 19–31.

Kitson, R. R. A., Millemaggi, A. & Taylor, R. J. K. 2009. The Renaissance of a -Methylene- g -butyrolactones : New Synthetic Approaches. *Angewandte Chemie International Edition 48*(50) 9426–9451.

Knuutila, S., Björkqvist, A. M., Autio, K., Tarkkanen, M., Wolf, M., Monni, O., Szymanska, J. et al. 1998. DNA copy number amplifications in human neoplasms: review of comparative genomic hybridization studies. *The American Journal of Pathology 152*(5): 1107–1123.

Kolesnikov, N., Hastings, E., Keays, M., Melnichuk, O., Tang, Y.A., Williams, E., Dylag, M., Kurbatova, N., Brandizi, M., Burdett, T. and Megy, K., 2014. ArrayExpress update—simplifying data submissions *Nucleic acids research*: gku1057

Koul, D. 2008. PTEN signaling pathways in glioblastoma. *Cancer Biology and Therapy 7*(9): 1321–1325.

Krakstad, C., & Chekenya, M. 2010. Survival signalling and apoptosis resistance in glioblastomas: opportunities for targeted therapeutics. *Molecular Cancer 9*(1): 1.

Krause, D. R., Jonnalagadda, J. C., Gatei, M. H., Sillje, H. H. W., Zhou, B.-B., Nigg, E. A. & Khanna, K. 2003. Suppression of Tousled-like kinase activity after DNA damage or replication block requires ATM, NBS1 and Chk1. *Oncogene 22*(38): 5927–5937.

Kubbutat, M. H., Jones, S. N. & Vousden, K. H. 1997. Regulation of p53 stability by Mdm2. *Nature 387*(6630): 299–303.

Kumar, R., Gururaj, A. E. & Barnes, C. J. 2006. p21-activated kinases in cancer. *Nature reviews. Cancer 6*(6): 459–471.

Labuhn, M., Jones, G., Speel, E. J., Maier, D., Zweifel, C., Gratzl, O., Van Meir, E. G. et al. 2001. Quantitative real-time PCR does not show selective targeting of p14(ARF) but concomitant inactivation of both p16(INK4A) and p14(ARF) in 105 human primary gliomas. *Oncogene 20*(9): 1103–1109.

Lacroix, M., Abi-Said, D., Fourney, D. R., Gokaslan, Z. L., Shi, W., DeMonte, F., Lang, F. F. et al. 2001. A multivariate analysis of 416 patients with glioblastoma multiforme: prognosis, extent of resection, and survival. *Journal of Neurosurgery 95*(2): 190–198.

Lai, Y.J., Tsai, J.C., Tseng, Y.T. and Benveniste, E.N., 2015. Small G protein Rac GTPases regulate the maintenance of glioblastoma stem-like cells.*Cancer Research 75*(15 Supplement): 4219-4219.

Laplante, M. & Sabatini, D. M. 2012. MTOR signaling in growth control and disease. *Cell 149*(2): 274–293.

Lee, J. C., Vivanco, I., Beroukhim, R., Huang, J. H. Y., Feng, W. L., DeBiasi, R. M., Yoshimoto, K. et al. 2006. Epidermal growth factor receptor activation in glioblastoma through novel missense mutations in the extracellular domain. *PLoS Medicine 3*(12): 2264–2273.

Lee, J., Kotliarova, S., Kotliarov, Y., Li, A., Su, Q., Donin, N. M., Pastorino, S. et al. 2006. Tumor stem cells derived from glioblastomas cultured in bFGF and EGF more closely mirror the phenotype and genotype of primary tumors than do serum-cultured cell lines. *Cancer Cell 9*(5): 391–403.

Lee, S. M., Koh, H.-J., Park, D.-C., Song, B. J., Huh, T.-L. & Park, J.-W. 2002. Cytosolic NADP(+)-dependent isocitrate dehydrogenase status modulates oxidative damage to cells. *Free Radical Biology & Medicine 32*(11): 1185–1196.

Li, Q. & Lozano, G. 2013. Molecular pathways: Targeting Mdm2 and Mdm4 in cancer therapy. *Clinical Cancer Research*, *19*(1), 34–41.

Li, T., Zhang, J., Zhu, F., Wen, W., Zykova, T., Li, X., Liu, K. et al. 2011. P21-activated protein kinase (PAK2)-mediated c-Jun phosphorylation at 5 threonine sites promotes cell transformation. *Carcinogenesis 32*(5): 659–666.

Li, Z., Gourguechon, S. & Wang, C. C. 2007. Tousled-like kinase in a microbial eukaryote regulates spindle assembly and S-phase progression by interacting with Aurora kinase and chromatin assembly factors. *Journal of Cell Science 120*(Pt 21): 3883–3894.

Li, Z., Umeyama, T. & Wang, C. C. 2008. The chromosomal passenger complex and a mitotic kinesin interact with the tousled-like kinase in trypanosomes to regulate mitosis and cytokines. *PLoS ONE 3*(11): e3814.

Liang, Y., Diehn, M., Watson, N., Bollen, A. W., Aldape, K. D., Nicholas, M. K., Lamborn, K. R. et al. 2005. Gene expression profiling reveals molecularly and clinically distinct subtypes of glioblastoma multiforme. *Proceedings of the National Academy of Sciences of the United States of America 102*(16): 5814–5819.

Lindqvist, A., Rodríguez-Bravo, V. & Medema, R. H. 2009. The decision to enter mitosis: feedback and redundancy in the mitotic entry network. *Journal of Cell Biology 185*(2): 193–202.

Linton, A., Cheng, Y. Y., Griggs, K., Kirschner, M. B., Gattani, S., Srikaran, S., Chuan-Hao Kao, S. et al. 2014. An RNAi-based screen reveals PLK1, CDK1 and NDC80 as potential therapeutic targets in malignant pleural mesothelioma. *British Journal of Cancer 110*(2): 510–9.

Lipinski, C. A., Lombardo, F., Dominy, B. W. & Feeney, P. J. 2001. Experimental and computational approaches to estimate solubility and permeability in drug discovery and development settings. *Advanced Drug Delivery Reviews 46*(1-3): 3–26.

Livak, K. J. & Schmittgen, T. D. 2001. Analysis of relative gene expression data using real-time quantitative PCR and the 2-ÄÄCT method. *Methods 25*(4): 402–408.

Logue, J. S. & Morrison, D. K. 2012. Complexity in the signaling network: Insights from the use of targeted inhibitors in cancer therapy. *Genes & Development 26*(7):

641–650.

Louis, D. N., Ohgaki, H., Wiestler, O. D., Cavenee, W. K., Burger, P. C., Jouvet, A., Scheithauer, B. W. et al. 2007. The 2007 WHO classification of tumours of the central nervous system. *Acta Neuropathologica 114*(2): 97–109.

Louis, D. N., Perry, A., Burger, P., Ellison, D. W., Reifenberger, G., von Deimling, A., Aldape, K. et al. 2014. International Society Of Neuropathology--Haarlem consensus guidelines for nervous system tumor classification and grading. *Brain Pathology 24*(5): 429–435.

Lu, P., Weaver, V. M. & Werb, Z. 2012. The extracellular matrix: A dynamic niche in cancer progression. *Journal of Cell Biology 196*(4): 395–406.

Lun, M., Lok, E., Gautam, S., Wu, E. & Wong, E. T. 2011. The natural history of extracranial metastasis from glioblastoma multiforme. *Journal of Neuro-Oncology 105*(2): 261–273.

Manning, B. D. 2009. Challenges and opportunities in defining the essential cancer kinome. *Science Signaling 2*(63): pe15-pe15

Manning, B. D. & Cantley, L. C. 2007. AKT/PKB signaling: navigating downstream. *Cell 129*(7): 1261–1274.

Manning, G., Whyte, D. B., Martinez, R., Hunter, T. & Sudarsanam, S. 2002a. The Protein Kinase Complement of the Human Genome. *Science 298*(5600): 1912–1934.

Mao, H., LeBrun, D. G., Yang, J., Zhu, V. F. & Li, M. 2012. Deregulated Signaling Pathways in Glioblastoma Multiforme: Molecular Mechanisms and Therapeutic Targets. *Cancer Investigation 30*(1): 48–56.

Mao, X.-G., Zhang, X., Xue, X.-Y., Guo, G., Wang, P., Zhang, W., Fei, Z. et al. 2009. Brain Tumor Stem-Like Cells Identified by Neural Stem Cell Marker CD15 *Translational oncology 2*(4): 247–257.

Marlin, J.W., Eaton, A., Montano, G.T., Chang, Y.W.E. and Jakobi, R., 2009. Elevated p21-activated kinase 2 activity results in anchorage-independent growth and resistance to anticancer drug–induced cell death. *Neoplasia 11*(3): 286-297.

Martin, S., Janouskova, H. & Dontenwill, M. 2012. Integrins and p53 pathways in glioblastoma resistance to temozolomide. *Frontiers in Oncology 2*: 157.

Masui, K., Cloughesy, T. F. & Mischel, P. S. 2012. Review: molecular pathology in adult high-grade gliomas: from molecular diagnostics to target therapies. *Neuropathology and Applied Neurobiology 38*(3): 271–291.

McEllin, B., Camacho, C. V., Mukherjee, B., Hahm, B., Tomimatsu, N., Bachoo, R. M.

& Burma, S. 2010. PTEN loss compromises homologous recombination repair in astrocytes: Implications for glioblastoma therapy with temozolomide or poly(ADP-Ribose) polymerase inhibitors. *Cancer Research 70*(13): 5457–5464.

Mellinghoff, I. K., Wang, M. Y., Vivanco, I., Haas-Kogan, D. A., Zhu, S., Dia, E. Q., Lu, K. V et al. 2005. Molecular determinants of the response of glioblastomas to EGFR kinase inhibitors. *The New England Journal of Medicine 353*(19): 2012–2024.

Middelbeek, J., Clark, K., Venselaar, H., Huynen, M.A. and Van Leeuwen, F.N., 2010. The alpha-kinase family: an exceptional branch on the protein kinase tree. *Cellular and Molecular Life Sciences 67*(6): 875-890.

Ministry of Health Malaysia. 2007. *National Cancer Registry Report*.

Mir, S.E., Hamer, P.C.D.W., Krawczyk, P.M., Balaj, L., Claes, A., Niers, J.M., Van Tilborg, A.A., Zwinderman, A.H., Geerts, D., Kaspers, G.J. and Vandertop, W.P., 2010. In silico analysis of kinase expression identifies WEE1 as a gatekeeper against mitotic catastrophe in glioblastoma. *Cancer Cell 18*(3): 244-257.

Moodie, S. A., Willumsen, B. M., Weber, M. J. & Wolfrnan, A. 1993. Complexes of Ras . GTP with Raf-1 and Mitogen-Activated Protein Kinase Kinase. *Science 260*(14): 1658–1661.

Mu, S., Kunkel, P., Lamszus, K., Ulbricht, U., Lorente, G. A., Nelson, A. M., Schack, D. Von et al. 2003. A role for receptor tyrosine phosphatase in glioma cell migration 6661–6668.

Muhammad, a. K. M. G., Candolfi, M., King, G. D., Yagiz, K., Foulad, D., Mineharu, Y., Kroeger, K. M. et al. 2009. Antiglioma immunological memory in response to conditional cytotoxic/immune-stimulatory gene therapy: Humoral and cellular immunity lead to tumor regression. *Clinical Cancer Research 15*(19): 6113–6127.

Mulloy, J. C., Cancelas, J. a, Filippi, M., Kalfa, T. a, Guo, F., Dc, W. & Zheng, Y. 2013. Rho GTPases in hematopoiesis and hemopathies Review article Rho GTPases in hematopoiesis and hemopathies. *Blood 115*(5): 936–947.

Mumtaz, A., Saeed, A., Fatima, N., Dawood, M., Rafique, H. & Iqbal, J. 2016. Imidazole and its derivatives as potential candidates for drug development. *Bangladesh J Pharmacology* 756–765.

Murphy, D. A. & Courtneidge, S. A. 2011. The “ins” and “outs” of podosomes and invadopodia: characteristics, formation and function. *Nature Reviews Molecular Cell Biology 12*(7): 413–426.

Nakamura, M., Watanabe, T., Klangby, U., Asker, C., Wiman, K., Yonekawa, Y., Kleihues, P. et al. 2001. p14ARF deletion and methylation in genetic pathways to glioblastomas. *Brain Pathology 11*(2): 159–168.

Narahara, K., Kimura, S., Kikkawa, K., Takahashi, Y., Wakita, Y., Kasai, R., Nagai, S. et al. 1985. Probable assignment of soluble isocitrate dehydrogenase (IDH1) to 2q33.3. *Human Genetics 71*(1): 37–40.

Nathanson, D. & Mischel, P. S. 2011. Charting the course across the blood-brain barrier. *The Journal of Clinical Investigation 121*(1): 31–33.

Newlands, E. S., Stevens, M. F., Wedge, S. R., Wheelhouse, R. T. & Brock, C. 1997. Temozolomide: a review of its discovery, chemical properties, pre-clinical development and clinical trials. *Cancer Treatment Reviews 23*(1): 35–61.

Newton, H. B. 2003. Molecular neuro-oncology and development of targeted therapeutic strategies for brain tumors. Part 1: Growth factor and Ras signaling pathways. *Expert Review Of Anticancer Therapy 3*: 595–614.

Ng, K., Kim, R., Kesari, S., Carter, B. and Chen, C.C., 2012. Genomic profiling of glioblastoma: convergence of fundamental biologic tenets and novel insights. *Journal of Neuro-Oncology 107*(1): 1-12

Nichol, D., & Mellinghoff, I. K. 2015. PI3K pathway inhibition in GBM—is there a signal?. *Neuro-Oncology 17*(9): 1183-1184.

Nigg, E. A. 1995. Cyclin-dependent protein kinases: key regulators of the eukaryotic cell cycle. *BioEssays : News And Reviews In Molecular, Cellular And Developmental Biology 17*(6): 471–480.

Nobusawa, S., Watanabe, T., Kleihues, P. & Ohgaki, H. 2009. IDH1 mutations as molecular signature and predictive factor of secondary glioblastomas. *Clinical Cancer Research 15*(19): 6002–6007.

Noel, G., Huchet, A., Feuvret, L., Maire, J. P., Verrelle, P., Le Rhun, E., Aumont, M. et al. 2012. Waiting times before initiation of radiotherapy might not affect outcomes for patients with glioblastoma: A French retrospective analysis of patients treated in the era of concomitant temozolomide and radiotherapy. *Journal of Neuro-Oncology 109*(1): 167–175.

Ogden, A. T., Waziri, A. E., Lochhead, R. A., Fusco, D., Lopez, K., Ellis, J. A., Kang, J. et al. 2008. Identification of A2B5+CD133- tumor-initiating cells in adult human gliomas. *Neurosurgery 62*(2): 505.

Ohgaki, H. & Kleihues, P. 2005a. Epidemiology and etiology of gliomas. *Acta Neuropathologica 109*(1): 93–108.

Ohgaki, H. & Kleihues, P. 2005b. Population-based studies on incidence, survival rates, and genetic alterations in astrocytic and oligodendroglial gliomas. *Journal of Neuropathology And Experimental Neurology 64*(6): 479–489.

Ohgaki, H. & Kleihues, P. 2007. Genetic pathways to primary and secondary

glioblastoma. *The American Journal of Pathology 170*(5): 1445–1453.

Ohgaki, H. & Kleihues, P. 2011. Genetic profile of astrocytic and oligodendroglial gliomas. (1). *Brain Tumor Pathology 28*(3): 177–183.

Ohgaki, H. & Kleihues, P. 2013. The definition of primary and secondary glioblastoma. *Clinical Cancer Research 19*(4): 764–772.

Okura, H., Golbourn, B. J., Luck, A. J., Smith, C. A. & Rutka, J. T. 2015. Abstract 4038: Role of the Rho-GTPase CDC42 in glioma migration. *Cancer Research 75* (15 Supplement): 4038.

Ostrom, Q.T., Gittleman, H., Farah, P., Ondracek, A., Chen, Y., Wolinsky, Y., Stroup, N.E., Kruchko, C. and Barnholtz-Sloan, J.S., 2013. CBTRUS statistical report: Primary brain and central nervous system tumors diagnosed in the United States in 2006-2010. *Neuro-oncology 15*(suppl 2): ii1-ii56.

Otero, J. J., & Tihan, T. 2011. Morphological analysis of CDC2 and glycogen synthase kinase 3β phosphorylation as markers of G2→ M transition in glioma. *Pathology Research International 2011*.

Liesi, P. 1983. Laminin and fibronectin in normal and malignant neuroectodermal cells. *Medical Biology 62*(3): 163-180.

Pajouhesh, H. & Lenz, G. R. 2005. Medicinal chemical properties of successful central nervous system drugs. *Neurorx : The Journal Of The American Society For Experimental Neurotherapeutics 2*(4): 541–553.

Palmer, R. H., Vernersson, E., Grabbe, C. & Hallberg, B. 2009. Anaplastic lymphoma kinase: signalling in development and disease. *The Biochemical Journal 420*(3): 345–361.

Pardridge, W. M. 1998. CNS drug design based on principles of blood-brain barrier transport. *Journal Of Neurochemistry 70*(5): 1781–1792.

Parkin, D. M. & Muir, C. S. 1992. Cancer Incidence in Five Continents. Comparability and quality of data. *IARC Scientific Publications* (120): 45–173.

Parsons, D.W., Jones, S., Zhang, X., Lin, J.C.H., Leary, R.J., Angenendt, P., Mankoo, P., Carter, H., Siu, I.M., Gallia, G.L. and Olivi, A., 2008. An integrated genomic analysis of human glioblastoma multiforme. *Science 321*(5897): 1807-1812.

Patel, M. N., Halling-Brown, M. D., Tym, J. E., Workman, P. & Al-Lazikani, B. 2012. Objective assessment of cancer genes for drug discovery. *Nature Reviews Drug Discovery 12*(1): 35–50.

Paulus, W. & Tonn, J. C. 1995. Interactions of glioma cells and extracellular matrix. *Journal of Neuro-Oncology 24*(1): 87–91.

Paw, I., Carpenter, R. C., Watabe, K., Debinski, W. & Lo, H.-W. 2015. Mechanisms regulating glioma invasion. *Cancer Letters 362*(1): 1–7.

Paz, M. F., Yaya-Tur, R., Rojas-Marcos, I., Reynes, G., Pollan, M., Aguirre-Cruz, L., García-Lopez, J. L. et al. 2004. CpG island hypermethylation of the DNA repair enzyme methyltransferase predicts response to temozolomide in primary gliomas. *Clinical Cancer Research 10*(15): 4933–4938.

Pegg, A.E., 2000. Repair of O 6-alkylguanine by alkyltransferases. *Mutation Research/Reviews in Mutation Research 462*(2): 83-100.

Pelloski, C.E., Lin, E., Zhang, L., Yung, W.A., Colman, H., Liu, J.L., Woo, S.Y., Heimberger, A.B., Suki, D., Prados, M. and Chang, S., 2006. Prognostic associations of activated mitogen-activated protein kinase and Akt pathways in glioblastoma. *Clinical Cancer Research 12*(13): 3935-3941.

Pierscianek, D., Kim, Y.-H., Motomura, K., Mittelbronn, M., Paulus, W., Brokinkel, B., Keyvani, K. et al. 2013. *MET* Gain in Diffuse Astrocytomas is Associated with Poorer Outcome. *Brain Pathology 23*(1): 13–18.

Pires, I.M., Bencokova, Z., McGurk, C. and Hammond, E.M., 2010. Exposure to acute hypoxia induces a transient DNA damage response which includes Chk1 and TLK1. *Cell Cycle 9*(13): 2502-2507.

Pitz, M. W., Eisenhauer, E. A., MacNeil, M. V., Thiessen, B., Easaw, J. C., Macdonald, D. R., Eisenstat, D. D. et al. 2015. Phase II study of PX-866 in recurrent glioblastoma. *Neuro-Oncology 17*(9): 1270–1274.

Pointer, K. B., Clark, P. A., Zorniak, M., Alrfaei, B. M. & Kuo, J. S. 2014. Glioblastoma cancer stem cells: Biomarker and therapeutic advances. *Neurochemistry International 71*(1): 1–7.

Pokorny, J. L., Calligaris, D., Gupta, S. K., Iyekegbe, D. O., Mueller, D., Bakken, K. K., Carlson, B. L. et al. 2015. The Efficacy of the Wee1 Inhibitor MK-1775 Combined with Temozolomide Is Limited by Heterogeneous Distribution across the Blood–Brain Barrier in Glioblastoma. *Clinical Cancer Research 21* (8): 1916–1924.

Polgar, D., Leisser, C., Maier, S., Strasser, S., R??ger, B., Dettke, M., Khorchide, M. et al. 2005. Truncated ALK derived from chromosomal translocation t(2;5)(p23;q35) binds to the SH3 domain of p85-PI3K. *Mutation Research - Fundamental and Molecular Mechanisms of Mutagenesis 570*(1): 9–15.

Pulgar, T., Benitah, S. A., Valeron, P. F., Espina, C. & Lacal, J. C. 2005. Gomez del and Rho GTPase expression in tumourigenesis: evidence for a significant link. *Bioessays 27*: 602–613

Radu, M., Semenova, G., Kosoff, R. and Chernoff, J., 2014. PAK signalling during the development and progression of cancer. *Nature Reviews Cancer 14*(1): 13-25.

Rajalingam, K., Schreck, R., Rapp, U. R. & Albert, Š. 2007. Ras oncogenes and their downstream targets. *Biochimica et Biophysica Acta - Molecular Cell Research 1773*(8): 1177–1195.

Ramirez, Y. P., Weatherbee, J. L., Wheelhouse, R. T. & Ross, A. H. 2013. Glioblastoma multiforme therapy and mechanisms of resistance. *Pharmaceuticals 6*(12): 1475–1506.

Rane, C. K. & Minden, A. 2014. P21 activated kinases: structure, regulation, and functions. *Small GTPases 5*(January 2015): 37–41.

Rao, J. S. 2003. Molecular mechanisms of glioma invasiveness: the role of proteases. *Nature Reviews. Cancer 3*(July): 489–501.

Rathmell, J. C., Fox, C. J., Plas, D. R., Hammerman, P. S., Cinalli, R. M. & Thompson, C. B. 2003. Akt-directed glucose metabolism can prevent Bax conformation change and promote growth factor-independent survival. *Molecular and Cellular Biology 23*(20): 7315–28.

Raub, T. J., Wishart, G. N., Kulanthaivel, P., Staton, B. A., Ajamie, R. T., Sawada, G. A., Gelbert, L. M. et al. 2015. Brain exposure of two selective dual CDK4 and CDK6 inhibitors and the antitumor activity of CDK4 and CDK6 inhibition in combination with temozolomide in an intracranial glioblastoma xenograft. *Drug Metabolism and Disposition 43*(9): 1360–1371.

Rauch, J., Volinsky, N., Romano, D., & Kolch, W. (2011). The secret life of kinases: functions beyond catalysis. *Cell Communication and Signaling 9*(1): 1.

Read, R.D., Fenton, T.R., Gomez, G.G., Wykosky, J., Vandenberg, S.R., Babic, I., Iwanami, A., Yang, H., Cavenee, W.K., Mischel, P.S. and Furnari, F.B., 2013. A kinome-wide RNAi screen in Drosophila Glia reveals that the RIO kinases mediate cell proliferation and survival through TORC2-Akt signaling in glioblastoma. *PLoS Genet 9*(2): e1003253.

Reifenberger, G., Ichimura, K., Reifenberger, J., Elkahloun, A. G., Meltzer, P. S. & Collins, V. P. 1996. Refined mapping of 12q13-q15 amplicons in human malignant gliomas suggests CDK4/SAS and MDM2 as independent amplification targets. *Cancer Research 56*(22): 5141–5145.

Rey, J., Lagorce, D., Vavru, M., Labb, M., Miteva, M. A., Sperandio, O., Villoutreix, B. O. et al. 2015. MTiOpenScreen : a web server for structure-based *43*(April), 448–454.

Rhodes, D.R., Yu, J., Shanker, K., Deshpande, N., Varambally, R., Ghosh, D., Barrette, T., Pander, A. and Chinnaiyan, A.M., 2004. ONCOMINE: a cancer microarray database and integrated data-mining platform. *Neoplasia 6*(1): 1-6.

Riemenschneider, M. J., Büschges, R., Wolter, M., Reifenberger, J., Boström, J., Kraus, J. A., Schlegel, U. et al. 1999. Amplification and overexpression of the MDM4

(MDMX) gene from 1q32 in a subset of malignant gliomas without TP53 mutation or MDM2 amplification. *Cancer Research, 59*(24), 6091–6096.

Riemenschneider, M. J., Mueller, W., Betensky, R. A., Mohapatra, G. & Louis, D. N. 2005. In situ analysis of integrin and growth factor receptor signaling pathways in human glioblastomas suggests overlapping relationships with focal adhesion kinase activation. *Am J Pathol 167*(5): 1379–1387.

Robertson, L. B., Armstrong, G. N., Olver, B. D., Lloyd, A. L., Shete, S., Lau, C., Claus, E. B. et al. 2010. Survey of familial glioma and role of germline p16INK4A/p14 ARF and p53 mutation. *Familial Cancer 9*(3): 413–421.

Roe, J. L., Nemhauser, J. L. & Zambryski, P. C. 1997. TOUSLED participates in apical tissue formation during gynoecium development in Arabidopsis. *The Plant Cell 9*(3): 335–353.

Roe, J. L., Rivin, C. J., Sessions, R. A., Feldmann, K. A. & Zambryski, P. C. 1993. The Tousled gene in A. thaliana encodes a protein kinase homolog that is required for leaf and flower development. *Cell 75*(5): 939–950.

Romano, J. D. & Kolch, W. 2011. The secret life of kinases functions beyond catalysis. *Cell Communication Signalling* 9:23

Ronald, S., Awate, S., Rath, A., Carroll, J., Galiano, F., Dwyer, D., Kleiner-Hancock, H. et al. 2013. Phenothiazine Inhibitors of TLKs Affect Double-Strand Break Repair and DNA Damage Response Recovery and Potentiate Tumor Killing with Radiomimetic Therapy. *Genes & Cancer 4*(1-2): 39–53.

Ronald, S., Sunavala-Dossabhoy, G., Adams, L., Williams, B. & De Benedetti, A. 2011. The expression of Tousled kinases in CaP cell lines and its relation to radiation response and DSB repair. *The Prostate 71*(13): 1367–1373.

Rooprai, H. K., Vanmeter, T., Panou, C., Schnüll, S., Trillo-Pazos, G., Davies, D. & Pilkington, G. J. 1999. The role of integrin receptors in aspects of glioma invasion in vitro. *International Journal of Developmental Neuroscience 17*(5-6): 613–623.

Roskoski, R. 2013. Anaplastic lymphoma kinase (ALK): structure, oncogenic activation, and pharmacological inhibition. *Pharmacological Research 68*(1): 68–94.

Ruoslahti, E. 1996. Brain extracellular matrix. *Glycobiology 6*(5): 489–492.

Salmena, L., Carracedo, A. & Pandolfi, P. P. 2008. Tenets of PTEN tumor suppression. *Cell 133*(3): 403–414.

Sami, A. & Karsy, M. 2013. Targeting the PI3K/AKT/mTOR signaling pathway in glioblastoma: Novel therapeutic agents and advances in understanding. *Tumor Biology 34*(4): 1991–2002.

Sampetrean, O. & Saya, H. 2013. Characteristics of glioma stem cells. *Brain Tumor Pathology*, *30*(4), 209–214.Sarbassov, D. D., Ali, S. M., Kim, D.-H., Guertin, D. A., Latek, R. R., Erdjument-Bromage, H., Tempst, P. et al. 2004. Rictor, a novel binding partner of mTOR, defines a rapamycin-insensitive and raptor-independent pathway that regulates the cytoskeleton. *Current Biology : CB*, *14*(14): 1296–1302.

Sarbassov, D. D., Ali, S. M., Kim, D.-H., Guertin, D. A., Latek, R. R., Erdjument-Bromage, H., Tempst, P. et al. 2004. Rictor, a novel binding partner of mTOR, defines a rapamycin-insensitive and raptor-independent pathway that regulates the cytoskeleton. *Current Biology 14*(14), 1296–1302

Sarker, D., Reid, A. H. M., Yap, T. A. & De Bono, J. S. 2009. Targeting the PI3K/AKT pathway for the treatment of prostate cancer. *Clinical Cancer Research 15*(15): 4799–4805.

Schnell, O., Krebs, B., Wagner, E., Romagna, A., Beer, A. J., Grau, S. J., Thon, N. et al. 2008. Expression of integrin αvβ3 in gliomas correlates with tumor grade and is not restricted to tumor vasculature. *Brain Pathology 18*(3): 378–386.

Schröder, L. B. W. & McDonald, K. L. 2015. CDK4/6 Inhibitor PD0332991 in Glioblastoma Treatment: Does It Have a Future? *Frontiers In Oncology 5*(November): 259.

Seals, D. F., Azucena, E. F., Pass, I., Tesfay, L., Gordon, R., Woodrow, M., Resau, J. H. et al. 2005. The adaptor protein Tks5/Fish is required for podosome formation and function, and for the protease-driven invasion of cancer cells. *Cancer Cell 7*(2): 155–165.

Sedo, A. & Mentlein, R. 2014. Glioma Cell Biology 3–23.

Seguin, L., Desgrosellier, J. S., Weis, S. M. & Cheresh, D. A. 2015. Integrins and cancer: Regulators of cancer stemness, metastasis, and drug resistance. *Trends in Cell Biology 25*(4): 234–240.

Seo, M., Lee, S., Kim, J.-H., Lee, W.-H., Hu, G., Elledge, S. J. & Suk, K. 2014. RNAi-based functional selection identifies novel cell migration determinants dependent on PI3K and AKT pathways. *Nature Communications 5*: 5217.

Shai, R., Shi, T., Kremen, T. J., Horvath, S., Liau, L. M., Cloughesy, T. F., Mischel, P. S. et al. 2003. Gene expression profiling identifies molecular subtypes of gliomas. *Oncogene 22*(31): 4918–4923.

Shalom, S. & Don, J. 1999. Tlk, a novel evolutionarily conserved murine serine threonine kinase, encodes multiple testis transcripts. *Molecular Reproduction and Development 52*(4), 392–405.

Sharma, G. V. M., Ramesh, A., Singh, A., Srikanth, G., Jayaram, V., Duscharla, D., Jun, J. H. et al. 2014. Imidazole derivatives show anticancer potential by inducing

apoptosis and cellular senescence. *Med. Chem. Commun 5*, 1751–1760.

Sharma, S. V, Bell, D. W., Settleman, J. & Haber, D. A. 2007. Epidermal growth factor receptor mutations in lung cancer. *Nature Reviews: Cancer 7*(3): 169–181.

Sharma, S., Salehi, F., Scheithauer, B. W., Rotondo, F., Syro, L. V. & Kovacs, K. 2009. Role of MGMT in tumor development, progression, diagnosis, treatment and prognosis. *Anticancer Research*, *29*(10): 3759–3768.

Shen, Q., Wang, Y., Kokovay, E., Lin, G., Chuang, S.-M., Goderie, S. K., Roysam, B. et al. 2008. Adult SVZ stem cells lie in a vascular niche: a quantitative analysis of niche cell-cell interactions. *Cell Stem Cell 3*(3): 289–300.

Shete, S., Hosking, F. J., Robertson, L. B., Dobbins, S. E., Sanson, M., Malmer, B., Simon, M. et al. 2009. Genome-wide association study identifies five susceptibility loci for glioma. *Nature Genetics 41*(8): 899–904.

Shinojima, N., Tada, K., Shiraishi, S., Kamiryo, T., Kochi, M., Nakamura, H., Makino, K. et al. 2003. Prognostic value of epidermal growth factor receptor in patients with glioblastoma multiforme. *Cancer Research 63*(20): 6962–6970.

Shvarts, A., Bazuine, M., Dekker, P., Ramos, Y. F., Steegenga, W. T., Merckx, G., van Ham, R. C. et al. 1997. Isolation and identification of the human homolog of a new p53-binding protein, Mdmx. *Genomics 43*(1): 34–42.

Sillje, H. & Nigg, E. 2001. Identification of human Asf1 chromatin assembly factors as substrates of Tousled-like kinases. *Curr Biol 11*(13): 1068–1073.

Sizoo, E. M., Braam, L., Postma, T. J., Pasman, H. R. W., Heimans, J. J., Klein, M., Reijneveld, J. C. et al. 2010. Symptoms and problems in the end-of-life phase of high-grade glioma patients. *Neuro-Oncology 12*(11): 1162–1166.

Solomon, D. A., Kim, J. S., Jean, W. & Waldman, T. 2008. Conspirators in a capital crime: Co-deletion of p18INK4c and p16INK4a/p14ARF/p15INK4b in glioblastoma multiforme. *Cancer Research 68*(21): 8657–8660.

Sonenberg, N. & Gingras, A. C. 1998. The mRNA 5’ cap-binding protein eIF4E and control of cell growth. *Current Opinion in Cell Biology 10*(2): 268–275.

Soroceanu, L., Murase, R., Limbad, C., Singer, E., Allison, J., Adrados, I., Kawamura, R., Pakdel, A., Fukuyo, Y., Nguyen, D. and Khan, S., 2013. Id-1 is a key transcriptional regulator of glioblastoma aggressiveness and a novel therapeutic target. *Cancer research 73*(5): 1559-1569.

Steelman, L. S., Chappell, W. H., Abrams, S. L., Kempf, C. R., Long, J., Laidler, P., Mijatovic, S. et al. 2011. Roles of the Raf/MEK/ERK and PI3K/PTEN/Akt/mtor pathways in controlling growth and sensitivity to therapy-implications for cancer and aging. *Aging 3*(3): 192–222.

Stettner, M. R., Wang, W., Nabors, L. B., Bharara, S., Flynn, D. C., Grammer, J. R., Gillespie, G. Y. et al. 2005. Lyn kinase activity is the predominant cellular Src kinase activity in glioblastoma tumor cells. *Cancer Research 65(13)*: 5535–5543.

Stock, C. and Schwab, A., 2009. Protons make tumor cells move like clockwork. *Pflügers Archiv-European Journal of Physiology 458*(5): 981-992.

Stommel, J.M., Kimmelman, A.C., Ying, H., Nabioullin, R., Ponugoti, A.H., Wiedemeyer, R., Stegh, A.H., Bradner, J.E., Ligon, K.L., Brennan, C. and Chin, L., 2007. Coactivation of receptor tyrosine kinases affects the response of tumor cells to targeted therapies. *Science 318*(5848): 287-290

Strebhardt, K., Becker, S. & Matthess, Y. 2014. Thoughts on the current assessment of Polo-like kinase inhibitor drug discovery. *Expert Opinion on Drug Discovery 0441*(December): 1–8.

Stummer, W., Pichlmeier, U., Meinel, T., Wiestler, O. D., Zanella, F. & Reulen, H. J. 2006. Fluorescence-guided surgery with 5-aminolevulinic acid for resection of malignant glioma: a randomised controlled multicentre phase III trial. *Lancet Oncology 7*(5): 392–401.

Stupp, R., Mason, W. P., van den Bent, M. J., Weller, M., Fisher, B., Taphoorn, M. J. B., Belanger, K. et al. 2005. Radiotherapy plus concomitant and adjuvant temozolomide for glioblastoma. *The New England Journal of Medicine 352*(10): 987–996.

Sugawa, N., Ekstrand, A. J., James, C. D. & Collins, V. P. 1990. Identical splicing of aberrant epidermal growth factor receptor transcripts from amplified rearranged genes in human glioblastomas. *Proceedings of the National Academy of Sciences of the United States of America 87*(21): 8602–8606.

Sun, H., King, A. J., Diaz, H. B. & Marshall, M. S. 2000. Regulation of the protein kinase Raf-1 by oncogenic Ras through phosphatidylinositol 3-kinase, Cdc42/Rac and Pak. *Current Biology CB*, *10*(5): 281–284.

Sun, L., Hui, A.-M., Su, Q., Vortmeyer, A., Kotliarov, Y., Pastorino, S., Passaniti, A. et al. 2006. Neuronal and glioma-derived stem cell factor induces angiogenesis within the brain. *Cancer Cell 9*(4): 287–300.

Sunavala-Dossabhoy, G. & De Benedetti, A. 2009. Tousled homolog, TLK1, binds and phosphorylates Rad9; TLK1 acts as a molecular chaperone in DNA repair. *DNA Repair 8*(1): 87–102.

Szczepanowska, J. 2009. Involvement of Rac /Cdc42/PAK pathway in cytoskeletal rearrangements. *Acta Biochimica Polonica*, *56*(2), 225–234.

Tait, M. J., Petrik, V., Loosemore, A., Bell, B. A. & Papadopoulos, M. C. 2007. Survival of patients with glioblastoma multiforme has not improved between 1993 and 2004: analysis of 625 cases. *British Journal Of Neurosurgery 21*(5): 496–500.

Takayama, Y., Kokuryo, T., Yokoyama, Y., Ito, S., Nagino, M., Hamaguchi, M. & Senga, T. 2010. Silencing of Tousled-like kinase 1 sensitizes cholangiocarcinoma cells to cisplatin-induced apoptosis. *Cancer Letters 296*(1): 27–34.

Tanaka, S., Louis, D. N., Curry, W. T., Batchelor, T. T. & Dietrich, J. 2012. Diagnostic and therapeutic avenues for glioblastoma : no longer a dead end ? *Nature Reviews Clinical Oncology 10*(1): 14–26.

Tarone, G., Cirillo, D., Giancotti, F. G., Comoglio, P. M. & Marchisio, P. C. 1985. Rous sarcoma virus-transformed fibroblasts adhere primarily at discrete protrusions of the ventral membrane called podosomes. *Experimental Cell Research 159*(1): 141–157.

Tavazoie, M., der Veken, L., Silva-Vargas, V., Louissaint, M., Colonna, L., Zaidi, B., Garcia-Verdugo, J. M. et al. 2008. A specialized vascular niche for adult neural stem cells. *Cell Stem Cell 3*(3): 279–288.

Thaker, N. G., Zhang, F., McDonald, P. R., Shun, T. Y., Lewen, M. D., Pollack, I. F. & Lazo, J. S. 2009. Identification of survival genes in human glioblastoma cells by small interfering RNA screening. *Molecular Pharmacology 76*(6): 1246–1255.

The Cancer Genome Atlas.(TCGA) Research Network. 2008. Comprehensive genomic characterization defines human glioblastoma genes and core pathways. *Nature* 455 (2008): 1061−1068

Thiery, J. P. 2002. Epithelial-mesenchymal transitions in tumour progression. *Nature Reviews. Cancer 2*(6): 442–454.

Thomas, a, Giesler, T. & White, E. 2000. p53 mediates bcl-2 phosphorylation and apoptosis via activation of the Cdc42/JNK1 pathway. *Oncogene 19*(46): 5259–5269.

Thomas, A. A., Brennan, C. W., DeAngelis, L. M. & Omuro, A. M. 2014. Emerging therapies for glioblastoma. *JAMA Neurology 71*(11): 1437–44.

Thoreen, C. C., Kang, S. A., Chang, J. W., Liu, Q., Zhang, J., Gao, Y., Reichling, L. J. et al. 2009. An ATP-competitive mammalian target of rapamycin inhibitor reveals rapamycin-resistant functions of mTORC1. *Journal of Biological Chemistry 284*(12): 8023–8032.

Tivnan, A., Zakaria, Z., O'Leary, C., Kögel, D., Pokorny, J. L., Sarkaria, J. N. & Prehn, J. H. M. 2015. Inhibition of multidrug resistance protein 1 (MRP1) improves chemotherapy drug response in primary and recurrent glioblastoma multiforme. *Frontiers in Neuroscience 9*(June): 218.

Tolcher, A. W., Gerson, S. L., Denis, L., Geyer, C., Hammond, L. A., Patnaik, A., Goetz, A. D. et al. 2003. Marked inactivation of O6-alkylguanine-DNA alkyltransferase activity with protracted temozolomide schedules. *British Journal of*

Cancer 88(7): 1004–1011.

Tsatsanis, C. & Spandidos, D. A. 2000. The role of oncogenic kinases in human cancer (Review). *International Journal of Molecular Medicine 5*(6): 583–590.

Tu, S. & Cerione, R. a. 2001. Cdc42 Is a Substrate for Caspases and Influences Fas-induced Apoptosis. *Journal of Biological Chemistry 276*(22): 19656–19663.

Uhlen, M., Fagerberg, L., Hallstrom, B. M., Lindskog, C., Oksvold, P., Mardinoglu, A., Sivertsson, A. et al. 2015. Tissue-based map of the human proteome. *Science 347*(6220): 1260419–1260419.

Vanhaesebroeck, B., Guillermet-Guibert, J., Graupera, M. & Bilanges, B. 2010. The emerging mechanisms of isoform-specific PI3K signalling. *Nature Reviews. Molecular Cell Biology 11*(5): 329–341.

Varuhese, J. F. & Li, Y. 2011. Molecular dynamics and docking studies on cardiac troponin C. *Journal of Biomolecular Structure & Dynamics 29*(1): 123–135.

Veeravalli, K. K. & Rao, J. S. 2012. MMP-9 and uPAR regulated glioma cell migration. *Cell Adhesion and Migration 6*(6): 509–512.

Vega, F.M. and Ridley, A.J., 2008. Rho GTPases in cancer cell biology.*FEBS Letters 582*(14): 2093-2101.

Vehlow, A. & Cordes, N. 2013. Invasion as target for therapy of glioblastoma multiforme. *Biochimica et Biophysica Acta - Reviews on Cancer 1836*(2): 236–244.

Verhaak, R. G. W., Hoadley, K. A., Purdom, E., Wang, V., Qi, Y., Wilkerson, M. D., Miller, C. R. et al. 2010. Integrated genomic analysis identifies clinically relevant subtypes of glioblastoma characterized by abnormalities in PDGFRA, IDH1, EGFR, and NF1. *Cancer Cell 17*(1): 98–110.

Verhoeff, J.J., van Tellingen, O., Claes, A., Stalpers, L.J., van Linde, M.E., Richel, D.J., Leenders, W.P. and van Furth, W.R., 2009. Concerns about anti-angiogenic treatment in patients with glioblastoma multiforme. *BMC cancer 9*(1): 44

Villano, J. L., Seery, T. E. & Bressler, L. R. 2009. Temozolomide in malignant gliomas: Current use and future targets. *Cancer Chemotherapy and Pharmacology 64*(4): 647–655.

Viswas, R. S. & Lee, H. 2011. Quinoline as a Privileged Scaffold in Cancer Drug Discovery. *Current Medicinal Chemistry*, *18*, 1–21.

Vivanco, I., Robins, H. I., Rohle, D., Campos, C., Grommes, C., Nghiemphu, P. L., Kubek, S. et al. 2012. Differential sensitivity of glioma- versus lung cancer-specific EGFR mutations to EGFR kinase inhibitors. *Cancer Discovery 2*(5): 458–471.

Vogelstein, B., Lane, D. & Levine, a J. 2000. Surfing the p53 network. *Nature 408*(6810): 307–310.

Volarević, S. & Thomas, G. 2001. Role of S6 phosphorylation and S6 kinase in cell growth. *Progress in Nucleic Acid Research and Molecular Biology 65*: 101–127.

Voudouri, K., Berdiaki, A., Tzardi, M., Tzanakakis, G.N. and Nikitovic, D., 2015. Insulin-Like Growth Factor and Epidermal Growth Factor Signaling in Breast Cancer Cell Growth: Focus on Endocrine Resistant Disease. *Analytical Cellular Pathology 2015*

Wang, J., Duncan, D., Shi, Z. & Zhang, B. 2013. WEB-based GEne SeT AnaLysis Toolkit (WebGestalt): update 2013. *Nucleic Acids Research 41*(Web Server issue): W77–83.

Wang, J., Zhang, J., Sun, J., Han, J., Xi, Y., Wu, G., Duan, K. X. et al. 2011. Prostacyclin administration as a beneficial supplement to the conventional cancer chemotherapy. *Medical Hypotheses 76*(5): 695–696.

Wang, X., Freeman, N. E., Patil, R., Patil, S. A., Mitra, S., Orr, W. E., Abner, C. W. et al. 2012. EDL-291 , a novel isoquinoline , presents antiglioblastoma effects in vitro and in vivo. *Anti-Cancer Drugs*, *23*, 494–504.

Wang, Y., Zhu, S., Cloughesy, T. F., Liau, L. M., & Mischel, P. S. 2004. p53 disruption profoundly alters the response of human glioblastoma cells to DNA topoisomerase I inhibition. *Oncogene 23*(6): 1283-1290.

Warner, S. J., Yashiro, H. & Longmore, G. D. 2010. The Cdc42/Par6/aPKC Polarity Complex Regulates Apoptosis-Induced Compensatory Proliferation in Epithelia. *Current Biology 20*(8): 677–686.

Wasik, M. A., Zhang, Q., Marzec, M., Kasprzycka, M., Wang, H. Y. & Liu, X. 2009. Anaplastic lymphoma kinase (ALK)-induced malignancies: novel mechanisms of cell transformation and potential therapeutic approaches. *Seminars in Oncology 36*(2 Suppl 1): S27–35.

Weinstein, I. B. & Joe, A. 2008. Oncogene addiction. *Cancer Research 68*(9): 3077–3080.

Wen, P.Y. and Kesari, S., 2008. Malignant gliomas in adults. *New England Journal of Medicine 359*(5): 492-507.

Westhoff, M.-A., Karpel-Massler, G., Brühl, O., Enzenmüller, S., La Ferla-Brühl, K., Siegelin, M. D., Nonnenmacher, L. et al. 2014. A critical evaluation of PI3K inhibition in Glioblastoma and Neuroblastoma therapy. *Molecular and Cellular Therapies 2*: 32.

Wheeler, A. P., Wells, C. M., Smith, S. D., Vega, F. M., Henderson, R. B., Tybulewicz,

V. L. & Ridley, A. J. 2006. Rac1 and Rac2 regulate macrophage morphology but are not essential for migration. *Journal of Cell Science 119* (Pt 13): 2749–2757.

Wheeler, D. L., Dunn, E. F. & Harari, P. M. 2010. Understanding resistance to EGFR inhibitors-impact on future treatment strategies. *Nature reviews. Clinical Oncology 7*(9): 493–507.

Whittaker, C. A., Bergeron, K. F., Whittle, J., Brandhorst, B. P., Burke, R. D. & Hynes, R. O. 2006. The echinoderm adhesome. *Developmental Biology 300*(1): 252–266.

Wiedemeyer, W. R., Dunn, I. F., Quayle, S. N., Zhang, J., Chheda, M. G., Dunn, G. P., Zhuang, L. et al. 2010. Pattern of retinoblastoma pathway inactivation dictates response to CDK4/6 inhibition in GBM. *Proceedings of the National Academy of Sciences of the United States of America 107*(25): 11501–11506.

Willems, L., Tamburini, J., Chapuis, N., Lacombe, C., Mayeux, P. & Bouscary, D. 2012. PI3K and mTOR signaling pathways in cancer: New data on targeted therapies. *Current Oncology Reports 14*(2): 129–138.

Winograd-Katz, S. E., Fässler, R., Geiger, B. & Legate, K. R. 2014. The integrin adhesome: from genes and proteins to human disease. *Nature Reviews: Molecular Cell Biology 15*(4): 273–288.

Wong, A. J., Bigner, S. H., Bigner, D. D., Kinzler, K. W., Hamilton, S. R. & Vogelstein, B. 1987. Increased expression of the epidermal growth factor receptor gene in malignant gliomas is invariably associated with gene amplification. *Proceedings of the National Academy of Sciences of the United States of America 84*(19): 6899–6903.

Wong, A. J., Ruppert, J. M., Bigner, S. H., Grzeschik, C. H., Humphrey, P. A., Bigner, D. S. & Vogelstein, B. 1992. Structural alterations of the epidermal growth factor receptor gene in human gliomas. *Proceedings of the National Academy of Sciences of the United States of America 89*(7): 2965–2969.

Wong, E.T., Hess, K.R., Gleason, M.J., Jaeckle, K.A., Kyritsis, A.P., Prados, M.D., Levin, V.A. and Yung, W.A., 1999. Outcomes and prognostic factors in recurrent glioma patients enrolled onto phase II clinical trials.*Journal of Clinical Oncology 17*(8): 2572-2572

Workman, P., Al-Lazikani, B. & Clarke, P. A. 2013. Genome-based cancer therapeutics: Targets, kinase drug resistance and future strategies for precision oncology. *Current Opinion in Pharmacology 13*(4): 486–496.

Wrensch, M., Jenkins, R. B., Chang, J. S., Yeh, R.-F., Xiao, Y., Decker, P. A., Ballman, K. V et al. 2009. Variants in the CDKN2B and RTEL1 regions are associated with high-grade glioma susceptibility. *Nature Genetics 41*(8): 905–908.

Wrensch, M., Minn, Y., Chew, T., Bondy, M. & Berger, M. S. 2002. Epidemiology of primary brain tumors: current concepts and review of the literature. *Neuro-*

Oncology 4(4): 278–299.

Xiang, W., Zhang, D., & Montell, D. J. 2015. Tousled-like kinase regulates cytokine-mediated communication between cooperating cell types during collective border cell migration. *Molecular Biology of The Cell 27*(1): 12-19.

Xie, Q., Mittal, S. & Berens, M. E. 2014. Targeting adaptive glioblastoma: an overview of proliferation and invasion. *Neuro-Oncology 16*(12): 1575–1584.

Xu, A. M. & Huang, P. H. 2010. Receptor tyrosine kinase coactivation networks in cancer. *Cancer Research 70*(10): 3857–3860.

Yachi, K., Watanabe, T., Ohta, T., Fukushima, T., Yoshino, A., Ogino, A., Katayama, Y. et al. 2008. Relevance of MSP assay for the detection of MGMT promoter hypermethylation in glioblastomas. *International Journal of Oncology 33*(3): 469–475.

Yamada, K., Tso, J., Ye, F., Choe, J., Liu, Y., Liau, L. M. & Tso, C. L. 2011. Essential gene pathways for glioblastoma stem cells: Clinical implications for prevention of tumor recurrence. *Cancers 3*(2): 1975–1995.

Yan, H., Parsons, D. W., Jin, G., McLendon, R., Rasheed, B. A., Yuan, W., Kos, I. et al. 2009. Mutations in Gliomas. *New England Journal of Medicine 360*(8): 765–773.

Yancopoulos, G. D., Davis, S., Gale, N. W., Rudge, J. S., Wiegand, S. J. & Holash, J. 2000. Vascular-specific growth factors and blood vessel formation. *Nature 407*(6801): 242–248.

Yang, J., Yan, R., Roy, A., Xu, D., Poisson, J. & Zhang, Y. 2015. The I-TASSER Suite: protein structure and function prediction. *Nature Methods*, *12*(1), 7–8.

Yang, X., Yang, S., Chai, H., Yang, Z. & Lee, R. J. 2015. A Novel Isoquinoline Derivative Anticancer Agent and Its Targeted Delivery to Tumor Cells Using Transferrin-Conjugated Liposomes. *PLoS ONE* 10(8).

Yeh, C. H., Yang, H. J., Lee, I. J. & Wu, Y. C. 2010. Caenorhabditis elegans TLK-1 controls cytokinesis by localizing AIR-2/Aurora B to midzone microtubules. *Biochemical and Biophysical Research Communications 400*(2): 187–193.

Zhang, X. D. 2007. A pair of new statistical parameters for quality control in RNA interference high-throughput screening assays. *Genomics 89*(4): 552–561.

Zhang, X. D., Yang, X. C., Chung, N., Gates, A., Stec, E., Kunapuli, P., Holder, D. J. et al. 2006. Robust statistical methods for hit selection in RNA interference high-throughput screening experiments. *Pharmacogenomics 7*(3): 299–309.

Zhang, Y., Cai, R., Zhou, R., Li, Y., & Liu, L. 2016. Tousled-like kinase mediated a new type of cell death pathway in Drosophila. *Cell Death & Differentiation 23*(1): 146-157.

Zheng, H., Ying, H., Yan, H., Kimmelman, A.C., Hiller, D.J., Chen, A.J., Perry, S.R., Tonon, G., Chu, G.C., Ding, Z. and Stommel, J.M., 2008, December. Pten and p53 converge on c-Myc to control differentiation, self-renewal, and transformation of normal and neoplastic stem cells in glioblastoma. In *Cold Spring Harbor symposia on quantitative biology* (sqb-2008). Cold Spring Harbor Laboratory Press.

Zhu, G., Wang, Y., Huang, B., Liang, J., Ding, Y., Xu, A. & Wu, W. 2012. A Rac1/PAK1 cascade controls β-catenin activation in colon cancer cells. *Oncogene 31*(8): 1001–1012.

Ziegler, D. S., Kung, A. L. & Kieran, M. W. 2008. Anti-apoptosis mechanisms in malignant gliomas. *Journal of Clinical Oncology 26*(3): 493–500.

Zoncu, R., Efeyan, A. & Sabatini, D. M. 2011. mTOR: from growth signal integration to cancer, diabetes and ageing. *Nature Reviews. Molecular Cell Biology 12*(1): 21–35.

APPENDIX A

ANIMAL ETHICS COMMITTEE APPROVAL – page 1 of 2

Jawatankuasa Etika Penggunaan Haiwan (UKMAEC) | UKM Animal Ethics Committee (UKMAEC)

UKM 1.5.24/138/61/2
12hb. Oktober, 2014

UKMAEC
d/a
Unit Sumber Haiwan Makmal
Fakulti Perubatan
Universiti Kebangsaan Malaysia
Jalan Raja Muda Abdul Aziz
50300 Kuala Lumpur.

Profesor Madya Dr. Roslan Harun,
Institut Perubatan Molekul UKM (UMBI)
Pusat Perubatan,
Universiti Kebangsaan Malaysia,
Jalan Yacob Latiff, Bandar Tun Razak,
56000 Cheras, Kuala Lumpur.

Tuan,

Kelulusan Dari Jawatankuasa Etika Penggunaan Haiwan (UKMAEC) Untuk Tajuk: "*In vivo* functional analysis of Tousled like kinase 1 in GBM xenograft model."

Dalam mesyuarat UKMAEC pada 24hb. September, 2014 telah memutuskan bahawa permohonan tuan diluluskan. Nombor kelulusan adalah seperti berikut:

UMBI/2014/ROSLAN/24-SEPT./607-SEPT.-2014-DEC.-2014

Bersama surat ini kami lampirkan sijil kelulusan dengan butiran penyelidikan yang berkaitan. Diharap sijil ini dapat dimanfaatkan pada masa hadapan.

Sekian, terima kasih.

Yang benar,

PROFESOR MADYA DR. KAMISAH YUSOF
Pengerusi UKMAEC
Universiti Kebangsaan Malaysia

s.k. - Pengarah CRIM

d/a Unit Sumber Haiwan Makmal, Fakulti Perubatan, Universiti Kebangsaan Malaysia, Jalan Raja Muda Abdul Aziz, 50300 Kuala Lumpur
Telefon: +603-9289 5086 / 5091 Faksimili: +603-2698 3743 E-mel: kuhaiwan@medic.ukm.my Laman Web:
http://www.medic.ukm.my/laru

ANIMAL ETHICS COMMITTEE APPROVAL – page 2 of 2

UNIVERSITI KEBANGSAAN MALAYSIA
ANIMAL ETHICS COMMITTEE
c/o Laboratory Animal Resource Unit
Faculty of Medicine, UKM
Jalan Raja Muda Abdul Aziz 50300 Kuala Lumpur
Tel: 92895086, 92895091, 92895087 Fax: 603-29683743

24th September, 2014

UKMAEC APPROVAL NUMBER:	**UMBI/2014/ROSLAN/24-SEPT./607-SEPT.-2014-DEC.-2014**
CHIEF INVESTIGATOR:	**Assoc. Prof. Dr. Roslan Harun**
DIVISION/DEPT. OF CHIEF INVESTIGATOR:	**UKM Medical Molecular Biology Institute (UMBI) UKM Medical Centre.**
FUNDING INSTITUTION (S):	**HICOE Project Grant, Ministry of Education, Malaysia**
GRANT NUMBER (S):	**JJ-008-2011**
PROJECT TITLE:	***In vivo* functional analysis of Tousled like kinase 1 in GBM xenograft model.**
CO-INVESTIGATOR:	**Prof. Datuk Dr. A. Rahman A. Jamal** **Dr. Mohd Hanafi Ahmad Damanhuri** **Dr. Nor Azian Abdul Murad**
STUDENT:	**Kamariah binti Ibrahim**
OTHER AUXILIARIES:	-
PROJECT CLASSIFICATION:	**C**
SOURCE OF ANIMALS:	**Biolasco, Taiwan**
HOUSING-LOCATION OF ANIMALS DURING PROJECT:	**UMBI, UKM.**
ESTIMATED DURATION OF PROJECT:	**From September 2014 to December 2014**

Assoc. Prof. Dr. Kamisah Yusof
Chairperson of UKMAEC
Universiti Kebangsaan Malaysia

APPROVED

Low Kiat Cheong
Secretary of UKMAEC
Universiti Kebangsaan Malaysia

APPENDIX B

FUNCTIONAL MICROARRAY GENE EXPRESSION ANALYSIS (CD)

APPENDIX C

MORPHOLOGY OF U87MG, LN18, A172 AND NORMAL HUMAN ASTROCYES GROWN IN CELL CUTURE CONDITION

LN-18 (ATCC®CRL-2610™)

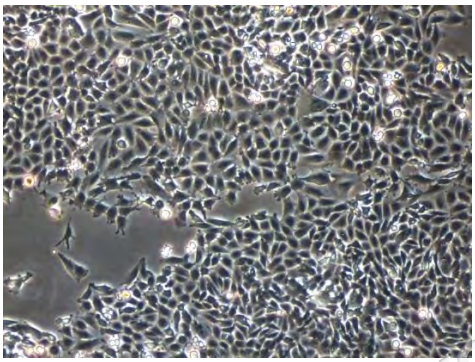

U-87 MG
(ATCC®HTB-14™)

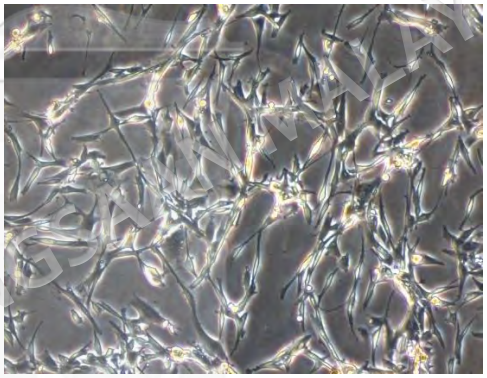

A-172 [A172]
(ATCC®CRL-1620™)

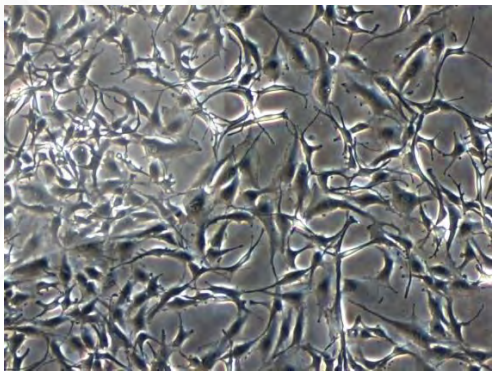

Clonetics™ Normal Human Astrocytes

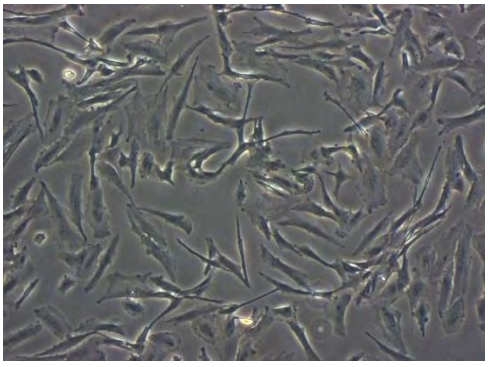

APPENDIX D

TLK1 ALTERATIONS IN GBM (cBIOPORTAL)

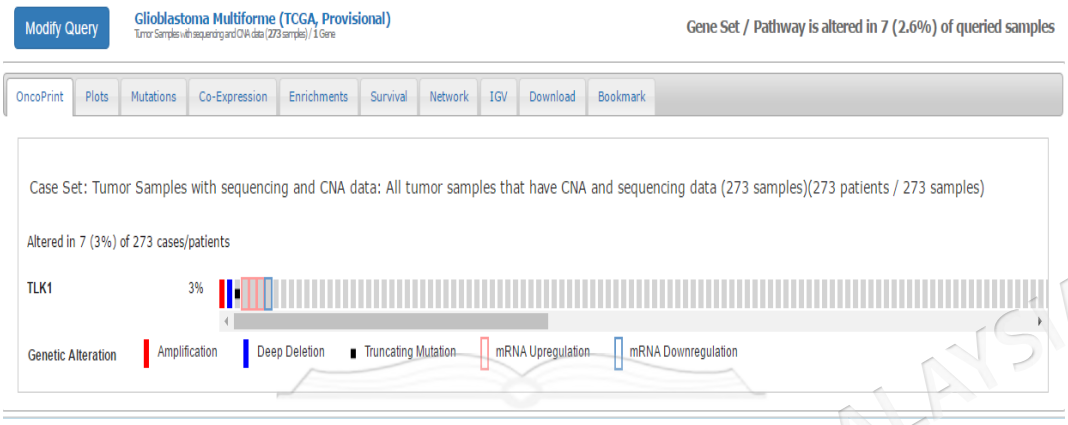

APPENDIX E

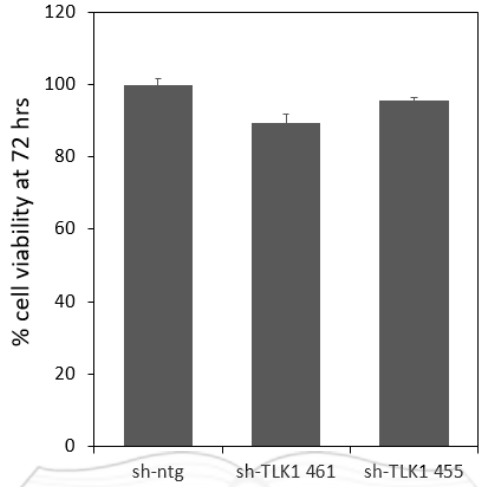

Appendix E1 Cell viability of U87MG knockdown with two shRNA sequences

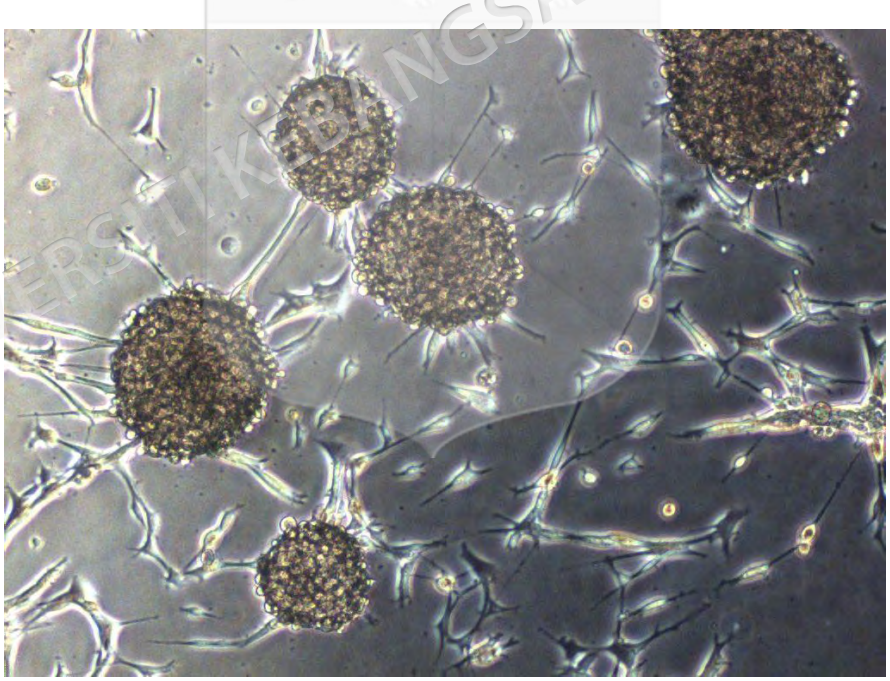

Appendix E2 Morphology of U87G which transformed into spheroids when cultured in a very confluent condition which did not allow wound healing analysis to be performed in this particular cell line

APPENDIX F

RNAI SCREENING OPTIMIZATION

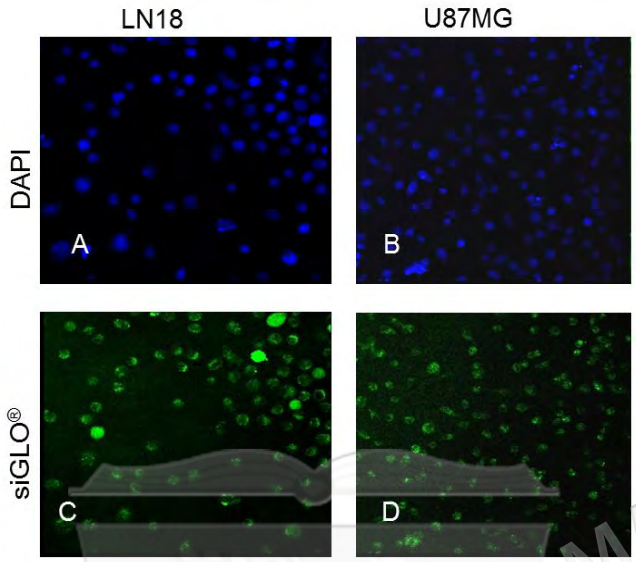

Appendix F1 Figure shows careful optimization prior RNAi screening. Transfection efficiency was measured using siGLO® and observed under confocal microscopy. Transfection efficiency achieved were more than 80% in both U87MG and LN18 cell lines.

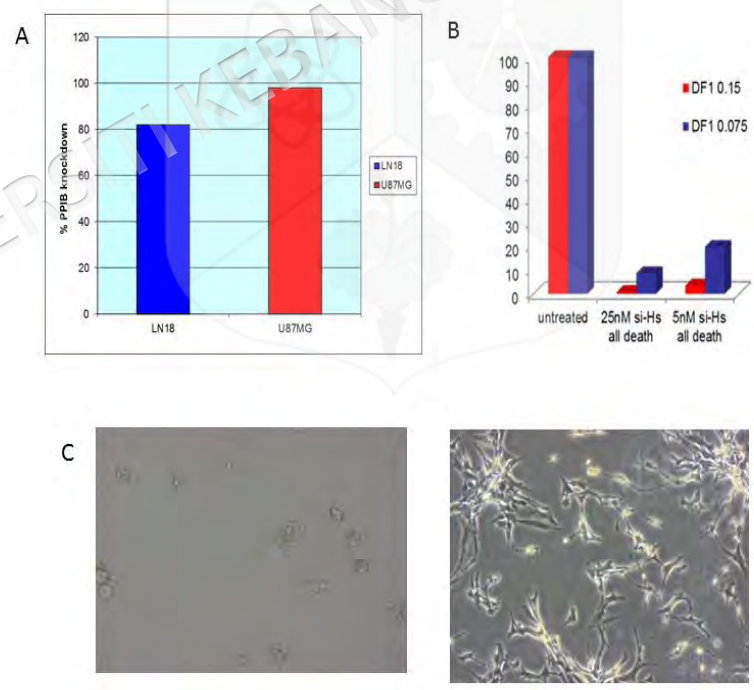

Appendix F2 Figure shows A) More than 80% control gene PPIB knockdown was achieved in U87MG and LN18. B) and C) Graph shows successful transfection in both cell ines using AllStars Hs Cell Death Control siRNA (Qiagen, USA) and Dharmafect1 1 transfection reagent.

APPENDIX G

VECTOR MAP

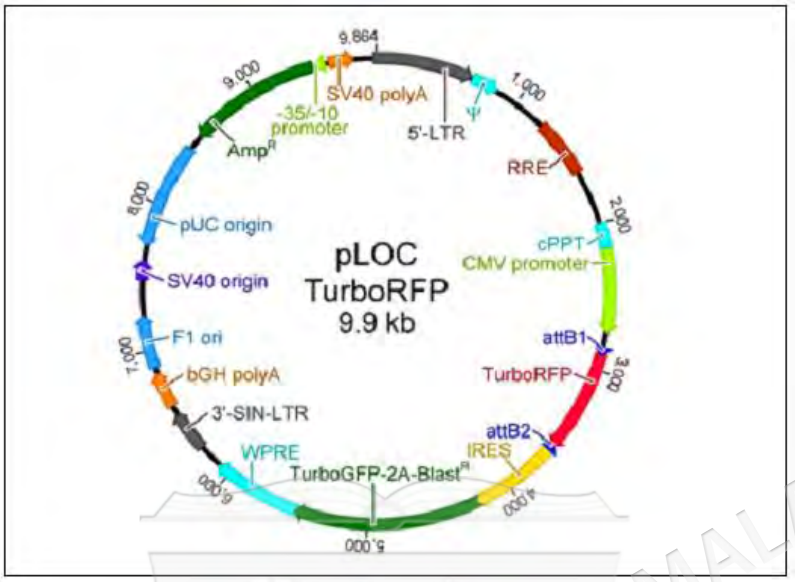

Detailed vector map of pLOC lentiviral vector containing the TurboRFP ORF. The lentiviral ORF clone contains attB1 and attB2; the ORF clone contains attL1 and attL2

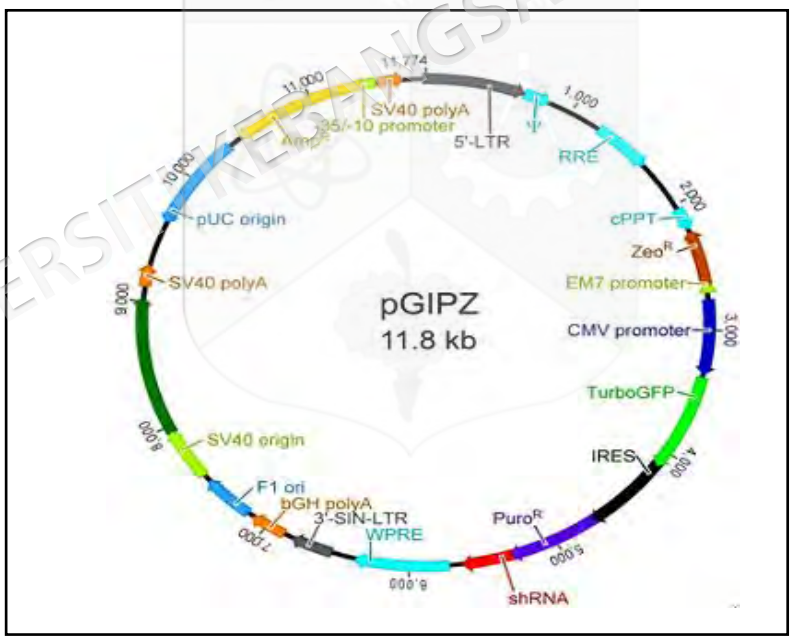

Detailed vector map of pGIPZ lentiviral vector.

APPENDIX H-1

CELL LINES CHARACTERISTICS – LN18

Cell line	LN18
Disease	Grade IV, glioblastoma; glioma
Company	American Type Culture Collection, ATCC, USA
Designation	ATCC® CRL-2610™
Characteristics	Adherent
Organisms	Homo sapiens
Morphology	Epithelium
Source	Brain/cerebrum; right temporal lobe
Tumourigenic	Yes
Information	65 years, male
Growth	Subculture Ratio: 1:4 to 1:6
Culture	The base medium for this cell line is ATCC-formulated Dulbecco's Modified Eagle's Medium, Catalog No. 30-2002. To make the complete growth medium, add the following components to the base medium: fetal bovine serum to a final concentration of 5%
Storage	Complete growth medium, 90%; Additional fetal bovine serum, 5%; DMSO, 5%.
Comments	The cells are negative for glial fibrillary acidic proteins and S100 (S-100) protein. The cells exhibit mutated p53 (TP53) and possible homozygous deletions in the p16 and p14ARF tumor suppressor genes. They have a wild-type PTEN gene. Stimulation of the cells with Fas ligand lead to apoptotic cell death within 16 hours. The cells were also killed by puromycin in a dose dependent manner. Bcl-2 protects these cells from Fas ligand-induced cell death but was shown to have only a small protective effect on puromycin-induced apoptosis. Reference: Forbes et al. 2014 (COSMIC cell lines project), and ATCC

APPENDIX H-2

CELL LINES CHARACTERISTICS – U87MG

Cell line	U87MG
Disease	glioblastoma; astrocytoma; classified as grade IV as of 2007
Company	American Type Culture Collection, ATCC, USA
Designation	ATCC® HTB-14™
Characteristics	Adherent
Organisms	Homo sapiens
Morphology	Epithelium
Source	Brain
Tumourigenic	Yes
Information	44 years, male
Growth	Subcultivation Ratio: A subcultivation ratio of 1:2 to 1:5 is recommended, Medium Renewal: 2 to 3 times per week
Culture	The base medium for this cell line is ATCC-formulated Eagle's Minimum Essential Medium, Catalog No. 30-2003. To make the complete growth medium, add the following components to the base medium: fetal bovine serum to a final concentration of 10%.
Storage	Complete culture medium described above supplemented with 5% (v/v) DMSO
Comments	CDKN2A homozygous c.1_471del471 p.0?, PTEN homozygous c.209+1G>T p.? CDKN2C homozygous c.1_507del507 p.0? Wild type TP53 gene (no mutations) Reference: Forbes et al. 2014 – COSMIC cell lines project and ATCC

APPENDIX H-3

CELL LINES CHARACTERISTICS – A172

Cell line	A172
Disease	glioblastoma; astrocytoma; classified as grade IV as of 2007
Company	American Type Culture Collection, ATCC, USA
Designation	ATCC® CRL-1620™
Characteristics	Adherent
Organisms	Homo sapiens
Morphology	Epithelium
Source	Brain
Tumourigenic	Yes
Information	53 years, male
Growth	Subcultivation Ratio: A subcultivation ratio of 1:3 to 1:8 is recommended. Medium Renewal: Every 2 to 3 days
Culture	The base medium for this cell line is ATCC-formulated Dulbecco's Modified Eagle's Medium, Catalog No. 30-2002. To make the complete growth medium, add the following components to the base medium: fetal bovine serum to a final concentration of 10%.
Storage	Complete culture medium described above supplemented with 5% (v/v) DMSO
Comments	CDKN2A homozygous c.1_471del471 p.0? Reference: Forbes et al. 2014 (COSMIC cell lines project), and ATCC

APPENDIX H-4

CELL LINES CHARACTERISTICS – NHA

Cell line	Clonetics™ Normal Human Astrocytes (NHA), Lonza
Company	Lonza Walkersville, Inc., USA
Designation	NHA
Characteristics	Adherent
Organisms	Homo sapeiens
Morphology	Epithelium
Source	Brain
Tumourigenic	No
Information	Obtained from a donor that was tested and found non-reactive by an FDA approved method for the presence of HIV-I, hepatitis B virus and hepatitis C virus.
Growth	Typical time from subculture to confluent monolayer 6 – 8 days. Additional population doublings guaranteed using Clonetics™ System 10
Culture	Clonetics™ ReagentPack™ provides the solutions required for successful subculture of primary cells. It contains 100 ml each of HEPES Buffered Saline Solution, Trypsin/EDTA, and Trypsin Neutralizing Solution (TNS). HEPES-BSS is used to neutralize the complex proteins in growth medium that may inactivate trypsin during trypsinization. Trypsin/EDTA is used to remove cells from culture vessel surfaces. TNS is used to effectively neutralize Trypsin/EDTA.

APPENDIX I

LIST OF PRIMERS

GENE NAME	Forward 5' to 3'	Reverse 5' to 3'
FYN	GGAAAAAGACCAGTCCTGCCT	GTCCGCCAACGATCACAAAC
ROCK2	CAGACCCTTTTGCCCGATCA	GGCAGTTAGCTAGGTTTGTTTG G
ARPC1B	GAACCTGGACAAGAAGGCGA	,GATCTGGCTGACGCTGTTCT
RAC2	CACCGACACTCTCCAGGCTC	ATAGTTGTCAAACACGGTGGG G
THBS2	AAAGTGAGTCCCTGCCTTCC	CCTGTGCAGGGCTGCTG
COL4A2	CCAGGTTTTAAAGGCAGCCG	TTTGCGCCCAGGTATCCTTT
PXN	CATGGACGACCTCGACGC	CAAGAACACAGGCCGTTTGG

APPENDIX J

TMZ TITRATION ASSAY

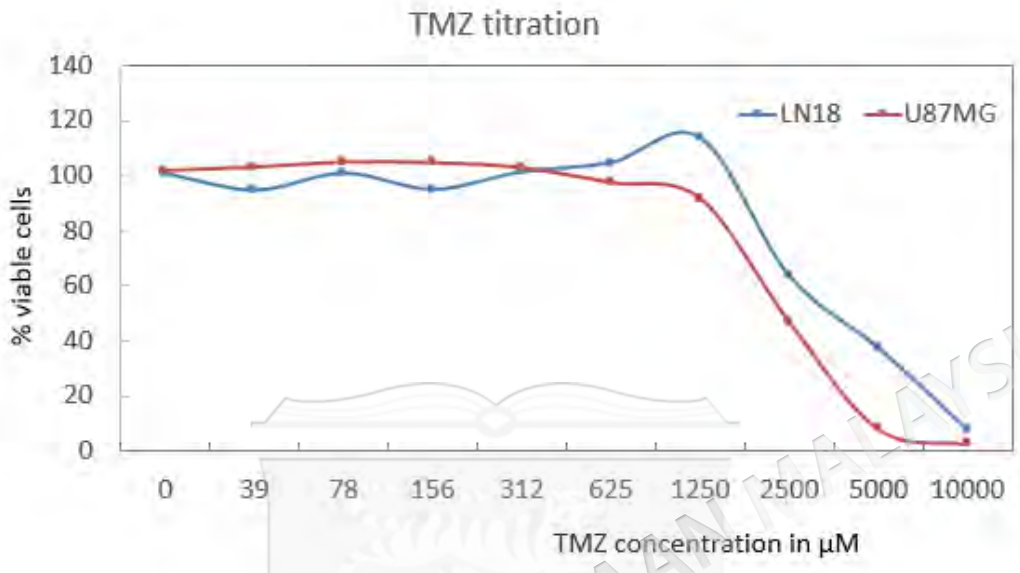

Appendix J Drug titration for TMZ. Sub-lethal dose of 1/10 of TMZ IC50; 250 µM (1:10) was selected for chemosensitization experiment

APPENDIX K

LIST OF PROCEEDINGS

1. ***Kamariah Ibrahim,*** Firdaus Che Mat, Nor Azian Abdul Murad, Norfilza Mohd Mokhtar, Nuraziah Mohammad Zain, Nurismah Md Isa, A Rahman A Jamal and Roslan Harun; Silencing of cell cycle related kinases sensitizes glioblastoma cells to temozolomide. 37th Malaysian Biochemistry and Molecular Biology Conference; Sime Darby; Kuala Lumpur;18-19 July 2012

2. ***Kamariah Ibrahim,*** Firdaus Che Mat, Nor Azian Abdul Murad, Norfilza Mohd Mokhtar, Wan Zurinah Wan Ngah, A Rahman A Jamal and Roslan Harun; Silencing of cell cycle kinases sensitizes glioblastoma cells to temozolomide Frontiers in Cancer Science, National University of Singapore; Silencing of cell cycle kinases sensitizes glioblastoma cells to temozolomide. 5-8 November 2012

3. ***Kamariah Ibrahim,*** Mohd Firdaus Che Mat, Nor Azian Abdul Murad, Norfilza Mohd Mokhtar, Nuraziah Mohamad Zin, Nurismah Md Isa, Wan Zurinah Wan Ngah, A Rahman A Jamal and Roslan Harun. Silencing of Tousled-like kinase 1 (TLK1) reduces survival, migration and invasion of glioblastoma multiforme cells, 1st National Conference for Cancer Research In Conjunction with 5th Regional Conference on Molecular Medicine (RCMM); 8-10 November 2013

4. ***Kamariah Ibrahim***, Abu Bakar Danjuma, Nor Azian Abdul Murad, Norfilza Mohd Mokhtar, Wan Zurinah Wan Ngah, A Rahman A Jamal and Roslan Harun. *In silico* homology modelling and docking study of Tousled-like kinase 1 identifies potential inhibitors for glioblastoma multiforme International Symposium & Workshop on Functional Genomics & Structural Biology 2014; 21-24 January 2014

5. ***Kamariah Ibrahim,*** Ahmad Hathim Ahmad Azman, Liyana Safinaz Abdul Kadir, Nurafifah Natrah Sakim, Nurul Qistina Hashim, A Rahman A Jamal and Roslan Harun. Overexpression of Tousled-like kinase 1 promotes survival and invasiveness in glioblastoma multiforme cells UKM Medical Molecular Biology (UMBI) Postgraduate Research Seminar 2014; 3rd June 2014

6. ***Kamariah Ibrahim,*** Nor Azian Abdul Murad, Wan Zurinah Wan Ngah, A Rahman A Jamal and Roslan Harun. Investigation of mechanisms involved in Tousled-Like Kinase 1 inhibition in the regulation of survival pathways in glioblastoma multiforme; 2nd National Conference for Cancer Research In Conjunction with 6th Regional Conference on Molecular Medicine (RCMM), 2015

APPENDIX L

LIST OF PUBLICATIONS

1. ***Kamariah Ibrahim,*** Firdaus Che Mat, Nor Azian Abdul Murad, Norfilza Mohd Mokhtar, Wan Zurinah Wan Ngah, A Rahman A Jamal and Roslan Harun. Silencing of PROS1 induces apoptosis and inhibits migration and invasion of glioblastoma multiforme cells. International Journal of Oncology 49(6) 2359-2366 (IF: 3.018)

2. ***Kamariah Ibrahim,*** Nor Azian Abdul Murad, A Rahman A Jamal and Roslan Harun. Knockdown of Tousled-like kinase 1 inhibits glioblastoma cell invasion and migration via the integrin-mediated cell adhesion pathway. Submitted 1st February 2017 Molecular Cancer (IF: 5.88)

3. ***Kamariah Ibrahim,*** Abu Bakar Danjuma, Nor Azian Abdul Murad, A Rahman A Jamal and Roslan Harun. *In silico* homology modelling and identification of Tousled-like kinase 1 inhibitors for glioblastoma therapy via high throughput virtual screening protein-ligand docking. Submitted 2nd August 2016. BMC Research Notes (ISI)

APPENDIX M

LIST OF AWARDS

1. UKM Postgraduate Mobility Travel Grant to participate and present at the Frontiers in Cancer Science Conference, Singapore, 2012

2. Best Poster Presentation; 37th Malaysian Biochemistry and Molecular Biology Conference, 2012

3. 1st Prize; Young Investigator Award in Cancer; 1st National Conference for Cancer Research in Conjunction with 5th Regional Conference on Molecular Medicine (RCMM), 2013

4. Best Poster Presentation in Structural Biology; International Symposium & Workshop on Functional Genomics & Structural Biology 2014

5. 3rd Prize for Three Minutes Thesis Competition, Varsity level, University Kebangsaan Malaysia, March 2015

6. 1st Prize; Young Investigator Award in Cancer; 2nd National Conference for Cancer Research in Conjunction with 6th Regional Conference on Molecular Medicine (RCMM), 2015